

Technische Universität München

TUM School of Engineering and Design

**Eco-Efficiency Assessment of Zero-Emission
Heavy-Duty Vehicle Concepts**

Sebastian Pascal Wolff

Vollständiger Abdruck der von der TUM School of Engineering and Design der
Technischen Universität München zur Erlangung des akademischen Grades eines

Doktors der Ingenieurwissenschaften

genehmigten Dissertation.

Vorsitz: Prof. Malte Jaensch, Ph.D.

Prüfer*innen der Dissertation: 1. Prof. Dr.-Ing. Markus Lienkamp
2. Prof. Dr.-Ing. Achim Kampker (RWTH Aachen)

Die Dissertation wurde am 30.09.2022 bei der Technischen Universität München eingereicht
und durch die TUM School of Engineering and Design am 27.12.2022 angenommen.

The more you know, the less you need.

YVON CHOUINARD
CLIMBER AND FOUNDER OF PATAGONIA

Danksagung

Diese Arbeit ist der Abschluss meiner Zeit als wissenschaftlicher Mitarbeiter am Lehrstuhl für Fahrzeugtechnik der Technischen Universität München. Obwohl diese Dissertation meine Forschungsarbeit von 2017 bis 2022 zusammenfasst, kann sie nicht im Ansatz widerspiegeln, was ich aus meiner Lehrstuhlzeit mitnehme.

Meinem Doktorvater Prof. Dr.-Ing Markus Lienkamp möchte ich für die Betreuung und seinen Input zum Gelingen dieser Arbeit danken. Vor Allem möchte ich ihm aber für sein Vertrauen in meine Arbeit im Truck 2030, später als Teamleiter, in der NPM und, nicht zuletzt, in meine Forschung danken. Die damit verbundenen Freiheiten weiß ich sehr zu schätzen — sie haben mir die Gelegenheit gegeben meine Ideen auch über diese Dissertation hinaus zu entwickeln.

Am Meisten aber prägen die Kollegen die Zeit am Lehrstuhl. Viele Kollegen sind in dieser Zeit zu Freunden geworden und ich möchte allen dafür danken, diese Zeit unvergesslich gemacht zu haben. Im Besonderen gilt mein Dank meiner Forschungsgruppe Fahrzeugkonzepte. Ihr habt nicht nur bei fachlichen Diskussionen, gemeinsamen Kaffee- und Mittagspausen sowie vielen Abendveranstaltungen meine Lehrstuhlzeit geprägt. Wegen euch war es auch immer eine Freude, dieses Team leiten zu dürfen. Stellvertretend für viele Kollegen und Freunde, möchte ich meiner langjährigen Bürokollegin Dr.-Ing. Svenja Kalt für die gemeinsame Zeit und ihr kritisches Lektorat meiner Veröffentlichungen danken. Weiterhin wären weder diese Veröffentlichungen noch diese Arbeit ohne die Gespräche, Diskussionen und Spaziergänge mit Dr.-Ing Matthias Brönnner möglich gewesen — vielen, vielen Dank dafür! Für die sorgfältige Durchsicht dieser Arbeit und daraus resultierende Hinweise bedanke ich mich auch bei Moritz Seidenfus, Manuel Ank und Lorenzo Nicoletti.

Mein Dank gilt ebenfalls den von mir betreuten Studenten, die mit ihren Arbeiten und viel persönlichem Engagement das Forschungsprojekt bereicherten und damit auch zum Erfolg dieser Dissertation beigetragen haben. Auch Dr.-Ing. Michael Fries gebührt ein besonderer Dank, insbesondere für die Motivation zur Promotion und die bereichernden Diskussionen. Ebenfalls möchte ich Prof. Dr.-Ing. Karl-Viktor Schaller für seine Einblicke in die Nutzfahrzeugtechnik und -industrie und die vielen Gespräche nach der Vorlesung Nutzfahrzeugtechnik danken.

Prof. Dr.-Ing. Achim Kampker danke ich für die Übernahme des Zweitgutachtens. Weiterhin gilt mein Dank Herrn Prof. Ph.D Malte Jaensch für die Übernahme des Prüfungsvorsitzes.

Meiner Familie, insbesondere meinen Eltern und Schwiegereltern gebührt größter Dank. Ihr habt mich in all meinen Vorhaben bestärkt und immer unterstützt. In ganz besonderem Maß danke ich meiner Frau Carolin für ihre Unterstützung, Motivation und nicht zuletzt für ihr Verständnis über alle Höhen und Tiefen während der gesamten Promotionszeit und darüber hinaus.

München, im Sommer 2022

Sebastian Wolff

Abstract

Despite the *Paris Climate Agreement* and pledges by governments to reduce anthropogenic carbon-dioxide emissions, road transportation emissions are increasing. In 2015, the European Union resolved penalties for exceeding CO₂-limits beginning in 2025. Besides global warming, the ongoing destruction of nature due to human-caused environmental impact is increasingly coming into focus. The automotive industry has a relevant role in changing these developments. On the one hand, the majority of vehicles require fossil fuels and, on the other hand, the production of automotive products contributes significantly to global resource consumption. While passenger cars are problematic mainly due to their large numbers, heavy commercial vehicles cause environmental damage due to high fuel and resource consumption per vehicle. Yet, they are irreplaceable for global supply chains and, thus, economic growth and prosperity.

Global and European commercial vehicle manufacturers are under high pressure to replace their diesel-powered vehicles with environmentally friendly and cost-efficient alternatives. In addition to hybrid vehicles, battery electric and hydrogen-powered fuel cells or internal combustion engines are considered alternatives. Giving recommendations to vehicle developers and decision-makers, this work combines an ecological and economic assessment. Having a unified cradle-to-grave system boundary, the presented eco-efficiency assessment provides a comprehensive and holistic technology forecast. An evolutionary algorithm accounts for future technological development and optimizes each vehicle concerning environmental, economic, and driving performance. With infrastructure being a decisive cost factor, a system cost approach combines vehicle-specific total cost-of-ownership with infrastructure costs. Based on vehicle stock development scenarios, the system costs approach estimates the eco-efficiency of the transition from fossil fuels to zero-emission alternatives in the current decade.

The study shows the impact of renewable energy on long-haul transportation and quantifies the associated costs, comparing eco-efficient vehicle concepts suitable for future transportation (Figure 1). The results indicate that battery electric trucks have competitive operating costs compared to diesel-powered vehicles. With today's European electricity mix, the environmental impact of battery-powered vehicles is 313 % higher than the reference diesel. However, with increasing renewable energy the battery electric vehicles outperform the diesel (-65 %). Operating the fuel cell with green hydrogen decreases environmental impact (-27 %) compared to methane-based hydrogen. In the long run, battery electric trucks outperform fuel cell trucks regarding environmental impact. Battery electric and fuel cell electric trucks potentially perform at the same costs as today's diesel. This applies to the total cost of ownership at the vehicle level and the system level, including the infrastructure costs of the future vehicle fleet.

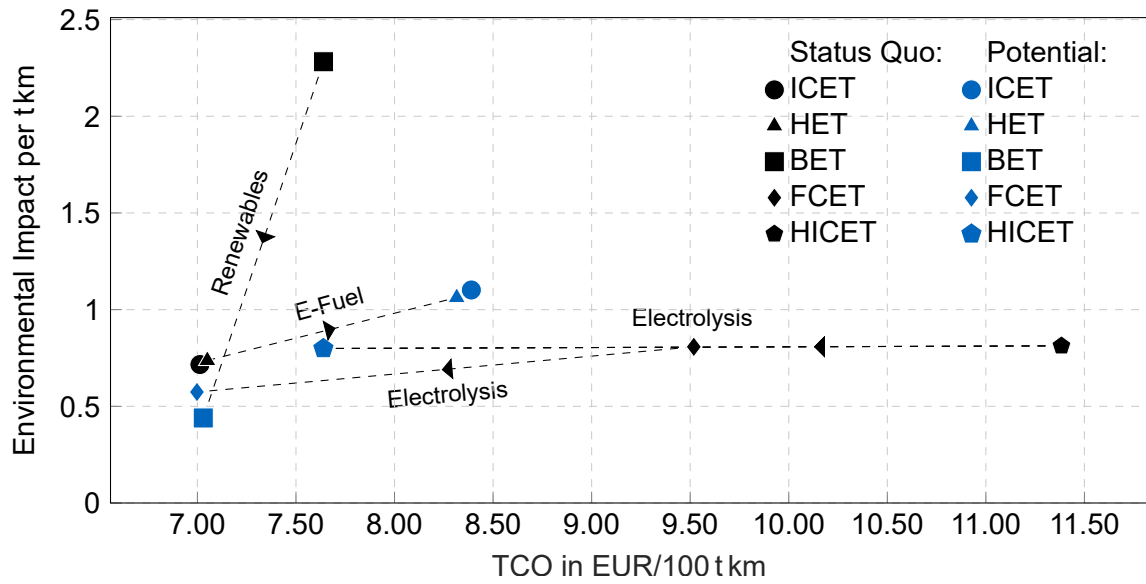


Figure 1: The vehicle concepts' technological potential (blue markers; ●) shows the improvement in eco-efficiency of the BEV and the FCEV, while the ICEV and HEV deteriorate. The black markers (black markers; ●) indicate the optimization results presented in this study. The potential scenario assumes renewable energy, hydrogen via electrolysis and synthetic diesel—both produced with renewable energy. [Note: ICET: Internal Combustion Engine Truck; HET: Hybrid Electric Truck; BET: Battery Electric Truck; FCET: Fuel Cell Electric Truck; HICET: Hydrogen Internal Combustion Engine Truck]

Contents

List of Abbreviations	III
Formula Symbols	VII
1 Introduction	1
1.1 Environmental Impact	2
1.2 Road Transportation	3
1.3 Relevance of Low Emission Freight Transport	5
2 State of Science	7
2.1 The Concept of Eco-Efficiency	7
2.1.1 Economic Dimension	9
2.1.2 Ecological Dimension	9
2.1.3 Impact Assessment and Interpretation	15
2.2 Application to Freight Transport	18
2.3 Alternative Powertrains for Heavy-Duty Vehicles	21
2.3.1 Diesel, Bio and Synthetic-Fuel-Powered Trucks	22
2.3.2 Battery Electric Trucks	23
2.3.3 Hybrid and Overhead Catenary Trucks	25
2.3.4 Hydrogen Powered Vehicles	27
2.4 Existing Assessment Models	33
2.5 Critics and Research Questions	34
3 System Boundary	37
3.1 Considered Systems	37
3.2 Scenarios	38
3.2.1 Status Quo	38
3.2.2 Potential in 2030	39
4 Eco-Efficiency Assessment	41
4.1 Life Cycle Costing	42
4.1.1 Infrastructure Costs	42
4.1.2 National Vehicle Stock	44

4.1.3	Overhead Catenary Costs	47
4.1.4	Concept of System Costs	47
4.2	Life Cycle Assessment	48
4.2.1	Life Cycle Inventory	48
4.2.2	Life Cycle Impact Assessment.....	50
4.3	Longitudinal Vehicle Simulation Model	51
4.3.1	Non-CO ₂ Emissions	55
4.3.2	Fuel Cell Electric Vehicle Model.....	57
4.3.3	Hydrogen Internal Combustion Engine Vehicle Model	59
4.3.4	Overhead Catenary Design.....	60
5	Multi-Objective Optimization Problem	63
6	Validation and Uncertainty	67
6.1	Validation	67
6.2	Uncertainty Quantification	69
7	Results	73
7.1	Life Cycle Costing Results	74
7.2	Life Cycle Assessment Results	75
7.3	Optimization Results	76
7.3.1	Vehicle Concepts	77
7.3.2	Individual Eco-Impact.....	85
7.4	Eco-Efficiency Potential	87
7.5	System Cost Results	89
8	Discussion and Conclusion	93
8.1	Stakeholder Survey	93
8.2	Conclusions	98
8.3	Outlook	99
9	Summary	101
	List of Figures	i
	List of Tables	v
	Bibliography	vii
	Appendix	xxxvii

List of Abbreviations

ACEA	European Automobile Manufacturers' Association
ANL	Argonne National Lab
AP	Acidification Potential
BET	Battery Electric Truck
BOM	Bill of Materials
CDF	Cumulative Distribution Function
CFA	Confirmatory Factor Analysis
CH ₂	Compressed Hydrogen
CI	Compression Ignition
CNG	Compressed Natural Gas
CTUe	Comparative Toxic Unit (eco-System)
DOD	Depth of Discharge
EC	European Commission
EEA	European Environmental Agency
EII	Environmental Impact Index
EM	Electric Machine
EP	Eutrophication Potential
EPA	Environmental Protection Agency
EU	European Union
FCET	Fuel Cell Electric Truck
FD	Fossil Resource Depletion
GCW	Gross Combination Weight
GDP	Gross Domestic Product
GHG	Greenhouse Gas
GREET	Greenhouse Gases, Regulated Emissions, and Energy Use In Technologies Model
GVW	Gross Vehicle Weight
GWP	Global Warming Potential
HC	Hydrocarbon
HET	Hybrid Electric Truck
HICET	Hydrogen Internal Combustion Engine Truck
HPDI	High-Pressure Direct Injection
HT	Human Toxicity

ICE	Internal Combustion Engine
ICET	Internal Combustion Engine Truck
ILCD	International Reference Life Cycle Data
IPBES	Intergovernmental Platform on Biodiversity and Ecosystem Services
IPCC	Intergovernmental Panel on Climate Change
IR	Ionizing Radiation
IUCN	International Union For Conservation of Nature
JRC	Joint Research Center
LCA	Life Cycle Assessment
LCC	Life Cycle Costing
LCI	Life Cycle Inventory
LEM	Lifecycle Emissions Model
LH	Long-Haul
LH2	Liquid Hydrogen
LNG	Liquid Natural Gas
MOP	Multiobjective Optimization Problem
MOVES	Motor Vehicle Emissions Simulator
NF	Normalization Factor
NMVOC	Non-Methane Volatile Organic Compounds
OBET	Overhead Catenary Battery Electric Truck
ODP	Ozone Depletion Potential
OEM	Original Equipment Manufacturer
PBox	Probability Box
PDF	Probability Density Function
PHET	Plug In Hybrid Electric Truck
PM	Particulate Matter
POCP	Photochemical Ozone Creation Potential
PSM	Permanent Synchronous Machine
PTX	Power-To-X
RCA	Remaining Climbing Ability
RD	Resource Depletion
RD	Regional Delivery
SDG	Sustainable Development Goal
SI	Spark Ignition
SMR	Steam Methane Reforming
SOC	State of Charge
TCO	Total Cost of Ownership
UD	Urban Delivery
UNEP	United Nations Environment Program

VECTO	Vehicle Energy Consumption Calculation Tool
VSP	Vehicle-Specific Power
VVUQ	Validation Verification Uncertainty Quantification Framework
WBCSD	World Business Council on Sustainable Development
WD	Water Depletion
WHSC	Worldwide Harmonized Stationary Cycle
WHTC	Worldwide Harmonized Transient Cycle
ZEV	Zero-Emission Vehicle

Formula Symbols

Formula Symbols	Unit	Description
α	%	Road Inclination
α_c	-	Charge Transfer Coefficient (Fuel Cell)
A_{cell}	m ²	Fuel Cell Surface Area
A_f	m ²	Frontal Area
$b_{\text{e-road}}$	%	E-Road Share of Total Road
b_{Tafel}	V	Tafel slope (Fuel Cell)
c	-	Impact Category
c_d	-	Drag Coefficient
C	EUR	Costs (Reference year: 2020)
C_I	EUR	Total Infrastructure Costs
C_{max}	1/h	Maximum (Dis-)Charge Rate
$C_{I, \text{e-road}}$	EUR/km	E-Road Costs
C_{unit}	EUR	Specific Infrastructure Costs (e.g., charging point)
C_S	EUR	System Costs
C_T	EUR	Transport Costs
d_{daily}	km/d	Daily Driving Distance
ΔG	kJ	Activation Energy Barrier
$\Delta H_{\text{m, LHV}}$	MJ/mol	Lower Hydrogen Heating Value
Δv	m ³	Activation Barrier Volume Factor
$E_{\text{Infrastructure}}$	kWh/d	Specific, Daily Energy Supply (Infrastructure)
E_{Vehicle}	kWh/km	Specific Energy Consumption (Vehicle)
EII	10 ⁻¹⁵	Environmental Impact Index
F	A s/mol	Faraday Constant
F_a	N	Aerodynamic Drag Force

F_g	N	Gravitational (Climbing) Resistance
F_i	-	Pareto Front
F_m	N	Acceleration resistance
F_r	N	Rolling Resistance Force
$F(\mathbf{x})$	-	Objective Function
g	m/s ²	Gravitational Acceleration
$g(\mathbf{x})$	-	Unequality Constraint
G_p^*	-	Payload Ratio
GVW	t or kg	Gross Vehicle Weight
h	J s	Planck Constant
$h(\mathbf{x})$	-	Equality Constraint
i_{end}	A/m ²	Single Fuel Cell Current Density at end of Ohmic Region
$i_{\text{nom,cell}}$	A/cm ²	Fuel Cell Current Density (Single Cell)
I_0	A	Current at 0 V (Fuel Cell)
$I_{\text{avg.}}$	A	Average Electric Motor Current
I_{end}	A	Current at the End of Ohmic Region (Fuel Cell)
I_{max}	A	Maximum Current (Fuel Cell)
I_{nom}	A	Nominal Current (Fuel Cell)
IS	multiple	Impact Score (different units possible)
IR	%	Improvement Ration
k	J/K	Boltzmann Constant
λ_m	-	Rotational Inertia Factor
$m_{\text{payload, max}}$	kg	Maximum Payload
$m_{\text{veh., empty}}$	kg	Empty Vehicle Mass
n	1/s	Rotational speed
$\eta_{\text{Bat.}}$	%	Charging efficiency
η_{engine}	%	Engine Efficiency
$\eta_{\text{fuelcell, nom}}$	%	Nominal Fuel Cell Stack Efficiency
$\eta_{\text{Pan.}}$	%	Conductive Pantograph Efficiency
$\eta_{\text{veh.}}$	%	Efficiency
n_c	-	Normalization Factor
n_{new}	-	Total New Vehicle Registration

$n_{\text{new,cat.}}$	-	Annual New Vehicle Registration per Vehicle Category
n_{Vehicle}	-	Number of Vehicles
n_{years}	-	Number of Years
N	-	Number of Parallel Fuel Cells
p_{H_2}	Pa	Absolute Hydrogen Supply Pressure
$P_{\text{new,cat.}}$	-	Annual Share of New Vehicle Registration per Vehicle Category
$P_{\text{new,cat.,total}}$	-	Total Share of New Vehicle Registration per Vehicle Category
p_{O_2}	Pa	Absolute Air Supply Pressure
P	kW	Power
$P_{\text{nom., Stack}}$	kW	Nominal (Fuel Cell) Stack Power
P_t	-	Parent Generation (Optimization)
\mathcal{P}^*	-	Set of Pareto-Optimal Individuals
Q_t	-	Offspring Generation (Optimization)
Q_T	t km (t km/a)	(Annual) Transport Performance
ρ_a	kg/m ³	Air Density
R	J/kmol	Ideal Gas Constant
R_i	Ω	Inner Resistance
$R_{i, \text{cell}}$	Ω	Internal Fuel Cell Resistance
T	N m	Torque
T_{fuelcell}	K	Fuel Cell Operating Temperature
$u_{\text{nom,cell}}$	V	Nominal Fuel Cell Voltage (Single Cell)
U_0	V	Stack Voltage at 0 V (Fuel Cell)
U_1	V	Stack Voltage at 1 V (Fuel Cell)
U_{min}	V	Minimum Stack Voltage (Fuel Cell)
U_{nom}	V	Maximum Stack Voltage (Fuel Cell)
$U_{\text{nom., Stack}}$	V	Nominal (Fuel Cell) Stack Voltage
v	m/s	Velocity
w_c	-	Weighting Factor
x	-	Vector of Design Variables
z	-	Number of Moving Electrons

1 Introduction

“Our house is on fire” [1]. During her speech at the 2019 *World Economic Forum* in Davos, Greta Thunberg used these words to describe the progress and urgency of the climate crisis. In the year 2015, 189 out of 196 signing parties ratified the *Paris Climate Agreement* and, thus, committed to limiting the global temperature increase to a maximum of 2 °C and, if possible 1.5 °C, above pre-industrial levels [2]. Given the fact that, according to the Intergovernmental Panel on Climate Change (IPCC), the global (land and sea) temperature is already 1.4 °C above the reference, Thunberg might be right.

In *The Uninhabitable Earth: A Story of the Future*, David Wallace-Wells vividly not only describes the environmental but also the economic and social consequences of climate change [3]. Wallace-Wells draws an increasingly dystopic picture for each IPCC scenario, discussing multiple topics, such as rising sea levels, extreme heat, droughts, fires, and disease outbreaks. Although the book’s intention is not to provide solutions, Wallace-Wells [3, p. 198] calls for action to “nothing short of a complete overhaul of the world’s energy systems, transportation, infrastructure and industry and agriculture.” However, the question remains on *how* to live sustainably.

The term sustainability is first referenced in the context of forestry in the 18th century and, consequently, in the context of resource depletion [4]. In 1987, the report *Our Common Future*—also known as the *Brundtland Report*—defines sustainability as development “that [...] meets the needs of the present without compromising the ability of future generations to meet their own needs” [5, p. 16]. Additionally, the report established the three pillars of sustainability [5, p. 16]. Accordingly, sustainable development includes an environmental, economic, and social dimension. During the Earth Summit in 1992, all three were set as equal goals for global development [6]. These, as well as other, events that have been or will be considered important for global sustainable development, are summarized in Figure 1.1.

Although, both the *Brundtland Report* and the *Earth Summit* address a wide range of issues, they refrain from concretizing actions. To overcome this “abstract nature of sustainability” [7], the United Nations formulated 17 Sustainable Development Goals (SDGs) at their 2015 general assembly [8]. The SDGs laid the ground for multiple initiatives and standards that were discussed in a previous publication [7]. This review showed that economically and environmentally related SDGs are stronger represented in terms of disclosures and indicators, in particular in a non-governmental or business context [7]. For example, the SDG Business Disclosures include 139 indicators for SDG 8 (Decent Work and Economic Growth) and 57 for SDG 13 (Climate Action), while SDG 2 (Zero Hunger, 7 disclosures), SDG 4 (Quality Education, 9), SDG 10 (Reducing Inequalities, 9 disclosures), and SDG 11 (Sustainable Cities and Communities, 11 disclosures) are listed with the lowest number of disclosures. While this does not mean, that the economic and environmental pillars are more important, it hints at the complexity of their assessment that results in a large number of disclosures and indicators. Particularly, the assessment of environmental impacts is a complex issue, which is reflected in the existence of several, specialized initiatives and NGOs covering individual areas and/or SDGs from the field of ecology.

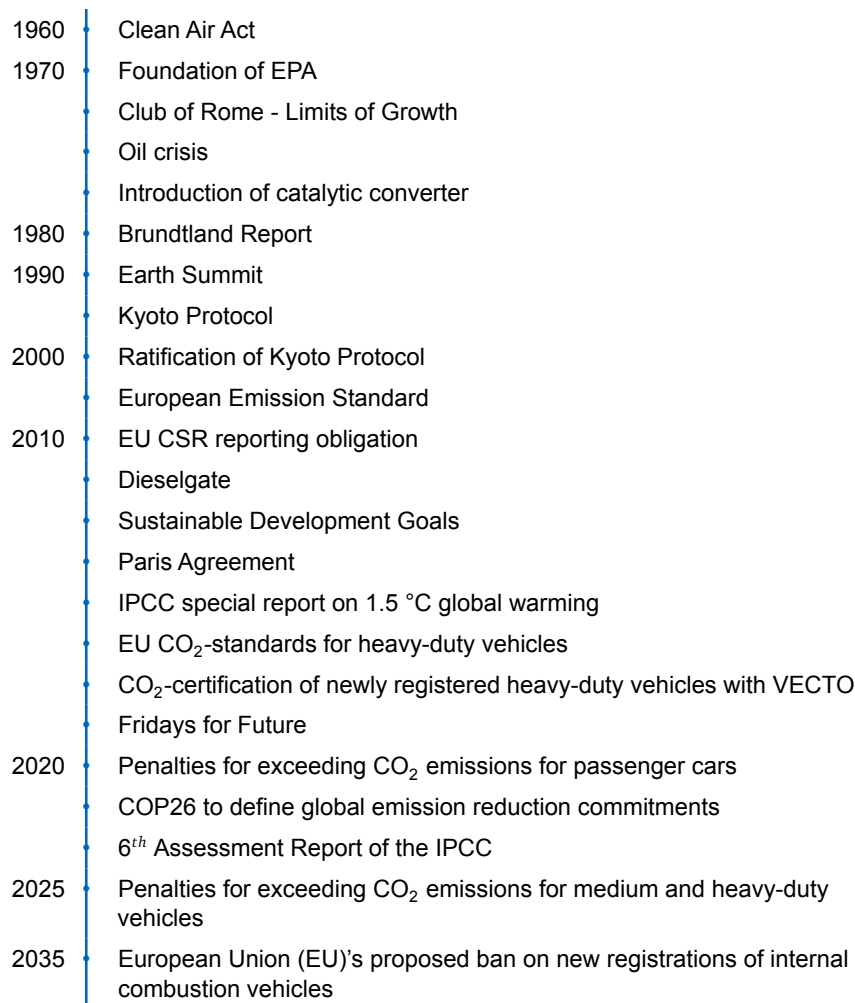


Figure 1.1: Important events that have been (or are expected to be) drivers for the development of sustainability in the automotive context [7]. [Note: EPA = Environmental Protection Agency; CSR = Corporate Social Responsibility; IPCC = Intergovernmental Panel on Climate Change; COP26 = 26th United Nations Climate Change Conference (“Conference Of the Parties”)]

1.1 Environmental Impact

The warnings from the IPCC give reason to believe that climate change is the most urgent environmental crisis to be solved [9]. While it is currently the most prominent, human-related environmental impact, it is neither the only one nor the first one to be discovered and discussed. For example, Figure 1.2 (marked as) shows that the global temperature anomaly—a measure of annual temperature increase compared to the period from 1951 to 1980—has tripled in the last 30 years alone [10, 11]. However, it is short-sighted to address environmental sustainability simply with a focus on the climate crisis, which is underlined by the complex inter-dependencies of climate change and sustainable development [12, p. 819f].

Corresponding to SDG 14 (Life Below Water) and SDG 15 (Life on Land), the loss of biodiversity provides another example of human-related environmental impact. Therefore, the International Union for Conservation of Nature (IUCN) regularly records how many animal species are threatened with extinction [13] and publishes their results, known as the *Red List*. The exponential increase of endangered species on the IUCN *Red List* from 11 046 in the year 2000 to 32 441 in 2020 illustrates (Figure 1.2), what is sometimes characterized as the earth’s sixth mass extinction [14].

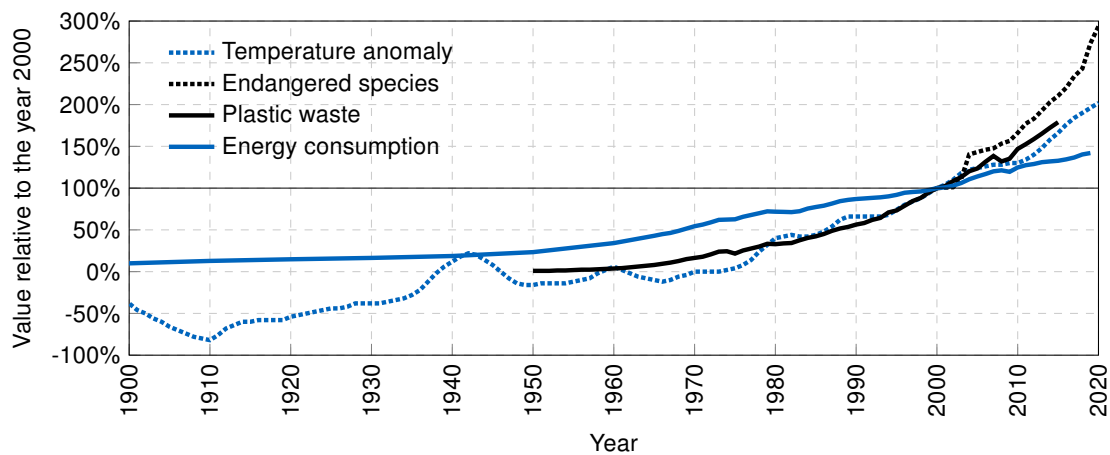


Figure 1.2: The examples of human-caused environmental damage within the Anthropocene show an exponential increase. All values are on a global scale and normalized to the year 2000. Global energy consumption includes all fossil and renewable energy sources [15–17]. The temperature anomaly describes the relative deviation of the global land and ocean temperature, compared to the average between 1951 and 1980. The increase after World War II is assumed to be caused by data discontinuity [10, 11]. Plastic waste correlates with global plastic production [18, 19]. Endangered species are those listed on the IUCN *Red List*.

The same trend can be seen in the increase of plastic waste (Figure 1.2 —). The production and consequently the amount of plastic waste increased from zero in the 1950s to more than 5000 Mt today and reaches 25 000 Mt until 2050 if the trend continues unchanged [19]. Yet plastic waste has not only negative effects on wildlife and biodiversity but also on human health [18]. Consequently, the reduction of plastic waste is embedded in SDG 12 (Responsible Production and Consumption).

Although far from complete, these examples illustrate that quantifying ecologic sustainability is a broad and complex topic, whereas global warming is one among many (possibly contradicting) problems. While the global energy consumption in Figure 1.2 (—) is not a direct environmental impact, its correlation with the previous examples hints at the relationship between human activities and ecological destruction. Furthermore, considering non-environmental aspects, such as energy consumption, shows the conflict between environmental impact and economic growth. For this, Belke et al. [20] showed that there is a strong, bidirectional relationship between energy consumption and economic growth. If “technological development brings economic growth” [21], the necessity to have tools evaluating the environmental impact of emerging technologies against their predecessors or seemingly similar alternatives becomes inevitable.

A common approach for such a technology impact assessment is a prospective life cycle assessment (LCA) [22, 23]. While a LCA covers environmental aspects of products and, thus, certain technologies, it lacks an economic dimension. The concept of eco-efficiency combines both, showing “ways of reducing their impact on the environment while continuing to grow and develop” [24]. The eco-efficiency assessment (Section 2.1), combining an economic (Section 2.1.1) and an ecological perspective (Section 2.1.2), is the starting point of this work. Beforehand, however, it must be clarified to what the concept is applied.

1.2 Road Transportation

The transport sector accounted for 19 % of global final energy consumption in 2015—the majority (99 %) provided by fossil fuels [25]. Khalili et al. [25] calculated that road transportation, including

passenger and freight, currently comprises approximately 75 % of the total transport energy demand. The remaining share is accounted for by rail, air, waterways, and marine transport. In the EU, the share of road transport is even higher, comprising 31 % of the final energy consumption in the year 2019—more than any other sector [26].

While energy demand directly correlates with greenhouse gas emissions, the combustion of fossil fuels leads to further emissions. Figure 1.3 compares selected road transport emissions to other modes of transportation. The European data from 2019 not only shows similar shares for emissions directly related to combustion (CO and NO_x) but also significant shares of non-exhaust emissions. These include fuel vapors (such as NMVOC) as well as brake and tire wear (primarily PM) [27]. While these emissions are used here for illustrative purposes only, they and their effects on humans and the environment are considered in detail in Section 2.1.2.

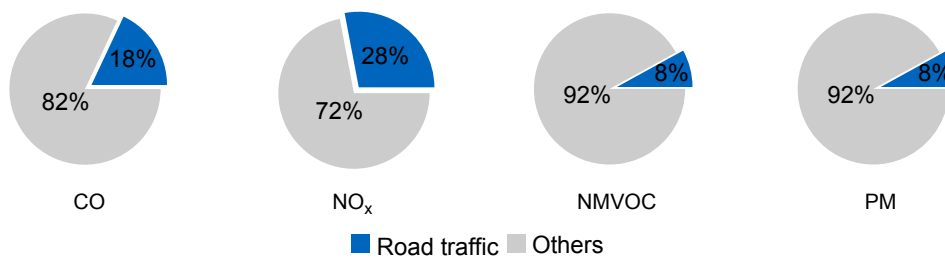


Figure 1.3: Emissions of selected air pollutants from road transport and other modes of transportation. The data shows European values for the year 2019. Road transportation includes exhaust as well as non-exhaust emission from fuel evaporation (NMVOC), and tire- and brake-wear (PM) [27].

The examples of energy demand and emissions caused by road transportation show that the automotive industry has long been related to environmental issues [7]. Beginning in the early 1960s, however, these issues became of public concern and led to the foundation of organizations, such as the Environmental Protection Agency (EPA). Eventually, emission standards were gradually introduced and tightened, which can be seen in Figure 1.1.

But it is not just the use phase of automotive products that leaves a global footprint: Upstream production and the associated consumption of resources further increase the industry's impact on people and the environment. Global automotive production, for example, is responsible for 12 % of global steel production [28] and even 26 % of aluminum production [29]—not yet including the current trend of battery electric mobility. The energy-intensive material processing and the environmental damage associated with any mining activity are, thus, a direct consequence of the industry and its products.

It becomes evident that the global automotive industry plays an important role not only in environmental impact but also in economic growth. The use of (fossil) energy, on-road emissions, and the production of technological products are highly intertwined with economic development, job creation, and innovation [30]. Consequently, the industry provides an important lever to reduce the global society's environmental footprint. At the same time, this transformation must be implemented economically to be successful. However, the industry's products and processes pose a complex challenge that cannot be solved by a one-fits-all solution. Therefore, road transportation is further categorized into passenger and freight transport. Both transport modes are facing equal challenges but require different solutions. The transformation of passenger cars is moving toward battery electric mobility because of both economic and environmental advantages over fossil fuels [31, 32]. However, driven by the introduction of European CO₂ reduction targets, road freight transport is just getting started [33]. The relevance of the road freight sector for sustainable development will be discussed in the following section.

1.3 Relevance of Low Emission Freight Transport

According to Khalili et al. [25], road freight transportation accounts for 25 % of the transport sector's final energy use in 2020. Similarly, the European Environmental Agency (EEA) stated that in 2017 27 % of the European greenhouse-gas emission came from transportation [34]. More than two-thirds of these emissions came from heavy-duty vehicles, comprising 5 % of the total European greenhouse gas emissions. This shows that heavy-duty vehicles alone provide a lever to reduce energy consumption and, thus, emissions and, ultimately, environmental impact, as discussed in a previous publication [35].

Low energy consumption is a key requirement for commercial vehicles. With fuel costs constituting approximately one-third of a heavy-duty vehicle's total cost of ownership (TCO), original equipment manufacturers (OEMs) have always made efforts to reduce the vehicles' fuel consumption. In the report of the German Federal Environmental Agency (Ger.: Umweltbundesamt), the average truck's energy consumption (including upstream processes) is 26 % lower compared to 1991-levels (Figure 1.4) [36]. This corresponds to an average reduction of 1.25 %/a, and is comparable with the average reduction of 1.1 %/a, reported by the European Automobile Manufacturers' Association (ACEA) [37].

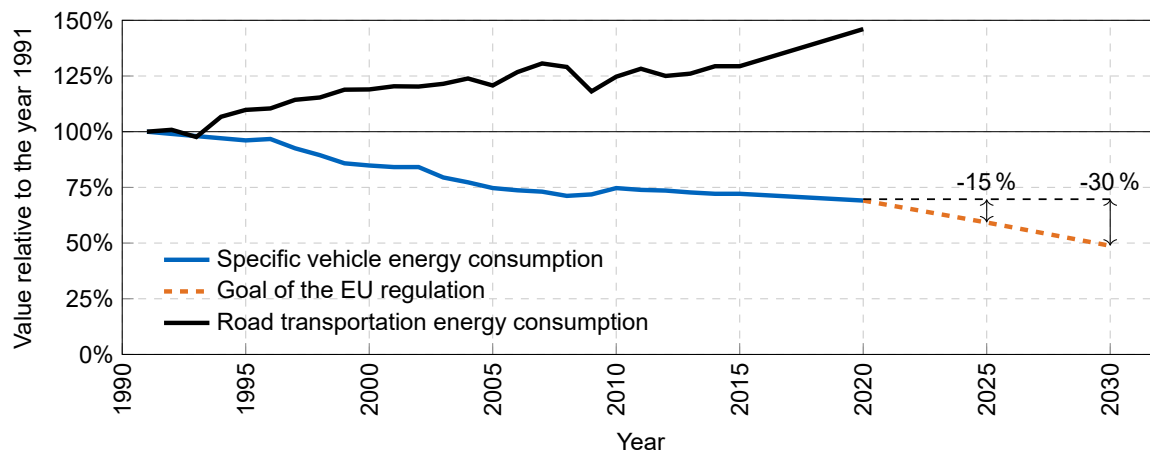


Figure 1.4: The historic development shows that since 1990 the road transport's total energy consumption increased, despite reduced vehicle consumption [36]. As a consequence, the EU agreed on CO₂ reduction goals of 15 % and 30 %, which have to be met by 2025 and 2030, respectively.

However, it is not only the challenge of reducing vehicle energy consumption that must be solved. Regarding economic development, the freight transport sector is connected in three ways: producing, using vehicles, and increasing economic growth by enabling road transportation. For instance, 64 % of the European freight is handled on road; more than half (57 %) over distances longer than 300 km [35, 38]. With constant economic growth—the European gross domestic product (GDP) increased on average by 1.8 %/a during the last 50 years [39]—transport performance also increases. This growth overcompensated for the reduction in specific vehicle consumption, which resulted in an overall increase of road transport energy consumption. Figure 1.4 visualizes this so-called rebound effect.

As a consequence, the EU introduced mandatory reduction targets for medium and heavy-duty vehicles [40]. European OEMs must reduce their average fleet consumption by 15 % until 2025 and 30 % until 2030 compared to the reference period from 2019 and 2021. For the average OEM, this requires an energy consumption reduction of 2.7 % to 3.8 %, tripling the historic development [41]. Furthermore, non-compliance is subject to penalties analogous to the passenger car regulation putting truck OEMs under severe pressure to develop and introduce new technologies.

In conclusion, this chapter showed the relevance of considering not only climate change but also further environmental impacts to achieve the goal of sustainable development. With its significant environmental footprint, the automotive industry plays an important role in achieving this goal. Considering the steadily growing demand for transportation and the reliance of the (European) economy on road transportation, it becomes evident that finding an equally environmentally and economically beneficial—or eco-efficient—solution requires new technologies.

Therefore, the following chapters summarize the basics of eco-efficiency (Section 2.1). Section 2.1.1 and Section 2.1.2 present current assessment methods for the economic and the ecologic dimension, respectively. The latter gives a detailed explanation on the measurement, normalization and weighting of environmental impacts, as required for a LCA. Being a comparative method, a LCA requires alternatives that are compared against each other. After summarizing the general requirements of heavy-duty vehicles (Section 2.2), Section 2.3 and 2.4 review existing vehicle assessment models as well as results from the literature. Additionally, the technical basics for the assessed vehicle technologies are summarized. Having shown the shortcomings of the state of science in Section 2.5, two research questions are derived.

To answer these research questions, Chapter 3 defines and justifies the methodological boundary conditions and the framework. Chapter 4 describes the eco-efficiency methodology combining life cycle costing and life cycle assessment (Section 4.1 and 4.2) followed by a description of the underlying vehicle simulation models (Section 4.3). In this context, the consideration of infrastructure as an essential component of freight transport is also integrated. To account for the technological potential of each vehicle technology, an evolutionary algorithm optimizes their design parameters, which is described in Chapter 5. The models are furthermore validated against existing data (Section 6.1) and the obtained results are subjected to uncertainty quantification (Section 6.2).

Based on the optimization results (Chapter 7), Section 7.4 shows the eco-efficiency potential for the vehicle technologies, providing recommendations to various decision makers. Additionally, Section 7.5 estimates the vehicles' system cost until 2030. Chapter 8 discusses the contribution of this work from a scientific, technological and societal point of view. A survey among different stakeholders Section 8.1 tests the underlying assumptions of using the eco-efficiency assessment for evaluating the transition towards zero-emission vehicles. The work finishes with a summary of the results and gives an outlook for further research (Chapter 9).

2 State of Science

The previous section showed the demand for a green transformation of the road transportation sector. The urgency is illustrated by the introduced CO₂-targets for the next decade. To achieve this transformation in an ecologically and also economically beneficial, the comparison of alternatives is a decisive factor in decision-making. This chapter will introduce the concept of eco-efficiency as a method for precisely this comparison. The second part of this chapter discusses the alternatives competing for technology leadership in the next decade and beyond. Therefore, based on current literature, the economic and ecologic potential of several vehicle concepts is shown and existing assessment models and their respective shortcomings are summarized.

2.1 The Concept of Eco-Efficiency

The concept of eco-efficiency emerged during the 1990s and was first mentioned by the World Business Council on Sustainable Development (WBCSD) as a framework that “brings together the essential ingredients—economic and environmental progress—which are necessary for economic prosperity to increase with more efficient use of resources and lower emissions” [24, p. 2]. Because the WBCSD is rooted in the *Earth Summit*, it is not surprising that eco-efficiency was created as part of sustainability assessment. Combining economic and ecologic performance as given in Equation (2.1), the concept allows reporting and progress tracking for products, geographic regions or processes [24, 42].

$$\text{Eco-Efficiency} = \frac{\text{Economic value}}{\text{Environmental impact}} \quad (2.1)$$

While this equation clearly shows the basic concept, its concrete application remains vague. As a result, the chemical group *BASF* published their approach of an eco-efficiency assessment in 2002, which became known as the *BASF Method* [43]. Figure 2.1 shows the initial method, as implemented in DIN EN ISO 14045 [43, 44]. Saling et al. [43] created a framework that combines a LCA with normalization and weighting to quantify the environmental impact. In conjunction with the LCA, a customer-oriented cost assessment represents the economic value. Subsequently, in 2021 the DIN EN ISO 14045 [44] published guidelines for an eco-efficiency assessment based on the *BASF-Method* [45].

Since then, eco-efficiency has been applied to different levels and disciplines. For example, Mickwitz et al. [46] assessed eco-efficiency on a regional level. Their case study on the Finnish region *Kymenlaakso*—located close to Helsinki—highlighted the temporal changes of the region regarding economic and ecologic indicators. They concluded that the tool facilitates (political) decision-making, although not being a guarantor for sustainable development. Comparing the eco-efficiency of 30 Chinese cities, Yin et al. [47] support this conclusion. Furthermore, they emphasized the difficulty of interpreting the

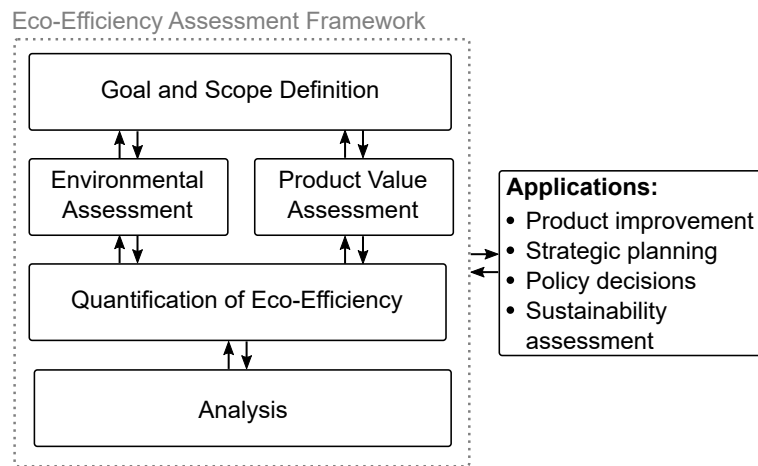


Figure 2.1: The process stages of an efficiency assessment according to the DIN EN ISO 14045 [44].

results, if the numerator and denominator of Equation (2.1) are coupled: “The higher the GDP of a city is, the higher its eco-efficiency but the higher its environmental pollutant emission” [47].

Onat et al. [48] performed a product-related approach analyzing the regionalized eco-efficiency of the introduction of battery electric passenger vehicles. Despite only including tank-to-wheel emissions and neglecting alternatives to battery electric vehicles, their approach can be used to derive policy and investment strategies. Focusing on the product level, Philippot et al. [49] analyzed the eco-efficiency of lithium-ion battery production. By comparing greenhouse gas emissions and battery pack costs, they not only estimated the eco-efficiency for different manufacturing countries but also the improvement associated with progressing manufacturing technology. Their research, thus, provides insights into the development of lithium-ion batteries and the improvement of eco-efficiency by technological advancement.

These examples demonstrate the real-world application of eco-efficiency. They are part of a trend of increasing research on eco-efficiency over the last 20 years [50]. However, John et al. [50] state that much of the research originates in academia and has little or no connection to industry or policy. Furthermore, eco-efficiency is mainly used in so-called developed parts of the world.

Huppés and Ishikawa [42, p. 31] state that the availability of data and technology is a common issue for eco-efficiency implementation. Additionally, the interpretation of the results and derivation of guidelines, policies, and decisions often requires expert knowledge, which further limits the wide application. Combined with the generic nature of the WBCSD definition, different approaches and thus interpretations of eco-efficiency as an indicator emerged [51].

In an earlier work, Huppés and Ishikawa [51] distinguished two types and their respective inverse of eco-efficiency:

- Environmental productivity and its inverse environmental intensity
- Environmental improvement cost and its inverse environmental cost-effectiveness

This formalization allows the categorization of an eco-efficiency assessment and is, therefore, a boundary condition for (in)comparability of results. Furthermore, Huppés and Ishikawa [51] discuss the methodological shortcomings of Equation (2.1) that Yin et al. [47] encountered: In addition to the simultaneous increase of both equation elements leading to an unchanged overall score, the choice of reference also plays a role. Depending on the reference, either the denominator, the numerator or both could experience a sign change (e.g., an alternative has lower costs than the reference) and

complicate the interpretation of the results. This highlights the importance of transparently selecting the indicators for economic and ecologic assessment, which will be part of Section 2.1.1 and 2.1.2. In the same way, the reference choice is crucial, which is why Section 2.2 gives a technological overview of current and future heavy-duty vehicle technologies.

2.1.1 Economic Dimension

According to the DIN ISO 14045, “monetary value may be expressed in terms of costs, price, willingness to pay, added value, profit, future investment, etc.” [44, p. 18]. Being more precise, Saling et al. [43] state that the TCO adequately represents the economic dimension from a customer’s point of view. For the transport sector, the TCO is the central element and a common choice for economic assessment [52, p. 19]. Although a large number of other economic parameters (e.g., GDP) can be used in the context of eco-efficiency [46–48], they are not described here because they are not related to a product such as a commercial vehicle.

Commercial vehicle TCO typically cover four cost categories [52, p. 74]:

- Variable
- Fixed
- Personnel
- Overhead

As part of the fixed costs and in the context of new technologies, vehicle acquisition costs are of special interest. Because they are difficult to determine, especially when production-ready vehicles are not yet available, Fries [53, p. 60-62] has developed a component-based manufacturing cost model. On the one hand, by splitting the model into components, it can represent different vehicle concepts, which can be used for vehicle concept optimization as presented in previous publications [54, 55]. On the other hand, changes in costs resulting from technological progress or new energy carriers, for example, can be easily included. For a detailed description of the remaining (cost)categories, please refer to chapter four in Wittenbrink’s *Transportmanagement* [52, p. 73-100] and the previously published life cycle costing methodology [56].

Without a reference, the TCO does not represent an economic value in the sense of the WBCSD definition. Therefore, Equation (2.2) introduces the difference ΔTCO between a reference $\text{TCO}_{ref.}$ and the alternative TCO_i to be assessed. The reference’s eco-efficiency is zero, per definition. Thus, the eco-efficiency improves if the alternative’s costs or its environmental impact decrease. This reasoning for the use of Equation (2.2) instead of the single TCO is previously published [56]. Consequently, this definition categorizes as environmental productivity [51] and the obtained scores are interpreted as “higher is better.”

$$\text{Economic value} := \Delta\text{TCO} = \text{TCO}_{ref.} - \text{TCO}_i. \quad (2.2)$$

2.1.2 Ecological Dimension

In their description of the *BASF Method*, Saling et al. [43] introduced a life cycle assessment to quantify the ecological dimension of eco-efficiency. In their 2020 review of the method, Grosse-Sommer et al. [57] suggested that the relevance and appropriateness of the impact categories, concerning the studied system, must be checked carefully. However, Grosse-Sommer et al. [57] still rely on the DIN EN ISO 14040 and 14044, which define the process and the requirements of carrying out a LCA but neither

the impact categories nor the system boundary to be used [58, 59]. Because of this, Grosse-Sommer et al. [57] defined the life cycle perspective, starting from raw material extraction, energy use, and end-of-life treatment, to be used in an eco-efficiency assessment. While the WBCSD did not originally intend this perspective, it provides a more holistic assessment. Nevertheless, the choice and definition of the system boundary remain an important aspect of any ecological assessment [60, p. 61f].

The DIN ISO 14040 [58] describes the general approach to carrying out an LCA, which is visualized in Figure 2.2. The four stages are mandatory to ensure the quality of a LCA and, thus, its results. Therefore this section describes the stages based on this norm with a special focus on the different impact categories.

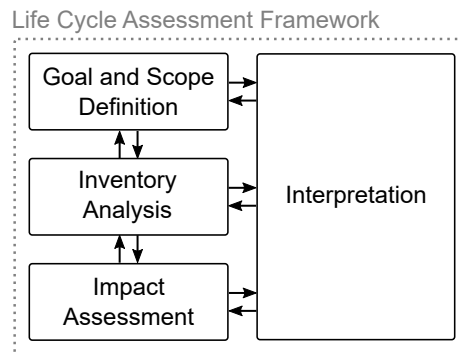


Figure 2.2: The four stages of a life cycle assessment according to the DIN EN ISO 14040 [58].

The first mandatory step of a LCA is the goal and scope definition. Besides the description of the intended application and audience, the goal and scope definition requires the definition of the studied systems, the impact categories, and the functional unit.

Special attention is, hereby, given to the functional unit, which provides the reference for the derived performance characteristics. All subsequent results refer to the functional unit. For example, the resulting global warming potential is given in kilogram CO₂ equivalent *per functional unit*. A typical functional unit in an automotive context is the number of kilometers during the vehicle lifetime or the derived *per kilometer* [61, p. 38, 62]. For commercial vehicles, either one vehicle with a specified lifetime [63] or tonne-kilometers per vehicle lifetime are typical functional units [64].

The selection of impact categories and associated indicators is part of the scope definition [60, p. 61]. Impact categories are further divided into midpoint and endpoint indicators [60, p. 25, 65, p. 2]. Although both describe environmental impacts, their interpretation differs largely. The former refers to an amount of an indicator without quantifying the consequence of this indicator. For example, global warming potential measured in kg CO₂-eq. does not describe climate change, being the consequence of an increase in greenhouse gas emissions. The temperature increase due to global warming potential would be attributed to an endpoint indicator, such as *ecosystem health*.

As Huppel et al. [66] pointed out, the use of endpoint indicators is subject to greater uncertainty than midpoint indicators. Although sets for endpoint indicators (e.g., ReCiPe2016 model [67]) exist, they concluded that there is less consensus on endpoint indicators; standardization is non-existent. Consequently, they are excluded from this work. On midpoint level, however, the International Reference Life Cycle Data (ILCD), under the coordination of the European Commission (EC) Joint Research Center (JRC), recommended a set of impact categories [68], which will be described in the next sections:

- Global warming potential (GWP)
- Acidification potential (AP)
- Ozone depletion potential (ODP)
- Photochemical ozone creation potential (POCP)
- Cancerous and non-cancerous human toxicity
- Ecotoxicity
- Particulate matter (PM)
- Ionizing radiation (IR)
- Freshwater, marine and terrestrial eutrophication potential (EP)
- Water, mineral, and fossil resource depletion (WD, RD, FD)

Global Warming Potential

Global warming potential is the most prominent example of environmental impact categories. It describes the effect of greenhouse gases absorbing radiation in the lower and upper atmosphere. This greenhouse gas effect is one of the key mechanisms of global warming [9]. Besides the well-known carbon dioxide (CO₂), several other emissions contribute to the greenhouse gas effect and are regulated in the Kyoto protocol [69]. Carbon-monoxide (CO), methane (CH₄), nitrous oxide (N₂O), fluorinated hydrocarbons, and chlorofluorocarbons are further gasses with similar atmospheric effects. However, the gases' different residence times and effectiveness require a normalization that is usually a conversion to carbon-dioxide-equivalent (kg CO₂-eq.) and frequently updated due to new scientific evidence. For example, the GWP of methane, as determined by the IPCC, increased from 21 kg CO₂-eq. in 2007 [70, p. 212] to 28 kg CO₂-eq. in 2014. It should be noted that methane's GWP depends on the observation period. The mentioned values from the Kyoto protocol assume 100 years. If the period is set to 20 years, the GWP increases to approximately 80 kg CO₂-eq. [71, p. 87]. The Greenhouse Gas Protocol provides a summary of further GWPs [72].

Acidification Potential

Acidification occurs when substances release protons into the ecosystem, causing a decline in the ecosystem's acid-neutralizing capacity (i.e., neutralizing hydrogen ions) [60, p. 215]. This local effect causes limited growth of terrestrial eco-systems and in severe cases, even die-back of forests and other plants, which could be observed especially in Central Europe and Scandinavia in the 1990s [73, p. 113]. When anions enter aquatic ecosystems, they cause the extinction of wildlife. However, acidification also has an effect on buildings and metallic surfaces, which resulted in significant damage in Europe and North America in the 1980s and 1990s [60, p. 214]. Since nitrogen oxides (NO_x)—in addition to ammonia (NH₃) and sulfur dioxide (SO_x)—contribute to acidification, they were strictly regulated. Eventually, this led to the introduction of catalytic converters [74, 75]. In LCA, moles of charge in *mol H⁺-eq.* quantify acidification potential [76].

Ozone Depletion Potential

Stratospheric (i.e., above 15 km from the Earth's surface) ozone protects life on earth from ultraviolet radiation [77]. On the one hand, ozone depletion describes the general decrease of stratospheric ozone, and, on the other hand, locally low concentrations, also known as ozone holes. The appearance of the largest ozone hole over Antarctica in the 1970s, primarily due to chlorofluorocarbon emissions, led to strict regulations and, as a consequence, to a steady reduction of the ozone hole [60, p. 209]. NASA reported the smallest extension of the antarctic ozone hole in the year 2019 [78]. Apart from crop

and plankton damage, low stratospheric ozone concentration causes skin cancer and eye cataracts [79, p. 152]. ODP is commonly measured as equivalent to the refrigerant Trichlorofluoromethane (CFC_3) in *kg CFC-11-eq.* [60, p. 213].

Photochemical Ozone Creation Potential

While the concentration of ozone in the stratosphere is essential for protecting life on earth, the presence of ozone in the troposphere—the lowest Earth's atmosphere [77]—causes severe health damage and impacts on vegetation. Ozone as well as other oxygen compounds are highly reactive, oxidizing organic surfaces. Thus, they can cause damage to respiratory organs and plant surfaces [60, p. 225]. The main precursors of ozone are nitrous oxides and non-methane volatile organic compounds that form ozone (O_3) under the influence of ultraviolet radiation [60, p. 225]. While ozone is an invisible gas, its precursors can cause localized fog-like clouds, also known as summer smog [80]. They are primarily caused by road transportation [60, p. 228]. However, with the introduction of catalytic converters [74, 75], NO_x emissions and, consequently, ozone concentration dropped [81]. In LCA, POCP is usually measured in *kg NMVOC-eq.* [82].

Human- and Eco-Toxicity

Due to a large amount of toxic substances, measuring their impact on the environment is challenging. Therefore, the United Nations Environment Program (UNEP) established a task force in 2005 to develop a comprehensive model for the toxicity of substances [83]. The *USEtox* model includes more than 3000 substances and quantifies their effect on ecosystems and human health [60, 83, p. 805]. Relevant sources for toxic substances are transportation, energy production, and industrial production [73, p. 146]. Although eco-toxicity is one of the most critically discussed impact categories, the UNEP, among the European Commission and the US EPA, recommends the *USEtox*-model [60, p. 236].

To cover the toxic impact on ecosystems, the model converts the substances to comparative toxic unit (eco-system) (CTUe). The indicator describes the estimated proportion of affected species integrated over time and volume per emitted kilogram of a chemical [83]. Although there is obviously damage to other eco-system, *USEtox* only addresses freshwater ecosystems and neglects maritime and terrestrial systems [68, p. 82].

Analogously, human toxicity describes the toxicological effects of biological and chemical substances on humans. Usually, the assessment distinguishes between carcinogenic and non-carcinogenic effects [60, p. 240]. The direct incorporation of the substances into nature as well as the ingestion via air and food are taken into account [60, p. 238]. The indicator comparative toxic unit (health) follows the same logic as CTUe and describes the estimated increase in morbidity of the entire population per kilogram of a chemical emitted [83].

Particulate Matter and Respiratory Inorganics

This indicator summarizes aerosols, causing damage to human health. These aerosols result directly from fine PM emissions (primary), but also chemical reactions with precursors (secondary) such as NO_x , NH_3 , and SO_x . Primary and secondary PM emissions cause damage to respiratory organs, which is why respiratory inorganics are used as a synonym. The smaller $\text{PM}_{2.5}$ emissions are even respirable. Major PM sources include road transportation, power plants, agriculture, and solid fuels (e.g., firewood) [60, p. 241f]. Although not commonly addressed in LCA studies [84], PM “is considered to be one of

the most important [...] global human disease burden[s]” [85, p. 2]. At the midpoint level, the indicator is measured in $kg\ PM_{2.5}\text{-eq.}$, while Fantke et al. [85] developed a model, directly measuring human disease incidents at the endpoint level, whereby the smaller, respirable $PM_{2.5}$ emissions contribute more than PM_{10} .

Ionizing Radiation

The radioactive decay of certain radioactive elements causes ionizing radiation (IR) in the form of gamma-rays. Because gamma rays carry high amounts of energy, they can remove electrons from the outer atom orbital. If exposed to this radiation, living organisms can suffer severe damage to the atoms of DNA and, thus, changes in the genetic code, eventually developing cancer [86, 87]. Man-made sources of radiation are—apart from nuclear power plants—mining activities for phosphate rock or coal extraction, and extraction of fossil oil and gas resources. Besides direct exposure due to airborne radionuclide emissions, ingestion of irrigated plants or animals, or inhalation of radioactive particles causes internal exposure to IR [86]. At the midpoint level, IR is measured in units of radioactive decay equivalent to the isotope Uranium 235 ($kBq^{235}\ U\text{-eq.}$). Although it can cause severe damage to living organisms, IR is seldomly discussed in LCA studies [84].

Aquatic and Terrestrial Eutrophication

Eutrophication describes the excessive release of nutrients into the ecosystem and is commonly divided into aquatic (freshwater and marine) and terrestrial. Large amounts of nutrients, such as nitrogen and phosphor, result in oxygen-intense algae growth that eventually causes hypoxic lakes, rivers or seas. This low oxygen saturation causes a decrease in water quality and ultimately the death of flora and fauna [88]. That is why in the 1970s there was talk of the “slow suffocation of lakes” [60, p. 219]. While the damage was concentrated in coastal areas, lakes, and rivers in the 1970s and 1980s, the effects now also become present in continental seas, such as the Baltic sea, the East China Sea or the Gulf of Mexico [88]. Agriculture and the associated use of fertilizers are considered one of the main sources of phosphor and nitrogen, among fuel combustion and municipal sewage [88, 89].

While the input of fertilizers into water bodies predominantly causes aquatic eutrophication, dispersal via the air also affects terrestrial systems. Agriculture is also the main polluter here, even though the industry is directly affected by reduced yields of crops due to eutrophication. Although the EEA reported decreasing nitrogen concentrations in the European soil between 2000 and 2010, the agency lists terrestrial eutrophication as a priority objective “to protect, conserve and enhance the Union’s natural capital” [89, p. 5].

The ILCD measures EP in phosphor or nitrogen equivalents. The unit $kg\ P\text{-eq.}$ or $mol\ P\text{-eq.}$ is used for freshwater and terrestrial eutrophication, respectively. Over this, marine eutrophication is measured in $kg\ N\text{-eq.}$, taking the prevailing mechanism in each case into account [82, p. 16].

Fossil and Mineral Resource Depletion

Resource depletion (RD) or fossil resource depletion (FD) is a measure of resource scarcity in particular concerning future generations [90]. The models distinguish between fossil and abiotic or mineral resource consumption depending on the extracted elements. In contrast to the other impact categories, resource depletion has no direct effect on ecosystems [60, p. 259] but can be regarded as a “recognizable value for society” [91]. It is, therefore, desirable to limit the use and, thus, the loss

of resources. Hauschild et al. [60, p. 259] distinguish consumptive and dispersive use: On the hand, the former describes the conversion of a resource to an unusable form. An example is the conversion of fossil fuels into carbon dioxide and water. On the other hand, dispersive resource use does not lose the resource per se but converts it into a less accessible form. Many metals fall into this category. “However, it is arguable whether resource availability is an environmental or economic issue and whether this should be subject to characterization models” [90].

Water Use

The global water cycle is closed, which is why water—as a renewable resource—does not deplete in the same way as fossil and mineral resources do. Due to precipitation and subsequent evaporation, approximately two-thirds of the global water are not accessible for human use. Only 3 % of the remaining amount is currently used by humanity, dominantly in agriculture (2.1 %) [60, p.251]. This means that water is sufficiently available on a global scale [60, p. 251]. Because water availability greatly varies geographically and seasonally, causing local water scarcity and complicating its assessment [92].

The example of lithium mining illustrates the difficulties of addressing environmental issues associated with water depletion (WD). As a key resource for automotive battery production, the demand for lithium strongly increased during the last decade [93, 94]. The application of lithium-ion batteries currently focuses on industrialized nations [94–96] of which most have a low or moderate water scarcity [92]. While this fosters the transition to renewable energy and, consequently, mitigates climate change in certain regions (e.g., USA, EU, China), mining activities cause water depletion or pollution in other regions. For example, about one-third of global lithium comes from the Atacama Desert, which has one of the world’s highest water scarcity ratings [95].

Common LCA approaches assess WD by the absolute water consumption in m³ or a water scarcity indicator as a fraction of consumption and availability [60, p. 251, 97, p. 156]. Frischknecht et al. [97], therefore, differentiate between six different scarcity levels: low, moderate, medium, high, very high and extreme. However, Schomberg et al. [95] argue that current LCA approaches lack the capability to fully account for regionalization. Consequently, supply chains, such as those of lithium-ion batteries, are not adequately represented. It becomes evident that there is still a missing consensus on the assessment of WD in LCA in the scientific community, despite the high importance of the impact category [60, p. 256, 92, 95].

Land Use

In LCA, land use describes anthropogenic actions that change the natural soil area in a specific region. Examples of land use or land cover are agriculture, infrastructure or open-pit mining [60, p. 245]. Environmental impacts include climate change, loss of biodiversity, and soil erosion [60, p. 248]. On the one hand, double accounting of environmental impacts must be avoided. Because direct emissions to the soil are covered by other categories (e.g., EP or eco-toxicity), they are not covered by land use. On the other hand, the severe and far-reaching direct effects of land use are hard to determine and still not well understood. For example, the loss of biodiversity due to the clearing of rainforests has many different, interrelated reasons: machine use, deforestation, and pesticides to name a few. It is impossible to know how much a single reason contributes to the overall biodiversity loss [60, p. 251]. Furthermore, the ecological consequences depend on the region. The severity of deforestation in Europe, for example, has a smaller impact on species loss than the same amount of deforestation in the Brazilian rainforest [60, p. 247f]. Frischknecht et al. [97, p. 149f] proposed a model to measure land

use as the annual conversion of land in km²/a. However, this is no direct measure of environmental impact and as data is scarce, further research is required to comprehensively include land use in LCA [98]. For this reason, data on land use is not included in the 2017 database version available for this research and is consequently excluded from this study.

Other Impact Categories

Apart from the impact categories included in the ILCD system, a variety of other impact categories exist. The JRC [68, p. 101] lists seven further categories that are excluded from their recommendations due to at least one of three reasons:

- No inventory data available.
- No characterization factor (i.e., model) available.
- No consensus on the characterization.

Among the categories are noise, accidents (e.g., oil spills or chemical accidents), and erosion [68, p. 101-105]. However, their exclusion from the ILCD recommendation does not reduce their potential severity, and they should be included depending on the goal of the study, as Guineé argues [99].

Inventory Analysis

After finishing the goal and scope definition, the product or system-specific data must be collected [60, p. 61, 58, p. 26]. The inventory analysis describes all relevant processes and material flows associated with the studied product system. This complexity often results in the use of generic data from databases [60, p. 61]. The result of the inventory analysis is a life cycle inventory (LCI), which quantifies all physical elementary flows (materials, energy, emissions) necessary to yield the functional unit. For heavy-duty vehicles, this step was performed in a previous publication [100], which is summarized in Section 4.2.1.

2.1.3 Impact Assessment and Interpretation

The impact assessment and subsequent interpretation are the final steps of a LCA. Both steps require a model of all relevant processes and material flows that were defined during the goal and scope definition and the inventory analysis. Typically a LCA software is used for building this model. In this model, the relevant elementary flows of the product system are reproduced and their corresponding characterizations are mapped with regard to the impact categories and the respective impact scores *IS* [60, p. 63]. The model that forms the basis of this thesis is described in Section 4.2. Although being an optional aspect of a LCA, the normalization and weighting of impact categories is an essential aspect of an eco-efficiency assessment [43, 44]. Therefore, their theoretical foundations are explained in the following.

Normalization of Environmental Impacts

Normalization places the environmental impact obtained in both a geographic and temporal reference [101, p. 12]. Saling et al. [43] used a comparative normalization approach, where the least favorable (technical) alternative was awarded a value of 7, while 1 was the most favorable. In 2017, Pizzol et al. [102] surveyed 216 LCA practitioners, showing that enhanced communication is the most common motive for using both, normalization and weighting, which corresponds well to the idea of the *BASF*

Method [43]. However, they point out that these two steps increase perceived uncertainty, which is why further research is required to enhance these methods.

For this, the EC JRC coordinated European research to develop a harmonized methodology to be used at the European level for interpreting LCA results and ultimately for improving decision-making [101]. As a result, Sala et al. [82] presented a comprehensive set of normalization factors n_c , after reviewing and rating existing approaches regarding their completeness, consistency, and robustness.

Their findings were further refined [82, 103, 104] and the obtained normalization factors (NFs) are shown in Table 2.1. As part of this process, Sala et al. [82, p. 26] put the obtained normalization factors into relation to planetary boundaries, which estimate the threshold for irreversible environmental consequences for each ILCD impact category. They concluded that global normalization factors are more robust and transparent than regional ones (e.g., Europe or per-person) [82, p. 71], which are, thus, not part of this study. The global NFs presented in the 2018 JRC report to the EC represent the most up-to-date set and are, therefore, considered for the presented approach [104]. Additionally, the characterization factor for PM changed from $kg PM_{2.5-eq.}$ to *disease incidents*. Because the latter was not available in the LCA software, the older NF had to be used to provide consistent results [82].

Table 2.1: The set of normalization factors presented by the JRC considers the impact categories recommended by the ILCD. The reference year for all shown regions is 2010. Except for PM, all factors are from the 2018 report representing the most recent version [104]. The values for PM are from the 2016 version [82] to sustain consistency with the LCA software, because the characterization changed from $kg PM_{2.5-eq.}$ to *disease incidents*.

Impact Category	Unit	Global	Europe	Person (EU)
GWP	kg CO ₂ -eq.	5.35×10^{13}	4.60×10^{12}	9.22×10^3
AP	mol H ⁺ -eq.	3.83×10^{11}	2.36×10^{10}	4.30×10^1
Ecotoxicity	CTUe	8.15×10^{13}	4.46×10^{12}	8.94×10^3
EP freshwater	kg P-eq.	5.06×10^9	8.44×10^9	1.69×10^1
EP marine	kg N-eq.	1.95×10^{11}	7.41×10^8	1.48
EP terrestrial	mol N-eq.	1.22×10^{12}	8.76×10^{10}	1.76×10^2
Human toxicity, cancer	CTUh	2.66×10^5	1.88×10^4	3.77×10^{-5}
Human toxicity, non-cancer	CTUh	3.27×10^6	2.69×10^5	5.39×10^{-4}
IR	kBq ²³⁵ U-eq.	2.04×10^{12}	5.64×10^{11}	1.13×10^3
ODP	kg CFC-11-eq.	1.61×10^8	1.08×10^7	2.16×10^{-2}
PM	kg PM _{2.5} -eq.	6.86×10^{10}	1.90×10^9	3.80
POCP	kg NMVOC-eq.	2.80×10^{11}	1.58×10^{10}	3.17×10^1
WD	m ³ water-eq.	7.91×10^{13}	4.06×10^{10}	8.14×10^1
RD, mineral	kg Sb-eq.	3.99×10^8	5.03×10^7	1.01×10^{-1}
RD, fossil	MJ	4.50×10^{14}	n.a.	n.a.
Land use	pt	1.98×10^{16}	3.78×10^{13}	7.58×10^4

Weighting of Environmental Impacts

In their original approach, Saling et al. [43] used the weighting to “develop[ed] a method whereby the ecological parameters are combined and ultimately plotted as a single point in a coordinate system.” Consequently, they applied a weighting scheme to obtain a single score. While their description remained vague, this topic was also discussed in several JRC reports [65, 82, 104] and accompanying research [102, 103, 105].

Weighting reflects the relative importance of an impact category and requires prior normalization [60, p. 192]. In the following, the resulting single score as given by Equation (2.3) is called Environmental Impact Index (EII):

$$\text{Environmental Impact Index} := \text{EII} = \sum_c w_c \frac{IS_c}{n_c}, \quad \forall c \in [1, \text{Impact Categories}]. \quad (2.3)$$

While the equation remains equal for different weighting approaches, the determination of the weighting factors w_c differs. In their review, Pizzol et al. [102] identified three (scientific) options for obtaining weighting factors:

- Distance-to-target
- Panel weighting
- Monetization

A distance-to-target approach ranks the impact categories according to their distance to either a policy or planetary-boundary-based target value [102, 104, p. 4]. An early example is the weighting set proposed by Hauschild and Potting [106] in 2005 that translates reduction goals for specific substances into weights for impact categories. Castellani et al. [105] applied a similar approach with a focus on European targets and policies to derive normalization factors for Europe and the year 2020. Their publication represents one of the most recent, policy-based distance-to-target weighting sets. In contrast, Tuomisto et al. [107] proposed a weighting approach taking the distance to planetary boundaries into consideration. Their approach was further developed by Bjørn and Hauschild [108]. Huppel et al. [66] used a meta-model to combine three weighting approaches into a single score. While this approach incorporates multiple perspectives, its interpretation becomes more complex [104, p. 59] and, thus, contradicts the purpose of weighting. Implemented in the ReCiPe model by Huijbregts et al. [67], Ponsioen and Goedkoop [109] proposed the conversion of mid- to endpoint weighting factors published in the JRC report [104, p. 127]. Table 2.2 summarizes these weighting approaches.

Table 2.2: The summary of environmental impact weighting methods and the respective scope shows the recently increasing attention to panel or mixed approaches [66, 105–109]. This trend can be attributed as a result of missing consensus on distance-to-target based methods as described in the JRC report [104].

Author	Year	Indicator	Method	Scope
Hauschild & Potting	2005	Mid-point	Distance-to-target	Global
Tuomisto et al.	2012	Mid-point	Distance-to-target	Global, Europe
Huppel et al.	2012	Mid-point	Meta model	Europe
Bjørn & Hauschild	2015	Mid-point	Distance-to-target	Global
Ponsioen & Goedkoop	2015	End-Point	Panel	Global, Europe
Castellani et al.	2016	Mid-point	Distance-to-target	Europe
Sala et al.	2018	Mid-Point	Mixed	Global, Europe

As these examples illustrate, a variety of weighting approaches exist and, as Table 2.3 shows, their ranking of impact categories differs broadly. For example, climate change is weighted between 2 % and 44 %, and ionizing radiation is only included in 4 out of 9 weighting sets. To create an appropriate

weighting set at the European level, the JRC organized an expert workshop in 2015—in which many of the previously mentioned authors participated—and evaluated available weighting approaches. Because they discussed scientifically based distance-to-target methods with an extensive expert panel, their approach categorizes as hybrid or mixed and provides the most recent and comprehensive weighting set. The resulting weighting set (Table 2.3, right column) was published by Sala et al. [104] and, subsequently, became part of the European Environmental Footprint method—a guideline for policy-making [110, p. 105].

Table 2.3: The summary of the weighting sets assessed and presented by the JRC shows the differences in the weighting as well as the number of considered impact categories [104]. For this work, the JRC weighting set is used (marked as **bold**). All values are given in %. Some categories are not considered by all weightings sets (marked as -). Differences to 100 % are due to rounding errors.

Impact Category	Castellani et al. WFSA	Castellani et al. WFsB	Tuomisto et al.	Bjørn et al. European	Bjørn et al. Global	Ponsioen et al.	Huppes et al.	Sala et al.
GWP	7.1	5.4	10	25	26	44.3	23.2	21.0
AP	7.2	5.5	8	1	1	-	4.2	6.2
Ecotoxicity	6.1	5.1	-	2	-	-	10.9	1.9
EP freshwater	6.2	4.7	7	9	2	-	2.3	2.8
EP marine	6.9	5.2	28	1	1	-	2.3	3.0
EP terrestrial	7.0	5.3	28	1	-	-	2.3	3.7
Human toxicity, cancer	6.9	5.2	-	-	-	1.4	6.5	2.1
Human toxicity, non-cancer	6.2	4.7	-	-	-	4.3	4.1	1.8
IR	6.1	4.6	-	-	-	0.3	6.5	5.0
ODP	6.4	4.9	8	1	2	-	3.6	6.3
PM	7.4	5.6	-	-	-	8.0	6.6	9.0
POCP	7.8	5.9	-	34	48	-	5.4	4.8
WD	6.1	29.6	5	1	4	3.2	5.1	8.5
RD and FD*	6.1	3.0	-	-	-	19.0	6.9	15.9
Land Use†	6.4	5.3	6	25	16	19.0	10.2	8.3

* Weighting sets do not distinguish types of resource depletion

† not included in the ILCD recommendations

Monetization methods rank environmental impact based on some economic value. Examples are estimations of a certain stakeholder's willingness or ability to pay for a specific environmental damage [104, p. 8]. Furthermore, abatement or mitigation costs can serve as a ranking. Although addressed in the report, Sala et al. [104, p. 53] conclude that monetization methods are not compatible with midpoint assessment and thus the ILCD recommended impact categories. Consequently, these methods are excluded in this work and reference is made to the JRC Report for further information [104].

2.2 Application to Freight Transport

A LCA models the life cycle of a defined product or system. As shown in the introduction, commercial vehicles, and heavy-duty vehicles, in particular, play a key role in the transformation of the transport

sector. Therefore, this section defines the general terminology and the requirements for heavy-duty vehicles, as the product is assessed. Furthermore, the underlying technological principles of each vehicle concept are summarized to provide a better understanding of the obtained results. Additionally, the state of science regarding the economic and ecological potential of heavy-duty vehicle concepts is presented. The section is structured by the vehicle concepts and their respective source of energy:

- Diesel as the reference, and alternative or synthetic fuels
- Hybrid (HET) and overhead catenary (OBET) powered trucks
- Battery electric trucks (BETs)
- Hydrogen-powered vehicles, including fuel cell trucks (FCET) and hydrogen internal combustion engine trucks (HICET)

Commercial vehicles are defined as vehicles for transporting goods (trucks) and people (buses). Trucks are further categorized by gross combination weight (GCW), vehicle concept, and purpose [111, p. 24-26, 112, p. 57, 113]. Regarding vehicle weight, three general categories exist: light, medium, and heavy-duty vehicles. However, the associated gross vehicle weight (GVW) varies depending on the country or source. The European legislation 2007/46/EG [114] distinguishes between vehicles lighter than 3.5 t (light-duty), between 3.5 t and 12 t (medium-duty), and above 12 t (heavy-duty). In the course of the introduction of CO₂ limits for heavy commercial vehicles in 2019, the regulation 2019/1242 [40] distinguishes by vehicle concept (axle configuration, cab type, and engine power) in addition to weight. The subgroup LH5 describes 4x2 tractors with a GCW above 16 t and is the most frequent (68 %) among nine subgroups [115], which are given in Appendix A. For this reason, in this work, the term heavy-duty refers to the vehicle with a GCW above 16 t, which includes the subgroups LH4, LH5, LH9, and LH10. Combined they comprise 84 % of all vehicles and all long-haul applications with a typical daily distance greater than 150 km [115, 116]. Mustafić [117] summarizes further legal requirements on the vehicle concepts.

Besides weight, mileage is an important characteristic of heavy-duty vehicles. As Figure 2.3a (a) shows, the average heavy-duty vehicle drives 120 000 km/a [118]. However, mileages above 150 000 km/a are rarely achieved. Due to their high mileage, the fuel consumption of heavy-duty vehicles is traditionally an important design objective. Besides that, general requirements for heavy-duty vehicles are discussed in previous publications [35, 100] and summarized as follows:

- Low total cost of ownership
- Sufficient payload or useful volume
- Sufficient range
- Low environmental impact (e.g., air and noise emissions)
- Safety
- Reliability
- Legal requirements (e.g., dimensions, GCW, and axle load)

From a customer perspective, range and payload are of special interest. Both can be regarded as a lower boundary that may lead to a decision being made for or against a particular vehicle. Gnann et al. [118] analyzed the daily ranges for heavy-duty vehicles. They found that, on average, vehicles travel approximately 400 km/d (Figure 2.3b). However, the daily distance follows a Gaussian distribution,

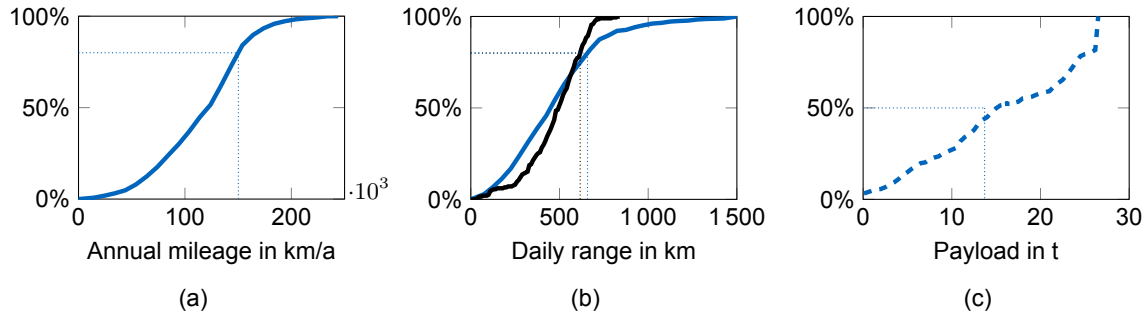


Figure 2.3: The data (n=1018 vehicles) highlights the importance of low fuel consumption due to high mileages (a) that require daily ranges of 400 km/d to 600 km/d (b). Different data sets from 2010 for heavy-duty vehicles (—; n=1018 vehicles) and 2016 for long-haul vehicles (—; n=51 trips) show a trend to slightly shorter ranges. For long-haul applications, the payload (---) shows a uniform distribution with an average of 13.6 t (n=264 trips) [118, 53, p. 35, 119, p. 79].

which means that a range of 658 km/d is sufficient for 80 % of the vehicles. The data collected by Fries et al. [53] focuses on long-haul vehicles, but yields similar results. The data’s average is at 495 km/d, while 80 % require less than 617 km/d. Consequently, a range of 400 km/d to 600 km/d imposes the lower boundary for current long-haul vehicles and the corresponding purchase decisions.

In contrast, the payload distribution (Figure 2.3c) obtained by Süßmann [119, p. 79] shows a uniform distribution and, accordingly, a linear, cumulative course. The average payload is at 13.6 t, which is comparable to the estimated payload for automotive goods by Fries et al. [53, p. 35] of 12 t to 13 t. However, the current EU certification tool VECTO uses a higher payload of 19.3 t. Apart from the absolute payload, the payload ratio can be used to compare different vehicle concepts. It is defined as the ratio of the maximum payload—depending on the allowed GVW—and empty vehicle weight (Equation (2.4) [111, p. 158f]:

$$G_p^* = \frac{m_{\text{payload,max}}}{m_{\text{veh.,empty}}} = \frac{GVW_{\text{max}} - m_{\text{veh.,empty}}}{m_{\text{veh.,empty}}}. \quad (2.4)$$

The question remains how these requirements can be fulfilled while reducing the overall environmental impact. The application of an eco-efficiency assessment can do just that: Combining economic with ecological objectives, it becomes possible to analyze different alternatives with regard to these objectives. Subsequent optimization minimizes costs and environmental impact, establishing eco-efficiency as an ideal concept to facilitate the cost-efficient transition to road transport’s low environmental impact.

Currently, there is a variety of alternatives aiming to achieve this goal. To give an overview of technologies, existing on the market, Bstieler [120] carried out a benchmark analysis. As a result, the morphological box presented in Figure 2.4 shows that European manufacturers focus on BETs, overhead catenary battery electric trucks (OBETs), and fuel cell electric trucks (FCETs).

It can also be seen that the alternatives differ strongly in the extent to which the requirements are met. Additionally, it becomes evident, that there is no common trend, incorporated by the OEMs. None of the shown vehicles excel prototypes or even the concept phase, no operating costs are available. Consequently, the following section will give a comprehensive overview of zero or near-zero-emissions technologies for heavy-duty vehicles. Besides the technological basics, a literature review assesses the economic and environmental potential.

Manufacturer	E-Force	DAF	Daimler	Scania	Reference					
Model	EF18	CF Electric	Gen H2	R450 Hybrid	EURO VI					
Powertrain	BET	HICE	FCET	OC	ICE					
Payload Ratio	<1,1	1,2	1,3	1,4	1,5	1,6	1,7	1,8	1,9	>2
Topology	Dual central, multiple gears	Central, fixed gear	Distributed, fixed gear	eAxle, fixed gear	Central, multiple gears					
Range in km	200-399	400-599	600-799	800-999	>1000					
Charging Power in kW	150	250	350	500	>1000					
Energy Storage	Batteries	Hydrogen, 350 bar	Hydrogen, 700bar	Hydrogen, liquid	Diesel					

Figure 2.4: The morphological box of current zero-emission prototype vehicles shows that there is no clear trend regarding the technologies. Neither the energy carrier nor corresponding storage nor powertrain topology is currently determined. However, the payload ratio increases from BET over FCET to diesel vehicles.

2.3 Alternative Powertrains for Heavy-Duty Vehicles

Although 97 %, diesel combustion engines dominate the transport sector [121], alternative powertrains have already been investigated in the past. Gaines et al. [122] performed the first published LCA for heavy-duty vehicles in 1998, comparing the environmental life-cycle impact of liquid natural gas (LNG) with conventional diesel. Although they concluded that LNG neither reduces energy demand nor greenhouse gases (GHGs), the technology currently experiences an upswing. In 2020, for example, 90 % of newly registered heavy trucks in Germany that do not run on diesel were powered by natural gas [123]. The reason for this is the lower fuel consumption (−22 % to −28 %) and, consequently, potential tank-to-wheel CO₂ savings between 12 % and 29 % [53, p. 93, 124]. However, compared to diesel sales, the total number of vehicles remains low: 201 LNG trucks and 18 BET compared to 128 814 diesel vehicles.

Yet LNG is not without controversy. Mottschall et al. [125, p. 7] concluded that LNG “is not a suitable measure for climate protection in road freight transport” because of extensive well-to-tank emissions. Similarly, Fries [53, p. 83f] showed marginal CO₂ reduction between 3 % and 5 % compared to diesel if methane slip (unburned fuel escaping the engine) is considered. Sen et al. [126] even showed increasing well-to-wheel emissions for compressed natural gas (CNG) vehicles used for road-transportation due to additional fuel production (GHG: 33 %; Pollutants: 200 %). However, there might be a cost reduction potential by using natural gas, which is not quantified in more detail due to model uncertainties. Fries [53, p. 83f] estimated cost savings between 8 % and 9 % for LNG vehicles. In contrast, Gnann et al. [118] forecasted a cost increase of LNG vehicles of 5 % to 12 % depending on vehicle mileage.

Nevertheless, LNG can contribute to GHG reduction if biogas or synthetic gas are considered. The former requires the planting of bioenergy crops, which “impedes the achievement of numerous Sustainable Development Goals” [127, p. 18], as stated in the joint IPBES and IPCC report on biodiversity and climate change. To be climate-positive, the latter has the same requirements for green energy as synthetic diesel, including a similar production process. Consequently, this work assumes these two options interchangeably. For these reasons, LNG is not regarded as an option for improving long-haul transport eco-efficiency and, consequently, is excluded from this study.

Apart from that, several non-gas-powered alternative powertrains exist. In the context of GHG emission reduction targets, Kirchner et al. [128] estimated the potential of reducing German GHG emissions by transitioning to alternative powertrains in heavy-duty vehicles at 20 % to 23 %. This study provides the basis for the German National Platform Mobility's (Ger.: Nationale Plattform Zukunft der Mobilität—a commission set up by the *German Ministry of Transport*) roadmap on the transition to zero-emission transportation [129]. As Prognos et al. [130] concluded, electrification will play a key role in that transition. Electrification with overhead catenary, battery, or hydrogen fuel cell electric trucks of 27 % by 2030 and 78 % by 2050 is required to achieve the goals set by the Paris Agreement [130, p. 23]. These vehicle concepts will be discussed in the subsequent chapters.

2.3.1 Diesel, Bio and Synthetic-Fuel-Powered Trucks

The diesel tractor, as depicted in Figure 2.5, is a state-of-the-art vehicle and provides the reference for further studies. These rear-driven vehicles are equipped with an internal combustion engine (ICE), mounted in the front of the vehicle underneath the driver's cab. Apart from the shown 4x2 configuration (5-LH), 6x2 (10-LH) axle configurations with an additional rear axle are common on European roads. For a detailed description of the structure and the components independent of the drivetrain, refer to the previous publication [100].

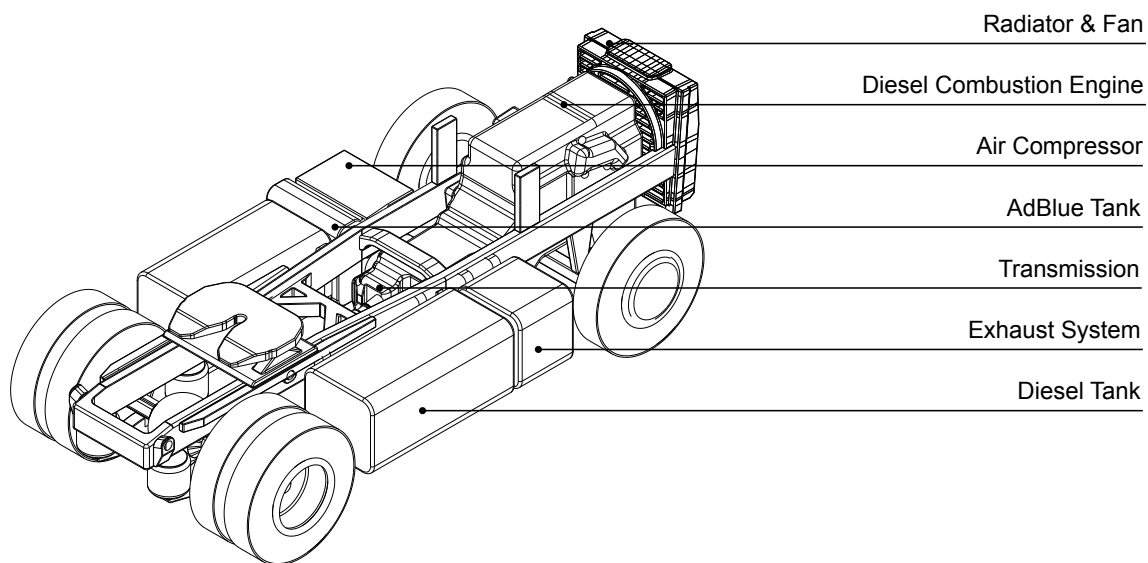


Figure 2.5: Isometric view of a diesel ICE heavy-duty vehicle package. The European cab-over-engine results in a short front overhang and a short wheelbase. Two diesel tanks mounted outside the frame hold up to 1200 L. Additionally, the exhaust treatment system including the AdBlue tank is mounted on the sides. The powertrain sits between the two side members [120, 112, p. 17].

The European tank-to-wheel reduction targets practically do not allow conventional diesel as future energy for transportation and, thus, in its current form, synthetic or biofuels either. The former refers to fuels produced by synthetic processes using raw materials and energy. For example, hydrogen is first obtained by electrolysis, which is then processed into liquid fuel by Fischer-Tropsch synthesis. If carbon is extracted from the air via direct air capture, these fuels are climate-neutral. Because the CO₂ emitted during combustion was extracted from the air before. Biofuels are also climate-neutral [131, 132]. Because they are processed from biomass (e.g., plants), which captured carbon during their life, they also emit the same amount of CO₂ during combustion. The complete processes are complex and not within the scope of this study. Therefore, refer to Schmidt et al. [131, p. 65-99] and the Agora study [132, p. 61-76] for further information.

Studies addressing either economic, ecological or both potentials of synthetic fuels are summarized in the following. Gaines et al. [122] pointed out that synthetic fuels could be beneficial if the overall process efficiency improves. Since then, several studies addressed this. First of all, den Boer et al. [133] forecasted a stagnation of costs for fossil diesel (−3 % to 5 %) until 2030 compared to 2012 levels. However, new regulations such as Germany’s carbon tax and EU GHG reduction targets, influencing the retail price were neither included nor foreseen.

Schmidt et al. [131] compared the well-to-tank greenhouse gas emissions, energy demand, and costs of synthetic fuels with those of hydrogen or battery electric vehicles. They estimated that synthetic fuel pathways—also known as power-to-x (PTX)—increase costs per kilometer for passenger cars by a factor of 3 to 5 in an optimistic scenario for the year 2050. Among the pathways, the direct use of hydrogen has the lowest CO₂ mitigation costs. The study only mentions internal combustion engine truck (ICET) and FCET as alternatives for long-haul transportation but quantifies neither their economic nor environmental potential.

Schmied et al. [134] analyzed the PTX and biofuel potential for the cross-modal transformation of national traffic with regard to the Paris Climate Agreement. With costs of 0.45 EUR/km to 0.65 EUR/km, they estimated the total costs for vehicles operated with PTX 13 % to 27 % higher than those operated with fossil diesel (0.40 EUR/km to 0.51 EUR/km) [134, p. 66]. They concluded that fuel cells are better in costs and GHG emissions than PTX and biofuels [134, p. 67]. Furthermore, they highlighted the limited availability of biofuels. Without extending first-generation bio-fuels, second-generation bio-fuels could supply 10 % of global transportation energy demand by 2050. However, this covers either air or sea transport [134, p. 51f]. Thus, the application for road transport is limited.

The primary reason for this cost increase was pointed out by Agora [132], who indicated the low well-to-wheel efficiency of power-to-liquid fuels. The fuel production has an efficiency of 44 % (well-to-pump) that equals approximately 17 % well-to-wheel for heavy-duty diesel engines [132, p. 12]. Consequently, the production plants must have a high proportion of full load hours [132, p. 34] to be profitable and use atmospheric carbon dioxide to achieve climate neutrality [132, p. 30]. Compared to fossil oil, they forecast a cost increase of 400 % to 600 % during the ramp-up-phase (2020 onward) and 100 % in 2030, if extensive production capacities (globally >100 GW) are achieved. Consequently, the study concluded that synthetic fuels (liquid or hydrogen) should only be applied where direct electrification is not possible—long-haul transport being none of the applications [132, p. 12]. Ueckerdt et al. [135] backed up this finding, concluding that PTX fuels have high climate mitigation costs and “should be prioritized for sectors inaccessible to direct electrification.” Nevertheless, PTX pathways are subject to great uncertainties, Ueckerdt et al. [135] left their assessment ambiguous. Six years earlier, Fulton et al. [136] also found no clear advantage of any technology, which underlines the process complexity, the associated uncertainties, and the potential risks.

2.3.2 Battery Electric Trucks

While bio and synthetic fuels both use the same vehicle setup as fossil diesel, a battery electric truck requires major changes to the vehicle components and package. As Figure 2.6 shows, the ladder frame with two side members remains unchanged. Because the electric powertrain can be built more compact, battery capacity utilizes the remaining space. Besides the powertrain, components such as the air compressor must be adopted from the ICET, ensuring compatibility with the pneumatic braking system of the vehicle and the trailer. A previous publication summarizes the similarities and differences between battery electric truck concepts and diesel-powered concepts [100]. Apart from the wheel-

independent hub motor concept shown in Figure 2.6, other vehicle architectures exist (Appendix B). A basic distinction can be made between central and wheel-independent drive. Furthermore, a central drive can be rigidly coupled to the drive axle or decoupled, as is the case with the diesel engine. Regardless of the engine position, direct-drive or shiftable transmissions can be used. The topologies efficiencies were discussed by Verbruggen et al. [137] and in a previously published simulative case study [138]. While Verbruggen et al. [137] found that a wheel-independent topology with a two-speed gearbox achieves the highest efficiency, the case study of current vehicles and prototypes shows that a central, direct-drive topology has the best efficiency [138]. These contradicting results highlight the necessity of comprehensive powertrain optimization and the need for further research. However, throughout this study, the central topology will be used for BET.

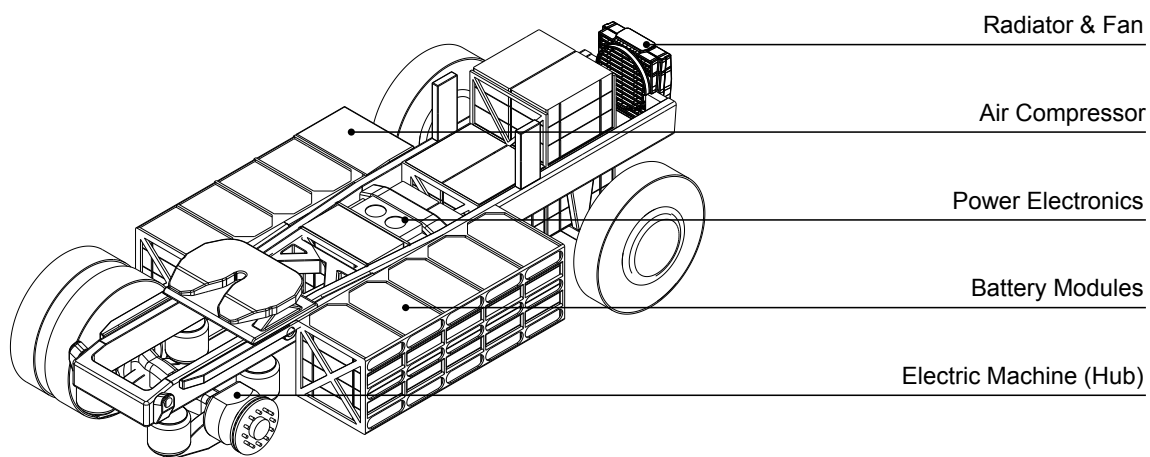


Figure 2.6: Isometric view of a battery electric heavy-duty vehicle package. The high-energy battery, the electric machine, and the power electronics are integrated into the frame and in the space freed up by the elimination of the conventional drivetrain. The auxiliary consumers (air compressor), the fan and the radiator remain, although the fan and radiator can be dimensioned smaller. The depicted maximum utilization of the package space results in a range of approximately 500 km to 600 km [120].

Although the efficiency of a battery electric truck is unbeaten, studies before 2017 did not consider them an option for long-haul transportation [124, 131, 133, 134, 136, 139–142]. For example, Den Boer et al. [133] estimated comparatively high costs between 1.12 EUR/km and 1.26 EUR/km for battery electric, regional delivery trucks in the year 2020. Due to the battery weight and the limited range, Den Boer et al. [133] did not consider BET an option for long-haul transport. However, it was not before the presentation of the battery electric *Tesla Semi* truck in 2017 [143], when BET received greater public attention for heavy-duty transport.

In 2017, Sen et al. [126] performed a simplified life cycle costing (LCC) and a LCA comparing diesel, hybrid electric truck (HET), CNG and BET long-haul trucks. They conclude that BET decrease costs by 16 % and 26 % compared to fossil diesel, while simultaneously reducing GHG emission by 16 % and air pollutants by 50 %. The BET outperformed all other vehicle concepts in their study.

Mareev et al. [144] indicated the energy consumption, including an 845 kWh battery, between 1.23 kW h/km and 1.94 kW h/km, which is 2.5 times more efficient than a diesel engine. Nevertheless, the battery weight reduces the maximum payload by 20 %. This might be acceptable given that most trucks only utilize about 70 % of their payload [144], and that “[T]he total life cycle costs show that battery electric trucks can perform at the level of the same costs as the conventional diesel trucks. However, the life cycle costs show also high dependency on battery lifetime and resulting battery exchanges” [144]. The study estimated the TCO between 0.69 EUR/km and 0.81 EUR/km, assuming battery pack costs

of 140 EUR/kWh, electricity costs of 0.139 EUR/kWh, and (net) diesel costs of 0.949 EUR/L [144]. A subsequent publication further specified the TCO at 0.76 EUR/km [145].

This conclusion is supported by Gnann et al. [118], who showed cost parity for BET in 2030 with costs between -5 % and 2 % compared to diesel (0.65 EUR/km to 0.843 EUR/km). Gnann et al. [118] assume battery pack costs of 186 EUR/kWh, electricity costs of 0.16 EUR/kWh, and diesel costs of 1.53 EUR/L, which is comparable to but less optimistic than the assumptions of Mareev et al. [144, 145]. Furthermore, they calculated CO₂ reductions of approximately 69 %. Hall and Lutsey [146] from the International Council on Clean Transportation also predicted the cost parity of electrified heavy-duty vehicles in the current decade. However, if infrastructure costs are included TCO could increase by 10 % in 2025 and 7 % in 2030 [146, p. 20].

2.3.3 Hybrid and Overhead Catenary Trucks

A hybrid powertrain consists of at least two energy converters and carriers [147, p. 4]. Typically these are an ICE with fuel as a chemical energy carrier combined with an electric machine and a battery. However, hydrogen fuel cell systems share these characteristics and can be referred to as HET. Combining two powertrains creates several degrees of freedom that save energy if designed optimally.

According to Fries [53, p. 12], the P2-hybrid topology has the biggest (economic) potential for long-haul applications, which is why other typologies are not further described in this work. For their description refer to Hofmann [147] and Reif et al. [148]. Fries [53, p. 83] concluded that diesel-hybrid drivetrains save 1.5 % to 2 % of costs compared to a conventional diesel, based on a TCO estimation. However, the CO₂ savings at 13 % are not sufficient to reach the EU targets beyond 2025 [53, p. 84]. Sen et al. [126] achieved similar results, with 13 % reduced GHG emissions and -16 % to -17 % air pollutants. They did, however, achieve cost savings between 11 % and 16 %. Rupp et al. [149] performed a LCA, comparing one conventional diesel with a diesel-hybrid long-haul truck. In the best case, they reported even lower emission savings of 6 % on a well-to-wheel perspective, including vehicle production. However, they highlighted the strong dependence of fuel savings on road topology, leaving no savings in the worst case [149].

Because of its two power sources and following the definition above, vehicles equipped with overhead catenary wires, which enable dynamic charging, categorize as HET. In this case, the overhead line is defined as a second energy carrier. Strictly speaking, however, the second energy converter is missing. The OBET is, consequently, described within this section. Figure 2.7 shows the vehicle package for such a vehicle, which is similar to the BET shown in Section 2.3.2. At this point, a central drive topology with a conventional rear axle is shown as an example. Figure 2.7 shows the maximum possible battery capacity, although it could be reduced due to the dynamic charging, which is the essential advantage of the OBET compared to BET. While the prototype vehicles, currently tested on German highways, still have a diesel engine combined with an electric machine, OBET achieve lower GHG emissions and costs [118, 150, p. 39, 45]. This is why overhead diesel hybrid trucks are only considered a transition technology and not further considered in this study.

Therefore, Wietschel et al. [140] and Gnann et al. [118] performed a feasibility study on the electrification of German highways with overhead catenary systems, assuming 2000 km of electrified road. The study compares electric highways (or e-roads) with diesel, LNG and hydrogen-powered vehicles [118]. Gnann et al. [118] estimated the costs of LNG and FCET as 10 % to 25 % higher than diesel, while the BET's—with or without pantograph—are similar to diesel. Specifically, they estimated the OBET's costs between 0.64 EUR/km and 0.80 EUR/km depending on the mileage, which is 2 % to 6 % lower than

the studied ICET. Thereby, a CO₂ reduction of 22 % was achieved, of which the secondary powertrain (i.e., diesel) comprises 82 %. The BET has 75 % lower well-to-wheel emissions compared to diesel, and the lowest of all vehicle concepts. Gnann et al. [118] concluded that battery electric trucks are superior. However, Gnann et al. [118] excluded the solution due to limitations of range and mass, because of the battery technology (at that time). This led to the conclusion that overhead catenary systems provide high efficiency and comparatively low emissions but at the expense of increased infrastructure costs. However, they argue that other systems also require infrastructure investments.

To overcome the diesel engine's emissions, Schmied et al. [134, p. 67] assumed the use of synthetic or biofuels for hybrid catenary vehicles, which results in well-to-wheel emissions comparable to the OBET. However, the OBET has the lowest emissions. Both overhead systems (diesel hybrid and fully electric) achieve costs of 0.3 EUR/km in 2050 and excluding taxes [134, p. 66], which is 25 % to 40 % lower than the projected diesel costs, whereby these costs do not include the required overhead infrastructure investment.

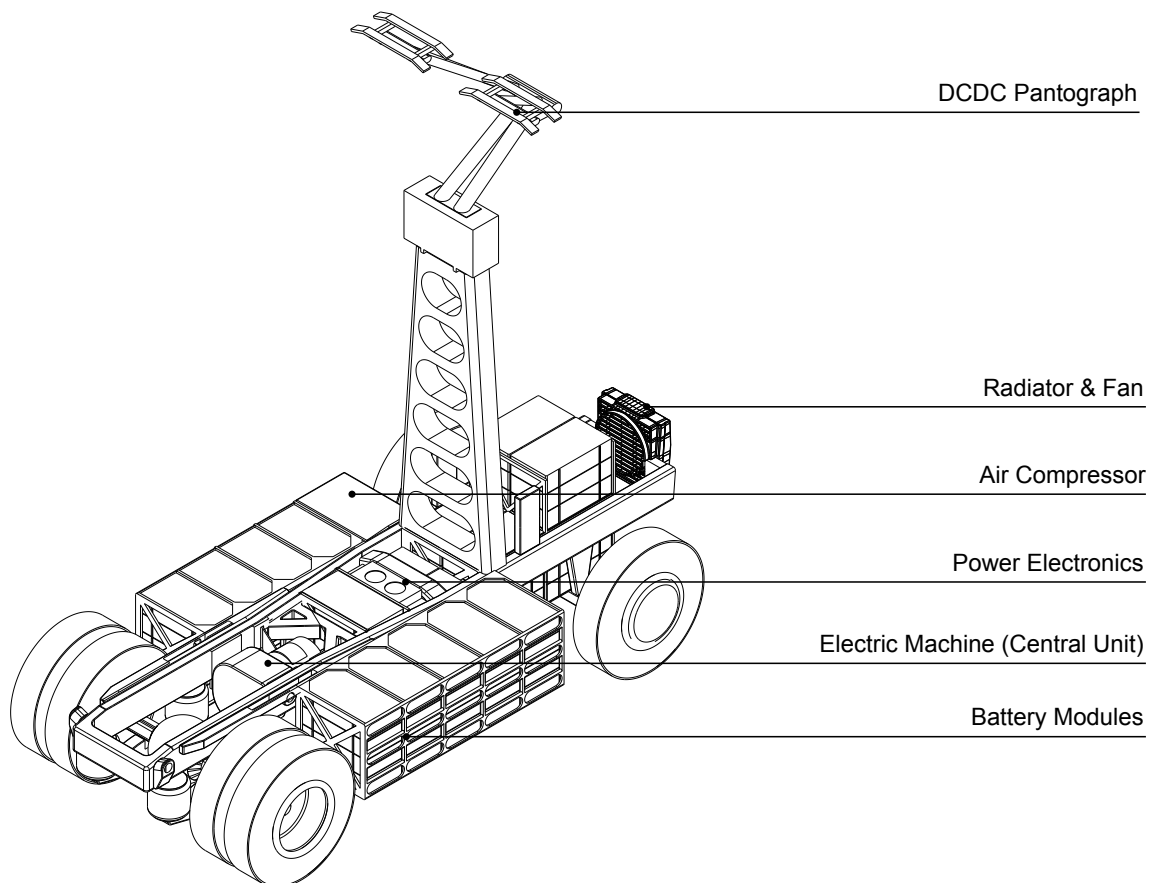


Figure 2.7: Isometric view of a battery electric overhead catenary vehicle package. The packaging is similar to a BET with an additional DCDC pantograph mounted behind the cab. The pantograph requires two contact points to achieve a closed electrical circuit. The total height of the shown, extended pantograph is 4.5 m. To reduce costs and weight, several battery modules can be omitted depending on the use case. The maximum utilization of the battery package space results in a range of approximately 400 km to 550 km without dynamic charging [120].

The life cycle costing approach presented by Mareev et al. [145] included the per-vehicle infrastructure costs. They found that despite superior energy consumption (1.66 kWh/km to 1.82 kWh/km), the costs remained equal to those of the ICET. The OBET achieved costs between 0.68 EUR/km and 0.72 EUR/km, depending on the e-road expansion, while the diesel obtained 0.71 EUR/km. This shows that the e-road network plays an important role in cost assessment. Mareev et al. [145] analyzed an

e-road network covering 3000 km, which corresponds to approximately 30 % of German highways. Additionally, they examined a network with 100 %, resulting in the upper-cost boundary. The former was first proposed by Wietschel et al [140, p. 2]. Without quantifying costs, Kirchner et al. [128] saw a potential already at an expansion of 2500 km or approximately 20 % of German highways.

Dynamic charging can also be achieved with inductive, wireless systems, integrated beneath the road surface. Olsson et al. [139] showed the technical feasibility of an inductive road system. They estimated the overall (well-to-wheel) efficiency at 79 % and 6 Mio. EUR/km as infrastructure costs—more than three times as high than overhead catenary systems. Nevertheless, den Boer et al. [133] forecasted the cost-parity of dynamically charged BETs in 2020. From 1.05 EUR/km to 1.17 EUR/km in 2020, the costs further decrease (1.02 EUR/km to 1.10 EUR/km), the lower limits being identical for catenary and inductive systems. Altogether, den Boer et al. [133] estimate the cost reduction potential of dynamically charged systems at 6 % to 9 % in 2020 and 12 % in 2030. In contrast, Limb et al. [151] estimated a 63 % economic benefit, comparing an electric US-class 8 truck with wireless, dynamic charging with diesel on a per-mile basis. However, they assumed infrastructure costs of only 1.6 Mio \$/km [151]. For the US, they calculated a GHG reduction between 49 % and 85 % depending on the state (i.e., electricity mix), which is similar to the other studies [118, 134]. Limb et al. [151] also addressed other emissions such as CO, NO_x, PM and SO_x finding that the former two decreased, while the latter two increased due to the average US electricity mix.

2.3.4 Hydrogen Powered Vehicles

Hydrogen is another alternative energy carrier for transport applications [152, p. 10, 153, p. 13]. In its national hydrogen strategy, the German *Federal Ministry for Economic Affairs and Energy* [154, p. 28] distinguishes between four hydrogen categories—sometimes referred to as colors—depending on the production process:

- Gray hydrogen is produced with steam methane reforming (SMR) and, thus, relies on fossil hydrocarbons. This process is currently the most used [153, p. 14].
- Blue hydrogen uses carbon capture and storage technology to prevent the CO₂ from gray hydrogen entering the atmosphere. It is, thus, carbon-neutral.
- Green hydrogen is produced from renewable electricity via electrolysis from water. Although it comprises 0.1 % of current, global hydrogen production, capacities increased rapidly during the last decade [153, p. 42, 45].
- Turquoise hydrogen relies on fossil hydrocarbons, similar to gray H₂. Due to a different, thermal process, the extracted carbon is solid and can be stored without affecting the atmosphere. However, the prerequisite is that the process heat is provided with renewable energy.

Being a precursor for synthetic fuels, hydrogen production via electrolysis requires fewer process steps and is approximately 50 % cheaper than synthetic fuels (independently of fluid or gaseous) [132, p. 24]. This renders direct hydrogen use attractive for cost-competitive industries, such as long-haul transportation. Therefore, FCET and hydrogen internal combustion engine truck (HICET) are among the technologies that allow direct hydrogen use, as the International Energy Agency states [153, p. 42, 45, 129]. Both technologies will be presented in the subsequent sections. For trucks, the Hydrogen Council [152, p. 17] estimates cost parity of hydrogen compared to battery electric trucks at a hydrogen price of 4 \$/kg to 6 \$/kg. According to the study, this can be achieved as soon as 2025 [152, p. 32].

Fuel Cell Electric Trucks

The powertrain of a fuel cell electric truck is equal to a BET, but with an additional fuel cell to convert the energy, chemically stored as hydrogen, and one or more tanks to store the hydrogen [155, p. 178f]. The battery enables recuperation and compensates for (fast) power peaks that cannot be handled due to the slower response characteristics of the fuel cell system. As Figure 2.8 shows, the battery can be designed smaller compared to a BET. The presence of the battery renders the FCET a hybrid, however, it is usually referred to separately.

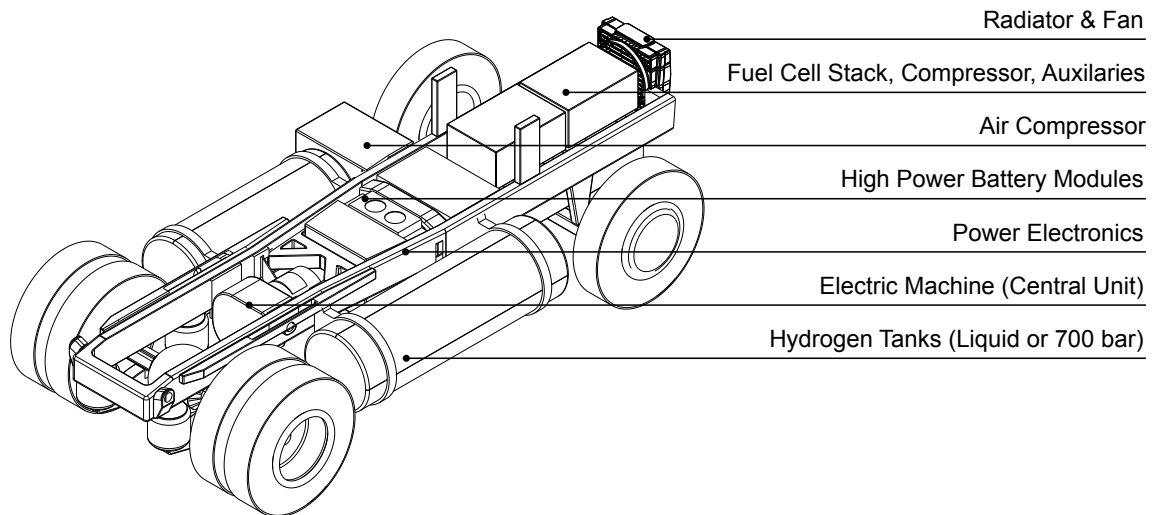


Figure 2.8: Isometric view of a fuel cell electric heavy-duty vehicle package. The packaging of the fuel cell stacks, their compressors, and auxiliaries (e.g., thermal control) is comparable to an ICE. The electric drivetrain is situated inside the frame while the two hydrogen tanks are located outside the side members. Their capacity depends on storage technology. The shown package space results in a range of approximately 500 km to 600 km [120].

The fuel cell's main advantage is its higher efficiency compared to combustion-based processes. On system-level, maximum efficiencies between 55 % and 60 % are possible [155, p. 148f and 154, 156, p. 17], which can be lower under dynamic operating conditions. However, fuel cells are also subject to three types of losses, which are depicted in the polarization curves (Figure 2.9) and depend on the cell current [155, p. 152f]. The fuel cell efficiency correlates with the cell voltage and decreases with higher currents. However, the power $P = UI$ increases until the voltage drops significantly.

The activation losses are caused by the limited load passage speed of electrons transferring between the electrode and electrolyte. The region of linear ohmic losses is determined by inner electrical resistance of the fuel cell and dominated by the electrolyte. This region is typically the main operating range. With increasing current, the physically limited gas transport slows down the reaction and causes the voltage drop and the diffusion losses, respectively. For further details on the reaction and the losses please refer to Klell et al. [155]. Despite its high efficiency, the fuel cell is subject to cold start difficulties [157, p. 86]. Furthermore, the fuel cell membrane's low durability remains a challenge, in particular for long-haul transportation [133, p. 126, 155, p. 141, 158, p. 52].

Regarding eco-efficiency, FCETs are frequently addressed for long-haul transport. Den Boer et al. [133] see the greatest GHG reduction potential in long-haul for the FCET, on the one hand. On the other hand, they forecast a cost increase between 12 % and 45 % in 2020 and 3 % to 37 % in 2030 compared to the respective diesel level (up to 52 % compared to 2012 diesel level). Furthermore, they highlight the high uncertainty in hydrogen cost assessment. Similarly, Gnann et al. [118] estimate a cost increase of 20 %, depending on the mileage. Accordingly, shorter distances are subject to a

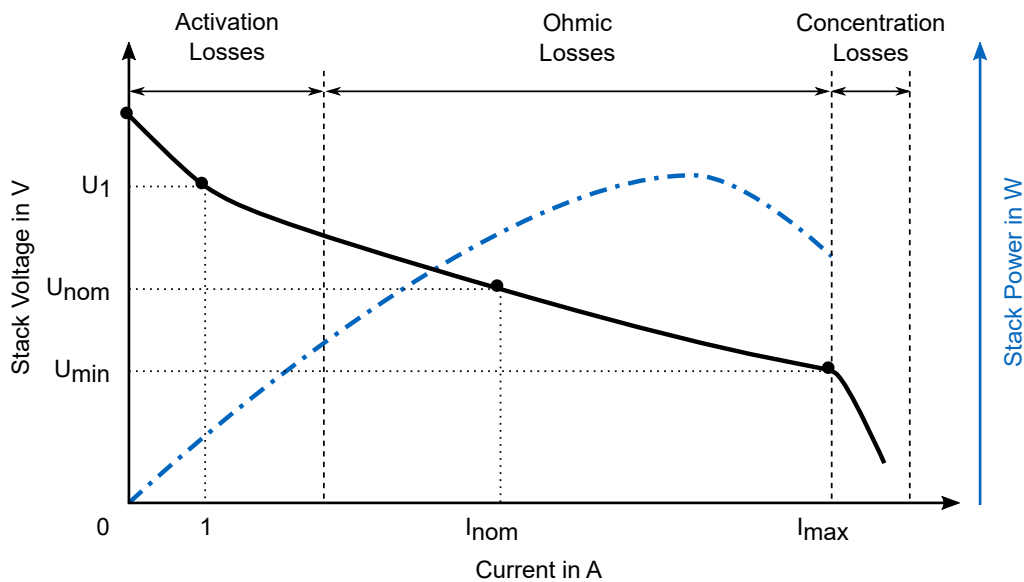


Figure 2.9: The polarization curve of a fuel cell with characteristic voltages and currents correlates with the thermodynamic efficiency. The three regions represent the different types of losses dominating the respective region.

greater increase in costs. However, they calculate a CO₂ reduction of 14 %, using gray hydrogen. Altenburg et al. [142, p. 72] regard FCET as the only valid option for heavy-duty vehicles. They calculate additional costs in the year 2015 of 260 % compared to the diesel (75 000 €/a vs. 200 000 €/a). The costs decline, however, eventually undercutting the diesel in the 2030 scenario by 6 %. According to their study, the shift towards FCET cuts emissions by 67 % compared to current diesel levels [142, p. 92], if green hydrogen is used. In contrast, Moultaq et al. [141] conclude that FCETs cost 5 % to 30 % less than conventional diesel, if hydrogen costs drop below diesel equivalent. According to Agora et al. [132, p. 24], this could be the case in 2050. Furthermore, TCO could increase by an additional 9 % if infrastructure investment is included [146, p. 20]. Thus, cost parity to diesel is only possible for high volumes (>10 000 trucks) [146, p. 24]. All of the mentioned studies share the conclusion that hydrogen costs are primarily responsible for the increase in TCO.

Hydrogen Internal Combustion Engine

The overall design of a hydrogen internal combustion engine truck (HICET) is similar to those of conventional (i.e., diesel) combustion engines. Apart from the hydrogen tanks, the system integration and packaging are equal to an ICET, which Figure 2.10 visualizes. However, due to the lower energy density of hydrogen compared to diesel, the required installation space can be—depending on the desired range—noticeably bigger. The vehicle package shown in Figure 2.10 represents the current maximum utilization resulting in approximately 1000 km to 1500 km of range [120]. In that case, the hydrogen tanks increase the weight by approximately 1 t, containing 100 kgH₂ to 150 kgH₂, when compared to a full diesel tank filled with 1000 L diesel (approximately 1 t). If only the side-mounted tanks are considered, the full tanks weight 60 % to 70 % less than a diesel system, although at the expense of significantly lower (i.e., -90 %) range. Nevertheless, with approximately 500 km, this range is comparable to BETs. In total, the vehicle weights are, however, still comparable to standard diesel. [159, p. 1173, 160, 161]. Hydrogen storage remains a critical component and is discussed separately in the next section.

As a combustion process, hydrogen combustion emits no carbon dioxide because no carbon atom is involved in the reaction [162, 163]. During the oxyhydrogen reaction, hydrogen reacts with oxygen and water is formed. However, in the internal combustion engine, the reaction takes place with a hydrogen-air mixture, so the high combustion temperatures also produce emissions such as nitrogen oxides. Because these emissions are also present in diesel engines, a similar exhaust gas treatment must be used to comply with emission standards. For example, NO_x emissions can be significantly reduced by SCR catalysts [164] or, in the case of stoichiometric operation, by three-way catalysts [157, p. 209].

Compared to diesel, hydrogen has good combustion properties [165, p. 4, 166], which are summarized in Table C.1. The properties allow a wide λ -range and, consequently, good qualitative combustion control and the possibility of direct injection. This reduces pumping losses and increases the engine's efficiency [157, p. 55, 167, p. 540, 165]. In addition, the higher combustion temperature improves the knocking behavior, which allows higher compression and, thus, also results in a higher efficiency compared to a diesel-powered engine [157, p. 55, 165, 167–170, p. 182]. However, high temperatures and compression ratios also increase mechanical stress on the components and lead to potentially increased engine weight [155, p. 222, 163, 168, 169, 171]. Additionally, the reported engine speed and resulting operating points are approximately twice as high as a heavy-duty diesel engine. The speed range is between 1000 min^{-1} and 5000 min^{-1} , with operating points between 1500 min^{-1} and 2000 min^{-1} [168, 172–174]. With a compression ratio between 11 to 16 and a stroke-bore ratio between 1.07 to 1.23, the research engines are comparable to modern heavy-duty engines [111].

Eidkum [175] reviewed state-of-the-art hydrogen combustion strategies and compared them regarding their respective indicated (i.e., thermal) efficiency, their possible exhaust treatment and their speed range. Appendix C contains further information on the combustion process timing, the induced efficiencies, and—where applicable—the respective ignition times. Table 2.4 summarizes his results and shows the superiority of compression ignition (CI) processes—equal to diesel combustion engines [157, p. 12]. Consequently, CI is well suited for heavy-duty applications, due to its low modification effort of the components as well as easy system integration.

Table 2.4: Overview of mixture formation and ignition possibilities with efficiency and required exhaust gas aftertreatment systems [175].

Combustion Strategy	Indicated Efficiency	Exhaust Treatment
External carburetion	40 % to 44 %	3-way catalytic converter
Direct injection, spark ignition	33 % to 45 %	SCR-catalytic converter
Direct injection, compression ignition	43 % to 46 %	SCR-catalytic converter
Direct injection, SI/CI	44 % to 46 %	SCR-catalytic converter
Direct injection, glow spark	44 % to 49 %	SCR-catalytic converter

In Table 2.4, it can also be seen that HICET have a lower efficiency compared to fuel cell systems. This translates to 20 % to 30 % increased fuel consumption and requires lower hydrogen costs of the same magnitude in order to be economically competitive [118]. However, compared to fuel cell systems, an advantage of hydrogen combustion is the lower H_2 -purity, required for the process [170, 172, 176]. This facilitates hydrogen production, logistics and storage, which can potentially yield lower costs.

Hydrogen Storage

Regardless of the energy conversion, the hydrogen tank is a critical component. Due to hydrogen's low density, its transport and storage are challenging. Klell et al. [155, p. 109] categorizes three typical storage processes:

- Gaseous, compressed at 300 bar to 700 bar is referred to as compressed hydrogen (CH₂)
- Fluid, at temperatures below $-252.85\text{ }^{\circ}\text{C}$ is referred to as liquid hydrogen (LH₂)
- Solid, chemically or physically stored in or at solids or fluids, currently in the laboratory stage

Currently, CH₂ is most frequently used for automotive applications. Because of the high pressure, fiber winding reinforced metal vessels (Type III) or solid carbon fiber vessels (Type IV) can be considered for this purpose [157, p. 88f]. Although the stainless steel Type III tanks are equally diffusion proof and secure [155, p. 117, 177, p. 487], carbon fiber reinforced Type IV tanks are—despite higher costs—preferred because of their lower weight [157, p. 88, 155, 178, p. 114]. In the following, therefore, this type of tank is used for further analysis. While high pressures increase the volumetric energy density of the hydrogen (Figure 2.11), they require heavier tanks, which reduces the gravimetric energy density of the tank system. According to Töpler et al. [157, p. 90], gaseous storage at 700 bar represents the best trade-off for automotive applications.

Liquid hydrogen storage offers further improvements in energy density (Figure 2.11). It is, thus, currently discussed for range-critical (i.e., long-haul) applications [155, p. 114]. Tanks for LH₂ have the same requirements as pressure tanks, but with additional isolation to maintain the temperature of $-252.85\text{ }^{\circ}\text{C}$ [155, p. 120f, 177, p. 488]. Because these cryo-tanks have no active cooling system, external heat input such as ambient temperature and solar radiation, however, results in hydrogen boil-off ($<3\text{ } \%/d$) due to increased pressure [155, p. 114]. The main disadvantages of LH₂ storage are the increased system complexity and the associated higher costs compared to gaseous storage alternatives. They are, consequently, not further considered in this work.

Apart from the state-of-the-art CH₂ and LH₂, hydrogen can also be stored as a solid state in metal hydrides—compounds of metals with hydrogen. Although prototypes of this storage technology have a lower energy density than CH₂ or LH₂, their theoretical densities are higher. Additionally, hydride storage is regarded as safer due to the lower operating pressure [155, p. 138, 157, p. 56]. The lower compression energy during refueling is also advantageous [179]. On the contrary, there is the higher weight, the higher consumption of resources, and the temperature differences when loading and unloading the hydrides [155, p. 138, 157, p. 56, 179].

Analogously, hydrogen can be chemically bound to liquid organic hydrogen carriers, which are in the experimental stage [179]. Currently, they offer poor energy release rates [180] and complex system integration due to required heat control and are, consequently, not pursued by any automotive OEM. However, their transport and storage are similar to current fuel logistics and thus the technology's primary advantage [176, 181]. Because of their currently not competitive energy densities neither solid-state nor LOHC are further considered in this work. A detailed summary of solid-state and LOHC can be found in Eidkum [175].

The same problems that occur with in-vehicle storage also occur with storage at service stations. Additionally, compressed hydrogen requires a pressure increase to approximately 900 bar at the station to exceed the storage pressure in the vehicle [156]. This compression results in energy losses of 15% [155, p. 133]. Furthermore, refueling times are slow (1 kg/min; 33 kWh/min) compared to diesel

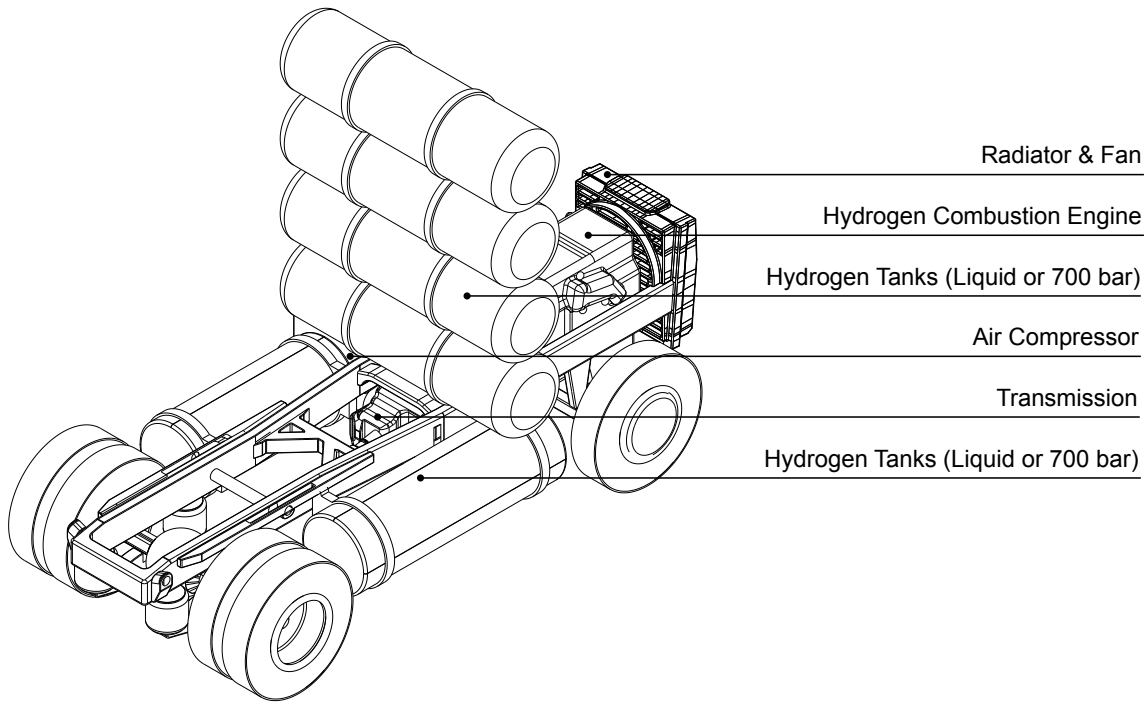


Figure 2.10: Isometric view of a hydrogen combustion heavy-duty vehicle package. The packaging of the hydrogen combustion engine is similar to a diesel engine. The two hydrogen tanks replace the diesel tanks. The shown packaging has additional tanks behind the cabin to extend capacity and thus range. This maximum utilization of the package space results in a range of approximately 1000 km to 1500 km depending on the hydrogen storage technology. The auxiliary consumers, fan, and radiator are equivalent to a conventional ICET [120].

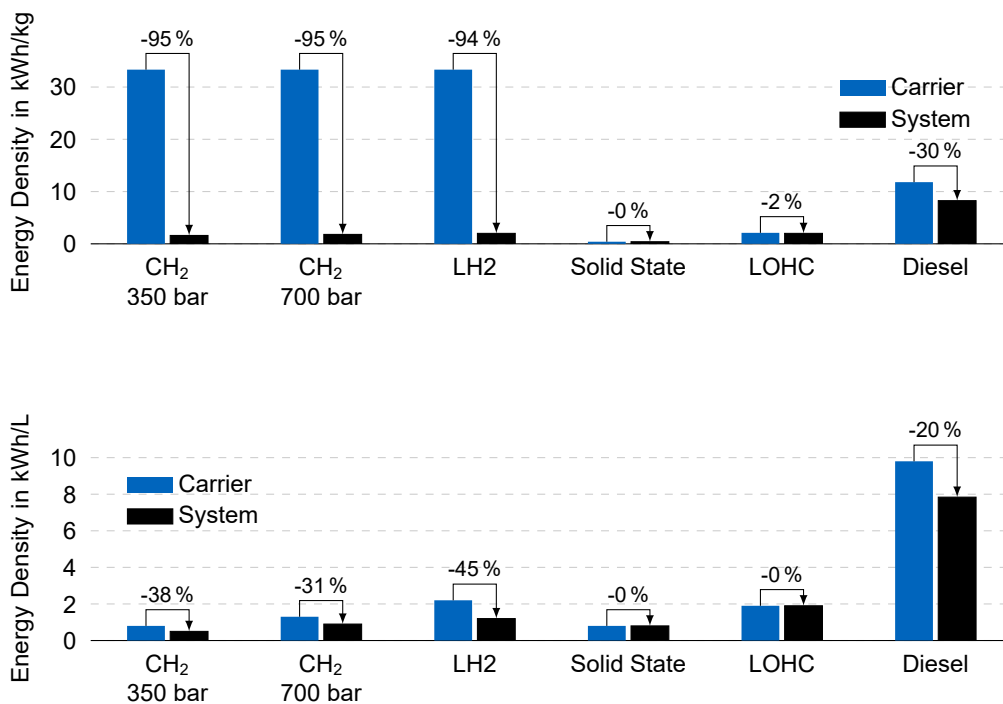


Figure 2.11: Comparing volumetric (top) and gravimetric (bottom) energy densities of hydrogen storage options for automotive applications shows that higher pressures or liquid storage offer the highest densities. However, losses between the energy carrier and system level are immense. They can also be interpreted as a measure of system complexity, rendering the solid-state or LOHC a valid option. For reference, the values for diesel are shown as well [175].

refueling (90 L/min; 882 kWh/min) [155, p. 120f, 182]. Fluid hydrogen stations also require boil-offs to reduce pressure. However, this boil-off hydrogen can produce electricity, operating the station. In addition, hydrogen liquefaction has a high energy demand, which amounts to 20 % to 46 % of the stored energy [155, p. 124, 177, p. 488].

2.4 Existing Assessment Models

The previous section summarized the technologies, currently being considered for zero-emission heavy-duty transport. Several studies estimated and compared their ecological as well as economic potential. Apart from these (high-level) studies, detailed assessment models exist, which replicate and compare different powertrains.

The Greenhouse gases, Regulated Emissions, and Energy use in Technologies Model (GREET) model is the first to mention. Published in 1996 by the Argonne National Lab (ANL), the first version only included the fuel cycle for 17 light-duty vehicle energy carriers [183]. The goal was to estimate their greenhouse gases and energy demands. In 2006, GREET was extended by a vehicle-cycle, rendering it a comprehensive, life-cycle-based approach for passenger vehicles [184]. The fuel cycles were combined with ICE, hybrid and fuel cell powertrains and supplemented with battery electric powertrains in further updates. Built on the knowledge and data of GREET, the ANL developed the Alternative Fuel Life-Cycle Environmental and Economic Transportation that combined environmental and ecological assessment for light and heavy-duty transportation [185]. While GREET is one of the most commonly used and extensive models, its applicability for the European market is limited due to their selection of—mostly US market—vehicles. Additionally, only the 2021 version includes a vehicle cycle for (US) heavy-duty vehicles, which was, consequently, not available for this work [186].

Due to the shortcomings of GREET and other models, Delucchi [187] created the Lifecycle Emissions Model (LEM). Although the overall approach is similar to GREET, LEM has a broader system boundary: “it covers more countries, wider time frames, more transport modes, more pollutants, more aspects of the life cycle (such as materials), and more relevant effects (such as price effects)” [187, p. 29]. The model’s major contributions are the full vehicle life cycle (i.e., cradle-to-grave), results for the years 1970 to 2050, 30 different countries and (simplified) infrastructure consideration. Compared to GREET, LEM can be used as a tool for showing certain trends and deriving policy recommendations. However, the model has not received updates since its publication in 2003, rendering it impractical for this work.

A recent extension to life cycle assessment models is the open-source model *calculator_truck*, published in 2021 by Sacchi et al. [188]. They focused on the different applications and size classes for road transport and included several relations between powertrain and vehicle weight or payload. Similar to Delucchi, they performed a prospective assessment until the year 2050. Additionally, they performed a LCA to evaluate the vehicles’ environmental impacts, which extends the scope of both, GREET and LEM. To the author’s knowledge, *calculator_truck* is the most recent addition to transportation life cycle models. Sacchi et al. [188] built on the life cycle inventory, previously published by the author [100], but performed the LCA separately. The approach of both works is therefore similar. However, *calculator_truck* focuses on LCA and does not consider the aspect of costs in detail as this work does.

2.5 Critics and Research Questions

The previous section discussed the necessity to address environmental impacts in conjunction with costs. This requirement applies, particularly, to the transportation sector. Although a variety of studies evaluate different transportation technologies from the environmental and cost perspective, there are several shortcomings in the current literature.

First of all, studies before 2017 completely neglect the possibility of battery-electric long-haul transportation. This even contradicts the conclusion of some of these studies that BETs provide a cost-efficient solution. At the latest, with the presentation of the *Tesla Semi* in 2017, this option was seriously considered in various studies.







Another shortcoming is the studies' incomparability because the studies do not have the same scope. This means that some studies consider either cost *or* environmental factors and only a few consider both together. Further, the different system boundaries are a major obstacle to the results' comparability. While some studies only consider the operation of the vehicle, others take a cradle-to-grave perspective. Likewise, the depth of the upstream processes varies and, accordingly, the influence of the energy sources or production supply chains is contained differently. Apart from this, the modeling depth is also different. Thus, all modeling depths can be found in the literature, from model-free conceptual considerations to component-exactly modeled (vehicle) systems.























Table 2.5 categorizes the sources, summarized in this section, by their sustainability pillar, vehicle modeling and system boundary. The last column shows the respective preferred technology for long-haul transportation. Altogether, it can be seen that a comprehensive assessment covering all relevant technological alternatives within a unified system boundary is missing. This section also showed that eco-efficiency provides a valuable concept for such a combined assessment, which has neither been applied to the transportation sector nor in a prospective manner. Based on this review of the state of science, the following two research questions are derived:

Which long-haul transport vehicle concept has the best eco-efficiency?

What is the most eco-efficient roadmap to low-emission freight transport if the infrastructure is included?

To answer these questions, an eco-efficiency assessment based on a detailed vehicle simulation—modeled at the component level—will be performed. This way, it is possible to include technological advancements, for example, cost decreases or efficiency improvements, and, consequently, enable a prospective approach. The assessment will be performed with the same system boundary and boundary conditions for all technologies. This means that all technologies are assessed with the same set of parameters—for example either best-case *or* worst-case. Apart from the vehicle perspective, an estimation of their influence on different decarbonization pathways will be performed. Therefore, the overall system costs, including vehicle and infrastructure, for a specific pathway will be calculated.

Table 2.5: Summary of the reviewed literature including the respective preferred vehicle concept for future road-transportation:  diesel or synthetic fuels;  natural gas;  overhead catenary or inductive power transfer;  hybrid electric;  battery electric;  hydrogen powered.

Author	Year	Sustainability			Vehicle			Scope			Preference
		Economy	Ecology	Social	Components	Passenger	Heavy-duty	Energy source	Infrastructure	Upstream	
Gaines et al.	1998	○	●	○	○	○	●	●	○	○	
Olsson	2013	●	●	○	●	●	●	●	●	○	 ¹
Zhao et al.	2013	●	●	○	●	○	●	●	○	○	
den Boer	2013	●	●	○	○	○	●	●	●	●	 
Fulton et al.	2015	●	●	○	○	○	●	●	●	○	  
Schmied et al.	2015	●	●	●	○	●	●	●	○	○	  ²
Reuter	2016	●	●	●	●	●	○	○	○	●	none
Schmidt et al.	2016	●	●	○	○	●	●	●	○	○	
Wietschel et al.	2017	●	●	○	●	○	●	●	○	○	
Sen et al.	2017	●	●	●	●	○	●	●	●	●	
Moultak et al.	2017	●	●	○	●	○	●	○	●	●	 
Gnann et al.	2017	●	●	○	○	○	●	○	●	○	
Altenburg et al.	2017	●	●	●	●	○	●	●	○	●	
Limb et al.	2018	●	●	○	○	○	●	○	●	○	 ¹
Fries	2018	●	●	○	●	○	●	●	○	○	
Agora Verkehrswende et al.	2018	●	○	○	○	○	○	●	●	○	none
Rupp et al.	2018	○	●	○	●	○	●	●	○	●	
Argonne National Lab	2018	●	●	○	○	○	●	●	○	●	none
Mareev et al.	2018a	●	○	○	●	○	●	○	●	○	
Mareev et al.	2018b	●	○	○	●	○	●	●	○	○	
Hall et al.	2019	●	○	○	○	○	●	○	●	○	 
Kirchner et al.	2019	●	●	○	○	●	●	●	○	○	  
Prognos et al.	2020	●	●	○	○	●	●	○	○	○	  
Hydrogen Council	2020	●	○	○	●	●	●	●	○	○	

¹wireless power transfer

²distribution and regional delivery only

3 System Boundary

The system boundary is at the base of the presented eco-efficiency assessment and—according to DIN EN 14044 [59]—a mandatory step in a LCA. To comprehensively estimate costs as well as environmental impact, a holistic system boundary is required. Figure 3.1 shows a cradle-to-grave system boundary, fulfilling this requirement. Each life cycle stage is characterized by material and energy inputs and outputs such as waste (i.e., material) and emissions to air, water or land. This boundary goes beyond the scope of a well-to-wheel analysis, which would only include the inputs and outputs of the use phase stage. A similar system boundary can be found in GREET and is also commonly used in LCA [60, p. 350]. The cradle-to-gate aspects that describe the flow from raw material extraction to the final manufactured product—in this case one heavy-duty truck—are described in a previous publication [100].

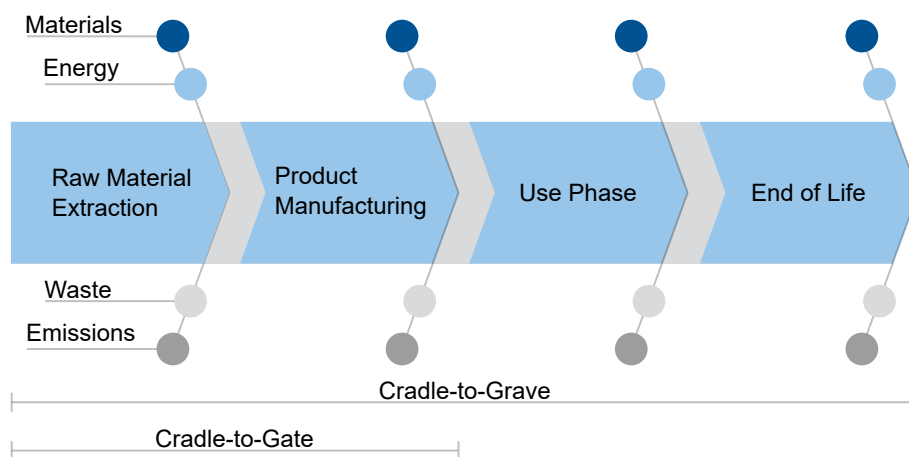


Figure 3.1: A simplified and linear representation of different system boundary definitions according to Hauschild et al. [60, p. 102] shows the four product life-cycle phases. The color coding represents the respective material and energy inputs (● ●) as well as waste and emission outputs (● ●). The well-to-tank fuel life-cycle is regarded as use-phase input and thus not explicitly shown. Fuel life-cycle combined with use-phase are regarded as well-to-wheel. The symbol sizes do not correlate with the respective inputs and outputs [100].

3.1 Considered Systems

The previous section summarized the most relevant technologies for zero-emission heavy-duty vehicles. Accordingly, these are the central components of the eco-efficiency assessment:

- Diesel vehicles provide the reference case and become zero-emission with the usage of e-fuels.
- Hybrid electric vehicles are considered analogous to diesel.

- Battery electric vehicles have only recently been considered technically feasible, although studies have already shown their potential. Additionally, overhead catenary concepts are addressed based on BETs.
- Fuel cell electric vehicles are equally zero-emission than BETs and they are attributed advantageous in practical operation.
- Hydrogen combustion engines are also considered, although only zero-emission regarding carbon-dioxide emissions.

However, it was also shown that infrastructure is of importance for most of these technologies. New energy carriers require new infrastructure for distribution and to ensure logistics operations. Particularly expensive concepts, such as overhead catenary infrastructure, highlight the importance to assess them in conjunction with vehicle technology. Therefore, the infrastructure, necessary to provide the respective energy carrier to the vehicle, will complement the vehicle-centered eco-efficiency assessment.

Infrastructure that is further upstream is not considered directly. Thus, neither the construction of renewable energy power plants (photovoltaic, wind) nor electrolyzers or e-fuel synthesis plants are included in the model. However, they are indirectly covered by aggregated environmental impacts and corresponding energy production costs.

3.2 Scenarios

After defining the system boundaries and the technical systems under consideration, two scenarios represent the time-dependent aspects. The first scenario, labeled *Status Quo*, poses the reference case. The second scenario shows the expected maximum potential of each technology in the current decade. Consequently, this best-case scenario is called *Potential*. The scenarios differ in the respective energy production pathways and the associated economic changes and environmental impacts.

It must be noted that all the costs exclude externalities such as taxes or subsidies. Without externalities, a solely technical comparison is possible, reducing the overall uncertainty [190]. Additionally, as Rebitzer et al. [191] conclude, such a free and unregulated market is valid if supplemented with an environmental assessment. Consequently, the costs represent production costs, which are lower than the prices paid by (end-)consumers, for example, at gas stations. As the International Energy Agency showed, energy production costs for crude oil are less volatile than the end consumer prices, which are subject to local policies and demand [192].

3.2.1 Status Quo

First, as a reference, the *Status-Quo* scenario describes the current status regarding fuel and technology costs. Furthermore, it excludes synthetic diesel for this scenario because it is not available in sufficient quantities. The conventional diesel is modeled with data from the *ecoinvent* database [193, 194]. Today's hydrogen comes exclusively from steam reforming and is, therefore, labeled gray [195]. The cost is assumed to be 8.67 EUR/kg, which corresponds to the current production cost without taxes. Both fuel cells and hydrogen tanks are currently produced in small batches, resulting in 130 EUR/kWh for the stacks and 580 EUR/kg for the type IV tank [33]. The electricity mix corresponds to the 2019 European electricity mix, which has 0.403 kg CO₂-eq./kWh. The battery production in China results in approximately 110 kg CO₂-eq./kWh and costs of 140 EUR/kWh at pack level. The scenario assumes

electricity costs of 0.11 EUR/kWh, again excluding all taxes and surcharges. Table 3.1 summarizes the cost assumptions of both scenarios. The data and underlying review and own assumptions are previously published [31, 33, 196].

Table 3.1: The production cost assumptions, used for the optimization, represent values from the year 2020 and assumed costs for the year 2030 (Potential) to account for the technological advancement [96, 196]. [Note: PtL = Power-to-Liquid]

Costs	2020	Potential	Unit
Diesel	0.45	0.54	EUR/L
PtL Diesel	-	1.21	EUR/L
Electricity	0.11	0.12	EUR/kWh
Hydrogen	8.67	2.47	EUR/kg
Battery	140	70	EUR/kWh
H ₂ Tank	580	290	EUR/kg
Fuel Cell System	130	33.5	EUR/kW

3.2.2 Potential in 2030

The *Potential* scenario assumes equally good development for all technologies until 2030. This is accompanied, above all, by cost reductions. The technology costs for batteries (70 EUR/kWh), hydrogen tanks (290 EUR/kg) and fuel cell stacks (33.5 EUR/kW) are approaching the material costs from today's perspective. The electricity is produced primarily with renewable energies (0.02 kg CO₂-eq./kWh) at a cost of 0.12 EUR/kWh [197]. Hydrogen is produced with electrolysis powered with renewables and thus reduced environmental impact [195, 198]. The electrolysis, as well as the e-fuel plants, run under high utilization in sunny regions of the Middle East and North Africa, which significantly reduces the production costs for hydrogen (2.47 EUR/kg) and synthetic diesel (1.21 EUR/L) [31, 196]. The environmental impact of synthetic diesel is based on data from the 2020 GREET model [199, 200].

4 Eco-Efficiency Assessment

Although the system boundary expands beyond it, the vehicle concept—in particular, the powertrain—is at the center of this work. However, the urgency to improve the transport sector’s environmental footprint also requires recommendations to policy and decision-makers. To support technical and political decisions, the tool considers vehicle concepts beyond their state of the art to map their technological progress. Therefore, the developed approach uses a genetic (or evolutionary) algorithm that optimizes each vehicle concept, improving its performance, and, thus, showing its technological progress. In the sense of an ex-ante LCA, this improvement is essential to derive consistent policy recommendations [22]. The optimization generates vehicle concepts that fulfill the trade-off between ecological and economic performances to varying degrees. It, thus, answers the question, of to which extent zero-emission vehicles solve the conflict between these two objectives. The methodology highlighting the novelty of using vehicle concept optimization as a prospective eco-efficiency assessment was previously published [56].

Figure 4.1 depicts the overall modeling concept (►). In the beginning, the vehicle model simulates the energy consumption for a given set of vehicle parameters and a defined driving cycle (I). The life cycle costing (IIa) and life cycle analysis (IIb) utilize the resulting energy consumption supplemented with component-specific models. As a result, the TCO and the environmental impact index—the weighted sum of environmental impacts—are combined as an eco-efficiency assessment (III). The outer loop (◀) feeds the eco-efficiency results into the optimization algorithm, which iteratively adapts the vehicle parameter inputs to step I. The following sections provide detailed descriptions of steps I-IV.

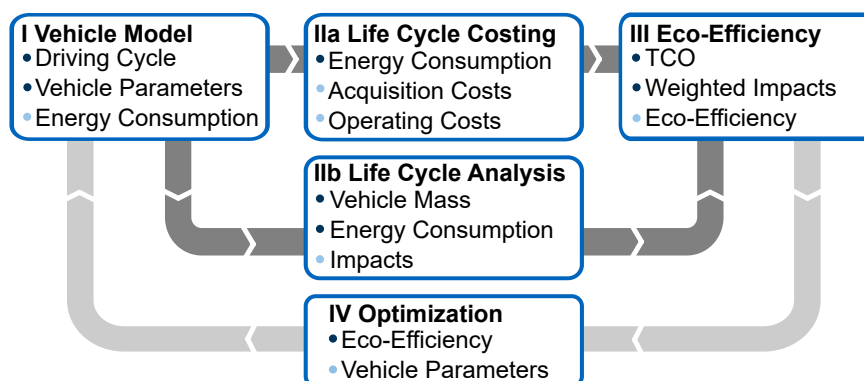


Figure 4.1: Vehicle concept optimization methodology with model flow ►, optimization loop ◀, essential inputs ●, and outputs ● of each process step [56].

4.1 Life Cycle Costing

A life cycle costing calculation captures the economic dimension as described in Figure 4.1 Ila. The energy consumption, as a crucial input, is the vehicle model's output and is described separately in Section 4.3. The life cycle costing builds on the work of Fries [53] who implemented a parametrizable total cost of ownership model in Matlab/Simulink. His model follows the calculation as described by Wittenbrink [52] and consists of four cost aspects:

- Variable costs
- Fixed costs
- Personell costs
- Overhead costs

A publication preceding this work [56] expanded Fries' model, which only covered the use phase, to account for the whole vehicle life cycle of ten years. Additionally, the component cost data was updated [196] to account for recent development in particular for zero-emission technologies. The Model's key assumptions are summarized in this section for ease of understanding. For details refer to the mentioned publications [53, 56, 196].

Apart from the energy consumption, the daily driving time and range are important inputs to calculate the variable costs. The latter is particularly critical for battery-electric vehicles. To account for the negative effects of low range, Fries' model was extended to either use for the total daily-driven distance, based on average speed and working hours, or the maximum possible range, which is limited by the battery capacity, depending on which is lower. This corresponds to the assumption that the vehicles are only charged in depots and overnight. The assumption is motivated by the limited charging power for BET, which does not yet allow sufficiently fast charging during rest breaks [201]. The daily-driven distance is the net driving time available multiplied by the average speed. Additional variable costs include maintenance such as tire exchange, which is based on a lifetime service of 140 000 km and 450 EUR per tire. Further costs are summarized as a lump sum of 0.13 EUR/km [202]. Except for energy consumption, the variable costs remain equal for all vehicle concepts.

Comprising the majority of the fixed costs, the acquisition costs are modeled for each set of vehicle parameters. The underlying models are component-specific regressions as proposed in the works of Fries [53, 54, 203]. His cost model was updated, as described in König et al. [196]. To account for the total vehicle cycle, an operation of ten years is assumed after which the residual vehicle value is zero [56]. For electric vehicle concepts, at a state of health of 80 %, the battery is replaced and transferred to recycling. Under these conditions, Rohr et al. [204] estimated the battery's residual pack value of 25 EUR/kWh_{gross} and 80 % state of health. The model assumes a battery cycle life of 3000 full cycles and a complete battery swap after the state of health falls below the threshold during the vehicle's operating time [205]. The model developed by Lajunen et al. [206] estimates the state of health in correlation with an average battery load, resulting from the vehicle operation. A discount rate of 3.5 %/a accounts for the time value of the vehicle acquisition [202].

The personnel and overhead costs are equal for all vehicle types. For details refer to the model described in an earlier publication [56]. All costs are given in EUR₂₀₂₀ and without considering inflation.

4.1.1 Infrastructure Costs

Section 2.3 showed that zero-emission heavy-duty vehicles require dedicated infrastructure. On the one hand, except for synthetic fuels, diesel refueling stations cannot be used further. On the other hand, the current zero-emission passenger car infrastructure is of limited use for heavy-duty applications.

Current hydrogen fuel stations for passenger cars already operate at 700 bar. However, the low flow rates limit the application for heavy-duty vehicles. Therefore, an additional system operating at 350 bar is currently being installed along German highways, despite the lower energy density and, thus, limited future viability [207].

Charging infrastructure can potentially be shared among passenger cars and heavy-duty vehicles, due to equal standardization (*Combined Charging System* and *Megawatt Charging System*) [201]. However, the higher energy demand, and thus larger battery capacity, leads to higher charging powers than passenger cars. Otherwise, satisfactory charging times cannot be achieved. For an overnight charging process, a power of 150 kW is sufficient to charge a long-haul vehicle (450 km range; approximately 500 kWh) in under nine hours [55, 144]. More frequent and shorter charging times require higher powers that are currently not available at large scale and—as a simplification—not considered in the infrastructure cost model [55].

Dynamically charged concepts, such as overhead wires or inductive charging, require a dense network of infrastructure. Regardless of the power transfer, several thousand kilometers of road network must be electrified in order to provide sufficient infrastructure. Depending on the use case, additional, charging infrastructure is required to charge the vehicles while they are not driving (e.g., overnight).

The developed model does not consider infrastructure further upstream: The expansion of renewable energies, the installation of electrolyzers for green hydrogen production, and the construction of plants for the synthesis of liquid fuels are not explicitly modeled. However, the costs for these measures are indirectly present in the production costs of the individual energy sources, whose system boundary in each case extends to distribution in the respective vehicles. Analogously, the losses during transport and refueling are already included in the fuel costs and represent average values independent of the storage technology. Table 4.1 summarizes the cost assumptions for the presented infrastructure.

Table 4.1: The cost per unit and the respective amount of energy that can be provided daily are required to obtain the vehicle-specific and total infrastructure costs. The costs are based on two prepublications [196, 55]. The selected assumptions for the model are marked **bold**.

Infrastructure Type		Investment Costs	Unit	Daily Energy*
E-Road	Catenary	2 - 2.5	MEUR/km [†]	n.a.
	Conductive	0.5 - 1.2	MEUR/km [†]	n.a.
	Inductive	2.6 - 3.6	MEUR/km [†]	n.a.
Charging Point	22 kW AC	5500	EUR	220 kWh/d
	24 kW DC	18 500	EUR	240 kWh/d
	50 kW DC	33 500	EUR	500 kWh/d
	150 kW DC	59 000	EUR	1.5 MW h/d
Fuel Station	Hydrogen dispenser	1.25	MEUR	5 MW h/d

* assuming 10 hours per day utilization; [†] costs per lane

As infrastructure is shared among multiple vehicles, it is necessary to convert the associated costs to a per-vehicle base. A model presented in a previous publication, uses the vehicle-specific energy demand E_{vehicle} to obtain the lower boundary of the infrastructure, satisfying this demand [55]. As shown in Equation (4.1), the resulting infrastructure costs C_I can be adapted for charging points and refueling stations. While each charging or refueling point can be used by a single vehicle, electrified

roads will be used by several vehicles at the same time. Consequently, dynamic charging costs require a specific amount of vehicles to be converted in per-vehicle costs.

$$C_I = \frac{E_{\text{vehicle}} d_{\text{daily}}}{E_{\text{infrastructure}}} C_{\text{Unit}}, \quad (4.1)$$

- C_I = Infrastructure costs on EUR
- E_{vehicle} = Vehicle energy consumption in kWh/km
- d_{daily} = Daily driving distance km/d
- $E_{\text{infrastructure}}$ = Specific, daily energy supply in kWh/d
- C_{Unit} = Specific infrastructure costs in EUR.

4.1.2 National Vehicle Stock

Estimation of vehicle stock is necessary for two reasons: 1) when infrastructure is used by several vehicles at the same time, and 2) in order to obtain a macroeconomic perspective in terms of infrastructure investment. For the former, the investment per vehicle decreases if more vehicles share the infrastructure. For the latter, a larger vehicle stock requires more infrastructure investment to satisfy the (energy-)demand as described in the previous section. Consequently, there is a dependency on economic performance and vehicle stock.

The German heavy-duty vehicle market is a lead market with approximately 25 % of the total European market share, followed by France and the UK with 15 % share each [208]. Two German heavy-duty OEMs (*Volkswagen/Traton* and *Daimler*) comprise 53 % of the European vehicle sales. For this reason, the German market does not only represent technological leadership but is also representative of the European market [209]. Accordingly, the market has an important role to play in meeting climate targets and the necessary transition to zero-emission powertrains.

In order to assess the development of the German commercial vehicle market the German Industry Association (Ger.: Bundesverband der Deutschen Industrie [BDI]), the German Ministry of Economics and the Ministry of Transport commissioned one study each [128, 210, 211]. Five future scenarios (Figure 4.2) have emerged from these studies to inform policy decisions:

- 80% climate protection path [210, p. 6]
- 95% climate protection path [210, p. 6]
- Climate Protection Program from Prognos study [211]
- BCG scenario E (Electrification) [128]
- BCG scenario K (Alternative and E-Fuels) [128]

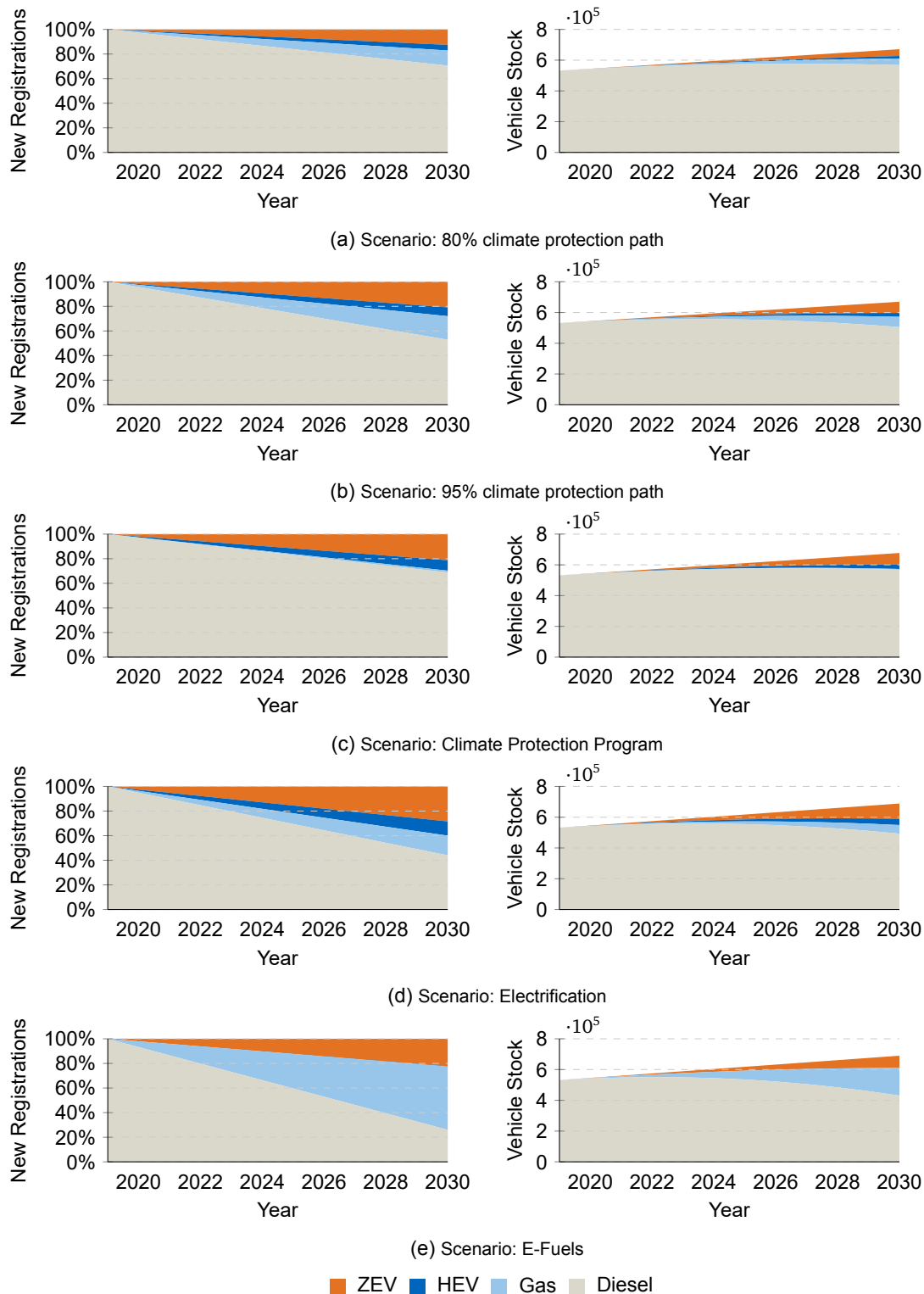


Figure 4.2: Assuming average, annual new vehicle registrations, the vehicle stocks from the five scenarios (right column) are converted to new vehicle registrations (left column). This enables a comparison with the penalties stipulated in EU regulation for exceeding emission limits. Kemmler et al. [211] developed the 80 % (a) and 95 % (b) reduction path scenarios for the German Ministry of Economics. Gerbert et al. [210] created the Climate Protection Program (c) on behalf of the German Industry Association. The electrification (d) and the carbon neutral fuel (e) scenario were developed by Kirchner et al. by order of the German Ministry of Transportation. It can be seen that the newer (c,d) or more ambitious scenarios (b) require higher electrification rates and a stronger transformation of the vehicle stock.

For details on the scenarios and their development, refer to the respective sources [128, 210, 211]. While all these scenarios forecast the vehicle stock composition in the year 2030, they do not disclose the temporal change, for example in new vehicle registration. However, the European CO₂-reduction targets for heavy-duty vehicles refer to new vehicle registration. Accordingly, OEMs are expected to develop a strategy that leads precisely to the achievement of these goals and, thus, the avoidance of the penalties. It is, therefore, necessary to compare the scenarios from the studies, with the EU regulation and evaluate them in terms of penalties.

The European legislation does not differentiate between zero-emission vehicles, as the three studies do. Instead, BET, FCET and OBET are all attributed 0 g CO₂/t km. For this reason, these technologies are summarized as zero-emission vehicles (ZEVs) (Figure 4.2). Based on average new vehicle registration and assuming a linear development of newly registered vehicles, the left column in Figure 4.2 shows the development of new registrations for each concept. Accordingly, the right column shows the total vehicle stock. The resulting deviation between the studies and the calculated vehicle stock is between 1 % and 4 % and, thus, considered sufficiently accurate. Appendix D summarizes the assumptions to obtain the missing data regarding new vehicle registrations.

To determine the amount of the penalties for exceeding the emission limits, Mustafić [117] used the new registrations to obtain an average European commercial vehicle OEM. For this purpose, an average vehicle sales value was calculated on the basis of the production figures of the European OEMs. Appendix D shows the underlying data and the resulting average OEM. In order to accurately reflect the vehicle categories, the studies' categories were leveled to match the specific vehicle concepts of the regulation (Table A.1). Mustafić [117] used the *LOTUS* simulation model [116] to derive each concept's energy consumption and further calculate the respective penalty.

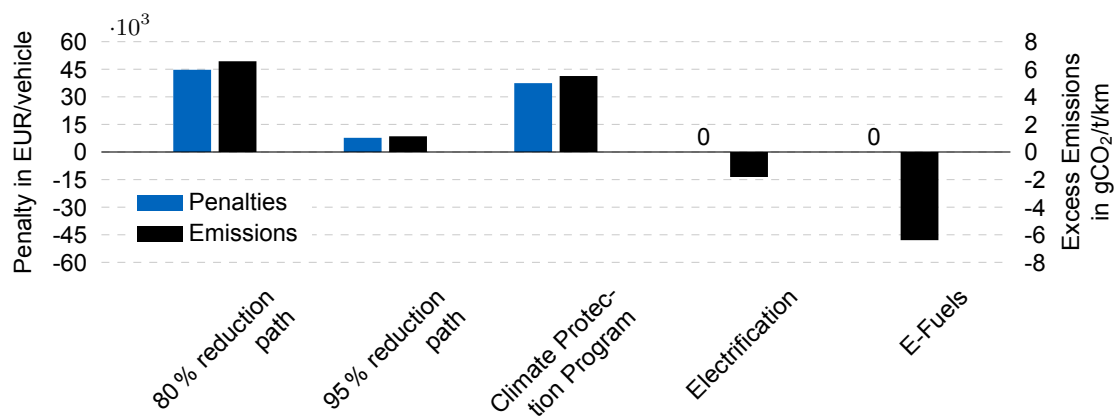


Figure 4.3: Different penalties per vehicle arise in the year 2030 due to varying excess CO₂-emissions. Penalties cannot fall below zero. Only the scenarios *Electrification* and *E-Fuels* achieve sufficient CO₂-reductions to avoid penalties.

Figure 4.3 shows the resulting penalty (■) and emissions (■) for each scenario. It becomes evident that both scenarios (BCG E and K) by Kirchner et al. [128] avoid penalties while the other three scenarios lead to significant additional costs. It is striking that the *carbon neutral fuel* scenario has the greatest savings in emissions, although the share of ZEV is low. This is achieved by the largest share of gas vehicles, lowering the total tank-to-wheel emissions. Achieving such a high share requires every second newly registered vehicle in 2030 to be gas-powered. Given that in 2020, their share was 2 % [212], this scenario requires the largest transformation, which is why this scenario is not considered further. As it is unlikely that OEM pursue any scenario resulting in fines, the former three scenarios

are also not further assessed. Consequently, only the electrification scenario (BCG E) will be further considered for the macro-perspective eco-efficiency assessment.

4.1.3 Overhead Catenary Costs

With data on new vehicle registration and vehicle stock trends, a model can convert e-road infrastructure costs $C_{I, e-road}$ to vehicle level (Equation (4.2)). To obtain the length of the e-road network, a ratio b_{e-road} relates the total road network to the expansion stages described in Section 2.3.3. To obtain a temporal resolution, linear infrastructure development is assumed. The National Platform Future of Mobility estimates the upper expansion speed at 500 km/a for the German road network (ca. 130 000 km) [213]. This equals an electrification rate of $\dot{b}_{e-road} = 4\%/a$.

$$C_{I, e-road} = \frac{b_{e-road} d_{road, total} C_{Unit}}{n_{vehicles}}, \quad (4.2)$$

where:

- $C_{I, e-road}$ = E-road infrastructure costs EUR
- b_{e-road} = E-road share of total road in %
- $d_{road, total}$ = Total road network length in km
- C_{Unit} = Specific infrastructure costs in EUR/km
- $n_{vehicles}$ = Number of e-road capable vehicles.

4.1.4 Concept of System Costs

The costs per vehicle described in the previous sections are an economic assessment from a business administration—or microeconomic—perspective. While these costs are highly relevant for OEMs or logistic companies, they are less relevant for policy-makers, because they do not scale to a national or international vehicle stock. Therefore, the system cost concept expands the per-vehicle perspective from a macroeconomic perspective, allowing policymakers to compare vehicle concepts.

A previous publication outlines the concept of system costs [55]. In this publication, the system costs provide a performance indicator to compare vehicle concepts on a national or international level. Therefore, the model relates the TCO and the infrastructure costs to the transportation performance and the vehicle stock, which is regionally confined (e.g., Germany, Europe etc.).

To obtain the system costs, the vehicle-specific TCO_i are multiplied by the transport performance Q_T , measured in tonne-kilometer per year. The performance indicator C_T is comparable to the total, monetary turnover of the transport industry. Based on the vehicle-specific energy consumption, the infrastructure costs are determined from the product of specific infrastructure costs C_I and the total vehicle stock n_{veh} . This relation is given by Equation (4.3). In this context, the system costs estimate a complete exchange of the vehicle stock. The concept-specific transportation demand $Q_{T,i}$ weights the total transportation demand Q_T by the powertrain split (Figure 4.2). This links the economic performance of a single vehicle—including the associated infrastructure costs—with the temporal development of the vehicle stock.

$$C_{S,i} = \overbrace{TCO_i Q_T}^{C_T} + C_I n_{veh.,i}. \quad (4.3)$$

4.2 Life Cycle Assessment

In addition to the life cycle costing, a life cycle assessment is the second component of the eco-efficiency analysis Figure 4.1. As described in Section 2.1.2, the LCA complies with the DIN 14040 and DIN 14044 [58, 59]. With the goal and scope definition as well as the system boundary, Chapter 3 already outlined the first and second steps of the LCA process. Additionally, the functional unit of the assessment is defined as the transport of one ton of goods over a distance of one kilometer [56]. The respective unit is tkm and, therefore, analogous to the TCO, which is measured in EUR/tkm. The subsequent inventory analysis and the selection of impact categories is part of Section 4.2.1 and 4.2.2.

4.2.1 Life Cycle Inventory

The life cycle inventory is necessary to quantify the inputs and outputs, relevant to the product system. Therefore, data must be collected that adequately describes the processes inside the system boundary. A bill of materials (BOM), which contains “component parts, raw materials, and quantities of each needed to produce one final product” [214, p. 529], summarizes this for technical products.

In 1998, Gaines et al. [122] presented a bill of materials for ICE heavy-duty trucks. However, this cannot be used for two reasons: 1) although the general appearance of trucks did not change significantly, this data lacks more than 20 years of technological advancement (e.g., exhaust treatment), and 2) the data address US class 8 trucks and cannot be completely transferred to European vehicles, due to their different cabs and dimensions. To overcome this lack, a life cycle inventory was developed in a previous publication [100].

The developed LCI has two advantages. On the hand, it also includes BET. Additionally, Mauk [215] expanded the model by fuel cell stacks and hydrogen type IV tanks based on Agostini et al. [179] and Simons and Bauer [216]. With this addition, all zero-emission technologies from Section 2.2 can be represented. On the other hand, the LCI links the bill of materials to vehicle-design specific parameters, which is shown in Figure 4.4. Thus, for example, gearbox input torque, the number of gears and transmission ratio can be used to determine the amount of steel, iron and other materials present in the gearbox. This enables the generation of any vehicle concepts with different drive types and design parameters and to transfer it to an LCI. To achieve this, multiple component-based mass models developed by Fries [53] were combined with generic component-based BOMs. For the model’s details, please refer to the previously published LCI [100].

The material mix is the output of the scalable LCI model. Figure 4.5 shows the resulting tractor for the five considered powertrain concepts. The vehicle design parameters for the shown results are summarized in Appendix E. They represent typical long-haul vehicles and—for BET, FCET, and HICET—a range of approximately 400 km. The shown results are an example, of how the scalable LCI links one specific set of design parameters to the output required for further LCA. It should be noted that the model can output any European heavy-duty vehicle design with an error of 5 % regarding material mix [100].

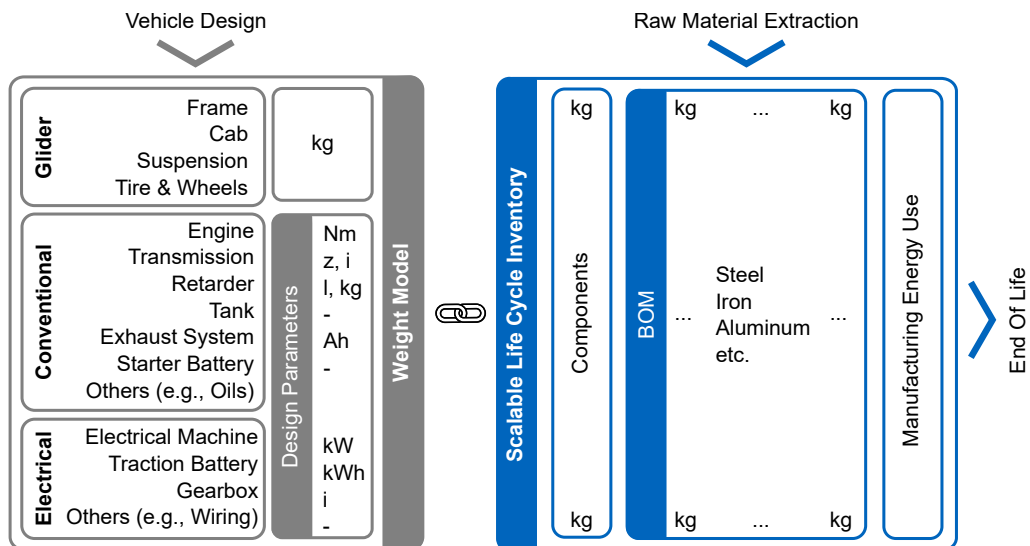


Figure 4.4: To obtain a scalable LCI, component-based mass models convert engineering design parameters (●) to a BOM. Subsequently, the respective materials are assigned and linked to the life cycle impact assessment (●) and, thus, to a database covering all the processes up to the extraction of raw materials. For detailed information refer to the previously published model [100].

It can be seen that the tractor mass of the BET is significantly higher than the remaining vehicle concepts. From Figure 4.5, it becomes evident that the Li-ion battery and the respective materials (aluminum, cathode powder, graphite, and copper) primarily cause the mass increase.

The model uses data for automotive batteries, published by Dai et al. [217], and, therefore, the NMC111 chemistry. Although this chemistry is not state of the art, their LCI is still the most recent, based on real-world data. For other chemistries, only model-based estimates exist. Advanced chemistries allow higher gravimetric energy densities, which is why the share of batteries in the material mix will decrease.

It must be noted that the FCET and HICET do not offer the same range as the diesel, albeit the mass is comparable. A further discussion on the changes in the material mix can be found in the publication [100].

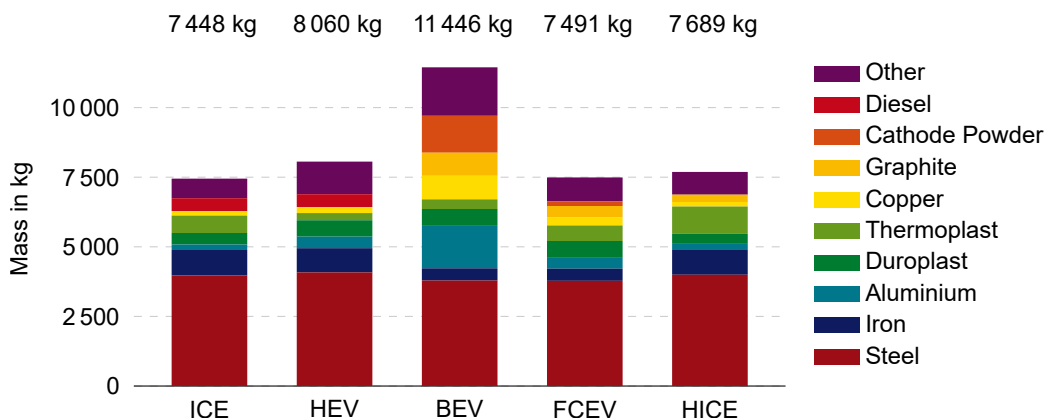


Figure 4.5: The LCI analysis of the absolute material masses shows decreases in steel and iron materials and an increase of battery-related materials (Cathode powder, graphite and aluminum) for the BEV concept. Only materials >5% are shown. Diesel is only present in ICET and plug in hybrid electric truck (PHET), while cathode powder and graphite are only relevant for BET and FCET, although in different quantities.

4.2.2 Life Cycle Impact Assessment

According to DIN EN ISO 14040 [58], the life-cycle impact assessment links the data gathered in the LCI with environmental impact categories (Section 2.1.2). According to the norm, there are three mandatory steps: 1) selection of impact categories, 2) classification based on LCI results, and 3) calculation of impact categories. This work uses the impact categories recommended by the ILCD, which were summarized in Section 2.1.2. To support the process of classification and calculation, different LCA software offer an extensive possibility for modeling. Gordon [218] and Álvarez [219] reviewed several applications with particular attention to applicability in an automotive context. In this context, the LCA software GaBi (Ger.: Ganzheitliche Bilanzierung [GaBi]), is widely used and suitable to answer the questions of this work [220].

To perform the classification (second step), Gordon [218] and Álvarez [219] built a LCA model for a generic tractor with a conventional, hybrid and battery electric powertrain. Mauk [215] expanded their model and added fuel cell-specific components (stack and tank). Because of their technical similarity, the same model represents both, the ICET and the HICET. However, the type IV hydrogen tanks replace the steel tanks of the ICET.

The models consist of multiple connected processes (Figure 4.6), of which there are three types [221, p. 35]. First, aggregated processes map materials, energies, and emissions up to a defined processing step (e.g., semi-finished product or electricity). These processes have a cradle-to-gate system boundary and include LCI data from the database linked to GaBi. For example, aggregated processes describe steel materials from raw material extraction (cradle) to a semi-finished product, ready for machining (gate). These processes only have data outputs and are used as input for other processes. As the second category, basic processes describe a gate-to-gate process and do not contain any LCI data or elementary flows and, thus, no direct emissions. The final assembly step is an example of this. These processes require additional data as input to yield an output—for example, a machined steel part. The third category is partly linked processes, which are a mixture of the other two. They have a cradle-to-gate system boundary but do contain certain inputs. In the given example, a partly-linked milling machining process contains LCI data on energy and lubricant usage but requires an (aggregated) semi-finished steel process as input.

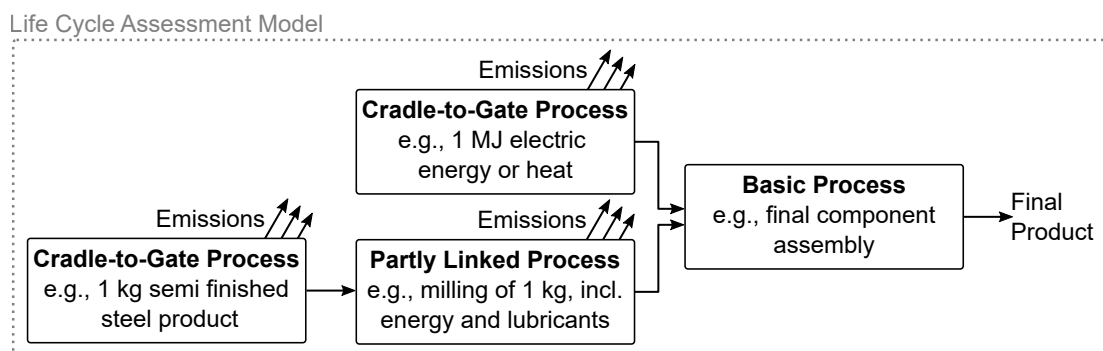


Figure 4.6: A simplified component model illustrates the three process categories in GaBi [221, p. 35]. A basic process itself has no direct emissions. In the assessment, these are only mapped via the upstream chain (i.e., cradle-to-gate processes).

A database contains the information, required to calculate the environmental impacts. Consistent with the system boundary, all built LCA models extend to raw materials and, thus, aggregated processes. This completely maps emissions and environmental impacts at the material level. However, processing and assembly steps are still necessary for the production of components and vehicles. These were either modeled with generic, aggregated processing data provided in the database or with partly linked

processes built on data from the literature. The latter was used primarily for the steps involved in manufacturing and assembling vehicle components and the associated energy input. The pre-published, scalable LCI [100] summarizes the vehicles' manufacturing data.

The *Technical University of Munich's Institute of Automotive Technology* owns licenses for the *thinkstep 2017* [222] and the *ecoinvent 3.3* [194] databases. Both were linked to GaBi and provided the background database for all LCA models. As discussed in previous publications [56, 100], the databases' validity represents a challenge, due to outdated data. However, because technological progress has mainly taken place at the component level (e.g. battery cells), this development is adequately represented via the use of up-to-date LCIs. Namely, the battery [217], electric machine [223], fuel cell system [179], the hydrogen [195] and synthetic fuel [199] pathways build on recent data. In order to represent the end-of-life or recycling of a vehicle, the material flows can be given a negative sign. This closes the material cycle in the material flow balance.

Although GaBi allows parametric modeling, it cannot be used directly as an element of the methodology shown in Figure 4.1. Mainly because there is no interface to external software, Seidenfus [224] transferred the aggregated LCA results to a vehicle simulation framework in Matlab/Simulink. This results in increased flexibility, modularity, scalability and, last but not least, automation capability, which is essential for vehicle concept optimization. However, the step loses the information about the individual elementary flows, which are only contained in the GaBi model. It should be mentioned that this step is only possible because GaBi exclusively represents linear relationships and all environmental factors scale linearly with material and energy demand. Consequently, the results also behave linearly. Since the information on material masses and energy demand is also available in the Matlab framework, the results can be scaled there without the intermediate step of the LCA model and integrated into the overall methodology.

The eco-efficiency assessment requires two additional steps, which are optional in the DIN EN ISO 14040: 1) Normalization of the results' magnitude, and 2) weighting of the results. Both steps follow the procedures described in Section 2.1.3 and 2.1.3. Seidenfus [224] applied the normalization and weighting factors presented in these sections and implemented them into the vehicle simulation framework. Both, the life-cycle costing and the life-cycle assessment, require vehicle-specific energy consumption as an input variable. This is calculated by the long-haul truck simulation *LOTUS* [116], whose structure is described in the following chapter.

4.3 Longitudinal Vehicle Simulation Model

Energy consumption is a crucial input to calculate a vehicle's economic and environmental performance. The fuel costs of a current diesel vehicle account for approximately one-third of its TCO [225]. Fuel consumption also dominates the use phase and, due to the high mileage, the environmental impact. An eco-efficiency assessment for heavy-duty vehicles, therefore, requires an adequate energy consumption model.

Every moving vehicle is subject to driving resistance forces and requires energy to overcome them. Equation (4.4) is a general description of these resistance forces [226, p. 23].

$$F_{\text{tot}} = \overbrace{m_{\text{veh}}g \cos \alpha}^{F_r} + \overbrace{m_{\text{veh}}g \sin \alpha}^{F_g} + \overbrace{\frac{1}{2}\rho c_d A v^2}^{F_a} + \overbrace{\lambda m_{\text{veh}} a}^{F_m}. \quad (4.4)$$

In addition to the mass-dependent rolling resistance F_r and the gravitational force F_g , there is also the velocity-dependent aerodynamic drag F_a . The last term describes the acceleration resistance F_m , which must be overcome to accelerate the vehicle. It depends on the vehicle mass and represents the inertia of the moving parts. Figure 4.7 shows the driving resistance forces for four typical heavy-duty use cases. In contrast to passenger cars, mass-related forces comprise the majority of energy consumption.

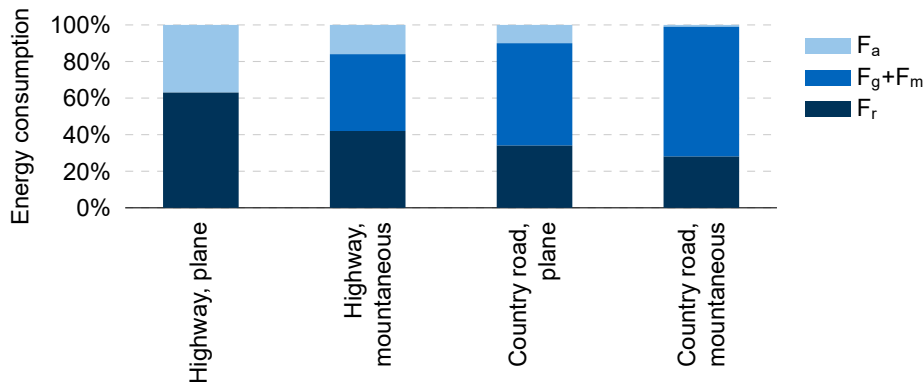


Figure 4.7: Energy consumption per driving resistance force of a 40 t diesel tractor for different types of operation. The vehicle cannot recuperate. The average velocity on the highway is 72 km/h, and 57 km/h on the country road [111, p. 37].

A longitudinal simulation implements the driving forces to calculate the energy consumption for any speed v , slope α , and acceleration a . [226, p. 38]. Consequently, the total mechanical power P_{tot} can be derived:

$$P_{\text{tot}} = F_{\text{tot}} v. \quad (4.5)$$

Considering the powertrain's efficiency η_{veh} yields the total energy E_{tot} :

$$E_{\text{tot}} = \int \frac{P_{\text{tot}}}{\eta_{\text{veh}}} dt. \quad (4.6)$$

Guzzella and Sciarretti [226, p. 34-41] distinguish between a (quasi-)static and a dynamic approach, which are both shown in Figure 4.8 a) and b), respectively. Both have a driving cycle in common, which must be known in advance. The key difference between the two simulations is the assumption that in a quasi-static simulation, the vehicle can reach *any* operating point of the driving cycle. Due to the low power-to-weight ratio (truck: 5 kW/t to 11 kW/t vs. car: >40 kW/t [227, p. 117, 228, p. 15]), this assumption is not valid for commercial vehicles. Especially on uphill gradients, trucks do not reach the desired speed, for example, 80 km/h on highways. Consequently, the quasi-static approach is not suitable (without adaptations) for the simulation of heavy-duty vehicles. Süssmann [119] discussed this issue in detail and derived the need for a dynamic simulation to accurately model driving characteristics and energy consumption.

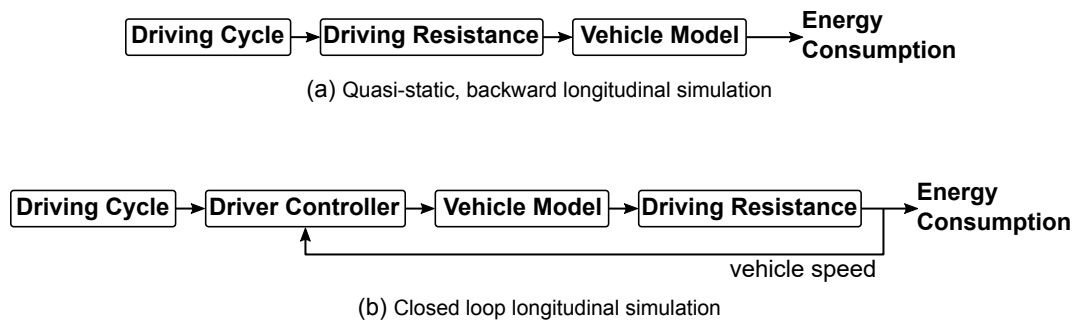


Figure 4.8: The diagrams show two simplified approaches to model a vehicle's energy consumption. The quasi-static approach (a) calculates the consumption based on static operating points, which result from the driving cycle, and efficiency or consumption maps. The dynamic approach (b) uses a driver controller, which accelerates the vehicle to minimize the deviation between the target and actual speed.

While the static approach essentially maps Equation (4.4), the driving resistances in the dynamic approach take the form of differential equations of motion:

$$m \ddot{x}(t) = F(x(t), u(t)), \quad x(t) \in \mathbb{R}^n, u \in \mathbb{R}^m. \quad (4.7)$$

This means that the force depends on position $x(t)$, tractive forces $u(t)$, and time t and yields the acceleration $\ddot{x}(t)$, which in turn depends on time. The considered system *vehicle* is both non-linear and discontinuous and, thus, cannot be solved analytically. The downside of a closed-loop simulation is the high computational effort and associated long computation times.

The EU regulation 2017/1151 stipulated that starting in January 2019, emissions from heavy-duty vehicles should be calculated and certified using a simulation program [229]. The *Graz University of Technology* was commissioned to develop the Vehicle Energy Consumption Calculation Tool (VECTO) for this purpose. Additionally, standardized test procedures to parametrize the models, generic data sets for driving cycles and driver behavior, and validation procedures were developed [230]. VECTO is a backward simulation with the ability to include driver behavior, which is primarily performed by limiting the acceleration [230, p. 35]. The tool has two main advantages: 1) the quasi-static simulation results in fast computation times and 2) all component models and the generic data are validated. However, VECTO cannot be used for this work because it does not offer any interfaces for automation (e.g., optimization algorithms) or extensions such as an eco-efficiency assessment. Furthermore, it currently does not include any zero-emission powertrains such as BET or FCET. The regulation aims to certify tank-to-wheel emissions, whereby these two powertrains are classified as zero-emissions and, consequently, do not have to be included in the simulation.

Süssmann [119] developed a dynamic, heavy-duty vehicle model in Matlab/Simulink to evaluate the fuel-savings of different measures, reducing the single driving forces. He used quasi-stationary engine models that utilize specific fuel consumption maps of EURO V combustion engines. The model calculated the consumption of a diesel vehicle on a real route with 2 % deviation from the measurement [119, p. 108]. In multiple works, Fries et al. [53, 54, 203, 231–233] further developed the model to include new powertrains (gas, dual-fuel and hybrid), an operating strategy, and a TCO model. Analogously to Süssmann, Fries implemented quasi-stationary efficiency maps for gas-powered engines, electric powertrain components and the transmission. Both, the consumption and cost results, are within the bounds of a validation space derived from real, published test drives and expert statements [53, p. 79]. Nevertheless, the closed-loop approach yields long computation times. The diesel model, for example,

requires—depending on the hardware—approximately 1 min, while VECTO requires approximately 3 s per simulation run.

In contrast to VECTO, the model's source code is open-source available, which allows diverse interfaces and extensions. Apart from the eco-efficiency assessment, the work at hand expanded certain aspects of Süssmanns and Fries' model, which are described in Section 4.3.1 to 4.3.4. The simulation model is previously published GitHub under the name *LOTUS* and contains the eco-efficiency framework of this work in addition to the publications by Süssmann and Fries [116].

Furthermore, a preliminary publication updates the map of internal combustion engines [234]. The *Institute of Internal Combustion Engines* at the *Technical University of Munich* developed and optimized a six-cylinder EURO VI engine model. The optimization of engine design parameters resulted in an induced best-point efficiency of 53 % ($\hat{=} 188 \text{ g/kWh}_{\text{Diesel}}$). The engine model's output provides a suitable input for the *LOTUS* simulation.

Until the introduction of VECTO, no standardized driving cycles, reflecting the use of commercial vehicles, existed. Instead, stationary engine test cycles determined the values of exhaust emissions. Therefore, Süssmann and Fries both derived their own driving cycles. While Süssmann recreated a route in Germany [235], Fries et al. [236] used a statistical representation of logged fleet test data. Assuming that the VECTO driving cycles set the new standard in the industry, their driving cycles were replaced with the VECTO driving cycles. A preliminary publication showed the distance-based version of the VECTO long-haul and regional delivery cycle, which can also be seen in Figure 4.9. Due to the focus on long-haul applications, the regional delivery cycle is also rejected in this work but included in the *LOTUS* GitHub repository [116].

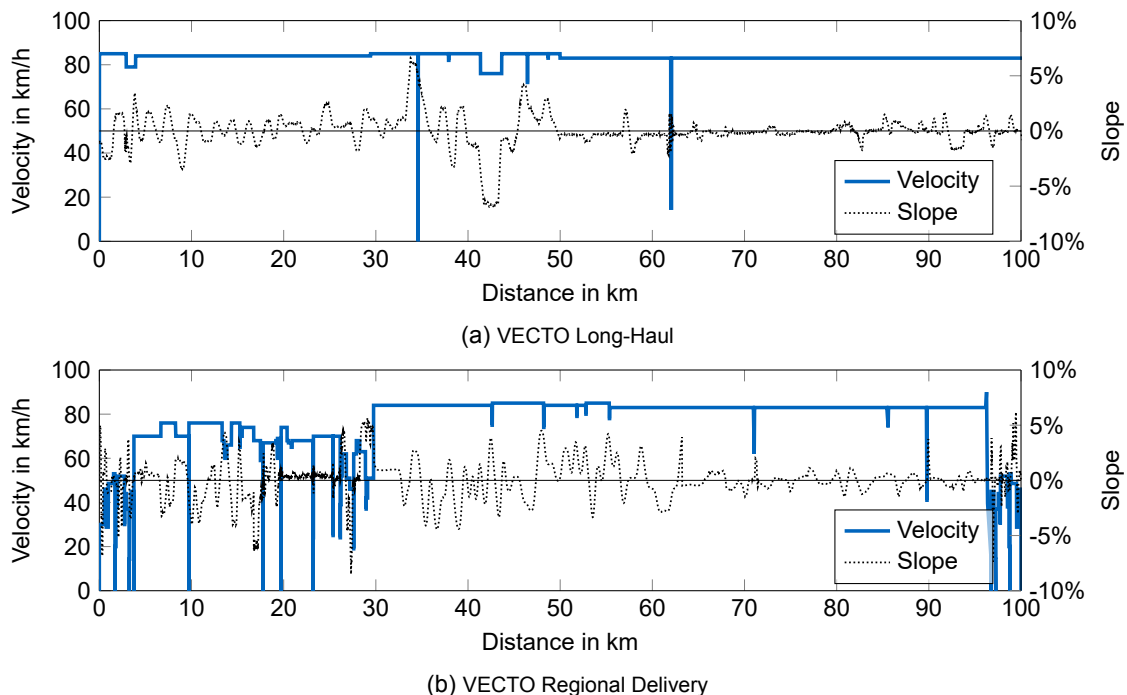


Figure 4.9: The speed profile and road gradient of the VECTO driving cycles characterize two use cases. The long-haul cycle (a) has an average velocity of 83 km/h and a stopping time of 67 s during two stops. The regional delivery cycle has a lower average velocity (66 km/h) but a higher dynamic with 11 stops and 746 s stopping time. Both cycles have a similar, average road gradient of 6.6 % and 6.2 %, respectively.

To be consistent and comparable with VECTO, the payload is also set to the according value (19.3 t). Table 4.2 summarizes the other vehicle parameters included in the driving resistance equation. The

values for the frontal area and drag coefficient are taken from Fries [53]. Verbruggen et al. [237] and Naunheimer [227] estimate the rolling drag coefficient at 7 ‰ and, thus, higher than Fries (5.2 ‰) [53]. *LOTUS* utilizes the more conservative value. Naunheimer [227] estimated the (dynamic) tire radius as well as the drivetrain efficiency, implemented in *LOTUS*. The transmission efficiency depends on the selected gear, modelled by an efficiency map [53, 227].

Table 4.2: Constant vehicle parameters to calculate tractive forces with the closed-loop longitudinal simulation model *LOTUS*.

Parameter	Symbol	Unit	Value	Source
Payload	m_{payload}	kg	19 300	[230]
Frontal area	A	m ²	10.2	[53]
Air drag (Pantograph)	c_D	-	0.53 (0.55)	[53]
Rolling drag	c_R	-	0.007	[227, 237]
Tire radius	r_{Tyre}	m	0.4465	[227]
Efficiency axle-drive	$\eta_{\text{Axle-drive}}$	-	0.98	[227]
Efficiency transmission	$\eta_{\text{Transmission}}$	-	0.96–0.99	[227]

4.3.1 Non-CO₂ Emissions

Neither Süssmann nor Fries nor VECTO addressed non-CO₂ emissions such as particulate matter, nitrogen oxides or hydrocarbon (HC). As shown in Section 2.1.2, these emissions have a major impact on ecosystems and human health, which is why they are also strictly regulated in many countries. The emission regulations include carbon monoxide, nitrogen oxides, hydrocarbons, and particulate matter. In Europe, EURO I to EURO VI and, expected between 2025 and 2030, the future EURO VII regulates these emissions for all vehicle classes [238, 239]. Similarly, the EPA defines emission standards for the United States of America, although there can be stricter local deviations (e.g., California) [240, 241]. Comparable standards exist in China, Japan, India, and other countries [242].

Before EURO VI, technical regulations for heavy-duty vehicles were based on the Worldwide Harmonized Stationary Cycle (WHSC) [238]. Introduced in 2011, the Worldwide Harmonized Transient Cycle (WHTC) replaced the stationary for heavy-duty vehicles [243]. Both test procedures are engine-only dynamometer tests. The effective EURO VI norm measures emissions in relation to the vehicle's fuel consumption in g/kWh or ppm/kWh, whereby the energy refers to the engine work in kWh. In contrast, CO₂ emissions are measured in absolute mass in kg [243, p. 75f] or related to the transport performance kg CO₂/t km.

Emissions from non-combustion-related sources, such as tire and brake wear are currently not regulated [244]. Both cause a significant amount of particulate matter, which, combined, are of the same magnitude as EURO VI exhaust emissions (8 mg/km) [244]. According to Grigoratos et al. [244], brake wear comprises 16 % to 55 % and tire wear 5 % to 30 % of the total PM₁₀-emissions. Aerosols from road dust and dirt cause the remaining amount (28 % to 59 %). The exact mechanisms are not fully understood, which explains the large variance. Furthermore, it is unclear how and to what extent the particulate matter is distributed in the air [244, p. 42].

Pan [245] reviewed (semi-)empirical non-CO₂ emission models and evaluated their integration in *LOTUS*. Regarding NO_x, PM, and HC, three models represent dynamic driving conditions and, thus, can be considered. The Comprehensive Modal Emissions Modeling is a physically-based approach

that calculates the emissions empirically in relation to the driving dynamics (speed, acceleration) and the engine's operating conditions [245, 246]. In contrast, the US EPA's Motor Vehicle Emissions Simulator (MOVES) is an empirical model that uses the vehicle-specific power $VSP = F_{tot} v_{veh}/m_{veh}$ in kWh/t as input. The model developed by Zhang et al. uses a similar approach with input data from a Chinese fleet test [247].

Pan [245] implemented these three models into the *LOTUS* framework. Table 4.3 summarizes the models' characteristics and the results from *LOTUS*. For reference, the EURO VI regulation is also shown. It can be seen that all models yield values below the emission regulation, which can be explained by different operating conditions. While both test cycles demand a high average engine torque, the average power during the VECTO cycle is higher (34 % vs. 25 % for a standard tractor with 2100 N m and 320 kW). In conclusion, differing test scenarios, limitations in data accessibility and lack of validated (EURO VI) experimental data limit the application of semi-empirical models. Altogether, Pan's [245] results underestimate EURO VI standard. To implement the more conservative values, the EURO VI limits were implemented in the LCA use-phase model.

Table 4.3: Pan's [245] study distinguishes four types (CO, HC, NO_x, PM) and three sources (exhaust, tires, brakes) of non-CO₂ emissions. The simulated exhaust emissions are all lower than the WHTC-test limits. The results for tire and brake wear show a large scatter, as well as a large deviation from the literature and thus a high uncertainty. [Note: FR=Fuel rate; VSP=Vehicle Specific Power]

Name	Source	Input	Emission			
			CO	HC	NO _x	PM
Exhaust Emissions in g/kWh						
EURO VI WHSC	[243]		1.50	0.13	0.40	0.01
EURO VI WHTC	[243]		4.00	0.16	0.46	0.01
CMEM	[246]	FR, Speed, Acceleration	1.38	0.13	0.16	-
MOVES	[248]	VSP, Speed	0.84	0.01	0.72	0.01
Zhang et al.	[247]	VSP	0.71	0.03	0.26	-
Tire Wear in g/km						
Lu et al.	[249]	PM ratio	-	-	-	8.90
MOVES	[248]	Speed	-	-	-	19.87
Pan	[245]					40.28
Brake Wear in g/km						
Iijima et al.	[250]	Speed, Braking Duration	-	-	-	1.99
MOVES	[248]	VSP, Speed	-	-	-	102.60
Pan	[245]					74.55

In the same way, Pan [245] implemented two empirical models each for brake and tire wear. The MOVES model includes calculation methods for both emission types and is also based on the vehicle-specific power. The model by Lu et al. [249] uses a statistical distribution of particle size. In combination with average tire wear rates, the mass of PM₁₀ can be derived. However, this neglects the vehicle's driving dynamics.

Iijima et al. [250] derived an empirical model for brake wear based on experimental brake dynamometer data. The model enables the calculation of individual braking processes depending on the vehicle

parameters and speed. Because no regulation for non-exhaust PM-emissions exists, Table 4.3 shows the average value for tire and brake wear based on the Pans [245] literature review. It becomes apparent that the models deviate and none of them matches the average literature values. On the one hand, different driving conditions and vehicle parameters explain this behavior. On the other hand, the approaches differ in their level of detail. None of the models can be validated for the given use case of European long-haul trucks.

Altogether, there is a high uncertainty associated with the use of empirical models for non-CO₂ emissions. Regarding exhaust emissions, the more conservative—compared to the simulation results—regulation values were used. This is also true in comparison to the real-driving emissions for EURO V and EURO VI commercial vehicles measured by Ko et al. [251]. Due to their high uncertainty, PM emissions from tire and brake wear are subsequently neglected. The deviation due to the neglect of tire wear is identical for all vehicle concepts and, thus, has no effect on the (relative) overall results. Brake wear also occurs in all vehicle concepts, but can vary in intensity due to recuperation. Only the model of Iijima et al. [250] can depict this relationship. However, the model is two orders of magnitude below the average literature values, and, therefore, the overall error is negligibly small.

4.3.2 Fuel Cell Electric Vehicle Model

To enable *LOTUS* to simulate fuel cell vehicles, Weiß [252] has integrated a fuel cell model. For this scope, he added the generic fuel cell stack model developed by Njoya et al. [253], which was already applied for passenger vehicles [254]. The electric components modeled by Fries [231] provide the remaining powertrain. Due to efficiency advantages, the *LOTUS* fuel cell model uses the central drive topology with a fixed gear ratio, as discussed in a previous publication [138]. Figure B.1 shows these topologies, and, for reference, other topologies.

The model only operates in the Ohmic region of the polarisation curve (Figure 2.9), thus neglecting activation and mass transport losses. A PT1 member models the stack dynamics.

Because it is based on existing data sheets, the electrical equivalent circuit requires only a few parameters to simulate a state-of-the-art fuel cell (proton exchange membrane). Njoya et al. [253] achieved a stack voltage accuracy between $\pm 1\%$. As parametrization, the model requires two cell-characteristic tuples ($[U_{\text{nom}}, I_{\text{nom}}]$ and $[U_{\text{max}}, I_{\text{max}}]$) from two regions of the polarization curve as inputs. Additionally, the voltages at 0 A and 1 A, U_0 and U_1 , are required. Typically these can be obtained from data sheets but in order to enable a scalable approach, the inputs are reduced to two—vehicle concept defining—stack-parameters:

- Nominal power $P_{\text{nom, stack}}$
- Nominal voltage U_{nom} .

These two parameters yield the nominal stack current I_{nom} (Equation (F.1)). The electrochemical correlations calculate the remaining unknown input variables, which were implemented in *LOTUS* by Weiß [252]. The model of a 50 kW fuel cell [253] as well as experimental data [255] provide assumptions for technical specifications of the fuel cell that cannot be calculated with the aforementioned correlations.

Consequently, the open circuit voltage can be derived as:

$$U_0 = U_{\text{nom}} + N b_{\text{Tafel}} \ln \frac{I_{\text{nom}}}{i_0} + R_i I_0, \quad (4.8)$$

Equation 4.8 requires further parameters that can be derived from electrochemical relations:

- Cell surface A
- Number of cells N
- Tafel slope b_{Tafel}
- Inner resistance R_i .

Equation (F.2) - (F.5) show their derivation based on physical relations. The Butler-Volmer equation (Equation (F.6)), which describes the reaction kinetics, can calculate the cell exchange current $i_0 = \frac{I_0}{A}$. Here, the hydrogen concentration- and temperature-dependent exchange current can be considered as a measure of the reaction speed [255, p. 71]. Consequently, all parameters are known in order to derive the characteristic voltages U_1 and U_{end} (Equation (4.9) and (4.10)). The stack current at the end of the Ohmic region I_{end} depends on the stack surface A (Equation (F.7)). Appendix F summarizes all derived formulas and assumptions for the fuel cell model.

$$U_1 = U_{\text{nom}} + N b_{\text{Tafel}} \ln I_{\text{nom}} + R_i I_0, \quad (4.9)$$

where:

U_1 = Cell voltage at 1 A.

$$U_{\text{end}} = U_0 + N b_{\text{Tafel}} \ln \frac{I_{\text{end}}}{I_0} + R_i I_{\text{end}}, \quad (4.10)$$

where:

U_{end} = Maximum cell voltage.

As discussed in Section 2.3.4, a FCET is a hybrid vehicle. That means that the fuel cell stack power is not (at all times) equal to the electric machine power and, thus, the vehicle requires an operating strategy controlling the power output. Schmid et al. [256] performed experiments with a *Hyundai ix35 FC* and showed that the vehicle uses the battery's state of charge (SOC) as a control variable. Their results hint at a discrete control strategy with fixed fuel cell operating points. Based on their findings, Weiß [252] implemented a discrete control strategy with five empirical operating points. Figure 4.10 shows the operating strategy for an exemplary FCET. Depending on the SOC, the focus is either on high efficiency (high SOC) or high power with decreasing efficiency at lower SOC. The strategy manipulates the fuel flow [257, p. 369f] and, thus, the corresponding power output. To prevent the fuel cell's output from oscillating, the switching between operating points is carried out under a hysteresis [252, p. 43f]. For example, if the SOC falls below 45 %, the power output increases until the SOC surpasses 50 %. The dotted lines (.....) in Figure 4.10 show the switching between operating points and the hysteresis.

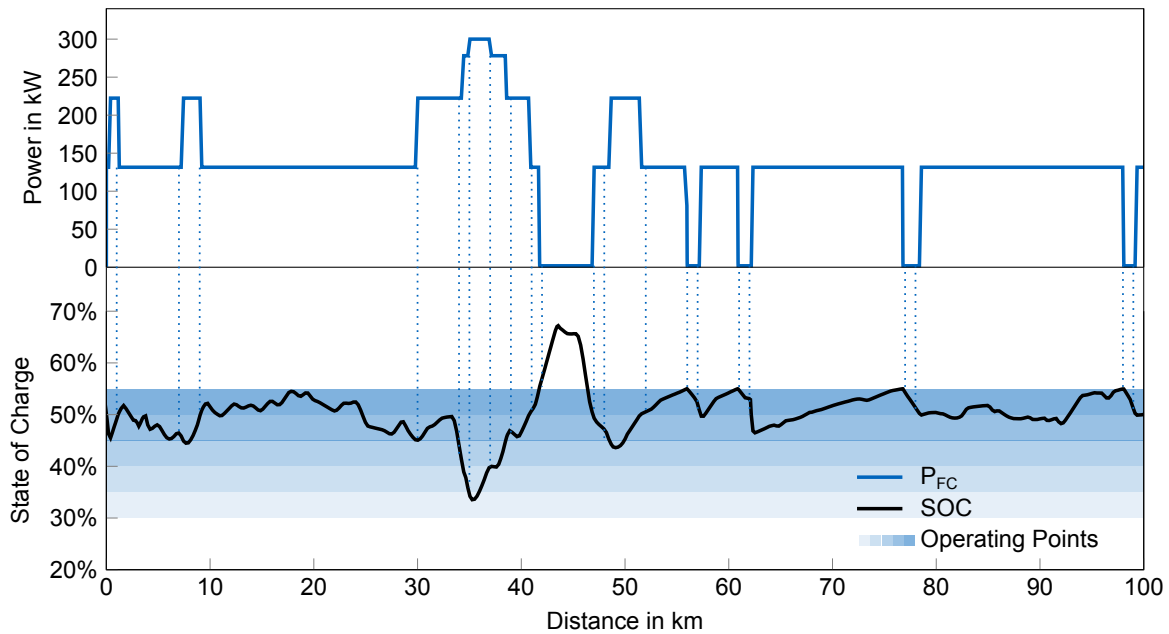


Figure 4.10: The discrete fuel cell operating strategy controls the power depending on the SOC. To prevent oscillating, each operating point consists of a hysteresis. The figure shows a FCET with a stack power of 300 kW, an electric motor with 2200 N m and a battery capacity of 40 kWh. The vehicle operates the VECTO long-haul cycle.

4.3.3 Hydrogen Internal Combustion Engine Vehicle Model

Regarding costs and environmental manufacturing impact, the hydrogen combustion engine is—apart from the tank—equal to its diesel counterpart (Section 2.3.4). However, *LOTUS* requires an extension to model the energy consumption of a HICET. Therefore, Eidkum [175] reviewed and modeled different hydrogen combustion technologies.

LOTUS uses specific consumption maps to obtain the fuel and, consequently, the energy consumption. Thus, the different hydrogen characteristics must be transferred to engine maps that can be used in *LOTUS*. In the first step, the specific diesel consumption map (in g/kWh) [234] is converted to an induced efficiency map (in %) [175]. Due to the lower overall efficiency of current hydrogen combustion engines, the map is scaled based on the average efficiency. This results in an efficiency conversion factor of $44/48.88 = 0.90$, which can be applied to any diesel consumption map.

Section 2.3.4 showed that hydrogen engines have a higher rotational speed than diesel engines. Therefore, the speed and, consequently, the efficiency map's torque, must be further adjusted. Due to the physical relationship $P = 2 \pi T n$, the resulting torque must be lower while the speed increases to have an equal power output. Figure 4.11 visualizes this correlation. The shifting points and gear ratios are adapted accordingly to yield the same behavior as the diesel ICET. Tschochner [258] and Fries et al. [203] successfully used this approach to simulate different, continuous combustion engine and electric motor maps.

Eidkum [175] obtained simulation results for two powertrain topologies using *LOTUS*. The standard HICET with compression ignition (CI) uses the efficiency map derived by Mährle et al. [234]. To check the approach's transferability, Eidkum [175] implemented the high-pressure direct injection (HPDI) process as developed by the *Westport* company [259]. The HPDI configuration is scaled, based on the LNG HPDI engine maps provided by Fries [53]. The hydrogen internal combustion engine and the HPDI process yield consumptions of 9.8 kg H₂/100 km and 9.6 kg H₂/100 km, respectively.

It must be noted that, although literature justifies the approach [203, 258], the conversion from one energy source to another is subject to simplifications. The obtained engine maps, therefore, only present an estimation of the HICET's energy consumption. In comparison, the optimized hydrogen combustion processes by Munshi et al. [259] achieve higher efficiencies. However, three (unpublished) expert opinions confirm the achieved consumption between 8 kg H₂/100 km and 10 kg H₂/100 km and, therefore, the model's plausibility. All expert opinions are from the year 2020 and incorporated into a previous publication [33]. Two of the experts are involved with the development of hydrogen combustion engines in a leading management position at a supplier and an OEM, respectively. The third expert is directly involved in development at an OEM.

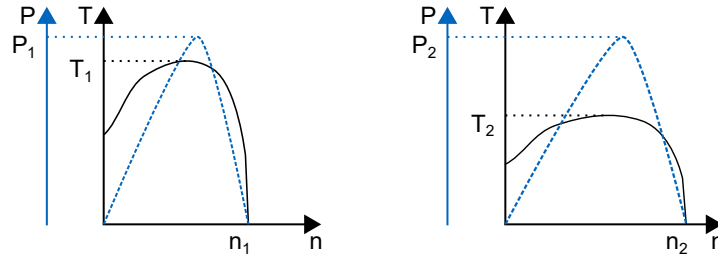


Figure 4.11: To convert engine maps with different characteristics into each other, the maps are scaled based on speed and torque. The power remains equal $P_1 = P_2$. To achieve this, the maximum rotational velocities as well as the maximum torque are adapted accordingly. Thereby applies $n_1 < n_2$ and $T_1 > T_2$.

4.3.4 Overhead Catenary Design

Section 2.3.3 showed that overhead catenary systems provide a solution to overcome the weight and range limitations of BETs. Dynamic charging enables smaller battery capacities while maintaining the same range. To investigate this relationship in more detail, Shen [260] studied various dynamic charging strategies and their impact on vehicle design.

Shen [260] based the BET's model on the *StratON* research project [150], where a DC-pantograph is connected to two contact wires above the road. The pantograph moves automatically to reduce aerodynamic drag when no overhead line is available. Shen [260] estimated the drag coefficient in the extended state at 8 %, compared to the retracted state, which equals an optimized version used for trains [261]. In the closed state, the drag coefficient is equal to a conventional truck [150].

The *LOTUS* implementation first calculates the minimum pantograph power $P_{Pan.}$ in order to sustain the velocity [145]. The power depends on the e-road segments' total length d_{OC} :

$$P_{Pan.} = E_{Vehicle} v \left(1 + \frac{1}{\eta_{Bat.} \eta_{Pan.}} \frac{d_{cycle}}{d_{OC}} \right), \quad (4.11)$$

where:

$E_{Vehicle}$ = Specific energy consumption, estimated at 1.83 kWh/km [150]

v = Vehicle velocity, 80 km/h

$\eta_{Pan.}$ = Conductive efficiency, estimated at 99 % [150]

$\eta_{Bat.}$ = Charging efficiency, estimated at 97 % [150].

Except for the electrified length d_{OC} , all parameters are known. The correlation between electrified road kilometers d_{OC} and their share on total utilization is non-linear because not all roads or road segments are equally frequented. If the electrified sections are located on the most frequently traveled highways, higher utilization can be achieved. This means that, in the best case, an e-road network of 15 % results in a share of 38 % of the mileage [140, p. 125]. For analyzing the effect of electrified roads on the vehicle concept, the mileage share represents the overall electrification. Additionally, it is assumed that a maximum of 90 % of the road network can be equipped with an overhead catenary system due to technical limitations such as tunnels and bridges [150, p. 96]. Figure 4.12 visualizes the correlation between possible electrification and e-road network expansion. Additionally, the three suggested e-road networks, as discussed in Section 2.3.3, are shown.

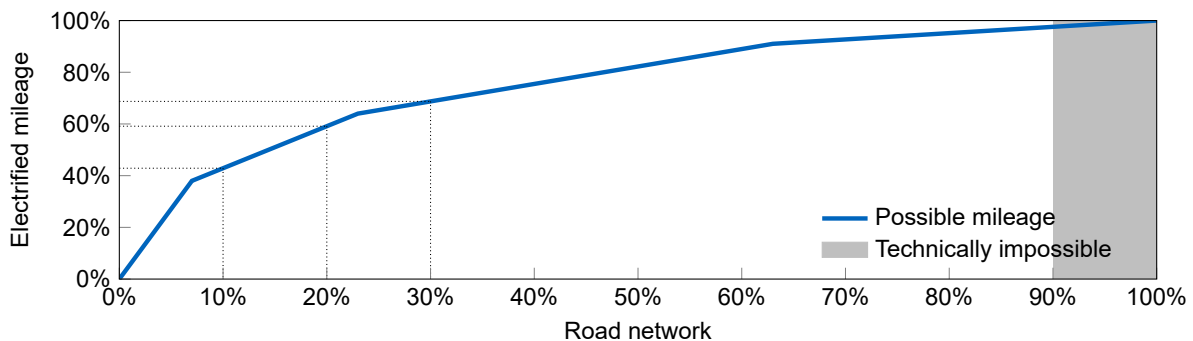


Figure 4.12: The relation between electrified road network length and electrified mileage (or utilization) is non-linear. For example, with 10 % of the most frequented road kilometers, 42 % of the mileage can be covered by an overhead contact line. The three expansion stages shown correspond to the proposal by Wietschel et al. [140]. An expansion above 90 % is technically impossible due to tunnels or bridges.

Consequently, these three network expansion stages are analyzed with the developed charging strategy and their respective electrification. Assuming that the overhead line can always provide the power according to Equation (4.11), Figure 4.13 shows the resulting SOC. The same vehicle completes the VECTO LH cycle with three increasing e-road expansion stages. For reference, the SOC without dynamic charging is shown. The vehicle is equipped with a battery capacity of 160 kWh. The interaction between battery size and expansion can be derived from this. Each electrified kilometer leads to a reduction in battery capacity of 1.1 kWh. The remaining range at the end of the cycle remains the same. For a typical daily driving distance of 400 km/d, this equals a reduction of 185 kWh for the e-road network of 10 % and 300 kWh for the network of 30 %, respectively.

Depending on traffic density, an overhead line would also allow higher charging capacities. This would not only keep the SOC constant but also charge the battery. However, the simulation yields technically impossible C-rates of 6/h to 7/h for the battery size investigated. Larger capacities would lower the C-rates, but the cost and weight advantage of the OC systems shrinks with it. In the following, the model uses a constant SOC strategy with variable power, representing a lower boundary regarding the range advantages.

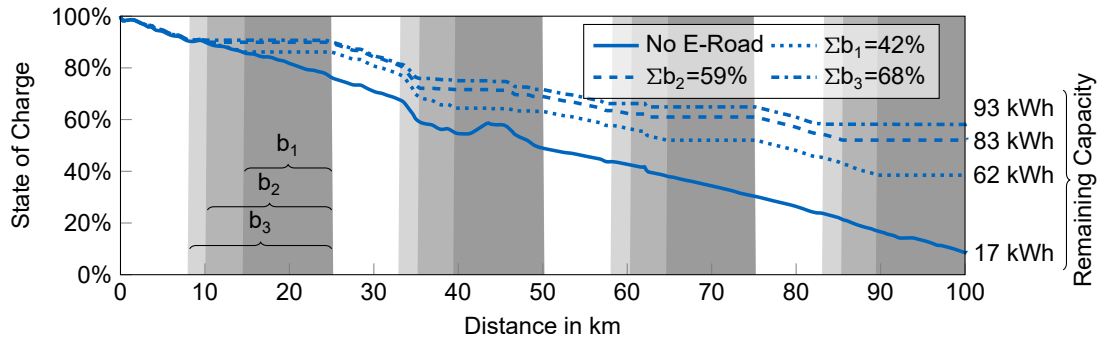


Figure 4.13: A vehicle with a 160 kWh achieves different remaining battery capacities depending on the e-road expansion b_1 , b_2 , and b_3 . The gray areas represent the road sections with dynamic charging. For the given VECTO LH driving cycle, each electrified road kilometer potentially decreases the battery capacity by 1.1 kWh.

5 Multi-Objective Optimization Problem

With the different powertrain models, a genetic (or evolutionary) algorithm optimizes each vehicle design. This can be regarded as an “ex-ante LCA” [22], which includes the technological improvements of each vehicle concept, enabling a fair and foremost prospective technology assessment. This is necessary to derive recommendations on future or emerging technologies. As discussed in a previous publication, this methodology is an innovation in the field of LCA and eco-efficiency analysis [56]. The evolutionary algorithm derives Pareto-optimal vehicle concepts, which help to analyze whether the conflict between environmentally and economically optimized vehicles can be resolved with alternative powertrains. This approach aspires to an easy selection by a decision-maker afterward (a posteriori).

This type of algorithm has already proven its applicability for improving vehicle performance in various applications. For example, Luo et al. [262] optimized the charging component’s efficiency of BETs. Yu et al. [263] and Da Silva et al. [264] both applied a genetic algorithm and optimized hybrid operating strategies. They achieved cost savings, lowered emissions, and extended the battery cycle life. Additionally, Ju et al. [265] and Pathak et al. [266] optimized vehicle concepts and aimed to resolve the conflicting customer requirements (e.g., acceleration and travel time) and costs. Fries [53] applied an evolutionary algorithm to heavy-duty vehicle design and optimized transport efficiency.

Before any optimization, the problem must be formulated in a mathematical form that the algorithm can solve. In the following, a summary of the multiobjective optimization problem (MOP) is given. Further fundamentals on optimization problems can be found in Kruse et al. [267] and Coello et al. [268]. As a mathematical definition, a multiobjective optimization problem (MOP) is the extension of a single objective optimization. The objective of evaluation function $F : \Omega \rightarrow \Lambda$ maps the vector x of n decision variables to an output vector y of k objectives. The decision variables can be continuous or discrete and are part of the decision variable space (some universe Ω). All possible solutions y are part of some universe Λ [268, p. 7]. Optimization problems can further be subject to a number of m inequality g_i or p equality h_j constraints. Equation (5.1) shows the standard form of such a MOP:

$$\begin{aligned} \min_x F(x) &= [f_1(x), \dots, f_k(x)]^T, \quad x = [x_1, \dots, x_n]^T \in \Omega \\ \text{s.t. } g_i(x) &\leq 0, \quad i = \{1, \dots, m\}, \text{ and} \\ h_j(x) &= 0, \quad i = \{1, \dots, p\}. \end{aligned} \tag{5.1}$$

Multi-objective problems typically have conflicting objectives. The improvement of one objective leads to the deterioration of another. Two solutions that fulfill this criterion are called Pareto optimal—named after the Italian engineer and economist Vilfredo Pareto. Equation (5.2) gives the mathematical expression of Pareto-optimality. It means that a set of solutions \mathcal{P}^* is Pareto-optimal, if no vector x' exists “which would decrease some criterion without causing a simultaneous increase in at least one other criterion” [268, p. 8] ($F(x') \preceq F(x)$).

$$\mathcal{P}^* := \{x \in \Omega \mid \nexists x' \in \Omega F(x') \preccurlyeq F(x)\}. \tag{5.2}$$

To solve a MOP, multiple objectives are to be solved simultaneously. At the point, where no solution can improve (i.e., minimize) one objective without increasing another one, the set \mathcal{P}^* achieved Pareto optimality [268, p. 11]. Consequently, there is no single, optimal solution, but a set of solutions, and the problem requires a posteriori decision maker [268, p. 7].

The non-dominated sorting algorithm II (NSGA-II) developed by Deb et al. [269] is an evolutionary, multi-objective algorithm. It is particularly capable “of preserving spread on the non-dominated front” [269] and shows a good convergence due to its selection method and good computational performance [268, p. 110, 269, 270]. Furthermore, the NSGA-II can handle non-linear and unsteady objective functions and continuous and discrete design variables. Both are present in a vehicle simulation. The presented approach builds on Fries’ [231] NSGA-II implementation into the vehicle simulation.

Figure 5.1 shows the algorithm’s procedure. The original population P_t contains a specified number of individuals. An individual is a set of design variables x —or genes in the evolutionary algorithm’s terminology. As a first step, stochastic operations (recombination and random mutation) generate the offspring generation Q_t from the starting population P_t . Non-dominated sorting divides the overall population R_t into individual (Pareto) fronts F_i of non-dominated individuals [270]. Because R_t is larger than the available slots for the new generation P_{t+1} , the least fit (i.e., the ones with the worst fitness value) individuals are rejected. To enhance diversity in the new population, a crowding distance sorting selects the individuals of the last front (here F_3), which are carried over to the new population. Because the algorithm allows individuals from the original population P_t to move to the new population, the selection is called *elitist* [268, p. 110]. The new population P_{t+1} is the start of the next iteration. Typically, for multi-objective optimizations, the user specifies a maximum number of iterations [270] as the termination criterion.

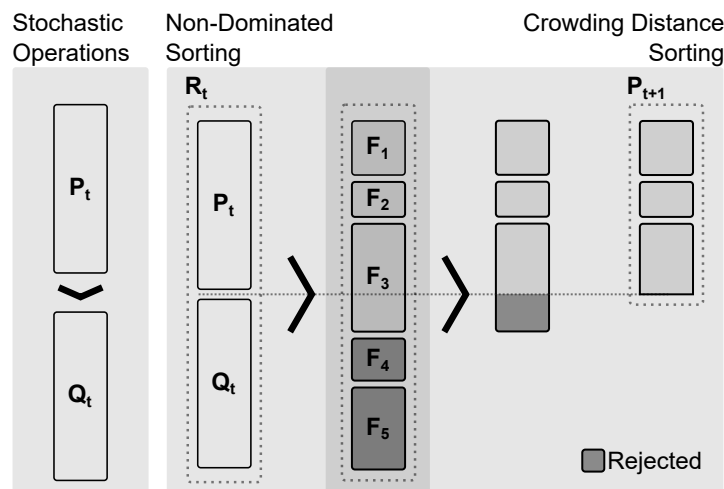


Figure 5.1: The evolutionary algorithm NSGA-II creates an offspring generation Q_t and evaluates its fitness. Subsequently, a non-dominated sorting applies. The algorithm sorts the obtained Pareto-fronts F_i based on crowding distance criteria to enhance the front’s diversity. The least *fit* Pareto-fronts are rejected.

Each set of design variables x denotes a unique vehicle that can be optimized with regard to the objectives f_i (Figure 4.1, IV). In addition to the economic (f_1) and environmental (f_2) objective, the third objective (f_3) is the remaining climbing ability (RCA), which represents a customer requirement. The

RCA is the maximum, additional gradient that a vehicle can travel at a certain speed (here: 85 km/h) without shifting gears. A low RCA results in frequent gear shifts, which is an unwanted property by the drivers. Thus, it represents a customer requirement, which can lead to *unreasonable* choices. For example, a customer does not always select the smallest possible engine to fulfill the requirements. Instead, a customer can choose the larger and more expensive—and thus economically unreasonable—engine based on subjective criteria. This example illustrates that optimizing such a customer requirement better reflects the customer’s choices and thus developed vehicles. Consequently, we define the climbing ability as the third objective instead of a boundary condition. To formulate a minimization problem, the remaining climbing ability has a negative sign so that it is maximized:

$$\begin{aligned}
 \min_{\mathbf{x}} \quad & F(\mathbf{x}) \quad \begin{cases} f_1(\mathbf{x}) := \text{TCO} \\ f_2(\mathbf{x}) := \text{EII} \\ f_3(\mathbf{x}) := -\text{RCA} \end{cases} \\
 \text{s.t.} \quad & g_1 : C_{\max} \leq \begin{cases} 5 \text{ h}^{-1}, \text{ if BEV} \\ 20 \text{ h}^{-1}, \text{ if HEV} \end{cases} \\
 & g_2 : I_{\text{avg}} \leq 400 \text{ A.}
 \end{aligned} \tag{5.3}$$

Supplementary to the two constraints g_1 and g_2 , limiting the battery’s (dis-)charge rate and average current to currently achievable values [138, 271], a hidden constraint applies if the vehicle cannot complete the driving cycle and stops. The algorithm excludes these vehicles from the solution space.

It must be noted that not all vehicle configurations are valid solutions because they result in the termination of the vehicle simulation (i.e., the vehicle stops because the slope cannot be climbed or the battery is empty). These vehicles are given an infinite objective value and the algorithm consequently excludes them from the population.

The boundaries for the ICET and HET design variables are borrowed from Fries et al. [203, 231]. The HICET optimization uses the same values as the ICET. Table 5.1 summarizes the design space for the BET and FCET optimization. There, the lower and upper bounds are selected based on a previously conducted benchmark [138]. It should be noted that a depth of discharge (DOD) below 50 %, would result in unfeasible large gross capacities for the BET, exceeding the GVW-limit. The battery is assumed a best-in-class high-energy battery with a gravimetric energy density of 161 kWh/kg on pack-level [196]. Extended limits allow the algorithm an exploration of the design space.

All optimizations were performed with 520 individuals and 100 generations—values, which Fries [53] successfully applied by. Due to the FCET model’s longer computation time, the optimization had to be performed with 160 individuals. The computation time for all optimization was approximately 8 h on a Linux cluster with 32 processors (Intel®Xeon®Gold 6148 CPU with 2.4 GHz).

In comparison to single-objective optimization problems, a MOP’s solution does not converge in the same way. Due to the solutions’ Pareto-optimality, a simple threshold cannot be used to determine when the algorithm terminates. Therefore, Goel and Stander [272] propose a metric to obtain a convergence curve for MOPs, which is specifically designed for genetic algorithms. Their proposed *improvement*

Table 5.1: Lower and upper boundaries for the design variables x for BEV and FCEV concept optimization. [Note: EM=Electrical Machine; RPM=Revolutions per Minute; DOD=Depth of Discharge; PSM=Permanent Synchronous Machine; ASM=Asynchronous Machine]

Design Variable	Unit	Lower	Upper
Max. torque T_{max}	Nm	500	2000
Rated EM RPM	min ⁻¹	1000	5000
DOD (Fuel Cell)	-	0.5 (0.1)	1
Capacity C_{bat}	kWh	560	1600
Ratio axle-drive	-	0.5	25
Gear spread	-	1	22
No. of gears	discrete		1, 2, 4, 6
Lower shift	min ⁻¹	750	1200
Upper shift	min ⁻¹	1200	1750
EM-type	discrete		PSM or ASM
Power fuel cell ¹	kW	100	140
Battery capacity ¹	kWh	50	300

¹only for FCEV concept optimization

ratio (Equation (5.4)) relates the population size $n(P)$ to the number of non-dominated individuals of the previous and the current generation $n(A_i)$.

$$IR = \frac{n(P)}{n(A_i)}, \quad P = \{a_{i-\Delta} : a_{i-\Delta} \prec a_i\}, \quad a_{i-\Delta} \in A_{i-\Delta}, \quad a_i \in A_i. \quad (5.4)$$

Figure 5.2 shows the improvement ratio obtained for the BET optimization. It can be seen that the optimization starts to converge after 70 generations (-----). “Since the evolution is locally random, the parameter Δ (generation gap) acts as a filter to reduce noise” [272]. Therefore, Figure 5.2 also shows the average improvement ratio (—) as a convergence metric. The generation gap delta corresponds to the number of generations ($\Delta = i$). Appendix G shows the convergence metrics for the remaining vehicle optimizations. Although all optimizations converge within the maximum generation, the different number of design variables causes the convergence to occur in varying generations.

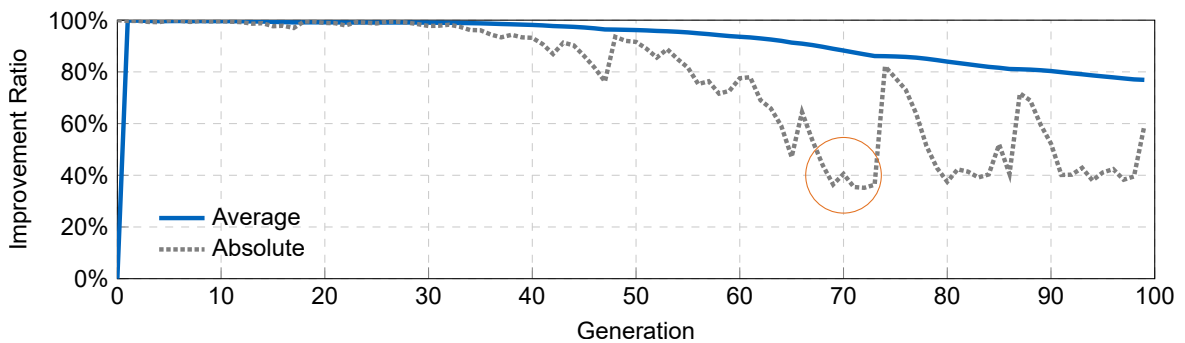


Figure 5.2: The absolute improvement ratio shows that the BET optimization converges after 70 generations (○). Locally random evolution creates noise, which the average improvement ratio filters out [272].

6 Validation and Uncertainty

Before presenting the results, the simulation model's correctness must be evaluated. Section 6.1 validates the model, comparing the diesel simulation to real-world data. Because no publicly available data on zero-emission vehicles exists, only validated submodels and physical completeness can verify the model. A Monte-Carlo-based uncertainty quantification extends the model's validation, counteracting this flaw. A framework quantifies and compares the system-inherent with the scenario-dependent (using the payload as an example) uncertainties.

6.1 Validation

To evaluate a model's quality, it can be verified and validated [273–275]. Danquah et al. [275] define verification and validation as follows:

- Verification: The process of determining that a computational model accurately represents the underlying mathematical model and its solution.
- Validation: The process of determining the degree to which a model is an accurate representation of the real world from the perspective of the intended uses of the model.

Süßmann [119] developed the predecessor of *LOTUS* to evaluate consumption reduction measures. Because some of these measures only yield a 0.3 L/100 km reduction, the simulation had to be able to show savings of this magnitude [119, p. 91]. Accordingly, the vehicle model had to represent the powertrain of a diesel vehicle in detail. Süßmann's model achieved an accuracy of 5.4 % when compared with test drives.

During the development of *VECTO*, ACEA [115] released consumption data for the European vehicle categories (Section 2.2 and Appendix A). Mustafić [117] modeled a diesel vehicle for each category with *LOTUS* and compared the results to the published data. Table 6.1 compares the simulation results with the real-world data, confirming Süßmann's results [119, p. 91]. Except for the 5-LD subgroup, all categories show a Gaussian distribution. Mustafić [117] compares the mean values of the data with the results from *LOTUS*. Because subgroup 5-RD has a near-uniform distribution, the comparison of the mean value is not representative and explains the comparatively high inaccuracy. However, the simulation results are within the 50 % confidence interval around the mean value. Furthermore, the subgroup represents a niche, with 0.8 % share of the total driving performance. It can be seen that *LOTUS* achieves an average accuracy of 5.3 % over the vehicle categories. This comparison and Süßmann's results show both the model's verification and its validity for simulating diesel powertrains.

To model other vehicle concepts, Fries et al. [203] included LNG engine maps. Furthermore, a previous publication [54] incorporates electrical components into the simulation to evaluate hybrid and LNG powertrains. For these vehicle concepts, no publicly available real-world data exists, which could

Table 6.1: To validate *LOTUS*, Mustafić [117] compared the results to previously published data. This data represents the preliminary average reference values from ACEA, which serve as a baseline for the consumption reductions set by the EU [115]. [Note: MAPE=Mean Absolute Percentage Error]

Vehicle Type	Subcategory	Vehicle sales	LOTUS g CO ₂ /t km	ACEA g CO ₂ /t km	MAPE %
Chassis	4-RD	7.9 %	206.31	198.1	4
Chassis	4-LH	1.9 %	97.59	102.9	3
Tractor	5-RD	0.8 %	73.53	84.0	12
Tractor	5-LH	62.8 %	57.98	56.5	3
Chassis	9-RD	7.2 %	113.65	110.9	2
Chassis	9-LH	9.2 %	60.84	64.7	6
Tractor	10-RD	0.1 %	78.99	84.0	6
Tractor	10-LH	9.7 %	61.79	58.6	5
Average					5.13

validate the overall simulation. Consequently, Fries [53, p. 78] did not validate the alternative powertrains from a vehicle perspective. Instead, he used validated submodels to ensure the results' quality.

As described in Section 4.3.2 and 4.3.3, both the FCET and HICET simulations use valid submodels. As with Fries [53], on the one hand, no publicly available data allows validation. Only the validated submodels can justify the validity of *LOTUS*. The (physically) complete representation of the different powertrains, on the other hand, represents the simulation's verification. Analogous to Süßmann [119] and Fries [53], *LOTUS* can represent all relevant relationships determining energy consumption.

As explained in Section 4.2.2, two previous publications discuss and verify the life cycle inventory's and the life cycle assessment's data quality [56, 100]. The LCC consists of four parts, of which two (personnel and overhead) are assumed identical for all vehicle concepts (Section 4.1). There is no data, explicitly evaluating the influence of zero-emission vehicle's on personnel and overhead costs [56]. However, it can be assumed that the logistic processes and, thus, personnel and overhead costs, remain unchanged by alternative powertrains—at least in the current decade. Dominating the fixed costs, the acquisition costs are essential for the costs' accuracy. The LCC builds on the specific component costs, which a previous publication [196] discusses. Furthermore, they are in line with current literature [49, 96, 276]. The same applies to the assumed energy costs, which comprise the majority of the variable costs. They correspond to current European cost forecasts [197, 277], which have been summarized in a previous publication [196].

Overall, the model cannot be fully validated due to a lack of experimental data. However, the model's physical completeness includes all primary powertrain components and, consequently, represents a verification. Lumped auxiliary consumers (here 3.5 kW) model the secondary powertrain components, such as thermal management. Advancements (e.g., Tesla's Octalink) in these components could easily be included if their effect on average auxiliary power consumption can be determined. Furthermore, all submodels are validated [53]. The assumptions for the economic evaluation can also not be validated because they are partly future costs of components or fuels. However, a comparison with data available in the literature [49, 96, 197, 276, 277] shows that these assumptions are plausible. The ecological assessment cannot be validated per se [278]. However, it was performed according to widely used standards DIN ISO 14040 and 14044 [58, 59] and the ILCD guidelines [68]. Data from current literature

allows the modeling of components [179, 217, 223], energy sources [195, 199], and electricity mixes [279, 280] down to material extraction. Data at this stage is scarce and seldomly updated [281]. An updated database version, therefore, does not significantly influence the results, because the data on the raw-material level remains the same. However, this cannot be evaluated conclusively, although the relative comparison remains valid regardless of the database version.

6.2 Uncertainty Quantification

Although single component models were validated for specific applications, it is necessary to quantify the associated overall uncertainty: While the use of simulations for product development is state of the art, Danquah et al. [282] highlighted the necessity of uncertainty quantification and model validation, which is rarely considered in an automotive context. These are, however, indispensable in order to derive valid conclusions and increase the overall system knowledge. This chapter, therefore, introduces a combined uncertainty quantification regarding the aleatoric and epistemic uncertainties. Apart from this, uncertainties may arise due to a lack of knowledge about the scenario. To counteract this, Section 3.2 defines the status quo and a best-case scenario, which can be achieved in 2030. Assuming that an improvement of the status quo in terms of energy mix and costs continues to take place, all possible solutions lie between today and this best-case scenario. Consequently, the scenario uncertainty is excluded from the uncertainty quantification and separately discussed in Section 7.4.

Aleatoric uncertainties are system-inherent variances [283, p. 4, 284, p. 50]. Because aleatoric uncertainties are known in advance, better system knowledge or more precise measurements cannot reduce these random fluctuations. For example, air pressure and temperature fluctuate naturally, affecting the calculation of driving resistances. According to Johnson et al. [285], probability density functions (PDFs) and cumulative distribution functions (CDFs) are adequate visual representations, typically in the shape of Gaussian, Weibull or exponential distribution. If these fluctuations are not known analytically (such as a coin toss), they can be measured experimentally and described mathematically, which expands the representation to an empirical probability density function. Seidenfus [286, p. 17] provides illustrating examples of PDFs and CDFs, respectively.

Epistemic uncertainties describe the lack of knowledge about the system [283, p. 4, 284, p. 50]. Sullivan [283, p. 17] further distinguishes between model shape and parametric uncertainty. The former reflects the doubt about the model's correctness, while the latter describes doubts about the correctness of certain parameters. In an engineering context, epistemic uncertainties are mathematically described by technically possible intervals $[a, b]$. The vehicle mass or the payload are examples of epistemic uncertainties. A vehicle's mass might be unknown because the exact mass of a vehicle depends on the individual vehicle configuration up to the exact filling level of individual liquids. Analogously, a commercial vehicle's payload depends on the use case and the type of goods. An interval in this case describes the uncertainties, for example via minimum and maximum values. According to Roy et al. [287], a probability box (PBox) visualizes combined aleatoric and epistemic uncertainties.

In order to quantify a model's uncertainty, aleatoric uncertainties are fed into the system with a fixed sample of epistemic uncertainties. This procedure is repeated with multiple samples from the epistemic probability boundaries [287, 288]. Danquah et al. [275, 289] and Riedmaier et al. [290] combined this approach with a Monte-Carlo sampling to create a unified framework for epistemic and aleatoric uncertainty quantification of technical, automotive systems. The generic Validation Verification Uncertainty Quantification Framework (VVUQ) is available at [GitHub](#) under open-source license [291].

Uncertainties are not an integral part of the DIN EN ISO 14044 and—even in a scientific—context seldom considered in LCA, although the topic’s attention is increasing [292, 293]. In particular for prospective LCA approaches, the scenario-related uncertainties can significantly influence the results [294]. In the case of use-phase-intense products—such as heavy-duty vehicles—uncertainties can shift the results and, thus, the LCA’s results [295]. Therefore, Seidenfus [286] quantified and analyzed the uncertainty associated with component and scenario-related parameters on the two eco-efficiency objectives EII and TCO. For this, he applied the VVUQ framework to the *LOTUS* eco-efficiency assessment.

The methodology allows the analysis of several indicators. Based on vehicle optimization, the TCO and the EII are the two variables of interest. Additionally, energy consumption provides a practical figure to analyze the results. Table 6.2 shows the range of parameters that Seidenfus [286] identified as aleatory errors. The *relative motor efficiency* represents the uncertainties of a motor map. The Truck 2030 engine map from *LOTUS* represents the reference (100 %), whose efficiency is changed with a variance of ± 3 %. The resulting constant factor is transferred to the entire map.

The payload represents an epistemic error, covering an interval from 10 t to 25 t, which is also identical for all vehicles. Payload is used here as an example of epistemic (or scenario-dependent) uncertainty, although the relationship between higher payload and higher consumption is obvious.

Table 6.2: Vehicle parameters and corresponding epistemic and aleatoric intervals [286]. The parameters are passed through the *LOTUS* vehicle simulation and evaluated with the VVUQ framework, developed by Danquah et al. [291].

Parameter	Symbol	Unit	Aleatoric	
			Mean μ	Variance σ
Air drag coefficient	c_D	-	0.5373	0.0037
Roll drag coefficient	c_R	-	0.007	0.0004
Relative Motor Efficiency	η_{engine}	%	100	0.3
Fuel Cell Stack Efficiency	$\eta_{\text{fuel cell}}$	%	55	4
			Epistemic	
			Min	Max
Payload	m_{payload}	kg	10 000	25 000

Figure 6.1 shows the resulting PBoxes for the two eco-efficiency objectives TCO and EII for the optimized BET concept (Section 7.3.1). Additionally, the figure shows the PBox for the overall energy consumption. It can be seen that the influence of the epistemic uncertainty (i.e., the payload) exceeds the influence of the aleatoric errors. While this effect is present in all scenarios, it is more pronounced for the two eco-efficiency objectives.

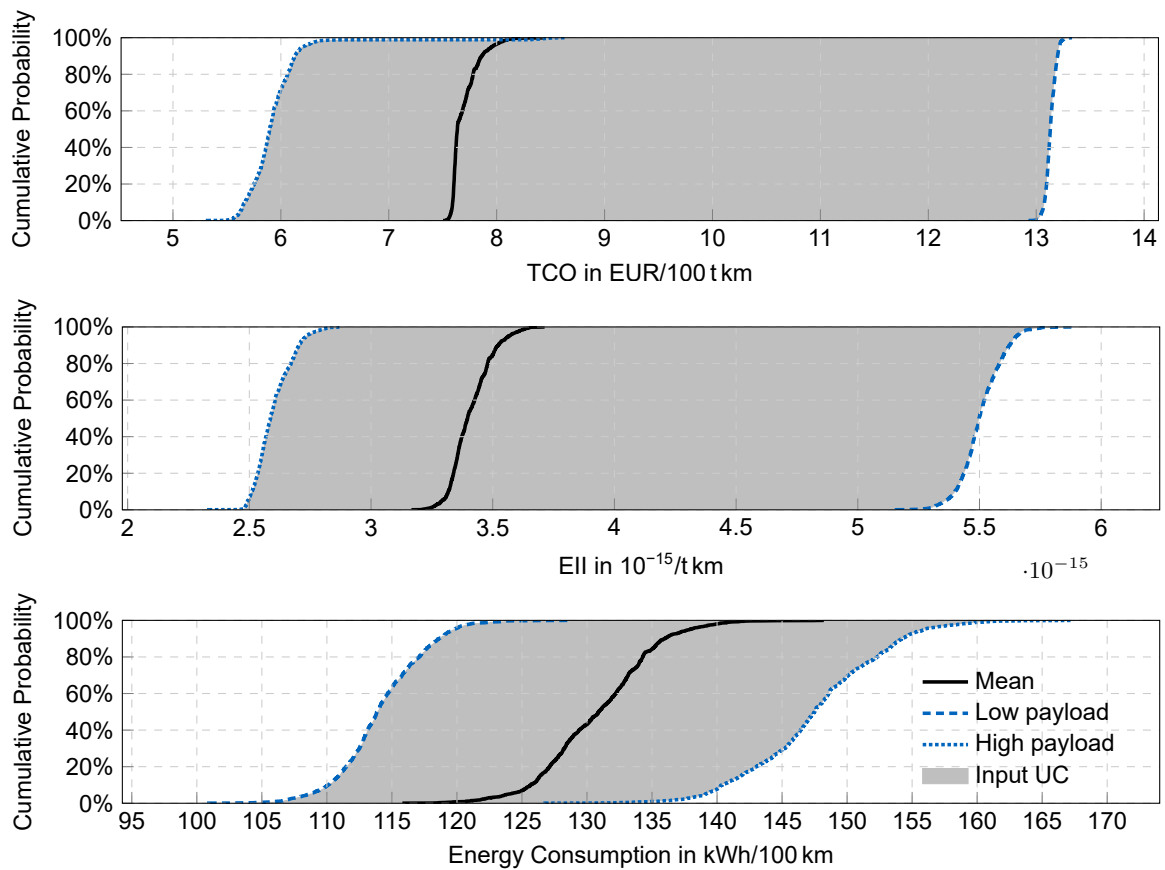


Figure 6.1: The cumulative distribution function shows the BET's uncertainty quantification of the two optimization objectives and its energy consumption. For each of the three aleatoric scenarios (mean, low, and high payload), the vehicle input parameters are altered in their epistemic intervals (Table 6.2). While the epistemic errors are visible in the energy consumption's uncertainty, their effect diminishes for the two objectives. Furthermore, the aleatoric uncertainty associated with differing payloads exceeds the epistemic uncertainties.

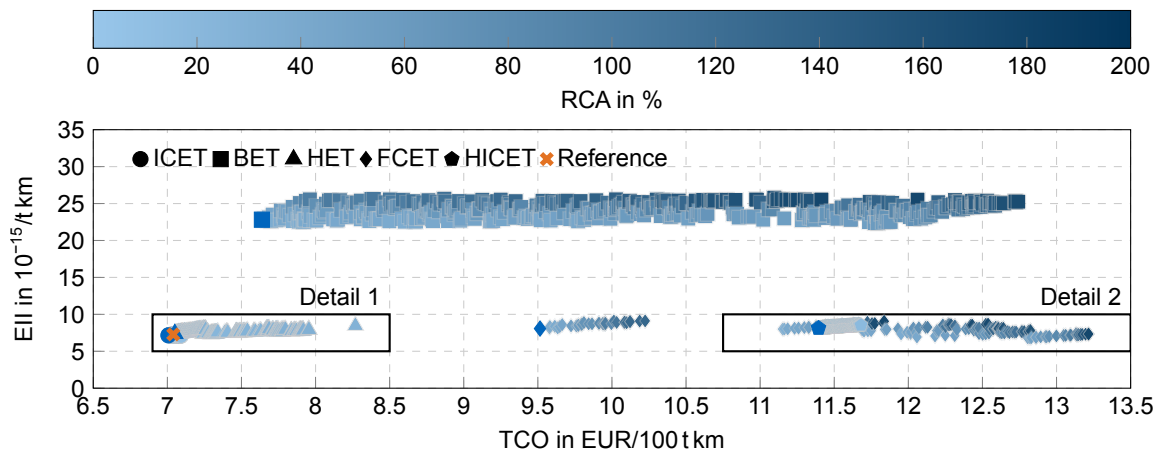
The same study was performed for the ICET, the HET, and the FCET concept. The HICET is not included as the results would be—apart from the engine map's conversion factor—identical to the ICET, due to equal simulation structure and scope. Appendix H shows these results. Although the absolute values differ, the picture is the same for all studies: The payload has a significantly higher influence on the results than the (not exactly determinable) vehicle parameters.

Uncertainty quantification allows a statement about how parameters that are not exactly known or determined influence the result. Seidenfus' [286] study on the uncertainty of vehicle parameters allows three conclusions:

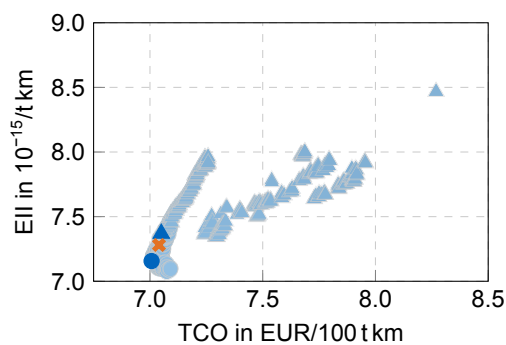
- Parameters such as rolling resistance or air resistance have a non-negligible influence on the consumption of individual vehicles. However, the resulting quality of the eco-efficient analysis is only marginally influenced by this for two reasons. First, these parameters are—except the OBET's dynamic air drag coefficient—identical for all vehicles, which is why the relative vehicle comparison is valid. Secondly, the validation of the previous work showed that for diesel vehicles a small deviation was obtained compared to different measurements. Therefore, it can be assumed that the selected set of vehicle parameters achieves high-quality results and that this quality is transferable to other vehicle concepts.
- The influence of the (epistemic) payload exceeds the influence of the aleatory uncertainties. This is especially true for the two eco-efficiency objectives TCO and EII, both of which are linked to the payload. In reality, the payload depends on the specific application. However, the simulation uses a generic payload published by the EU, which is used by VECTO to certify commercial vehicle emissions. Although the reference to reality cannot be conclusively ensured, the eco-efficiency analysis results are, nevertheless, valid in comparison with VECTO.
- The payload example shows that a scenario comparison can ignore aleatoric uncertainties. In particular, for results normalized on the functional unit (t km), it can be assumed that there are no fundamentally different results when aleatoric uncertainties are included. Therefore, the remainder of this work does not present these. However, it should always be noted that these uncertainties occur in reality.

7 Results

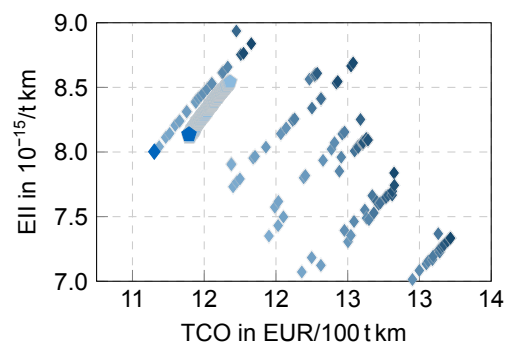
The following section presents the vehicle concept optimization results, which are Pareto-optimal regarding costs and environmental impact. First, Section 7.1 describes the LCC results and Section 7.2 summarizes the obtained LCA results. Both are based on a previous publication [138] and supplemented by the HICET concept. Figure 7.1 shows the solution space with a Pareto-front for each vehicle concept. In addition, a diesel vehicle, representing a modern tractor (such as *MAN TGX EURO VI*), provides a reference to compare the results [53]. Table 7.1 shows the three optimization objectives with additional vehicle performance indicators for each vehicle concept. For each indicator, the mean, minimum, and maximum value from the respective Pareto-front is shown, which indicates the degrees of freedom of the respective vehicle design. The optimization was performed with the *Status Quo* scenario assumptions.



(a) Complete solution space



(b) Detail 1 of solution space



(c) Detail 2 of solution space

Figure 7.1: Trade-off (a) between Eco-Impact Index and cost of ownership for Diesel, HET, BET, FCET, and HICET concept optimization. For the TCO, a vehicle lifetime of 10 years is assumed. The reference vehicle has a RCA of 14 %. The color-coding shows the superior climbing ability at 85 km/h of all electrified vehicle concepts (darker) compared to the diesel. For better readability, the individuals with the lowest TCO are highlighted and two details of the solution space (b, c) are shown.

Each vehicle concept will be described separately and from a technological point of view in Section 7.3.1. Because no vehicle concepts are compared there, these results apply regardless of the chosen scenario (here: *Status Quo*).

Choosing the most cost-efficient (i.e., the lowest TCO) vehicle from each Pareto-front, Section 7.3.2 analyzes the environmental impact of each cost-optimal vehicle concept. Section 7.4 shows the resulting changes of each vehicle, if the *Potential* scenario assumptions are applied. Eventually, Section 7.5 combines the two scenarios with an assumed vehicle stock development, providing a macroeconomic perspective beyond single vehicles.

Table 7.1: Summary of the three Pareto-optimal optimization objectives per vehicle. Additionally, the values for the EURO VI reference vehicle are shown. Additionally, the energy consumption has a significant influence on both costs and environmental impact, especially during the use phase. With the average speed, the TCO model calculates the annual mileage and the functional unit. The tractor mass provides is factor for the environmental production-phase impacts, which are scaled by the respective vehicle mass.

		Reference	Diesel	HEV	BEV	FCEV	HICE
TCO (EUR/t km)	Mean		0.071	0.074	0.102	0.118	0.115
	Min	0.070	0.070	0.071	0.076	0.095	0.114
	Max		0.071	0.083	0.127	0.132	0.117
EII (10⁻¹⁵/t km)	Mean		7.23	7.66	24.23	8.04	8.33
	Min	7.28	7.07	7.34	22.35	6.80	8.11
	Max		7.42	8.47	25.72	9.11	8.54
RCA (%)	Mean		14	24	92	91	13
	Min	14	9	17	33	28	8
	Max		17	30	173	173	17
Consumption (kWh/100 km)	Mean		313	306	140	204	329
	Min	317	303	296	128	184	317
	Max		324	314	149	226	340
Mileage (km/a)	Mean		102 984	105 420	70 096	105 287	103 989
	Min	103 777	100 640	105 046	49 600	103 729	102 310
	Max		104 177	105 723	105 185	105 732	104 704
Tractor mass (kg)	Mean		7187	7668	9006	7993	7250
	Min	7237	6937	7380	7852	7057	7106
	Max		7379	7984	10 950	9847	7379

7.1 Life Cycle Costing Results

Compared to the reference vehicle, the optimized diesel has a low potential of improving TCO (cf. Figure 7.1 b), despite lower energy consumption (Table 7.1). However, the concept has the lowest TCO of all alternatives.

The HET reduces the energy consumption by up to 7 % and simultaneously increases the mileage (1 % to 2 %) due to improved longitudinal dynamics and, consequently, higher average velocity. On the

one hand, both aspects lead to lower costs. On the other hand, the powertrain's complexity increases acquisition costs, which reduces the advantage due to the two aforementioned aspects. It should be noted that the cost of diesel and electricity does not include externalities (taxes, subsidies etc.). This makes diesel cheaper than electricity. Consequently, the HET increases TCO by up to 17 % compared to the reference vehicle.

The BET has the lowest energy consumption of all vehicle concepts, which is 53 % to 60 % lower than the reference. As Figure 7.1 shows, the BET has a large range regarding TCO, resulting in a cost increase between 8 % and 81 % compared to the reference. In the same way, the mileage shows a large spread, which explains the spread in costs due to the measurement in “per ton kilometer.” The reason for this is the calculation of the mileage, which depends on the battery capacity, as explained in Section 4.1. Here, higher mileage correlates with a larger battery and lower TCO (Section 7.3.1).

Compared to the reference, the FCETs achieve a higher mileage and—on average—perform better than the BETs. However, the TCO of the FCET concepts are up to 88 % higher than those of the diesel-powered concepts and, thus, equally high as the BETs'. Here, the high energy consumption in conjunction with high hydrogen costs, explains the high TCO. Regarding TCO, Figure 7.1 shows that two Pareto-fronts emerged. The technical relationships among the design variables that lead to this are discussed in Section 7.3.1.

The HICET achieves similar driving performance as the reference vehicle. Due to the same reasons as the FCET, the HICETs' TCO are 63 % to 67 % higher than those of the reference. Although the HICET concepts have the highest energy consumption, their average costs are in the same range as the FCET. Due to the simpler powertrain, the HICET concepts can partly compensate for their higher energy consumption. However, as Figure 7.1 shows, the FCETs' left Pareto-front achieves lower TCO than the HICET.

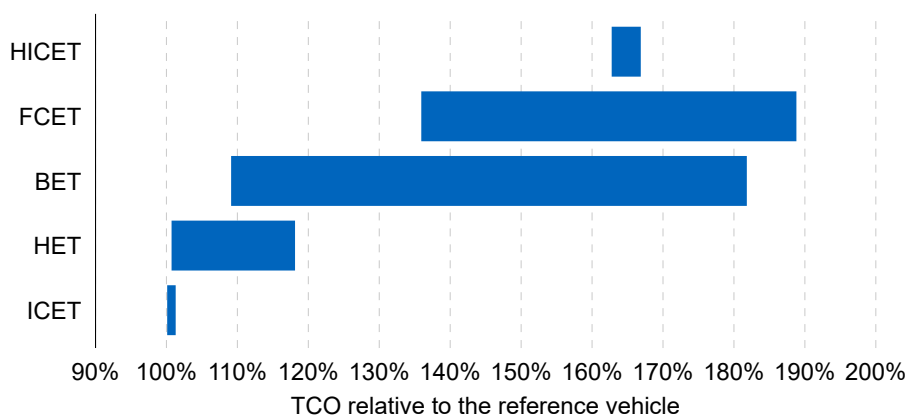


Figure 7.2: The normalized TCO of each vehicle concept show that only the optimized diesel achieves cost parity with the reference vehicle. Due to the higher production costs of electricity compared to diesel, the HET cannot achieve a cost advantage. Both fully electric concepts show (significantly) increased costs in the status quo scenario. Due to the high energy consumption and expensive hydrogen, the HICET costs are also higher. The wide range covered by the two electric concepts is striking, which is explained by the strong influence of the battery as a key component.

7.2 Life Cycle Assessment Results

Similar to the total costs, the energy consumption and mileage comprise the EII's majority. The tractor mass (Table 7.1) is an additional indicator, hinting at the environmental performance during the

production phase: higher mass equals higher material consumption and, thus, increased environmental impact.

As Figure 7.1 shows, the optimized diesel concepts perform better than the reference. This is due to a similar vehicle design (tractor mass) but lower energy consumption. Nevertheless, the bow-shaped Pareto-front (Figure 7.1, Detail 1) suggests that combinations with worse environmental performance *and* increased costs exist.

The electrified HET, BET, and FCET concepts all require additional powertrain components and (partly) rely on electric energy. Due to the assumed European electricity mix during the production and use phase, these concepts perform worse than the reference [138]. In the given status-quo scenario, the BET performs worst and increases EII by 307 % to 353 % compared to the reference. Only single individuals in the FCETs' right Pareto-front (i.e., most expensive) fall below the reference by a maximum of 7 %. Due to the higher hydrogen consumption, the HICETs' simpler powertrain and, thus, lower production phase-related EII cannot compensate for the increased use-phase impact. Section 7.3.1 explains the details of the technical relationships leading to the results for each vehicle concept.

Regarding the tractor mass, the optimized diesel, HETs, FCETs, and HICET are comparable to the reference (6 % to 10 %). The hybrid and the fuel cell powertrain are the most complex among the vehicle concepts, which explains their additional tractor mass compared to the reference. As expected, the BETs have the highest tractor mass; 9 % to 51 % above the reference. Their high mass suggests that the BETs' environmental performance is more dependent on their production phase than is the case for the other concepts. This will be discussed in Section 7.3.2.

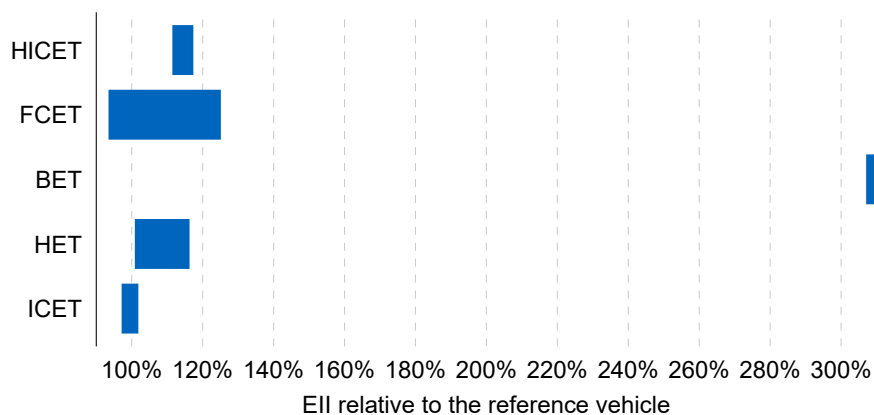


Figure 7.3: In the status quo scenario, the optimized diesel and the FCETs (SMR hydrogen) outperform the reference vehicle. The European energy mix diminishes the HETs' environmental performance. For the same reason, the BET performs worst. In addition, battery production worsens the EII.

7.3 Optimization Results

The vehicle concepts studied differ from each other technically. Section 7.3.1, therefore, analyzes which technological relationships have a relevant influence on the three objectives. Additionally, Section 7.3.2 shows the composition of the environmental impact. The most cost-efficient vehicle is selected from the optimization results, and its life cycle phases are evaluated based on the individual impact categories.

7.3.1 Vehicle Concepts

Section 7.1 and 7.2 summarized the differences between the vehicle concepts regarding their economic and environmental performance. Each vehicle concept has distinct design parameters and, accordingly, other degrees of freedom that the engineer can utilize, resulting in technical correlations between the parameters and the objectives. These interrelationships are discussed below for each concept. The results are previously published [138] and extended by the HICET in this work. Within this publication, the optimization results' raw data has been published on *Github* as part of *LOTUS* [116].

Diesel Concept

Figure 7.4 shows the correlation between the three objectives TCO, EII, and RCA for the optimized diesel concepts. This representation highlights the trade-offs resulting from the Pareto-optimality. On the one hand, TCO and EII behave similarly in certain solution space regions (top center, and center left). They can be optimized together, reducing costs and environmental impact at the same time. On the other hand, an improved (i.e., higher) RCA always correlates with deteriorating EII. It must be noted that the results show an optimal trade-off between costs and RCA at approximately 14 %.

The histograms in the diagonal are an indicator of the optimization algorithm's performance. The algorithm sorts the Pareto-optimal individuals to achieve an even distribution among the Pareto-front. This results in a near-uniform distribution as can be seen in the center and the bottom right corner of Figure 7.4. The accumulation of individuals around a TCO of 7.05 EUR/100 km (top left) can be explained by the minimum TCO at a RCA of approximately 14 %.

If RCA is taken as an indicator of driving characteristics, a simple insight is reflected in the results: higher-performing vehicles have higher costs and environmental impacts. An analysis of the design variables shows that the maximum engine torque $T_{ICE,max}$ is the significant technical lever for this.

Figure 7.5 shows that the optimization algorithm utilizes the complete engine torque design space with $T_{ICE,max}$ between 1500 N m and 2500 N m. Figure 7.5 (left) shows the correlation between engine torque, TCO and EII. Regarding costs, the torque has an optimum of approximately 2000 N m. Less torque reduces the average velocity and impairs the costs. In contrast, higher torque also increases the (average) energy consumption and, thus, costs (5 %). In EII, the influence of the average speed is subordinate, which is why a higher motor torque always leads to increased resource input and higher energy consumption. With increasing engine torque, the EII deteriorates up to 10 %. However, increased torque strongly improves the RCA (80 %). Besides the ICET torque, the gearbox design influences the objectives. Most solutions (97 %) have eight gears with an average gear spread of 21.6 with a standard deviation $\sigma = \pm 1.2$ and an average rear-axle ratio of 2.70 ± 0.03 .

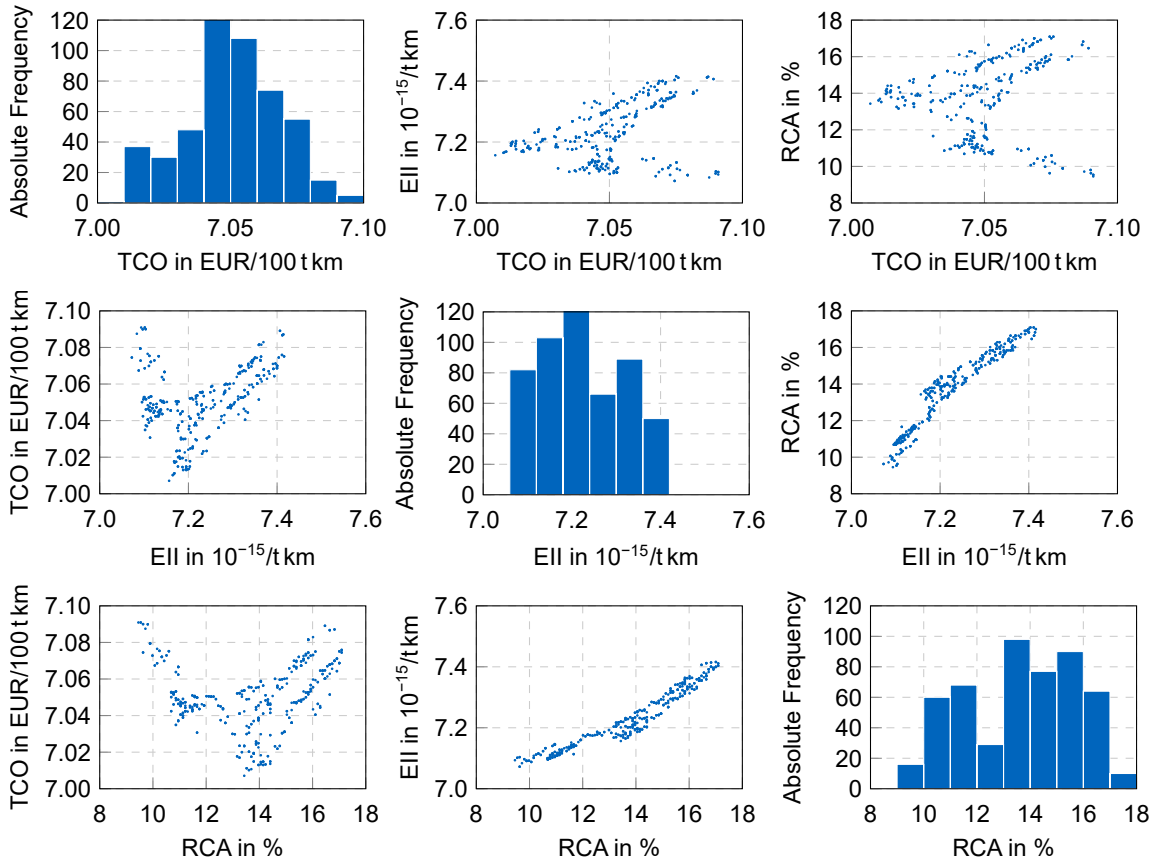


Figure 7.4: The plot matrix for the diesel optimization results shows the correlation between the three objectives as well as their distribution on the diagonal. While the algorithm can reduce costs and environmental impact at the same time, improving driving performance or RCA leads to a deterioration of the other two target variables. However, the TCO has a minimum at an RCA of approximately 14 % because a lower driving speed reduces the average vehicle speed and, thus, increases the costs per tonne-kilometer.

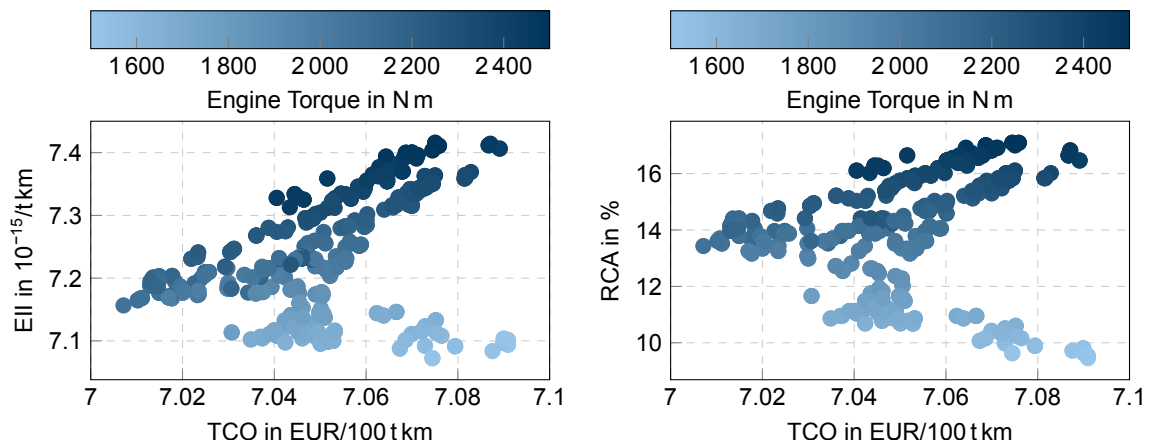


Figure 7.5: The engine torque $T_{ICE,max}$ has the largest influence on the three optimization objectives. Higher torque always improves RCA and deteriorates EII. Regarding costs, there is an optimum torque of approximately 2000 N m. Higher torque increases energy consumption and, thus, TCO, while lower torque reduces the average vehicle speed and, thus, mileage, which also increases costs.

Hybrid Electric Concept

Figure 7.6 shows the correlation between the three objectives as a result of the HET optimization. The results show a similar picture to diesel optimization: costs and environmental impact are not conflicting objectives. However, it is noticeable that there is no optimum concerning the RCA and, thus, the engine torque. The electric motor compensates for the disadvantage of smaller combustion engines. Furthermore, it can be seen that the RCA of the HET population is higher than that of the diesel population. Here, the electric motor leads to an improvement in driving performance for all vehicles.

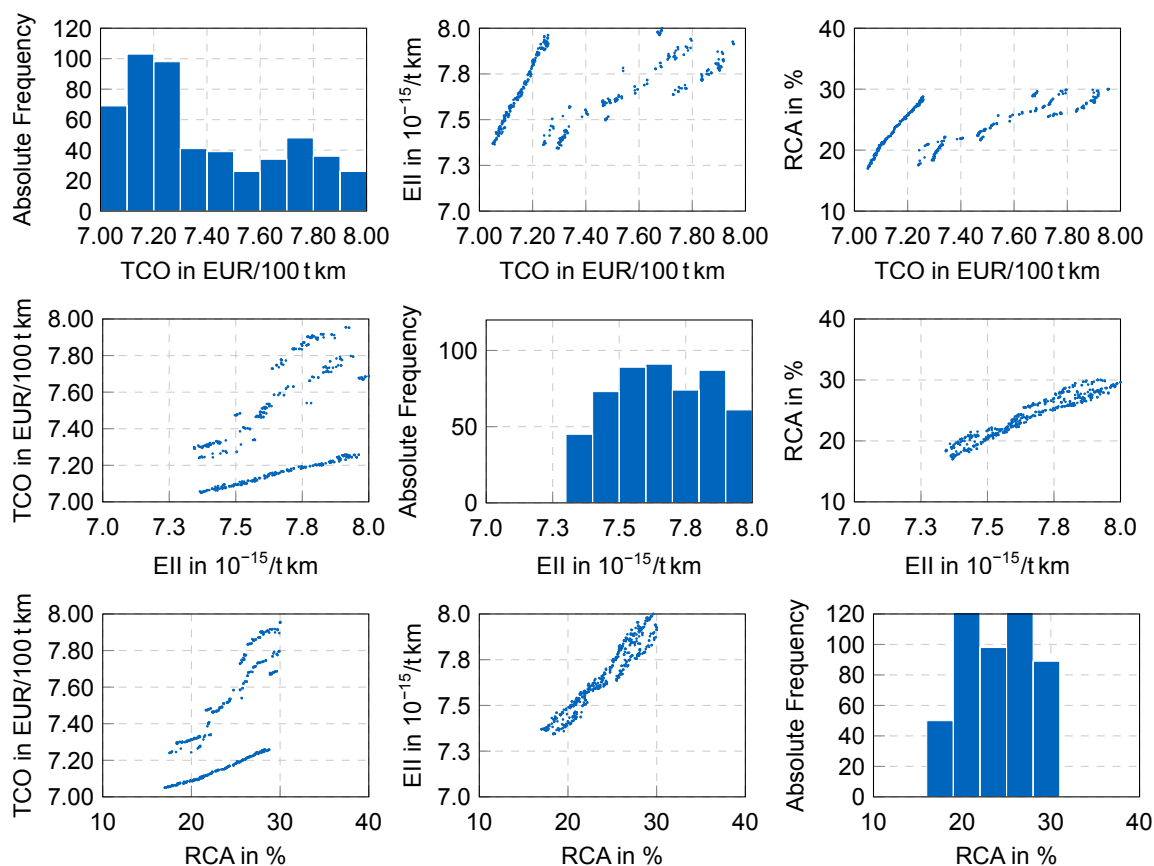


Figure 7.6: The plot matrix for the HETs show the same correlation as the diesel results. While TCO and EII can be minimized together, an improvement in RCA always leads to a deterioration of the other two objectives. Due to the additional torque provided by the electric machine, the HETs' RCA are higher than the diesel.

Figure 7.7 (left) shows that the electric machine torque $T_{EM,max}$ has the same effect on costs and EII as the ICET torque: With increasing torque, both TCO and EII also increase. In addition, the battery capacity C_{Bat} has a strong influence on the two objectives. Here, higher C_{Bat} yields lower TCO while it does not significantly affect the EII (Figure 7.7, right). However, most individuals have a small-sized battery capacity of 29.0 ± 6.3 kWh. The algorithm chose an asynchronous electrical machine for all individuals. Because the threshold for electric-only driving is at a low torque of 226.0 ± 80.6 Nm, the electric machine is used foremost for load-point shifts and boosting and not for electric-only driving. Accordingly, $T_{EM,max}$ is also low (725.0 ± 82.6 N m) compared to the average ICET torque (2458.0 ± 88.0 N m).

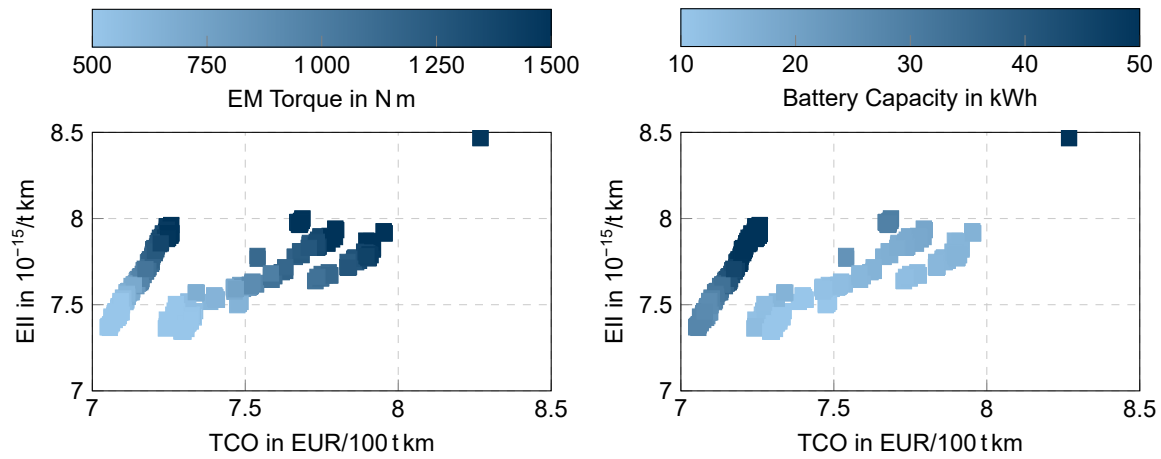


Figure 7.7: The two HET design variables electric machine torque $T_{EM,max}$ (left) and gross battery capacity C_{Bat} (right) have the largest impact on the objectives. In this context, an increase in motor torque predominantly leads to a worsening of the environmental impact with no influence on the TCO. In contrast, the battery capacity affects the costs but not the EII.

Battery Electric Concept

Figure 7.8 shows the BETs' large spread in TCO and at the same time low spread in the EII. Analogously to the two previous concepts, the BETs show that low TCO correlates with reduced environmental impact, while a better RCA deteriorates the other two objectives. The plot matrix shows no visible correlation between costs and environmental impact, which can explain the wide spread in TCO.

Figure 7.9 (left) indicates that the large spread in costs is related to battery capacity. Here, larger battery capacities achieve lower costs, due to higher mileage. Although this increases the vehicles' weight and, consequently, their energy consumption, there is no clear correlation between battery capacity and EII. On the right side in Figure 7.9, it can be seen that increasing motor torque leads to improved RCA and higher environmental impact. This suggests that the use phase and the associated energy consumption dominate the EII, with the electric torque being the important design variable. On average, the battery capacity is 515.0 ± 119.8 kWh, and the average electrical torque is 2444.0 ± 432.4 Nm provided by a permanent synchronous machine (PSM). All solutions have a direct-drive transmission with a gear spread between 10 to 14 and a rear-axle ratio between 1 to 1.36.

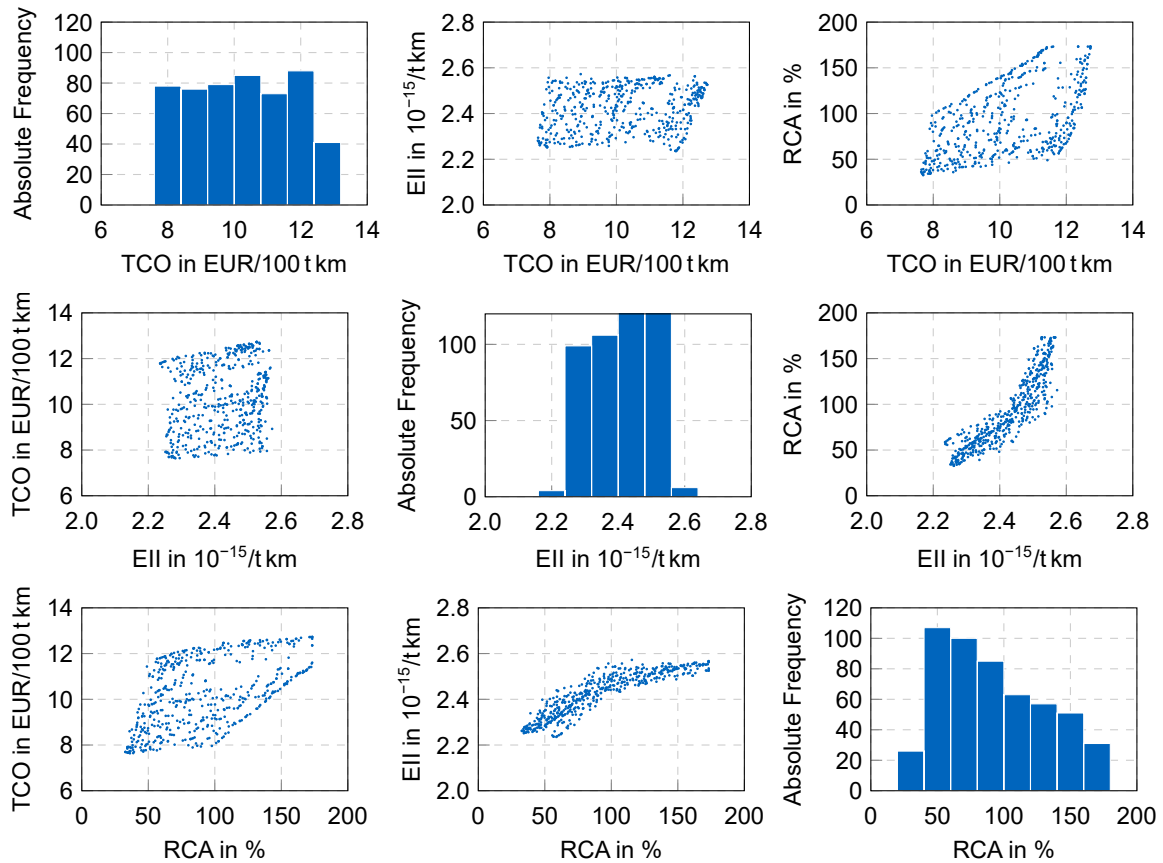


Figure 7.8: The plot matrix for the BET optimization shows that there is no visible correlation between TCO, EII, and RCA, which could explain the large spread in costs. However, improved RCA leads to higher environmental impact.

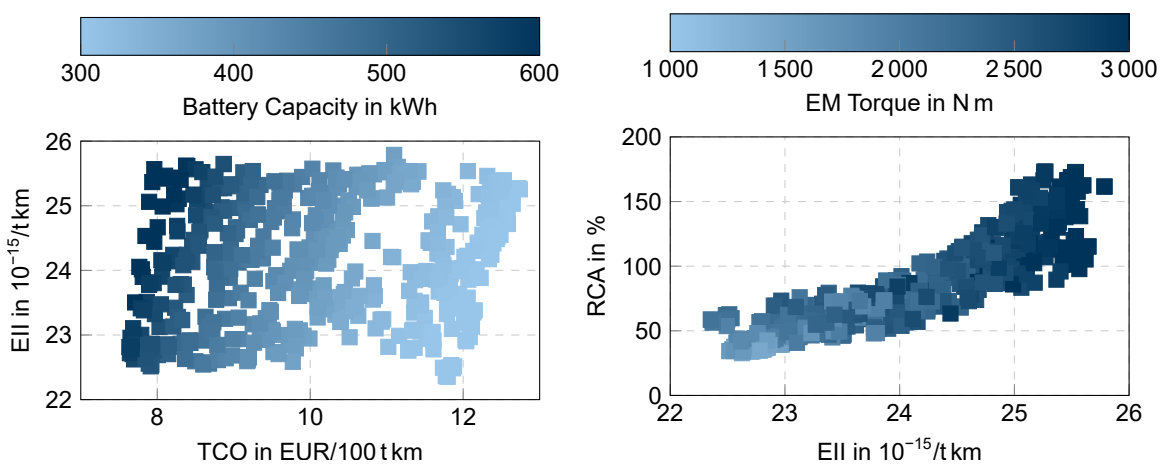


Figure 7.9: The two BET design variables battery capacity (left) and electric machine (EM) torque (right) have the greatest influence on the objectives. A higher battery capacity enables greater ranges and, thus, mileage resulting in lower costs. However, the influence of capacity on the EII is small. The EII is mainly influenced by the motor torque: improving the RCA by increasing the torque worsens the EII.

Fuel Cell Electric Concept

Similar to the other results, costs and environmental impacts increase with RCA improvement (Figure 7.10). The first feature standing out about the FCET results are the two Pareto-fronts that emerged (Figure 7.1 and Figure 7.10). One Pareto-front is located at approximately 10 EUR/t km, the other between 11 EUR/t km and 13 EUR/t km. The DOD is the prevailing design variable here.

While all individuals have a similar and small battery capacity of 63.0 ± 1.0 kWh, the DOD varies between 13 % and 80 % (Figure 7.11), where a higher DOD correlates with increased TCO due to reduced battery life. The effect on the EII, however, is small, as this is again dominated by energy consumption. This means that there is mainly a trade-off between battery utilization and costs. All solutions are equipped with a PSM with an average torque of 3586.0 ± 95.0 Nm and have a fuel cell power P_{FC} of 283.0 ± 12.8 kW close to the upper boundary of 300 kW. Although a truck requires only approximately 120 kW to drive at cruising speed on the highway, the high fuel cell powers can be explained by their improved efficiency under partial load. The, consequently, more expensive fuel cell stack is offset by the gain in efficiency and is, thus, worthwhile from a cost perspective.

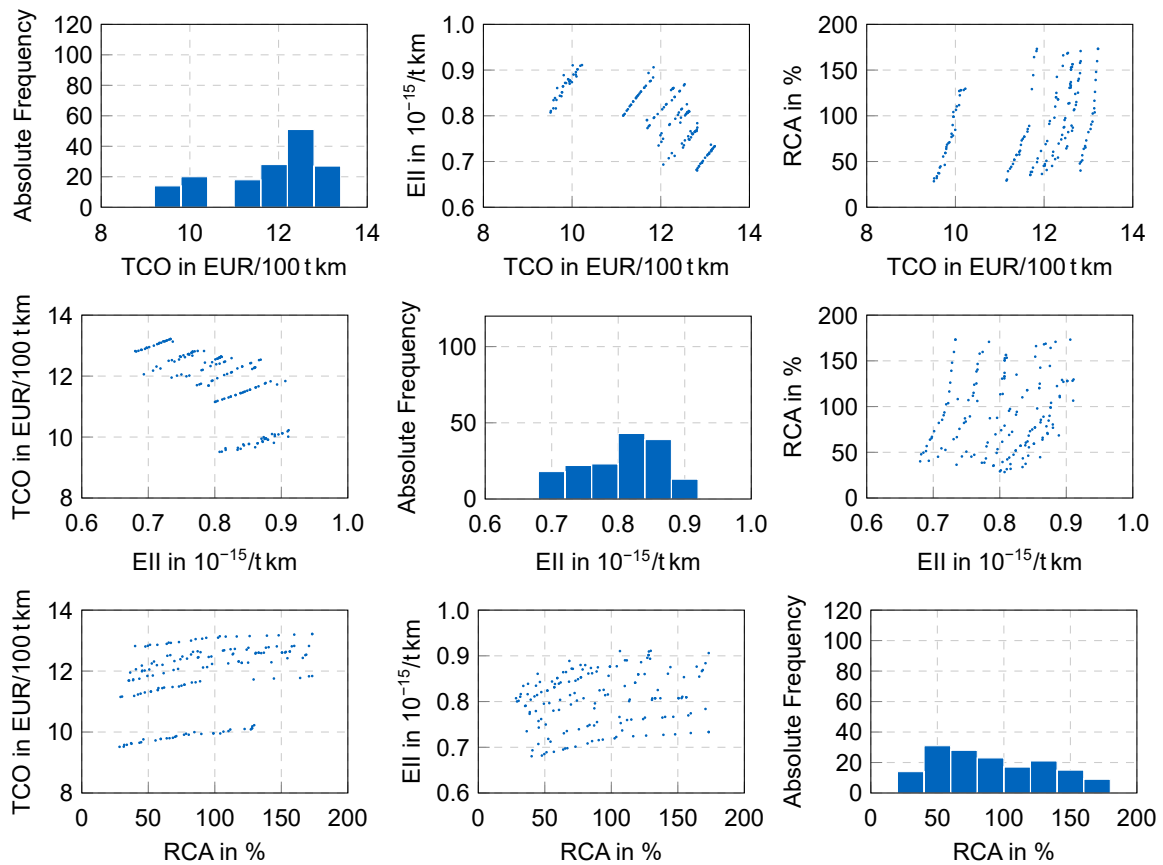


Figure 7.10: The plot matrix for the FCET optimization shows that six distinct Pareto-fronts with different costs emerged. One is located around 10 EUR/t km, while the other have costs in the range 11 EUR/t km to 13 EUR/t km.

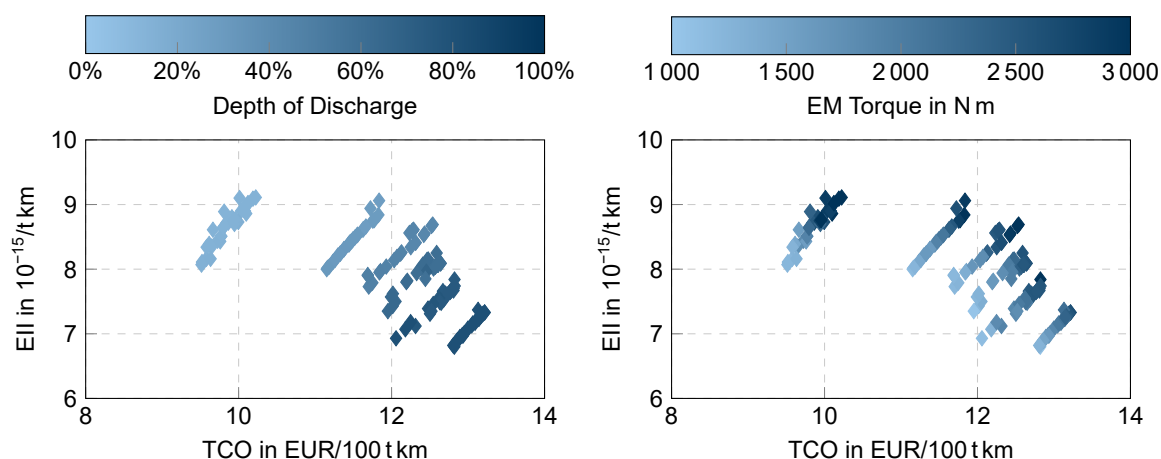


Figure 7.11: The two design variables DOD (left) and EM torque (right) have the greatest influence on the objectives. A higher DOD enables longer ranges and, thus, mileage at the expense of reduced cycle life. The latter effect dominates, resulting in higher costs. The influence of the DOD on the EII is small. The EII is mainly influenced by the motor torque: improving the RCA by increasing the torque worsens the EII.

Hydrogen Combustion Engine Concept

The plot matrix of the HICET optimization (Figure 7.12) shows the same behavior as the diesel optimization with increased TCO and EII in favor of RCA. However, there is no cost minimum as seen in the diesel results, although both optimizations were performed with the same system power and are based on the same engine maps. While underpowering of vehicles explains this behavior in the case of diesel, the HICET results do not allow this conclusion. The conversion of the diesel engine map into the hydrogen engine map yields a *flatter* maximum torque curve (Section 4.3.3), which means that the maximum torque can be delivered in a wider speed band. As a result, the torque curve is flatter in the engine's operating range and noticeable underpowering does not occur in the operating range of the drive cycle. Nevertheless, the correlation of higher torques, which yield better RCA, at the expense of higher costs and worse environmental performance remains. It should be noted, however, that the HICET optimization results' range is wider than that of diesel optimization.

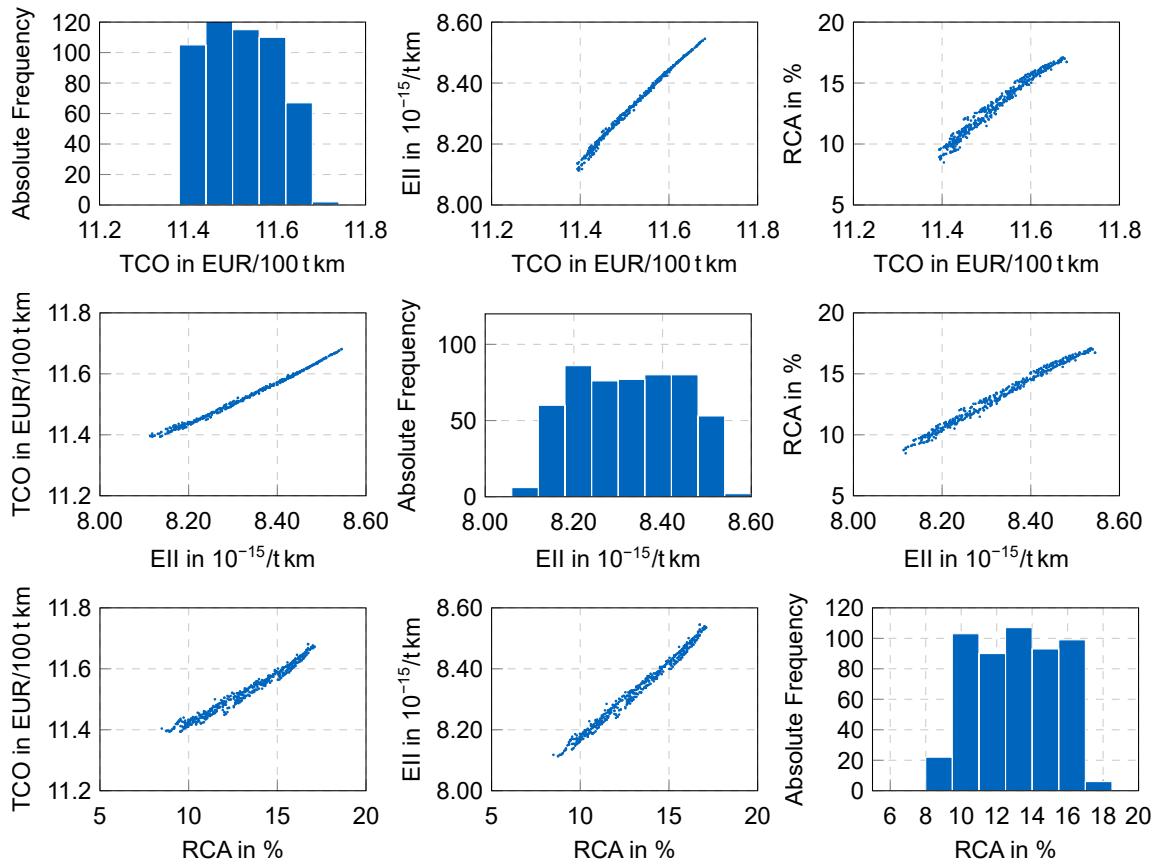


Figure 7.12: The plot matrix for the HICET optimization shows a distinctive Pareto-front. Similar to diesel optimization, the trade-off between good RCA at the expense of costs and environmental performance, exists.

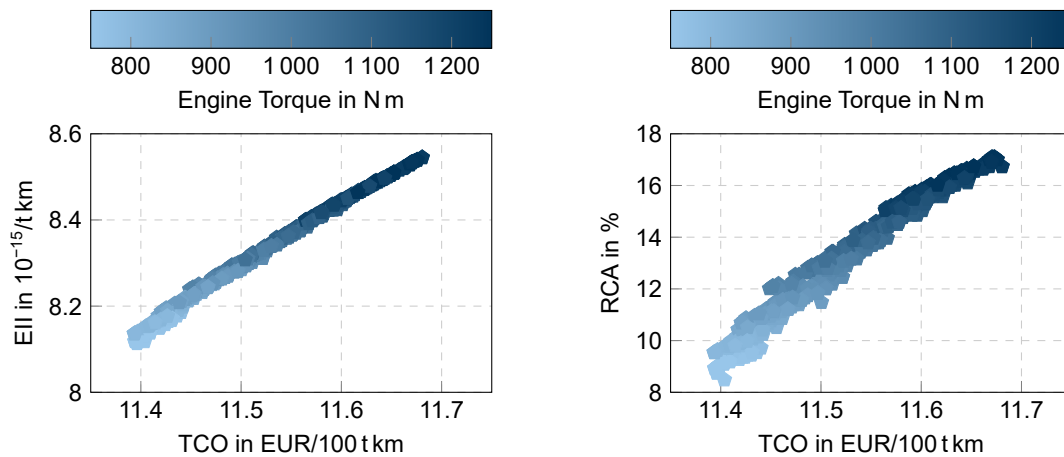


Figure 7.13: The HICET engine torque has the greatest influence on the objectives. TCO, EII, and RCA are all primarily influenced by the engine torque: improving the RCA by increasing the torque worsens the other two.

7.3.2 Individual Eco-Impact

As an aggregated and weighted metric, the EII shows the relative performance without the influence of the individual impact categories (Section 2.1.2). Because the powertrain concepts presumably differ in these categories, the individuals with the lowest TCO will be compared. Therefore, Figure 7.14 shows a breakdown of the environmental impact categories. Because normalization applies, the (dimensionless) categories can be compared against each other.

The optimized diesel vehicle shows the second highest values for GWP, almost exclusively caused by the combustion of diesel, which is also reflected in the fossil resource depletion value. Compared to the diesel, the HET concept has a higher total EII ($7.37 \times 10^{-15}/\text{t km}$ vs. $7.16 \times 10^{-15}/\text{t km}$), caused by the electricity mix and the battery production impact, which can be seen as increased eutrophication, human toxicity, ionizing radiation, and resource depletion. For the BET, this effect becomes more dominant, rendering the vehicle worst in total environmental impact ($22.3 \times 10^{-15}/\text{t km}$), although it has, for example, the best performance in GWP. The nuclear power share in the European electricity mix and the associated up and downstream nuclear fuel processes are responsible for the high values of human toxicity and ionizing radiation. Additionally, the resource depletion increases due to the share of photovoltaic power plants and their manufacturing. This applies equally to the electricity used in the production and use phase. Regarding electricity and battery production, the FCET concept ($8.08 \times 10^{-15}/\text{t km}$) performs similar to the HET. The FCET, however, has better performance in the remaining categories due to the lack of fuel combustion. Furthermore, the FCET production impact of each category is lower than the BET's, which is due to a smaller battery and, consequently, less energy and resource consumption in the production phase. Due to its lower efficiency, the HICET has higher GWP than the diesel. It should be noted that the SMR hydrogen production, here, is accounted as use-phase impact (Figure 3.1).

The recycling impact for all vehicles is one to two magnitudes smaller than the other two life cycle phases, which is primarily due to lower energy consumption, particularly compared to the use phase. Although recycling lowers the impact of raw material extraction (Section 4.2.2), its influence is negligible. Thus, the recycling impact cannot be seen in the figure.

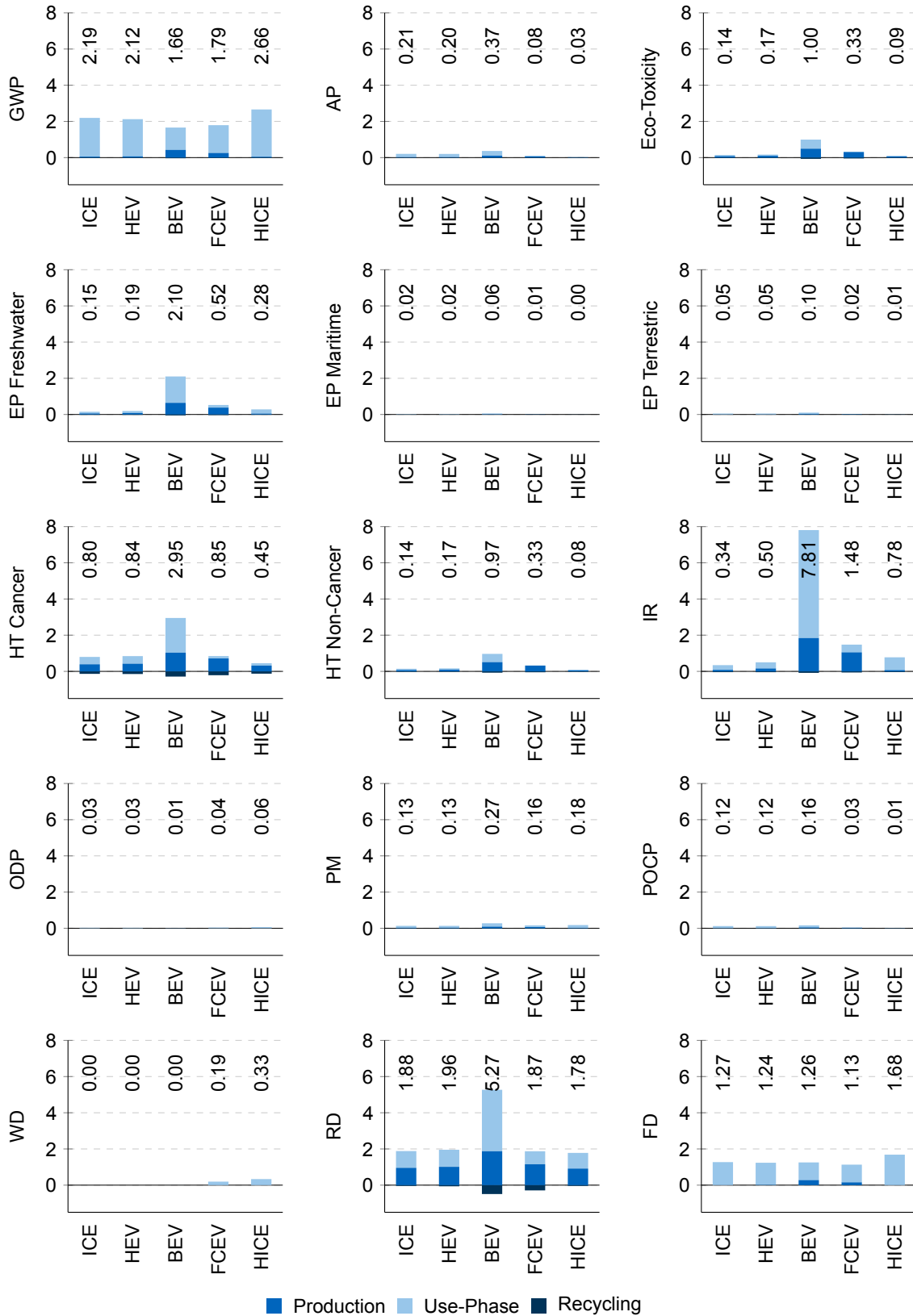


Figure 7.14: Selection of normalized environmental impact categories for the individuals with lowest TCO. For comparison between the categories, all values are given in $10^{-15}/t.km$. Because the diesel optimization results are very close to the reference vehicle, the latter is not shown. The normalization is based on Sala et al. [104] and the factors are given in Table 2.1. [Note: GWP=Global Warming Potential; AP=Acidification Potential; EP=Eutrophication Potential; HT=Human Toxicity; IR=Ionizing Radiation; ODP= Ozone Depletion Potential; PM= Particulate Matter; POCP=Photochemical Ozone Creation Potential; WD=Water Depletion; RD=Resource Depletion, Minerals; FD=Fossil Resource Depletion]

7.4 Eco-Efficiency Potential

The presented optimization results assume the status-quo energy mix, energy production paths, and energy and component costs (Section 3.2.1). In the *Status Quo* scenario, none of the alternative powertrain concepts outperforms the diesel, being either worse in costs or environmental impact or both. The question remains, how future developments affect the results and if or how much the alternative powertrain concepts can improve? The *Potential* scenario (Section 3.2) represents these developments with the major influencing factors regarding environmental and economic impact being changed. The prospective assessment (Section 7.4), hereby, shows eco-efficiency potential for each vehicle concept. Again, the individuals with the lowest TCO are used, applying the new parameter set.

Figure 7.15 compares the eco-efficiency potential for each powertrain concept (blue markers; ●) with the optimization results (blue markers; ●). While the BET mainly improves in EII, which is due to the use of renewable energy, the hydrogen-powered vehicles strongly improve their costs, primarily because of decreasing hydrogen costs. Utilizing synthetic diesel, both the diesel and the HET deteriorate.

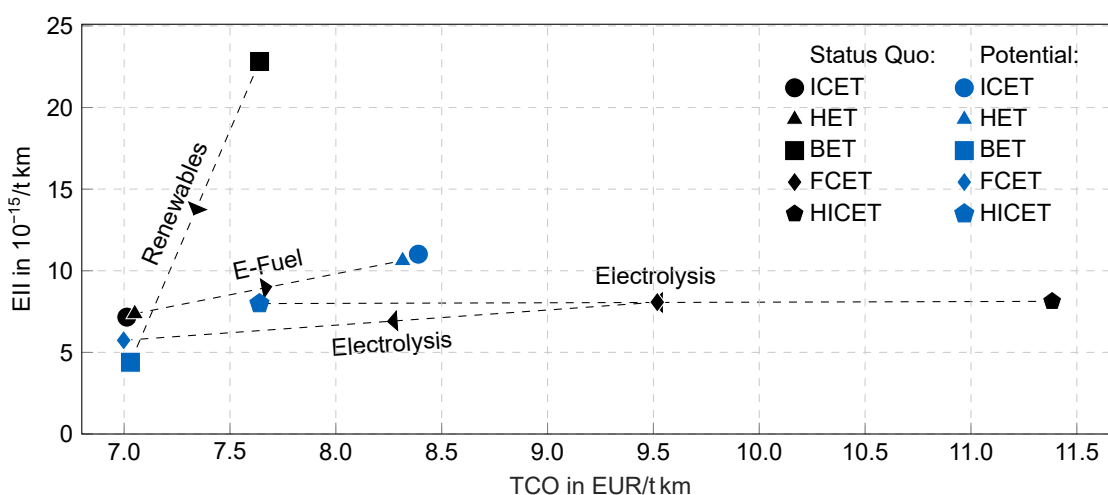


Figure 7.15: The vehicle concepts' technological potential (blue markers; ●) shows the improvement in eco-efficiency of the BEV and the FCEV, while the diesel and HEV deteriorate. The black markers (black markers; ●) indicate the optimization results presented in this study. The potential scenario assumes renewable energy, hydrogen via electrolysis, and synthetic diesel—both produced with renewable energy.

The assumed battery cost reduction benefits the BET's acquisition costs and its TCO. The significant improvement in EII highlights the importance of a renewable energy mix for electric vehicles. This is particularly important for use-phase intense applications, such as heavy-duty vehicles. With the future developments considered, the BET outperforms the state-of-the-art diesel-powered vehicles, undercutting their EII at similar TCO.

The electrolysis hydrogen path results in EII improvement, but due to the lower well-to-wheel efficiency, the resource depletion is also worse than the BET. Accordingly, the FCETs' EII is 2% higher than the BET. The FCET shows the highest cost reduction potential, with costs also at the level of today's diesel vehicles.

It should be noted that synthetic diesel reduces global warming potential by approximately 35%; yet, the overall EII worsens due to the additional well-to-tank emissions. Furthermore, there are still non-CO₂ tank-to-wheel emissions present in both diesel-powered powertrains, albeit, due to lower energy consumption, the effect is smaller on the HET. Thus, neither the use of synthetic diesel nor the hybridization of heavy-duty vehicles provides an improvement in eco-efficiency.

With 94 %, the HICET shows the highest GWP reduction (Figure 7.16). At the same time, the FCET and the BET reduce their cradle-to-grave GWP by 91 % and 80 %, respectively. The lower GWP is also reflected in decreasing fossil resource consumption. However, the results show that the reduced FD comes at the expense of increased mineral resource depletion, whereby photovoltaic electricity generation and rare earth metals, present in the battery and the electric motor, contribute the most. In both cases, though, research is underway to reduce rare earth metals [296, 297].

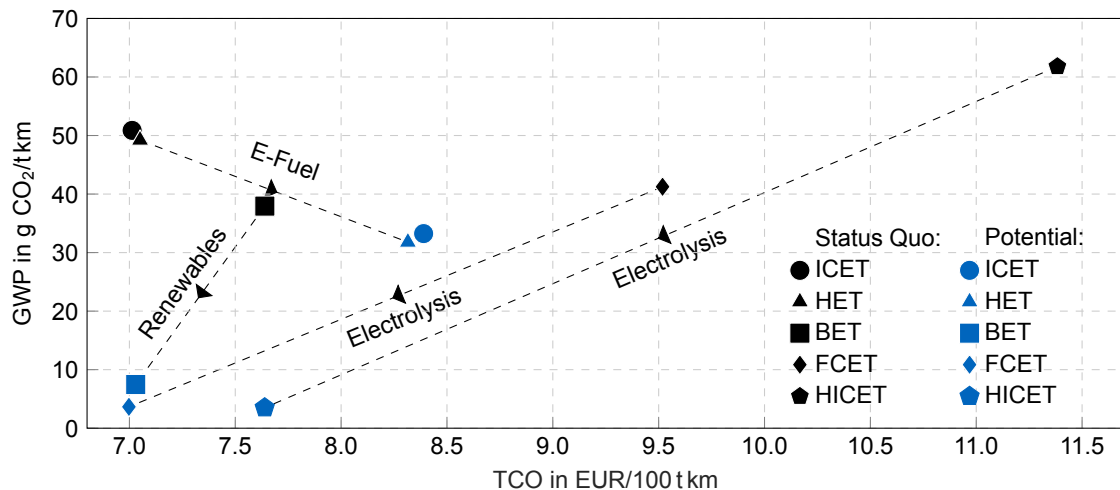


Figure 7.16: The technological potential (blue markers; ●) shows vehicle concepts' reduction of life-cycle GWP. The black markers (black markers; ●) indicate the optimization results presented in this study. The potential scenario assumes renewable energy, hydrogen via electrolysis, and synthetic diesel—both produced with renewable energy. It should be noted that these values are not relevant for the tank-to-wheel EU regulation.

The reduction of greenhouse gases is a key reason to develop alternative powertrains. Nevertheless, the results show that reduced fossil consumption comes at the cost of increased mineral resource depletion. Altenburg et al. [142, p. 97] confirm that there is a “shift towards resources that are currently not intensely used ones. Cobalt is critical, but overall environmental improvements prevail.” Resource depletion is a measure of resource scarcity and, thus, refers to inter-generational sustainability. Therefore, it is an important, time-dependent, socio-economic measure, but as Klinglmaier et al. [90] conclude, “it is arguable whether resource availability is an environmental or economic issue and whether this should be subject to characterisation models.” Furthermore, Slowik et al. [298] found that no resource shortages occur, due to increased (global) electric-vehicle shares. Consequently, and as discussed in a previous publication [56], the application of resource depletion as part of a prospective environmental assessment is questionable.

In addition to the results according to the ILCD impact categories, Figure 7.17 shows the status-quo (○) and the potential scenario (○) with an adapted weighting set, excluding both resource depletion categories. As expected, the environmental impact index decreases for all vehicle concepts. Compared to the status-quo diesel, battery electric and hydrogen-powered powertrains reduce EII by nearly half. Synthetic diesel, on the other hand, increases EII. All costs remain unchanged.

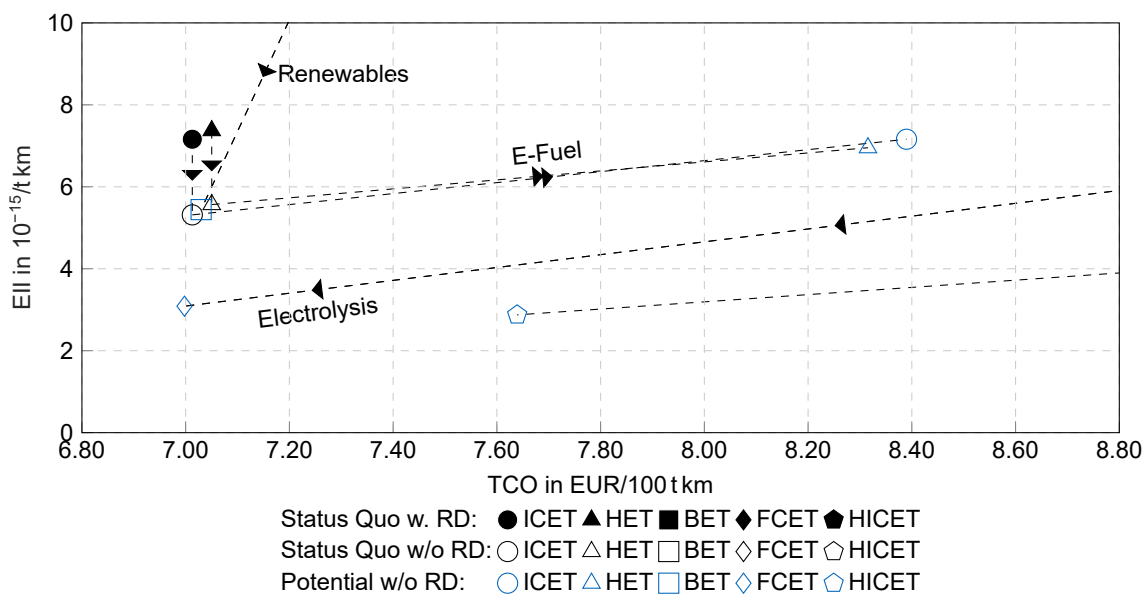


Figure 7.17: An adapted weighting set excludes the mineral and fossil resource depletion as a measure of direct environmental impact. The filled markers (●) indicate the results including RD and FD. The empty markers show the optimization results (○) and the potential scenario (○), each excluding RD and FD from the weighting. For a better visibility, only the potential results, excluding RD and FD, for the BET, FCET, and HICET are shown.

7.5 System Cost Results

The preceding considerations describe the conclusions related to the comparison of individual vehicles and, consequently, a micro(-economic) perspective. As described at the beginning, a macroeconomic perspective is still required for policymakers. The system cost approach transfers the results from a single-vehicle perspective to a likely, future vehicle stock, estimating its eco-efficiency and including infrastructure costs.

To perform this analysis, the zero-emission powertrain's system costs, which fulfill the long-term EU reduction targets, are used. Accordingly, neither Diesel nor HET are included. The BCG electrification scenario (Section 4.1.4) serves as a basis for this. On the one hand, this scenario fulfills the requirements of the EU regulation, so that no penalties are due. On the other hand, it requires a smaller change in the vehicle stock, which means that this scenario is easier to implement and is, therefore, assumed to be more likely. Furthermore, the assumption is made that the entire share of ZEVs is represented by one vehicle concept in each case. This simplification is necessary because the model assumes best-case costs for each vehicle concept. This assumption is only valid if economies of scale are exploited to the best possible extent, which is not the case with a distribution between technologies. Accordingly, a distribution would inevitably lead to higher costs than would be the case for a single technology. The costs are probably non-linearly related to the distribution, which the system cost approach cannot represent. This relationship is outside the scope of this work and could be investigated in further work. Additionally, a correct distribution, for example between BET and FCET, is impossible to predict and, thus, the uncertainty of the observation is inadmissibly increased.

To consider the technology development based on the two scenarios, the status quo scenario is assigned to the year 2020. The potential scenario corresponds to the year 2030. The values in between are interpolated linearly.

Furthermore, the battery electric overhead catenary truck is considered here. According to the results from Section 4.3.4, a reduced battery size is assumed, which has no impact on the daily range. This reduces the acquisition costs and, consequently, the TCO. It is assumed that starting in 2022, an overhead line network of 3000 km is built by 2030 (which corresponds to a realistic expansion of 500 km/a). Over this period, the TCO reduce linearly: Beginning with equal costs as a BET (7.5 EUR/100 km), they decrease to 6.5 EUR/100 km, including the maximum battery reduction of 300 kWh. For reference, the optimized BET has a battery capacity of 675 kWh.

Figure 7.18 shows the resulting system costs with the vehicle stock development for reference. Because the system costs multiply the different TCO of the vehicle concepts with increasing vehicle population, the previous results are more clearly reflected here: While hydrogen-powered vehicles in particular benefit from cost reductions, the costs of the BET decrease less. However, all vehicle concepts can compensate for the progressive stock growth, showing a degressive course in system costs. Comparing the two BET with the two hydrogen-powered concepts, this course is more pronounced for the latter. Because the transportation costs—comparable to total industry turnover—correlate with the TCO and comprise the majority of the system costs, the hydrogen cost reduction leads to a more degressive course. Additionally, Figure 7.18 shows that, despite lower TCO, the OBET's system costs are the highest, due to the high infrastructure costs, starting in 2022. It has to be mentioned, that after 2030, no or little additional catenary infrastructure has to be built. This means that the OBET system cost slope decreases and only increases with the continued need for charging infrastructure.

For the two assumed scenarios, the FCET outperforms the BET regarding TCO from the mid-decade onward. By the year 2030, the BET system costs reach the level of the HICET, which is because of lower infrastructure costs.

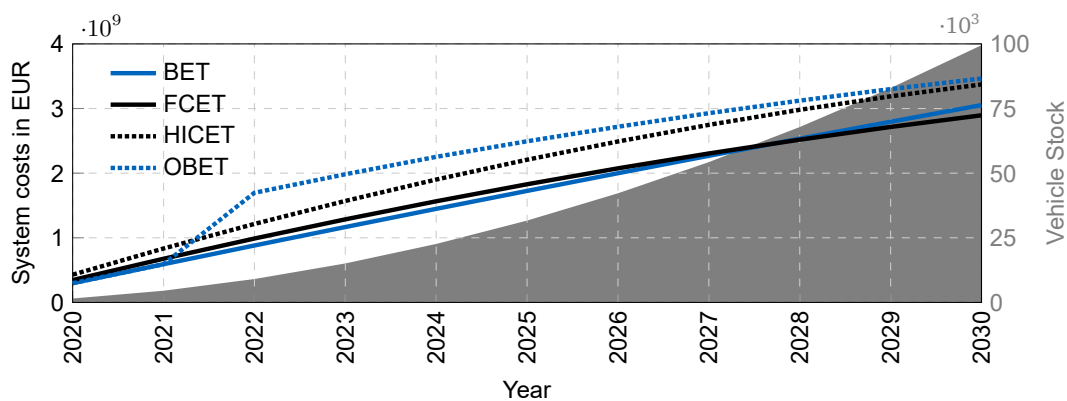


Figure 7.18: The system costs for the BCG E scenario show that all vehicle concepts overcompensate for the progressive vehicle stock growth. From the system costs perspective, FCET and BET perform best, achieving similar overall performance. HICET and OBET deviate due to lower efficiency and higher infrastructure costs, respectively.

Analogous to the system costs, the total EII can be obtained from Equation (4.3) by replacing TCO_i from C_T with the vehicle-specific EII. Figure 7.19 shows the results for the BCG electrification scenario. The vehicle-specific effects also intensify, so that both BETs benefit from their improvement in EII. The effect is strong enough that around the year 2025, despite the growing vehicle stock, there is a declining overall EII. In contrast, the hydrogen-powered vehicles EII show a slightly degressive course.

Overall, the BET and the OBET are the better vehicle concepts for reducing environmental impact in the long term. However, the OBET is always the most expensive option due to its infrastructure costs. Because of lower infrastructure costs and stronger TCO reduction, the FCET is preferable from a cost perspective, although the BET obtains similar infrastructure costs by the end of the decade. It

should be noted that the charging and hydrogen infrastructure costs are sensitive to the daily usage parameter (Appendix I). However, assuming equal usage for both, the hydrogen infrastructure remains less expensive. At the end of the period under review, the FCET is the vehicle concept with the best (i.e., highest) overall eco-efficiency. However, due to the improvement of the electricity mix and the declining EII, it can be assumed that post-2030, the BET will achieve better eco-efficiency.

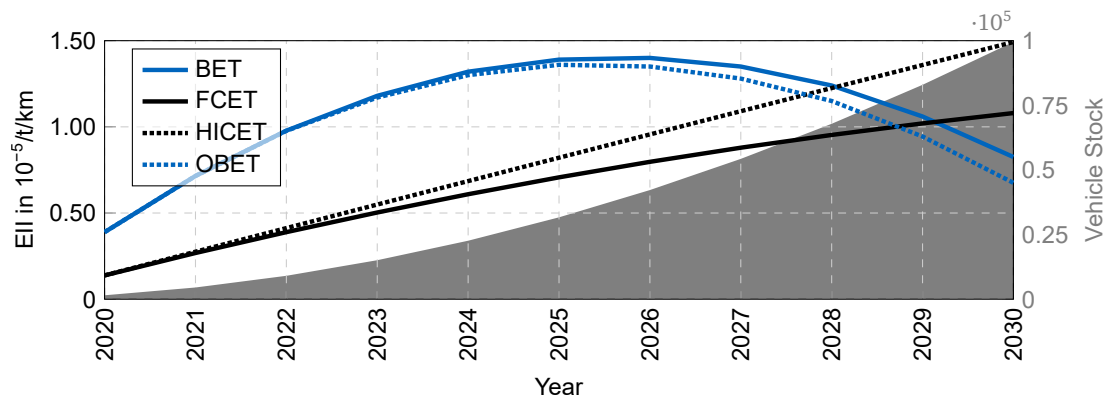


Figure 7.19: The total EII for the BCG E scenario show that all vehicle concepts overcompensate the progressive vehicle stock growth. From the environmental perspective, the BET perform best. The increasingly renewable energy mix results in the BET's decreasing environmental impact mid-decade. FCET, HICET, and OBET deviate due to lower efficiency and higher infrastructure costs, respectively.

8 Discussion and Conclusion

The optimization showed that eco-efficiency provides good and robust objectives for vehicle concept optimization. Applying a normalized and weighted life cycle assessment and a life cycle costing, the eco-efficiency yields understandable and intuitive results and is suitable for comparing emerging technologies.

However, the EII is a lumped index, losing the information of the single impact categories. Furthermore, as Sala et al. [104, p. 16] conclude, “no science can tell whether weighting based on the distance to policy, precautionary boundaries, stakeholders’ and experts’ opinions or any other method is the ‘right’ one to be applied, in general terms.” This can lead to individual positive effects being weakened by others, worsening effects or even disappearing altogether. Due to this, the weighted and normalized EII should never be used as the *only* measure to assess technology, but always in conjunction with the individual impact categories. Only the analysis of individual categories allows well-founded trade-offs to be made.

Nevertheless, this easy-to-use method does not only support engineers in the early design phase to develop cost-efficient vehicles with reducing environmental impact at the same time. The method also helps the scientific community by, first, applying vehicle concept optimization as a method of prospective technology assessment. Second, generic data sets for the cost and environmental assessment of heavy-duty vehicles have been published as part of the preliminary publications [31, 55, 56, 100, 196]. In particular, the life cycle inventory of heavy commercial vehicles [100] enables the scientific community to perform its own calculations on the environmental impact of commercial vehicles.

8.1 Stakeholder Survey

The eco-efficiency assessment has the underlying assumption that costs (vehicle and infrastructure) and environmental impact are sufficient objectives to compare zero-emission vehicle concepts. Furthermore, this work assumes that a transition towards zero-emission vehicles will occur. Dominated by environmental reasons, the current EU regulation mandates this transition. However, it should be checked if there are further, possibly contradicting, motives for the industry’s stakeholders. A survey-based confirmatory factor analysis (CFA) will, therefore, determine whether relevant stakeholders confirm these assumptions and how these stakeholders relate to the transition towards zero-emission vehicles.

Barré’s stakeholder survey [299], identified relevant stakeholders and determined their attitudes toward the powertrain technologies. Based on a literature review, he identified four stakeholders:

- The OEM due to their responsibility not only in vehicle development but also customer education and (public) communication [300].

- The public, on the one hand, due to their (increasingly *green*) consumer choices and, on the other hand, being represented by the politics and their governmental choices [301].
- The fleet owners or operators, being the products' customers, represent a crucial stakeholder. Apart from economical choices, their attitude (e.g., brand image, emotions, sense of responsibility) towards a technology strongly influences the decision-making process [301, 302].
- The drivers who—although rarely addressed—play a key role in technology acceptance [303].

Barré [299, p. 29f] analyzed the four stakeholders using 16 attributes of ZEVs taken from the literature [304]:

- | | |
|--------------------------------|---|
| 1. Travel range | 9. Local air quality |
| 2. Charging or refueling time | 10. Global CO ₂ -emissions |
| 3. Acquisition costs | 11. Traffic noise |
| 4. Energy costs | 12. Traffic safety |
| 5. Maintenance costs | 13. Job creation |
| 6. Infrastructure costs | 14. Industry and job attractiveness |
| 7. Infrastructure availability | 15. National energy independency ¹ |
| 8. Incentive needed | 16. Economic development |

The attributes 1 to 8 reflect the economic and operational performance of the vehicles. These attributes can be directly assigned to the individual vehicle concepts and compared with each other. In addition, the attributes 9 to 16 represent socio-ecological influences. These cannot be directly assigned to a vehicle concept, but refer to the transition to zero-emission vehicles in general. Besides BET and FCET, Barré included LNG vehicles as an option, because these vehicles currently experience a strong market growth (Section 2.3). Overhead catenary vehicles were also included, but the response rate was too low to allow a statistical evaluation.

The 16 attributes were first grouped into six independent variables, which in turn can be correlated into two higher-level factors. To correlate the former variables with the proposed two factors, Barré applied a CFA. In terms of data reduction, this statistical method infers a few factors from many, independent variables. The CFA produces a value that indicates the extent to which the variance of the independent variables is reflected by the underlying factors. Multiple studies [305–307], successfully applied this method in the case of electric passenger vehicles to answer similar problems. Figure 8.1 shows the 16 attributes (left column) with their respective independent variables (center column) and the two high-level factors (right column, ● and ●). The complete survey is given in Section J.1.

Figure 8.2 shows the three aggregated, economic and technical variables for each vehicle concept. Overall, there is a low variation in responses among stakeholders. However, it can be observed that OEMs assess the technologies more positively. Drivers and the public, in particular, are more critical of all technologies. Only the FCET infrastructure is rated worst by the OEMs. While this reflects the results of the literature review (Section 2.3.4), it is unclear whether the participants

¹This study was performed in 2021 and, thus, does not reflect potential changes due to the war in Ukraine and the subsequent discussion about Russian oil and gas imports.

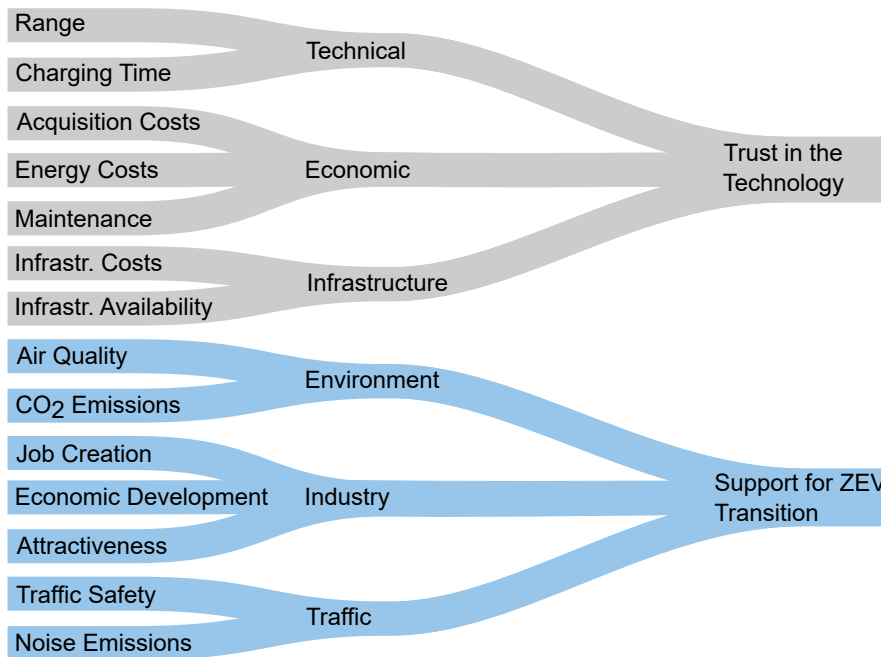


Figure 8.1: Two regression models evaluate the trust for each technology ● and the general support for the transition to ZEVs ●. Therefore, a survey ($n = 61$) collected 16 independent variables (left column), which were subsequently aggregated (center column). A CFA correlated them with the two factors (right column).

evaluated only the (comparatively low) fuel dispenser costs or the development of an overall hydrogen infrastructure. Altogether, the survey's results adequately reflect the obtained eco-efficiency results, although participants are closer to the status quo scenario.

Figure 8.3 shows the stakeholder's response to the socio-environmental attributes. It is striking that—regardless of the technology—a transition to ZEV is generally viewed positively. Throughout all stakeholders, the weighting, shown as circle-size, renders CO₂-emissions and air quality the two most important reasons for this transition, which is in line with the literature review. Again, the OEMs have a more positive attitude towards the transition than the drivers and the public.

Across all stakeholders, economic factors as well as infrastructure costs and availability have a significant (p -value < 0.05) or barely non-significant (p -value < 0.1) influence on trust in technology (Table J.4). Applying the R^2 -test, both models (*Trust in the technology* and *Support for ZEV transition*), show a goodness-of-fit of at least 70 % among the four stakeholders (Table J.3). Only the OEMs' trust in the technology could not be related sufficiently. This model failed the R^2 -test with 47 %, which could be due to the imbalance in knowledge level and expertise about the technologies: Assuming that the OEM-participants know much more about the technologies, they can give more differentiated answers.

Overall, the survey, thus, confirms the two key assumptions of the eco-efficiency assessment. CO₂-emissions and air quality, and, thus, environmental impact are relevant drivers for ZEV introduction. Assessing these (and other) environmental impacts is, therefore, necessary to weigh up the technologies against each other. From a technical perspective, economic factors and infrastructure play a crucial role. These aspects were represented in the eco-efficiency assessment, on the one hand, by a detailed TCO model, and, on the other hand, by the system cost approach.

Eventually, the question remains as to who should make the first move. Therefore, Barré [299] asked the participants to estimate their own and the remaining stakeholder's responsibility in the transition toward ZEV. In a departure from the previous survey, politics and charging operators are also assessable

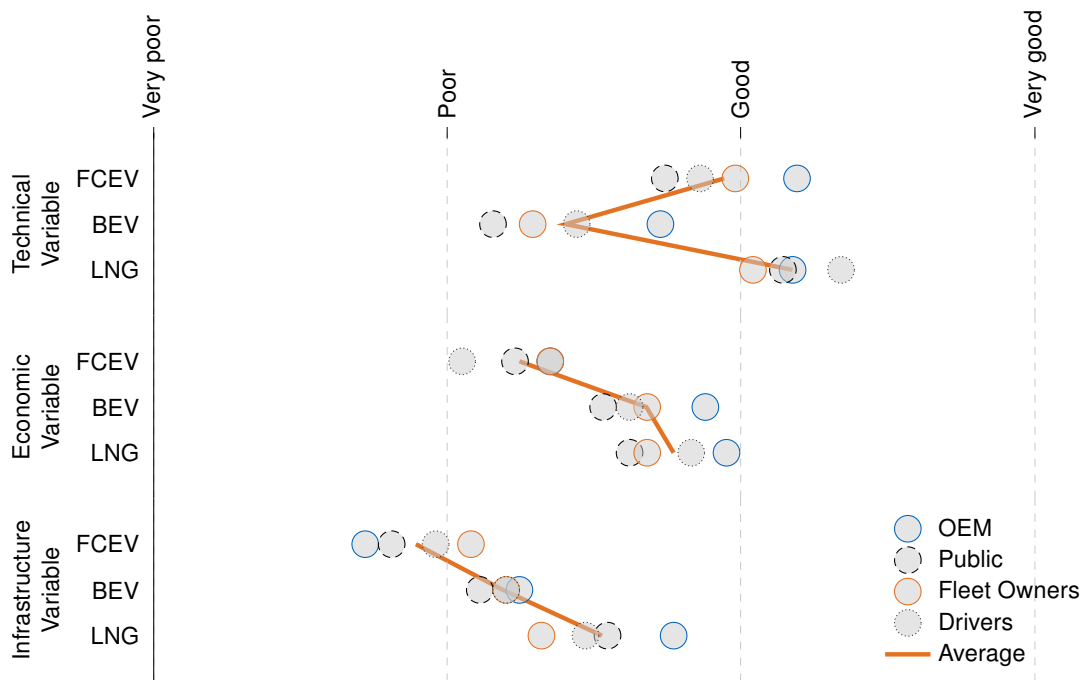


Figure 8.2: Based on Barré's [299] 2021 data, the survey ($n = 61$) results describe each stakeholder's (OEM, public, fleet owners, and driver) trust in three technologies (FCET, BET, LNG). A Likert scale assesses three independent, aggregate variables for this purpose. Overall the OEMs evaluate the technologies more positively, while the drivers and the public are less optimistic.

options there. The gathered data allows mapping the perceived and assigned responsibilities between the stakeholders, which Figure 8.4 shows. There, each row shows the responsibility assigned to the respective column. For the first four columns, the values in the diagonal are the self-perceived responsibilities of these four stakeholders.

The data shows two things: First, each stakeholder overestimates their own responsibility so that the own value in the column is always the highest. Second, the government has, on average, the highest assigned responsibility, followed by the OEMs and fleet owners, which have almost the same values. The government's important role in the transition can also be found in the literature. Moultaq et al. [141, p. 34] highlight the necessity of governments not only "in setting a clear vision," but also in creating incentives and investing in new technologies. In the same way, Altenburg et al. [142, p. 101] give concrete recommendations for political measures:

- Financial benefits
- Stricter regulations for conventional vehicles during registration and at the local level (e.g. driving bans)
- Extended standardization

The financial benefits are not limited to the vehicles but—more importantly—refer to the infrastructure. This conclusion is reached by Lozzi et al. [308], as well as Mathieu et al. [309], both of which identify targeted support for (charging) infrastructure as an important political measure. ACEA [310] even calls for binding targets for infrastructure development. Accordingly, there is an important relationship between the government and charging infrastructure, which the survey data also reflect.

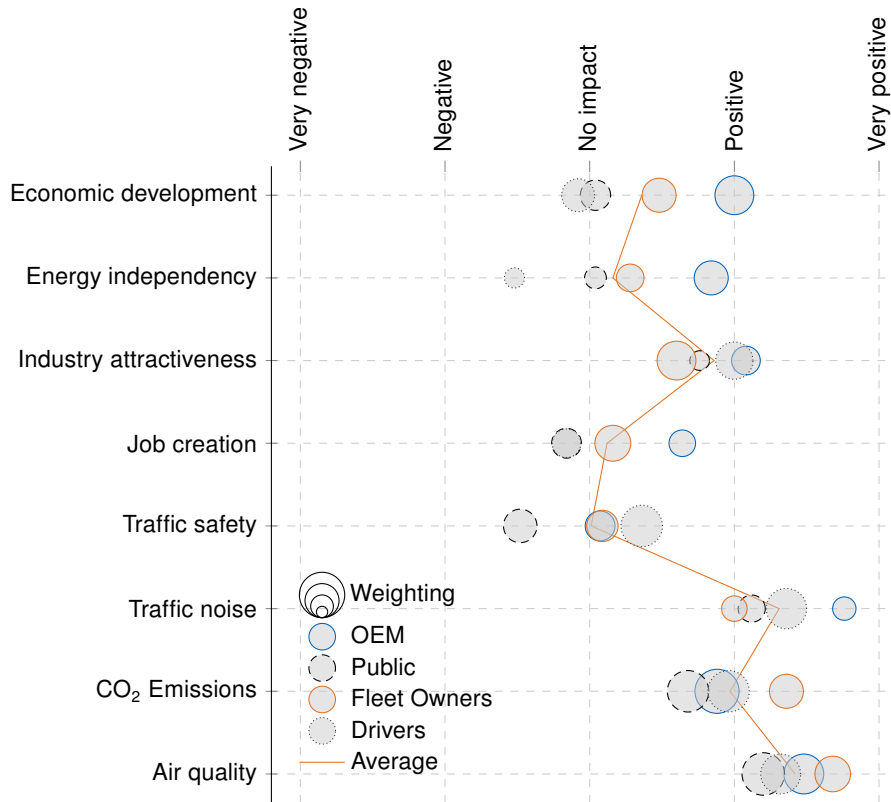


Figure 8.3: In Barré’s [299] survey ($n = 61$), eight independent variables assess the general support of each stakeholder (OEM, public, fleet owners, and driver) for the transition to ZEVs. All stakeholders have a positive or very positive attitude toward the transition. The weighting highlights CO₂-emissions and air quality as the transition’s most important drivers. Overall, OEMs have a more positive attitude than the public and the drivers.

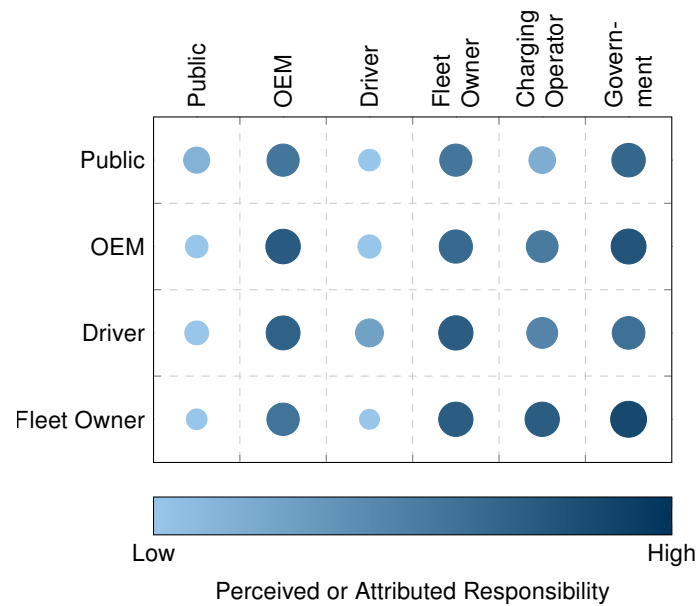


Figure 8.4: The correlation matrix shows how each stakeholder (row) assigns responsibility (color coding and circle size) in the transition to ZEVs to the other stakeholders (column). The diagonal of the first four columns represents the self-perceived responsibility, where all stakeholders overestimate themselves. The most responsibility is assigned to the government, followed by OEM and fleet owners.

8.2 Conclusions

The eco-efficiency assessment, combined with the system cost approach, can aid policy-makers. Likewise, OEMs benefit from the prospective method of vehicle concept optimization, which enables a comparison of concepts and identifies future technological developments and relevant technical levers. This is particularly relevant in the early vehicle development phase, where fundamental concept decisions are made. The generic approach has been developed specifically for this purpose. Both fleet operators and charging operators can use the results of the method to estimate the potential of the technologies, which helps to improve planning reliability. In the sense of a technology impact assessment, both methods can contribute to making technically sound decisions.

Based on the vehicle optimization and the two scenarios, the following conclusions can be made from a technological perspective:

- Electrified powertrains solve the trade-off between low costs, low environmental impact and good practicability (i.e., climbing ability) better than ICETs.
- As of today, no vehicle concept can outperform conventional diesel. Either costs are too high, due to increased energy and acquisition costs, or environmental impact increases because of the current electricity production. Thus, while the BET shows near cost parity with diesel, the electricity mix leads to a significantly higher environmental impact. In contrast, an SMR hydrogen-powered vehicle has similar environmental impacts to diesel but results in significantly higher costs.
- The BET, as well as both hydrogen-powered vehicles, have great potential if their technological progress is taken into account. The BET benefits from the renewable energy mix in the *Potential* scenario, improving its production and use phase impact and, consequently, reducing environmental impact. Furthermore, falling battery costs lead to a reduction in TCO to a level comparable to today's vehicles. The FCET also benefits from this: Falling hydrogen costs mean that the TCO of both hydrogen powertrains fall and, in the case of the FCET, are lower than that of today's diesel vehicles. Additionally, GWP decreases by 66 % to 86 % in the potential scenario. Here, the BET has the largest reduction, followed by the FCET. Due to its higher hydrogen consumption, the HICET performs worse among the three vehicle concepts.
- Synthetic diesel leads to a deterioration in eco-efficiency. Apart from increasing costs, large amounts of well-to-tank energy required for synthetic diesel result in increased mineral resource depletion. Although this also applies to the other powertrains, its negative effect on environmental impact strongly correlates with decreasing powertrain efficiency.
- The *Potential* scenario causes a shift from fossil resource depletion to mineral resource depletion. Although both, the BET and the FCET, require large amounts of rare earth metals, they still perform better than the conventional and synthetic diesel in EII. Excluding resource depletion from the weighting set shows that all options reduce environmental impacts albeit at different costs. From an economic perspective, the FCET and the BET are the best future alternatives.

8.3 Outlook

Apart from the powertrain, future vehicle technology could enhance the vehicles' economic and environmental performance. For example, Sen et al. [63] showed the positive impact of autonomously driving trucks in reducing costs and environmental impact.

The currently installed capacities of charging stations are not sufficient to enable fast intermediate charging (e.g., rest areas). This work, therefore, assumes that trucks are only charged overnight at depots. However, current developments already indicate that megawatt charging systems will be available soon. Due to the strong dependency on battery size, charging time and charging strategy, there are further potentials that speak for the use of BETs [311–313].

The rapid increase in battery-powered passenger cars leads to synergy effects that can soon be exploited by commercial vehicles. For example, Teichert et al. [314] showed that particular Li-ion cells already bring the TCO of heavy commercial vehicles to the level of diesel vehicles. Candar [296] highlighted the influence of different cell chemistries on their costs, environmental, and social impact. Furthermore, Duffner et al. [315] showed the potential (and challenges) of post-lithium-ion battery cell production. Thus, future research should, on the one hand, include other cell chemistries and new battery technologies in the eco-efficiency assessment. On the other hand, an expansion towards a life cycle sustainability assessment, as proposed by Candar [296], covering all three pillars of sustainability, should be pursued.

9 Summary

The commercial vehicle industry experiences severe changes. These are not only caused by tightened regulations in order to reduce greenhouse gas emissions and limit global warming. The ongoing destruction of nature leads to social change, which is reflected in changing consumer choices, ultimately demanding new, *green* products. Commercial vehicles significantly contribute to global warming and require large amounts of resources, yet they are indispensable for global economies.

This work, therefore, deals with the economic performance and environmental impacts of emerging heavy-duty vehicle technologies. Combining a total cost of ownership-model with a life cycle assessment, an eco-efficiency assessment compares the performances of diesel, hybrid electric trucks, battery electric trucks, fuel cell electric trucks, and hydrogen internal combustion engine trucks. An evolutionary algorithm optimizes each powertrain's technical design variables, minimizing costs and environmental impacts while improving driving performance. This optimization predicts technological progress in the sense of a prospective technology assessment. The comparison of the simulation results and published data, used for the current EU legislation, validates the underlying consumption model. Subsequently, uncertainty quantification of the most cost-efficient Pareto-optimal vehicles justifies the scenario-based comparison.

The charging or refueling infrastructure is crucial for the success of each technology. The system cost approach merges the vehicle-specific costs with the respective infrastructure costs in a single economic figure. Eventually, vehicle stock development scenarios, taken from literature, compare the system costs and environmental impacts of BET, FCET, and HICET for the current decade.

The results show that neither diesel nor hybrid trucks achieve the reduction mandated by the EU regulation. The use of synthetic diesel reduces CO₂-emission but increases overall environmental impact with simultaneously increased costs. Status-quo, the BET performs comparable to today's diesel costs but with significantly worse eco-impact. The FCET results are the contrary, with higher costs but slightly lower environmental impact. An optimistic, future scenario shows that the BET's environmental impact reduces with increasing renewable electricity in production and use-phase. At the same time, hydrogen costs decrease. Eventually, both powertrains outperform the current diesel in costs as well as environmental impact. While in a direct comparison of the individual vehicles, both technologies are almost on par, the system costs show an advantage for the FCET until 2030, which can be attributed to marginal lower infrastructure costs. The BET, on the other hand, leads to a lower environmental impact. Consequently, the eco-efficiency assessment cannot favor any technology but it shows the respective advantages and disadvantages and the relevant developments: On the one hand, the share of renewable energies must be increased for both BETs and hydrogen-powered vehicles. On the other hand, energy costs must decrease to reduce the high costs of hydrogen production.

The presented method can not only support this future research but also facilitate the vehicle concept development process for OEMs. Eventually, it can motivate them to reduce their products' environmental footprint and "to act as you would in a crisis" [1].

List of Figures

Figure 1.1:	Important events that have been (or are expected to be) drivers for the development of sustainability.....	2
Figure 1.2:	Examples of human-caused environmental damage within the last century.	3
Figure 1.3:	Emissions of selected air pollutants from road transport and other modes of transportation.....	4
Figure 1.4:	Historic development of total road transport energy consumption and vehicle-specific consumption relative to the year 1990.....	5
Figure 2.1:	The process stages of an efficiency assessment according to the DIN EN ISO 14045 [44].	8
Figure 2.2:	The four stages of a life cycle assessment according to the DIN EN ISO 14040 [58].....	10
Figure 2.3:	Mileage and payload distribution of European heavy-duty vehicles.	20
Figure 2.4:	Morphological box, comparing current prototype vehicles.	21
Figure 2.5:	Isometric view of a diesel ICE heavy-duty vehicle package.....	22
Figure 2.6:	Isometric view of a battery electric heavy-duty vehicle package.....	24
Figure 2.7:	Isometric view of a battery electric overhead catenary vehicle package.	26
Figure 2.8:	Isometric view of a fuel cell electric heavy-duty vehicle package.....	28
Figure 2.9:	Fuel cell polarization curve with characteristic voltages and currents.....	29
Figure 2.10:	Isometric view of a hydrogen combustion heavy-duty vehicle package.	32
Figure 2.11:	Gravimetric and volumetric comparison of hydrogen storage technologies.	32
Figure 3.1:	Cradle-to-grave system boundary definition.	37
Figure 4.1:	Vehicle concept optimization methodology.	41
Figure 4.2:	Development of vehicle registration and stock for five scenarios.....	45
Figure 4.3:	Penalties per vehicle due to exceeding CO ₂ -emissions for five scenarios.....	46
Figure 4.4:	Scalable life cycle inventory methodology.	49
Figure 4.5:	Material mix for five vehicle concepts.	49
Figure 4.6:	GaBi component model with three process categories.	50
Figure 4.7:	Four driving forces and their contribution to total energy consumption.	52
Figure 4.8:	Two longitudinal vehicle simulation approaches.	53
Figure 4.9:	The two VECTO driving cycles with speed and road gradient over distance.....	54
Figure 4.10:	Discrete fuel cell operating strategy controlling the power depending on the SOC.	59
Figure 4.11:	Approach to convert and scale engine efficiency maps.....	60
Figure 4.12:	Relation between electrified (catenary) road network length and electrified mileage.....	61
Figure 4.13:	Influence of e-road expansion on the vehicle's SOC.	62
Figure 5.1:	Overview of the evolutionary algorithm NSGA-II program.	64
Figure 5.2:	Improvement ratio of the BET optimization.....	66

Figure 6.1:	The CDF shows the BET’s uncertainty quantification of the two optimization objectives and its energy consumption.	71
Figure 7.1:	Trade-off (a) between Eco-Impact Index and total cost of ownership for ICET, HET, BET, FCET, and HICET concept optimization.	73
Figure 7.2:	TCO of each vehicle concept normalized to the reference vehicle.	75
Figure 7.3:	EII of each vehicle concept normalized to the reference vehicle.	76
Figure 7.4:	Diesel optimization plot matrix.	78
Figure 7.5:	Influence of engine torque on the diesel optimization objectives.	78
Figure 7.6:	Plot matrix for the HET optimization.	79
Figure 7.7:	Influence of electric motor torque and battery capacity on two HET optimization objectives.	80
Figure 7.8:	Plot matrix for the BET optimization.	81
Figure 7.9:	Influence of electric motor torque and battery capacity on two BET optimization objectives.	81
Figure 7.10:	Plot matrix for the FCET optimization.	82
Figure 7.11:	Influence of DOD and electric torque on two FCET optimization objectives.	83
Figure 7.12:	Plot matrix for the HICET optimization.	84
Figure 7.13:	Influence of engine torque on two HICET optimization objectives.	84
Figure 7.14:	Selection of normalized environmental impact categories for the individuals with lowest TCO.	86
Figure 7.15:	Vehicle concepts’ eco-efficiency potential due to technological progress.	87
Figure 7.16:	Vehicle concepts’ life-cycle global warming potential due to technological progress.	88
Figure 7.17:	Eco-efficiency potential with an adapted weighting set, excluding resource depletion.	89
Figure 7.18:	System costs for the BCG E scenario.	90
Figure 7.19:	EII for the BCG E scenario.	91
Figure 8.1:	The two regression models used in the CFA.	95
Figure 8.2:	Survey results describing each stakeholder’s trust in three technologies.	96
Figure 8.3:	Stakeholder survey, assessing the general support towards zero-emission trucks.	97
Figure 8.4:	The correlation matrix shows how each stakeholder (row) assigns responsibility in the transition to ZEVs to the other stakeholders (column).	97
Figure B.1:	Depending on the number and position of the electric machine(s), and the number of shiftable gears, there are six BET drivetrain topologies. The topologies are based on a preliminary publication [138].	xi
Figure C.1:	Operating point of a hydrogen engine with late direct injection and spark plug ignition at 2000 rpm at part load [175].	xlii
Figure C.2:	Operating point of a hydrogen engine with direct injection and compression ignition at 2000 rpm at part load [175].	xlii
Figure C.3:	Operating point of a hydrogen engine with dual direct injection and compression ignition at 2000 rpm in partial load [175].	xlii
Figure C.4:	Operating point of a hydrogen engine with dual direct injection, spark ignition, and compression ignition at 2000 rpm at part load [175].	xliii
Figure C.5:	Operating point of a hydrogen engine with direct injection and glow plug at 2000 rpm at part load [175].	xliii
Figure E.1:	Relative material mix for five vehicle concepts.	xlvii

Figure G.1:	The absolute improvement ratio shows that the diesel optimization converges after 15 generations. Locally random evolution creates noise, which the average improvement ratio filters out [272].	I
Figure G.2:	The absolute improvement ratio shows that the HET optimization converges within the set generations. Locally random evolution creates noise, which the average improvement ratio filters out [272]. The optimization terminated at generation 85 and had to be restarted. Due to server issues, the earlier generation data was lost, which is why the plot starts at generation 85. The proof of convergence as well as the final optimization results are not affected by this.	I
Figure G.3:	The absolute improvement ratio shows that the FCET optimization converges after 70 generations. Locally random evolution creates noise, which the average improvement ratio filters out [272].	I
Figure G.4:	The absolute improvement ratio shows that the HICET optimization converges after 70 generations. Locally random evolution creates noise, which the average improvement ratio filters out [272].	II
Figure H.1:	The CDF shows the diesel's uncertainty quantification of the two optimization objectives and its energy consumption.	III
Figure H.2:	The CDF shows the HET's uncertainty quantification of the two optimization objectives and its energy consumption.	III
Figure H.3:	The CDF shows the FCET's uncertainty quantification of the two optimization objectives and its energy consumption.	IV
Figure H.4:	The CDF shows the HICE's uncertainty quantification of the two optimization objectives and its energy consumption.	IV
Figure I.1:	The infrastructure costs (BCG E scenario) for BET and FCET are sensitive to the usage parameter. However, if the same assumptions for both are used, the relative results are not affected.	VI

List of Tables

Table 2.1:	Set of normalization factors for ILCD impact categories as developed by the JRC.	16
Table 2.2:	Summary of environmental impact weighting methods and the respective scope.	17
Table 2.3:	Weighting sets of ILCD impact categories as presented by the JRC.	18
Table 2.4:	Overview of mixture formation and ignition possibilities with efficiency and required exhaust gas aftertreatment systems.	30
Table 2.5:	Summary of the reviewed literature including the respective preferred vehicle concept for future road-transportation.	35
Table 3.1:	Production cost assumptions for the year 2020 and the technology potential scenario (2030).	39
Table 4.1:	Infrastructure types, investment costs, and daily energy supply.	43
Table 4.2:	Constant vehicle parameters to calculate tractive forces with the closed-loop longitudinal simulation model <i>LOTUS</i> .	55
Table 4.3:	Overview of non-CO ₂ emission models, literature, and regulations.	56
Table 5.1:	Lower and upper boundaries for the design variables x for BEV and FCEV concept optimization.	66
Table 6.1:	Validation of <i>LOTUS</i> vehicle sub-groups (diesel) based on the published data by ACEA.	68
Table 6.2:	Vehicle parameters and corresponding epistemic and aleatoric intervals.	70
Table 7.1:	Summary of the three Pareto-optimal optimization objectives.	74
Table A.1:	The regulation 2019/1241 defines the vehicle concepts, respectively subgroups, subject CO ₂ targets for heavy-duty vehicles.	xxxix
Table C.1:	General and combustion-specific properties of hydrogen and hydrogen-air-mixtures.	xli
Table D.1:	Average European truck OEM based on 2019 vehicle sales.	xliv
Table E.1:	Powertrain design parameters for five different long-haul vehicle concepts.	xlvi
Table J.1:	The total number of valid (i.e., complete answering of all questions) answers for each stakeholder sums up to $n = 61$. Despite direct inquiries, the response rates were low for OEMs and fleet owners. Because drivers were reached via flyers, it is not possible to determine a response rate [299].	lvii
Table J.2:	Stakeholder survey developed by Barré [299]. The survey was conducted online. Participants were acquired via direct e-mailing or, in the case of the drivers, flyers.	lvii
Table J.3:	R ² -test for the two exogenous variables of the CFA. A threshold for $R^2 \geq 0.1$ renders a model valid.	lx
Table J.4:	P-value and β -coefficient test.	lx

Bibliography

- [1] G. Thunberg. „*Our House is on Fire: Speech at the World Economic Forum 2019, Davos*,“ Cologny, Switzerland, 2019. Available: <https://www.youtube.com/watch?v=U72xkMz6Pxx>.
- [2] European Commission. „Paris Agreement - Climate Action - European Commission,“ 2021. [Online]. Available: https://ec.europa.eu/clima/policies/international/negotiations/paris_en#tab-0-0 [visited on 12/14/2021].
- [3] D. Wallace-Wells, *The uninhabitable earth: Life after warming*, First edition, New York, Tim Duggan Books, 2019, ISBN: 9780525576709.
- [4] H. C. von Carlowitz, K. Irmer and U. Grober, *Sylvicultura oeconomica: Anweisung zur wilden Baum-Zucht*, (Veröffentlichungen der Bibliothek "Georgius Agricola" der Technischen Universität Bergakademie Freiberg). vol. 135, Reprint der Ausg. Leipzig, Braun, 1713, Freiberg, TU Bergakademie, 2000, ISBN: 3860121154.
- [5] G. Brundtland et al., *Our Common Future ('Brundtland report')*, Oxford University Press, USA, 1987. Available: http://www.bne-portal.de/fileadmin/unesco/de/Downloads/Hintergrundmaterial_international/Brundtlandbericht.File.pdf?linklisted=2812.
- [6] United Nations Sustainable Development, „United Nations Conference on Environment & Development: Agenda 21,“ Rio de Janeiro, 1992. Available: <https://sustainabledevelopment.un.org/content/documents/Agenda21.pdf>.
- [7] S. Wolff, M. Brönner, M. Held and M. Lienkamp, „Transforming automotive companies into sustainability leaders: A concept for managing current challenges,“ *Journal of Cleaner Production*, vol. 276, p. 124179, 2020, DOI: 10.1016/j.jclepro.2020.124179.
- [8] U. Nations, „Transforming our World: The 2030 Agenda for Sustainable Development: A/RES/70/1,“ New York, 2015. Available: <https://sustainabledevelopment.un.org/content/documents/21252030%20Agenda%20for%20Sustainable%20Development%20web.pdf>.
- [9] Intergovernmental Panel on Climate Change, *Global warming of 1.5°C*, Geneva, Switzerland, Intergovernmental Panel on Climate Change, 2018. Available: <https://www.ipcc.ch/sr15/>.
- [10] N. J. L. Lenssen et al., „Improvements in the GISTEMP Uncertainty Model,“ *Journal of Geophysical Research: Atmospheres*, vol. 124, no. 12, pp. 6307–6326, 2019, DOI: 10.1029/2018JD029522.
- [11] GISTEMP Team. „GISS Surface Temperature Analysis (GISTEMP), version 4,“ 2021. [Online]. Available: <https://data.giss.nasa.gov/gistemp/> [visited on 02/02/2021].
- [12] G. Yohe et al., „Perspectives on climate change and sustainability,“ in *Climate Change 2007: Impacts, Adaptation and Vulnerability: Contribution of Working Group II to the Fourth Assessment Report of the Intergovernmental Panel on Climate Change*, M. L. Parry, O. F. Canziani, J. P. Palutikof, P. J. van der Linden and C. E. Hanson, ed. Cambridge, UK: Cambridge University Press, 2018. Available: https://www.ipcc.ch/site/assets/uploads/2018/03/ar4_wg2_full_report.pdf.

- [13] International Union for Conservation of Nature. „IUCN Red List of Threatened Species,“ 2021. [Online]. Available: <https://www.iucnredlist.org/resources/summary-statistics> [visited on 02/02/2021].
- [14] A. D. Barnosky et al., „Has the Earth’s sixth mass extinction already arrived?,“ *Nature*, vol. 471, no. 7336, pp. 51–57, 2011, DOI: 10.1038/nature09678.
- [15] H. Ritchie. „Energy Production and Consumption,“ 2021. [Online]. Available: <https://ourworldindata.org/energy-production-consumption> [visited on 02/02/2021].
- [16] British Petrol, „bp Statistical Review of World Energy 2020,“ London, UK, 2020. Available: <https://www.bp.com/content/dam/bp/business-sites/en/global/corporate/pdfs/energy-economics/statistical-review/bp-stats-review-2020-full-report.pdf> [visited on 12/14/2021].
- [17] V. Smil, *Energy transitions: Global and national perspectives*, Second edition, Santa Barbara, California, Praeger an imprint of ABC-CLIO LLC, 2017, ISBN: 9781440853241.
- [18] H. Ritchie and M. Roser. „Plastic Pollution,“ 2021. [Online]. Available: <https://ourworldindata.org/plastic-pollution> [visited on 02/02/2021].
- [19] R. Geyer, J. R. Jambeck and K. L. Law, „Production, use, and fate of all plastics ever made,“ *Science advances*, vol. 3, no. 7, e1700782, 2017, DOI: 10.1126/sciadv.1700782.
- [20] A. Belke, F. Dobnik and C. Dreger, „Energy consumption and economic growth: New insights into the cointegration relationship,“ *Energy Economics*, vol. 33, no. 5, pp. 782–789, 2011, DOI: 10.1016/j.eneco.2011.02.005.
- [21] H. K. Çalışkan, „Technological Change and Economic Growth,“ *Procedia - Social and Behavioral Sciences*, vol. 195, pp. 649–654, 2015, DOI: 10.1016/j.sbspro.2015.06.174.
- [22] S. Cucurachi, C. van der Giesen and J. Guinée, „Ex-ante LCA of Emerging Technologies,“ *Procedia CIRP*, vol. 69, pp. 463–468, 2018, DOI: 10.1016/j.procir.2017.11.005.
- [23] D. R. Cooper and T. G. Gutowski, „Prospective Environmental Analyses of Emerging Technology: A Critique, a Proposed Methodology, and a Case Study on Incremental Sheet Forming,“ *Journal of Industrial Ecology*, vol. 24, no. 1, pp. 38–51, 2020, DOI: 10.1111/jiec.12748.
- [24] World Business Council for Sustainable Development, „Measuring eco-efficiency: a guide to reporting company performance,“ London, 2000, ISBN: 978-2-9402-4014-2.
- [25] S. Khalili, E. Rantanen, D. Bogdanov and C. Breyer, „Global Transportation Demand Development with Impacts on the Energy Demand and Greenhouse Gas Emissions in a Climate-Constrained World,“ *Energies*, vol. 12, no. 20, p. 3870, 2019, DOI: 10.3390/en12203870.
- [26] Eurostat, „Energy statistics - an overview,“ Luxembourg, 2021. Available: https://ec.europa.eu/eurostat/statistics-explained/index.php?title=Energy_statistics_-_an_overview#Final_energy_consumption [visited on 06/11/2021].
- [27] European Environment Agency, „Emissions of air pollutants from transport,“ Copenhagen, Denmark, 2019. Available: https://www.eea.europa.eu/ds_resolveuid/IND-112-en [visited on 02/02/2021].
- [28] Trefis Team, „Trends In Steel Usage In The Automotive Industry,“ *Forbes*, vol. 2015, 20.05.2015. Available: <https://www.forbes.com/sites/greatspeculations/2015/05/20/trends-in-steel-usage-in-the-automotive-industry/?sh=6f469ec51476> [visited on 02/02/2021].

- [29] Statista. „Verteilung des weltweiten Aluminiumbedarfs nach Sektoren 2019 [Distribution of global aluminum demand by sector in 2019],“ 2021. [Online]. Available: <https://de.statista.com/statistik/daten/studie/240721/umfrage/verteilung-des-weltweiten-aluminiumbedarfs-nach-sektoren/> [visited on 02/02/2021].
- [30] G. Klink, M. Mathur, R. Kidambi and K. Sen. „The contribution of the automobile industry to technology and value creation,“ 2021. [Online]. Available: <https://www.es. Kearney.com/automotive/article/?/a/the-contribution-of-the-automobile-industry-to-technology-and-value-creation> [visited on 06/11/2021].
- [31] M. Lienkamp, W. Schmid, S. Wolff, M. Hessel and F. Homm, *Status Elektromobilität: Das Endspiel nach der Corona Krise*, Munich, Germany, 2020. Available: https://www.researchgate.net/publication/341670568_Status_Elektromobilitat_2020_Das_Endspiel_nach_der_Corona-Krise [visited on 05/28/2020].
- [32] European Commission, Directorate General for Climate Action and Ricardo Energy & Environment, *Determining the environmental impacts of conventional and alternatively fuelled vehicles through LCA: final report*, Luxembourg, Publications Office of the European Union, 2020, ISBN: 978-92-76-20301-8. DOI: 10.2834/91418.
- [33] S. Wolff, M. Lienkamp and K.-V. Schaller, *Status Nutzfahrzeuge 2020: Alles auf eine Karte? [Status Commercial Vehicles 2020: All on One Card?]*, Munich, Germany, 2021. Available: https://www.researchgate.net/publication/350580546_STATUS_NUTZFAHRZEUGE_2020_ALLES_AUF_EINE_KARTE [visited on 05/28/2020].
- [34] European Environment Agency, „Greenhouse gas emissions from transport in Europe,“ Copenhagen, 2019. Available: https://www.eea.europa.eu/ds_resolveuid/7009a89effc04d8ea8b5f94ff0a39912 [visited on 04/23/2020].
- [35] L. Nicoletti et al., „Review of Trends and Potentials in the Vehicle Concept Development Process,“ in *2020 Fifteenth International Conference on Ecological Vehicles and Renewable Energies (EVER)*, Monte-Carlo, Monaco, 2020, pp. 1–15, ISBN: 978-1-7281-5641-5. DOI: 10.1109/EVER48776.2020.9243115.
- [36] Umweltbundesamt. „Endenergieverbrauch und Energieeffizienz des Verkehrs,“ 2020. [Online]. Available: <https://www.umweltbundesamt.de/daten/verkehr/endenergieverbrauch-energieeffizienz-des-verkehrs#textpart-5> [visited on 02/01/2020].
- [37] Association des Constructeurs Européens d’Automobiles, „Reducing CO2 emissions from heavy-duty vehicles: An Integrated Approach,“ Brussels, 2017. Available: <http://reducingco2together.eu/assets/pdf/trucks.pdf> [visited on 12/14/2021].
- [38] Eurostat. „Road freight transport statistics,“ 2018. [Online]. Available: http://ec.europa.eu/eurostat/statistics-explained/index.php/Road_freight_transport_statistics [visited on 07/13/2018].
- [39] „World Economic Outlook Database: Update January 2021,“ Cologny, Switzerland, 2021. Available: <https://www.imf.org/en/Publications/WEO/weo-database/2020/October> [visited on 06/11/2021].
- [40] European Parliament. „Regulation (EU) 2019/1242 of the European Parliament and of the Council of 20 June 2019 setting CO2 emission performance standards for new heavy-duty vehicles and amending Regulations (EC) No 595/2009 and (EU) 2018/956 of the European Parliament and of the Council and Council Directive 96/53/EC,“ 20.06.2019. Available: <https://eur-lex.europa.eu/eli/reg/2019/1242/oj>.

- [41] K.-C. Scheel. „Kommentar: Klimaschutz im Transportsektor – Innovation vs. Regulierung,“ unpublished presentation. Munich, Germany, 2019.
- [42] G. Huppel and M. Ishikawa, *Quantified Eco-Efficiency: An Introduction with Applications*, (Eco-Efficiency in Industry and Science). vol. 22, Dordrecht, Berlin, and Heidelberg, Springer, 2007, ISBN: 9781402053986. DOI: 10.1007/1-4020-5399-1. Available: <http://nbn-resolving.de/urn:nbn:de:1111-200708027633>.
- [43] P. Saling et al., „Eco-efficiency analysis by basf: the method,“ *The International Journal of Life Cycle Assessment*, vol. 7, no. 4, pp. 203–218, 2002, DOI: 10.1007/BF02978875.
- [44] Umweltmanagement – Ökoeffizienzbewertung von Produktsystemen – Prinzipien, Anforderungen und Leitlinien (ISO 14045:2012) [Environmental management – Eco-efficiency assessment of product systems – Principles, requirements and guidelines], DIN EN ISO 14045, 2012.
- [45] BASF. „Ökoeffizienz-Analyse,“ 2021. [Online]. Available: <https://www.basf.com/global/de/who-we-are/sustainability/we-drive-sustainable-solutions/quantifying-sustainability/eco-efficiency-analysis.html> [visited on 12/14/2021].
- [46] P. Mickwitz, M. Melanen, U. Rosenström and J. Seppälä, „Regional eco-efficiency indicators – a participatory approach,“ *Journal of Cleaner Production*, vol. 14, no. 18, pp. 1603–1611, 2006, DOI: 10.1016/j.jclepro.2005.05.025.
- [47] K. Yin, R. Wang, Q. An, L. Yao and J. Liang, „Using eco-efficiency as an indicator for sustainable urban development: A case study of Chinese provincial capital cities,“ *Ecological Indicators*, vol. 36, pp. 665–671, 2014, DOI: 10.1016/j.ecolind.2013.09.003.
- [48] N. C. Onat et al., „How eco-efficient are electric vehicles across Europe? A regionalized life cycle assessment-based eco-efficiency analysis,“ *Sustainable Development*, 2021, DOI: 10.1002/sd.2186.
- [49] M. Philippot, G. Alvarez, E. Ayerbe, J. van Mierlo and M. Messagie, „Eco-Efficiency of a Lithium-Ion Battery for Electric Vehicles: Influence of Manufacturing Country and Commodity Prices on GHG Emissions and Costs,“ *Batteries*, vol. 5, no. 1, p. 23, 2019, DOI: 10.3390/batteries5010023.
- [50] I. John, E. M. Kwofie and M. Ngadi, „Two decades of eco-efficiency research: a bibliometric analysis,“ *Environmental Sustainability*, vol. 3, no. 2, pp. 155–168, 2020, DOI: 10.1007/s42398-020-00105-1.
- [51] G. Huppel and M. Ishikawa, „Eco-efficiency and Its Terminology,“ *Journal of Industrial Ecology*, vol. 9, no. 4, pp. 43–46, 2005, DOI: 10.1162/108819805775247891.
- [52] P. Wittenbrink, *Transportmanagement: Kostenoptimierung, Green Logistics und Herausforderungen an der Schnittstelle Rampe [Cost optimization, green logistics and challenges at the loading ramp]*, 2., vollst. neu bearb. u. erw. Aufl. 2014, Wiesbaden, Springer Gabler, 2014, ISBN: 978-3-8349-3825-1. DOI: 10.1007/978-3-8349-3825-1.
- [53] M. Fries, „Maschinelle Optimierung der Antriebsauslegung zur Reduktion von CO₂-Emissionen und Kosten im Nutzfahrzeug [Mechanical optimization of drive design to reduce CO₂ emissions and costs in commercial vehicles],“ Dissertation, Institute of Automotive Technology, Technical University of Munich, Munich, Germany, 2018. [Visited on 12/19/2018].
- [54] M. Fries et al., „Optimization of hybrid electric drive system components in long-haul vehicles for the evaluation of customer requirements,“ in *2017 IEEE 12th International Conference on Power Electronics and Drive Systems (IEEE PEDS 2017): Hawaii Convention Center, Honolulu, Hawaii, USA, 12-15 December 2017*, Honolulu, HI, 2017, pp. 1, 141–1, 146, ISBN: 978-1-5090-2364-6. DOI: 10.1109/PEDS.2017.8289236.

- [55] S. Wolff, M. Fries and M. Lienkamp, „Technoecological analysis of energy carriers for long–haul transportation,“ *Journal of Industrial Ecology*, vol. 49, no. 11, p. 6402, 2019, DOI: 10.1111/jiec.12937.
- [56] S. Wolff, M. Seidenfus, M. Brönnner and M. Lienkamp, „Multi-disciplinary design optimization of life cycle eco-efficiency for heavy-duty vehicles using a genetic algorithm,“ *Journal of Cleaner Production*, vol. 318, p. 128505, 2021, DOI: 10.1016/j.jclepro.2021.128505.
- [57] A. P. Grosse-Sommer, T. H. Grünenwald, N. S. Paczkowski, R. N. van Gelder and P. R. Saling, „Applied sustainability in industry: The BASF eco-eEfficiency toolbox,“ *Journal of Cleaner Production*, vol. 258, p. 120792, 2020, DOI: 10.1016/j.jclepro.2020.120792.
- [58] Umweltmanagement – Ökobilanz – Grundsätze und Rahmenbedingungen (ISO 14040:2006); Deutsche und Englische Fassung EN ISO 14040:2006, DIN EN ISO 14040, 2009.
- [59] Umweltmanagement – Ökobilanz – Anforderungen und Anleitungen (ISO 14044:2006 + Amd 1:2017); Deutsche Fassung EN ISO 14044:2006 + A1:2018, DIN EN ISO 14044, 2018.
- [60] M. Z. Hauschild, R. K. Rosenbaum and S. I. Olsen, *Life Cycle Assessment*, Cham, Springer International Publishing, 2018, ISBN: 978-3-319-56474-6. DOI: 10.1007/978-3-319-56475-3.
- [61] A. Del Duce et al., „eLCAR: Guidelines for the LCA of electric vehicles,“ Aachen, Germany, 2013. Available: http://elcar-project.eu/uploads/media/eLCAR_guidelines.pdf [visited on 12/14/2021].
- [62] F.-S. Boureima et al., „Comparative LCA of electric, hybrid, LPG and gasoline cars in Belgian context,“ *World Electric Vehicle Journal*, vol. 3, no. 3, pp. 469–476, 2009, DOI: 10.3390/wevj3030469.
- [63] B. Sen, M. Kucukvar, N. C. Onat and O. Tatari, „Life cycle sustainability assessment of autonomous heavy–duty trucks,“ *Journal of Industrial Ecology*, vol. 2602, pp. 1–48, 2019, DOI: 10.1111/jiec.12964.
- [64] M. Pizzol, R. Sacchi, S. Köhler and A. Anderson Erjavec, „Non-linearity in the Life Cycle Assessment of Scalable and Emerging Technologies,“ *Frontiers in Sustainability*, vol. 1, 2021, DOI: 10.3389/frsus.2020.611593.
- [65] G. Huppés and L. van Oers, „Background Review of Existing Weighting Approaches in Life Cycle Impact Assessment (LCIA),“ European Commission, Joint Research Centre, Institute for Environment and Sustainability, Luxembourg, 2011. Available: <https://publications.jrc.ec.europa.eu/repository/handle/JRC67215>.
- [66] G. Huppés, L. van Oers, U. Pretato and D. W. Pennington, „Weighting environmental effects: Analytic survey with operational evaluation methods and a meta-method,“ *The International Journal of Life Cycle Assessment*, vol. 17, no. 7, pp. 876–891, 2012, DOI: 10.1007/s11367-012-0415-x.
- [67] M. A. J. Huijbregts et al., „ReCiPe2016: a harmonised life cycle impact assessment method at midpoint and endpoint level,“ *The International Journal of Life Cycle Assessment*, vol. 22, no. 2, pp. 138–147, 2017, DOI: 10.1007/s11367-016-1246-y.
- [68] European Commission, Joint Research Centre, Institute for Environment and Sustainability, *International reference life cycle data system (ILCD) handbook: General guide for life cycle assessment: provisions and action steps*, (EUR, Scientific and technical research series). vol. 24571, First edition, Luxembourg, Publications Office, 2011, ISBN: 978-92-79-17451-3. DOI: 10.278/33030.

- [69] United Nations Framework Convention on Climate Change, „Kyoto Protocol Reference Manual: On Accounting of Emissions and Assigned Amount,“ 2008. Available: https://unfccc.int/resource/docs/publications/08_unfccc_kp_ref_manual.pdf [visited on 01/21/2021].
- [70] P. Forster et al., „Changes in Atmospheric Constituents and in Radiative Forcing,“ in *Climate Change 2007: The Physical Science Basis. Contribution of Working Group I to the Fourth Assessment Report of the Intergovernmental Panel on Climate Change* Cambridge, United Kingdom and New York, USA: Cambridge University Press, 2007. Available: <https://www.ipcc.ch/site/assets/uploads/2018/02/ar4-wg1-chapter2-1.pdf> [visited on 01/21/2021].
- [71] Intergovernmental Panel on Climate Change, *Climate Change 2014: Synthesis Report. Contribution of Working Groups I, II and III to the Fifth Assessment Report of the Intergovernmental Panel on Climate Change*, Geneva, Switzerland, Intergovernmental Panel on Climate Change, 2014, ISBN: 9291691437. Available: https://www.ipcc.ch/site/assets/uploads/2018/02/SYR_AR5_FINAL_full.pdf [visited on 01/16/2019].
- [72] Greenhouse Gas Protocol, „Global Warming Potential Values,“ Washington DC, USA and Maison de la Paix, Switzerland, 2016. Available: https://www.ghgprotocol.org/sites/default/files/ghgp/Global-Warming-Potential-Values%20%28Feb%2016%202016%29_1.pdf [visited on 01/22/2021].
- [73] H. K. Stranddorf, L. Hoffmann and A. Schmidt, „LCA technical report: Impact categories, normalisation and weighting in LCA. Update on selected EDIP97-data,“ Brøndby, 2003. Available: <https://lca-center.dk/wp-content/uploads/2015/08/LCA-technical-report-impact-categories-normalisation-and-weighting-in-LCA.pdf> [visited on 11/06/2020].
- [74] M. Simons. „Europe Bans Leaded Gas To Cut Smog,“ 1998. Available: <https://www.nytimes.com/1998/07/03/world/europe-bans-leaded-gas-to-cut-smog.html> [visited on 12/17/2019].
- [75] S. R. Craxford, „Pollution from lead in petrol,“ *Oil and Petrochemical Pollution*, vol. 1, no. 4, pp. 285–290, 1983, DOI: 10.1016/S0143-7127(83)80006-4. Available: <https://www.sciencedirect.com/science/article/pii/S0143712783800064>.
- [76] M. Posch et al., „The role of atmospheric dispersion models and ecosystem sensitivity in the determination of characterisation factors for acidifying and eutrophying emissions in LCIA,“ *The International Journal of Life Cycle Assessment*, vol. 13, no. 6, pp. 477–486, 2008, DOI: 10.1007/s11367-008-0025-9.
- [77] H. Zell. „Earth’s Atmospheric Layers,“ 2021. [Online]. Available: https://www.nasa.gov/mission_pages/sunearth/science/atmosphere-layers2.html [visited on 01/29/2021].
- [78] S. Blumberg, „2019 Ozone Hole is the Smallest on Record Since Its Discovery,“ NASA, 21.10.2019. Available: <https://www.nasa.gov/feature/goddard/2019/2019-ozone-hole-is-the-smallest-on-record-since-its-discovery> [visited on 12/14/2021].
- [79] V. N. Bashkin, „Stratospheric Ozone Depletion,“ in *Environmental Chemistry: Asian Lessons*, V. N. Bashkin, ed. Dordrecht: Kluwer Academic Publishers, 2003, pp. 137–159, ISBN: 1-4020-1004-4. DOI: 10.1007/0-306-48020-4_6.
- [80] A. Baklanov, L. T. Molina and M. Gauss, „Megacities, air quality and climate,“ *Atmospheric Environment*, vol. 126, pp. 235–249, 2016, DOI: 10.1016/j.atmosenv.2015.11.059.
- [81] R. Derwent et al., „Photochemical ozone formation in north west Europe and its control,“ *Atmospheric Environment*, vol. 37, no. 14, pp. 1983–1991, 2003, DOI: 10.1016/S1352-2310(03)00031-1.

- [82] S. Sala, L. Benini, E. Crenna and M. Secchi, „Global environmental impacts and planetary boundaries in LCA: Data sources and methodological choices for the calculation of global and consumption-based normalisation factors,” Luxembourg, 2016, DOI: 10.2788/64552. [Visited on 01/07/2021].
- [83] R. K. Rosenbaum et al., „USEtox—the UNEP-SETAC toxicity model: recommended characterisation factors for human toxicity and freshwater ecotoxicity in life cycle impact assessment,” *The International Journal of Life Cycle Assessment*, vol. 13, no. 7, pp. 532–546, 2008, DOI: 10.1007/s11367-008-0038-4.
- [84] S. C. McClelland, C. Arndt, D. R. Gordon and G. Thoma, „Type and number of environmental impact categories used in livestock life cycle assessment: A systematic review,” *Livestock Science*, vol. 209, pp. 39–45, 2018, DOI: 10.1016/j.livsci.2018.01.008.
- [85] P. Fantke et al., „Health effects of fine particulate matter in life cycle impact assessment: findings from the Basel Guidance Workshop,” *The International Journal of Life Cycle Assessment*, vol. 20, no. 2, pp. 276–288, 2015, DOI: 10.1007/s11367-014-0822-2.
- [86] R. Frischknecht, A. Braunschweig, P. Hofstetter and P. Suter, „Human health damages due to ionising radiation in life cycle impact assessment,” *Environmental Impact Assessment Review*, vol. 20, no. 2, pp. 159–189, 2000, DOI: 10.1016/S0195-9255(99)00042-6.
- [87] World Health Organisation. „Ionizing radiation, health effects and protective measures,” 2021. [Online]. Available: <https://www.who.int/news-room/fact-sheets/detail/ionizing-radiation-health-effects-and-protective-measures> [visited on 01/22/2021].
- [88] R. J. Diaz, H. Eriksson-Hägg and R. Rosenberg, „Hypoxia,” in *Managing Ocean Environments in a Changing Climate: Sustainability and Economic Perspectives*, K. J. Noone, U. R. Sumaila and R. J. Diaz, ed. Burlington: Elsevier Science, 2013, pp. 67–96, ISBN: 9780124076686. DOI: 10.1016/B978-0-12-407668-6.00004-5.
- [89] European Environment Agency, *Environmental indicator report 2018: in support to the monitoring of the Seventh Environment Action Programme*, Copenhagen, Publications Office, 2018, DOI: 10.2800/180334.
- [90] M. Klinglmair, S. Sala and M. Brandão, „Assessing resource depletion in LCA: a review of methods and methodological issues,” *The International Journal of Life Cycle Assessment*, vol. 19, no. 3, pp. 580–592, 2014, DOI: 10.1007/s11367-013-0650-9.
- [91] H. A. U. de Haes et al., „Best available practice regarding impact categories and category indicators in life cycle impact assessment,” *The International Journal of Life Cycle Assessment*, vol. 4, no. 2, 1999, DOI: 10.1007/BF02979403.
- [92] A.-M. Boulay et al., „The WULCA consensus characterization model for water scarcity footprints: assessing impacts of water consumption based on available water remaining (AWARE),” *The International Journal of Life Cycle Assessment*, vol. 23, no. 2, pp. 368–378, 2018, DOI: 10.1007/s11367-017-1333-8.
- [93] H. Vikström, S. Davidsson and M. Höök, „Lithium availability and future production outlooks,” *Applied Energy*, vol. 110, pp. 252–266, 2013, DOI: 10.1016/j.apenergy.2013.04.005.
- [94] Y. Ding, Z. P. Cano, A. Yu, J. Lu and Z. Chen, „Automotive Li-Ion Batteries: Current Status and Future Perspectives,” *Electrochemical Energy Reviews*, vol. 2, no. 1, pp. 1–28, 2019, DOI: 10.1007/s41918-018-0022-z.

- [95] A. C. Schomberg, S. Bringezu and M. Flörke, „Extended life cycle assessment reveals the spatially-explicit water scarcity footprint of a lithium-ion battery storage,“ *Communications Earth & Environment*, vol. 2, no. 1, 2021, DOI: 10.1038/s43247-020-00080-9.
- [96] Z. P. Cano et al., „Batteries and fuel cells for emerging electric vehicle markets,“ *Nature Energy*, vol. 3, no. 4, pp. 279–289, 2018, DOI: 10.1038/s41560-018-0108-1.
- [97] R. Frischknecht, R. Steiner and N. Jungbluth, „The Ecological Scarcity Method – Eco-Factors 2006. A method for impact assessment in LCA: Environmental studies no. 0906,“ Bern, 2012. Available: https://www.researchgate.net/publication/309630158_The_Ecological_Scarcity_Method_-_Eco-Factors_2006_A_method_for_impact_assessment_in_LCA [visited on 03/05/2021].
- [98] S. Sala, M.-A. Wolf and R. Pant, „Characterisation factors of the ILCD Recommended Life Cycle Impact Assessment methods. Database and supporting information,“ Luxembourg, 2012, DOI: 10.2788/60825.
- [99] J. B. Guinée, „Selection of Impact Categories and Classification of LCI Results to Impact Categories,“ in *Life cycle impact assessment (LCA compendium - the complete world of life cycle assessment)*, M. Z. Hauschild, ed. Dordrecht: Springer, 2015, pp. 17–37, ISBN: 978-94-017-9743-6. DOI: 10.1007/978-94-017-9744-3_2.
- [100] S. Wolff et al., „Scalable Life-Cycle Inventory for Heavy-Duty Vehicle Production,“ *Sustainability*, vol. 12, no. 13, p. 5396, 2020, DOI: 10.3390/su12135396.
- [101] L. Benini et al., *Normalisation method and data for environmental footprints*, Luxembourg, Publications Office, 2014, DOI: 10.2788/16415.
- [102] M. Pizzol et al., „Normalisation and weighting in life cycle assessment: quo vadis?,“ *The International Journal of Life Cycle Assessment*, vol. 22, no. 6, pp. 853–866, 2017, DOI: 10.1007/s11367-016-1199-1.
- [103] S. Sala, L. Benini, L. Mancini and R. Pant, „Integrated assessment of environmental impact of Europe in 2010: data sources and extrapolation strategies for calculating normalisation factors,“ *The International Journal of Life Cycle Assessment*, vol. 20, no. 11, pp. 1568–1585, 2015, DOI: 10.1007/s11367-015-0958-8.
- [104] S. Sala, A. K. Cerutti and R. Pant, „Development of a weighting approach for the Environmental Footprint,“ Luxembourg, 2018, DOI: 10.2760/945290.
- [105] V. Castellani, L. Benini, S. Sala and R. Pant, „A distance-to-target weighting method for Europe 2020,“ *The International Journal of Life Cycle Assessment*, vol. 21, no. 8, pp. 1159–1169, 2016, DOI: 10.1007/s11367-016-1079-8.
- [106] M. Hauschild and J. Potting, „Spatial Differentiation in Life Cycle Impact Assessment – The EDIP 2003 Methodology,“ *Environ news*, vol. 80, 2005. Available: <https://www2.mst.dk/udgiv/publications/2005/87-7614-579-4/pdf/87-7614-580-8.pdf>.
- [107] H. L. Tuomisto, I. D. Hodge, P. Riordan and D. W. Macdonald, „Exploring a safe operating approach to weighting in life cycle impact assessment – a case study of organic, conventional and integrated farming systems,“ *Journal of Cleaner Production*, vol. 37, pp. 147–153, 2012, DOI: 10.1016/j.jclepro.2012.06.025.
- [108] A. Bjørn and M. Z. Hauschild, „Introducing carrying capacity-based normalisation in LCA: framework and development of references at midpoint level,“ *The International Journal of Life Cycle Assessment*, vol. 20, no. 7, pp. 1005–1018, 2015, DOI: 10.1007/s11367-015-0899-2.

- [109] T. C. Ponsioen and M. J. Goedkoop, „Midpoint weighting based on endpoint information,“ personal communication in ”Development of a weighting approach for the Environmental Footprint”, Sala et al., 2018, 2015.
- [110] L. Zampori and R. Pant, „Suggestions for updating the Product Environmental Footprint (PEF) method: EUR 29682 EN,“ Luxemburg rep. JRC115959, 2019, DOI: 10.2760/424613.
- [111] E. Hoepke, W. Appel, H. Brähler and U. Dahlhaus, *Nutzfahrzeugtechnik*, (ATZ / MTZ-Fachbuch), Wiesbaden, Springer Fachmedien, 2010, ISBN: 978-3-8348-0995-7.
- [112] MAN Nutzfahrzeug Gruppe, „Grundlagen der Nutzfahrzeugtechnik: Basiswissen Lkw und Bus,“ 2007. [Visited on 11/16/2016].
- [113] M. Hilgers, *Einsatzoptimierte Fahrzeuge, Aufbauten und Anhänger [Application-optimized vehicles, bodies and trailers]*, (Nutzfahrzeugtechnik lernen). vol. Sammelordner für 9 Lehrhefte, Wiesbaden and s.l., Springer Fachmedien Wiesbaden GmbH, 2017, ISBN: 9783658146443.
- [114] European Parliament. „*DIRECTIVE 2007/46/EC OF THE EUROPEAN PARLIAMENT AND OF THE COUNCIL of 5 September 2007 establishing a framework for the approval of motor vehicles and their trailers, and of systems, components and separate technical units intended for such vehicles: Directive (EU) 2007/46,*“ 2007. Available: <http://data.europa.eu/eli/dir/2007/46/oj> [visited on 06/24/2021].
- [115] Association des Constructeurs Européens d’Automobiles, „CO2 emissions from heavy-duty vehicles: Preliminary CO2 baseline (Q3–Q4 2019) estimate,“ Acea, Brüssel, 2020. Available: https://www.acea.auto/files/ACEA_preliminary_CO2_baseline_heavy-duty_vehicles.pdf [visited on 03/24/2020].
- [116] S. Wolff. „LOTUS - Long-Haul Truck Simulation: Longitudinal Dynamic Simulation for Heavy Duty Vehicles,“ [Online]. Available: <https://github.com/TUMFTM/LOTUS>.
- [117] B. Mustafić, „Technische und politische Rahmenbedingungen für den wirtschaftlichen Einsatz von elektrischen schweren Nutzfahrzeugen [Technical and political framework conditions for the economic use of electric heavy commercial vehicles],“ Master’s thesis, Institute of Automotive Technology, Technical University of Munich, Munich, Germany, 2020.
- [118] T. Gnann, P. Plötz, M. Wietschel and A. Kühn, „How to decarbonise heavy road transport,“ in *eceee 2017 Summer Study - consumption, efficiency and limits: 29 May-3 June 2017, Belambra Les Criques, Toulon/Hyères, France : eceee Summer Study proceedings*, T. L. Lindström, ed. Stockholm, Sweden: eceee Secretariat, 2017, ISBN: 9789198387803. [Visited on 11/06/2020].
- [119] A. Süßmann, „Kundenspezifische Bewertung von Maßnahmen zur Reduktion des Kraftstoffverbrauchs bei schweren Nutzfahrzeugen [Customer-specific evaluation of measures to reduce fuel consumption in heavy commercial vehicles],“ Dissertation, Institute of Automotive Technology, Technical University of Munich, Munich, Germany, 2021. [Visited on 04/03/2020].
- [120] M. Bstieler, „Packageanalyse zur Bewertung von Zero-Emission Technologien für schwere Nutzfahrzeugkonzepte [Package-Analysis for the Evaluation of Zero-Emission Technologies for Heavy-Duty Vehicle Concepts],“ Semester project thesis, Institute of Automotive Technology, Technical University of Munich, Munich, Germany, 2021.
- [121] International Energy Agency, *The Future of Trucks*, Paris, IEA, 2017, DOI: 10.1787/9789264279452-en. [Visited on 06/12/2018].
- [122] L. Gaines, F. Stodolsky and Cuenca R., „Lifecycle-analysis for heavy vehicles,“ in *91st Air and Waste Management Association Meeting and Exhibition*, San Diego, 1998. Available: <https://www.osti.gov/biblio/10731>.

- [123] Kraftfahrtbundesamt, „Fahrzeugzulassungen (FZ) Bestand an Kraftfahrzeugen nach Umwelt-Merkmalen 1. Januar 2021 [Vehicle registrations (FC) Stock of motor vehicles by environmental characteristics January 1, 2021],“ Flensburg, 2021. Available: https://www.kba.de/SharedDocs/Downloads/DE/Statistik/Fahrzeuge/FZ13/fz13_2021.pdf?__blob=publicationFile&v=4.
- [124] H. Zhao, A. Burke and L. Zhu, „Analysis of Class 8 hybrid-electric truck technologies using diesel, LNG, electricity, and hydrogen, as the fuel for various applications,“ in *World Electric Vehicle Symposium and Exposition (EVS 27), 2013: Barcelona, Spain, 17 - 20 Nov. 2013*, Barcelona, Spain, 2013, pp. 1–16, ISBN: 978-1-4799-3832-2. DOI: 10.1109/EVS.2013.6914957.
- [125] M. Mottschall, P. Kasten and F. Rodríguez, „Decarbonization of on-road freight transport and the role of LNG from a German perspective,“ Berlin, 2020. Available: https://theicct.org/sites/default/files/publications/LNG-in-trucks_May2020.pdf [visited on 11/06/2020].
- [126] B. Sen, T. Ercan and O. Tatari, „Does a battery-electric truck make a difference? - Life cycle emissions, costs, and externality analysis of alternative fuel-powered Class 8 heavy-duty trucks in the United States,“ *Journal of Cleaner Production*, vol. 141, pp. 110–121, 2017, DOI: 10.1016/j.jclepro.2016.09.046.
- [127] H.-O. Pörtner et al., „IPBES-IPCC co-sponsored workshop report synopsis on biodiversity and climate change,“ 2021, DOI: 10.5281/ZENODO.4782538.
- [128] A. Kirchner et al. „Analyse Klimapfade Verkehr 2030,“ 2019. Available: <https://www.prognos.com/de/projekt/klimapfade-verkehr-2030>.
- [129] Nationale Plattform Zukunft der Mobilität, „2. Kurzbericht der AG 2 - Einsatzmöglichkeiten Unter Realen Rahmenbedingungen [2. short report of the working group 2 - application possibilities under real conditions],“ Berlin, 2020. Available: https://www.plattform-zukunft-mobilitaet.de/wp-content/uploads/2020/06/NPM-AG-2_Einsatzm%C3%B6glichkeiten-unter-realen-Rahmenbedingungen.pdf [visited on 04/08/2020].
- [130] Prognos, Öko-Institut and Wuppertal-Institut, „Towards a Climate-Neutral Germany: Three Steps for Achieving Climate Neutrality by 2050 and an Intermediate Target of -65% in 2030 as Part of the EU Green Deal-Executive Summary,“ 2020. Available: https://static.agora-verkehrswende.de/fileadmin/Projekte/2020/KNDE2050/A-EW_193_KNDE_Executive-Summary_EN_WEB.pdf [visited on 11/06/2020].
- [131] P. R. Schmidt, W. Zittel, W. Weindorf and T. Raksha, „Renewables in Transport 2050: Empowering a sustainable mobility future with zero emission fuels from renewable electricity,“ Ludwig-Bölkow-Systemtechnik GmbH, Frankfurt a. M., 2016. Available: http://www.lbst.de/news/2016_docs/FVV_H1086_Renewables-in-Transport-2050-Kraftstoffstudie_II.pdf [visited on 02/08/2018].
- [132] Agora Verkehrswende and Agora Energiewende, „Die zukünftigen Kosten strombasierter synthetischer Brennstoffe,“ 2018. Available: https://www.agora-energiewende.de/fileadmin/Projekte/2017/SynKost_2050/Agora_SynCost-Studie_WEB.pdf [visited on 12/14/2021].
- [133] L. C. den Boer, *Zero Emissions Trucks: An Overview of State-of-the-art Technologies and Their Potential : Report*, CE Delft, 2013. Available: <https://www.osti.gov/etdweb/biblio/22122374>.
- [134] M. Schmied, P. Wüthrich, R. Zah, H.-J. Althaus and C. Friedl, „Postfossile Energieversorgungsoptionen für einen treibhausgasneutralen Verkehr im Jahr 2050 – eine verkehrsträgerübergreifende Bewertung,“ 2015. Available: https://www.umweltbundesamt.de/sites/default/files/medien/378/publikationen/texte_30_2015_postfossile_energieversorgungsoptionen.pdf [visited on 04/30/2018].

- [135] F. Ueckerdt et al., „Potential and risks of hydrogen-based e-fuels in climate change mitigation,“ *Nature Climate Change*, vol. 11, no. 5, pp. 384–393, 2021, DOI: 10.1038/s41558-021-01032-7.
- [136] L. Fulton and M. Marshall, „Strategies for Transitioning to Low-Carbon Emission Trucks in the United States,“ Davis, 2015. Available: <https://steps.ucdavis.edu/files/06-11-2015-STEPS-NCST-Low-carbon-Trucks-in-US-06-10-2015.pdf> [visited on 02/21/2020].
- [137] F. J. R. Verbruggen, E. Silvas and T. Hofman, „Electric Powertrain Topology Analysis and Design for Heavy-Duty Trucks,“ *Energies*, vol. 13, no. 10, p. 2434, 2020, DOI: 10.3390/en13102434.
- [138] S. Wolff, S. Kalt, M. Bstieler and M. Lienkamp, „Influence of Powertrain Topology and Electric Machine Design on Efficiency of Battery Electric Trucks—A Simulative Case-Study,“ *Energies*, vol. 14, no. 2, p. 328, 2021, DOI: 10.3390/en14020328.
- [139] O. Olsson, „Slide-in Electric Road System: Inductive project report,“ Viktoria Swedish ICT, Göteborg, 2013. Available: <https://www.diva-portal.org/smash/get/diva2:1131846/FULLTEXT02> [visited on 11/29/2017].
- [140] M. Wietschel et al., „Machbarkeitsstudie zur Ermittlung der Potentiale des Hybrid-Oberleitungs-Lkw,“ Fraunhofer Institut für System und Innovationsforschung, Karlsruhe, 2017.
- [141] M. Moultak, N. Lutsey and D. Hall, „Transitioning to zero-emission heavy-duty freight vehicles,“ International Council on Clean Transportation, 2017. Available: <https://theicct.org/publications/transitioning-zero-emission-heavy-duty-freight-vehicles> [visited on 12/14/2018].
- [142] S. Altenburg et al., „Nullemissionsnutzfahrzeuge: Vom ökologischen Hoffnungsträger zur ökonomischen Alternative,“ Stuttgart, 2017. Available: <https://www.nweurope.eu/media/2663/2017-nfz-studie.pdf> [visited on 12/14/2021].
- [143] Tesla, Inc. „*Tesla Press Information*,“ 2019. Available: https://www.tesla.com/de_DE/presskit.
- [144] I. Mareev, J. Becker and D. Sauer, „Battery Dimensioning and Life Cycle Costs Analysis for a Heavy-Duty Truck Considering the Requirements of Long-Haul Transportation,“ *Energies*, vol. 11, no. 1, p. 55, 2018, DOI: 10.3390/en11010055. [Visited on 12/20/2018].
- [145] I. Mareev and D. Sauer, „Energy Consumption and Life Cycle Costs of Overhead Catenary Heavy-Duty Trucks for Long-Haul Transportation,“ *Energies*, vol. 11, no. 12, p. 3446, 2018, DOI: 10.3390/en11123446.
- [146] D. Hall and N. Lutsey, „Estimating the infrastructure needs and costs for the launch of zero-emission trucks,“ 2019, DOI: 10.13140/RG.2.2.17010.86724.
- [147] P. Hofmann, *Hybridfahrzeuge: Ein alternatives Antriebssystem für die Zukunft [Hybrid vehicles: An alternative powertrain for the future]*, 2. Aufl., Wien, Springer, 2014, ISBN: 978-3-7091-1779-8.
- [148] K. Reif, K.-E. Noreikat and K. Borgeest, *Kraftfahrzeug-Hybridantriebe: Grundlagen, Komponenten, Systeme, Anwendungen [Automotive Hybrid Powertrains: Basics, components, systems, applications]*, (ATZ / MTZ-Fachbuch), Wiesbaden, Vieweg+Teubner Verlag, 2012, ISBN: 9783834807229. DOI: 10.1007/978-3-8348-2050-1. Available: <http://gbv.ebib.com/patron/FullRecord.aspx?p=1083174>.
- [149] M. Rupp, S. Schulze and I. Kuperjans, „Comparative Life Cycle Analysis of Conventional and Hybrid Heavy-Duty Trucks,“ *World Electric Vehicle Journal*, vol. 9, no. 2, p. 33, 2018, DOI: 10.3390/wevj9020033.

- [150] S. Kühnel, F. Hacker and W. Görz, „Oberleitungs-Lkw im Kontext weiterer Antriebs- und Energieversorgungsoptionen für den Straßengüterfernverkehr [Catenary trucks in the context of further drive and Energy supply options for long-distance road freight transport],“ Freiburg, 2018. Available: <https://www.erneuerbar-mobil.de/sites/default/files/2018-09/Teilbericht%201%20O-Lkw-Technologievergleich-2018.pdf> [visited on 03/23/2021].
- [151] B. J. Limb et al., „Economic Viability and Environmental Impact of In-Motion Wireless Power Transfer,“ *IEEE Transactions on Transportation Electrification*, p. 1, 2018, DOI: 10.1109/TTE.2018.2876067.
- [152] Hydrogen Council, „Path to hydrogen competitiveness: A cost perspective,“ 2020. Available: https://hydrogencouncil.com/wp-content/uploads/2020/01/Path-to-Hydrogen-Competitiveness_Full-Study-1.pdf [visited on 02/21/2020].
- [153] International Energy Agency, „The Future of Hydrogen,“ Paris, France, 2019. Available: https://iea.blob.core.windows.net/assets/9e3a3493-b9a6-4b7d-b499-7ca48e357561/The_Future_of_Hydrogen.pdf [visited on 06/30/2021].
- [154] Bundesministerium für Wirtschaft und Technologie, „The National Hydrogen Strategy,“ Berlin, Germany, 2020. Available: https://www.bmbf.de/files/bmwi_Nationale%20Wasserstoffstrategie_Eng_s01.pdf [visited on 06/30/2021].
- [155] M. Klell, H. Eichlseder and A. Trattner, *Wasserstoff in der Fahrzeugtechnik [Hydrogen in automotive technology]*, Wiesbaden, Springer Fachmedien Wiesbaden, 2018, ISBN: 978-3-658-20446-4. DOI: 10.1007/978-3-658-20447-1.
- [156] W. Artl, „Wasserstoff und Speicherung im Schwerlastverkehr: Machbarkeitsstudie [Hydrogen and storage in heavy-duty transport: Feasibility study],“ Friedrich-Alexander Universität Erlangen-Nürnberg, Erlangen, 2018. Available: https://www.encn.de/fileadmin/user_upload/Studie_Wasserstoff_und_Schwerlastverkehr_WEB.pdf [visited on 05/02/2018].
- [157] J. Töppler and J. Lehmann, *Wasserstoff und Brennstoffzelle [Hydrogen and Fuel Cell]*, Berlin, Heidelberg, Springer Berlin Heidelberg, 2017, ISBN: 978-3-662-53359-8. DOI: 10.1007/978-3-662-53360-4.
- [158] „Shell Nutzfahrzeug-Studie: Diesel oder Alternative Antriebe - Womit fahren LKW und Bus morgen? [Shell Commercial Vehicle Study: Diesel or Alternative Drives - What Will Trucks and Buses Use Tomorrow?],“ Hamburg, 2016.
- [159] R. van Basshuysen and F. Schäfer, *Handbuch Verbrennungsmotor [Internal combustion engine handbook]*, Wiesbaden, Springer Fachmedien Wiesbaden, 2015, ISBN: 978-3-658-04677-4. DOI: 10.1007/978-3-658-04678-1.
- [160] A. Burkert, „Wasserstoff lässt sich auch gut verbrennen [Hydrogen can also be combusted well],“ *MTZ - Motortechnische Zeitschrift*, vol. 78, no. 04|2017, pp. 8–13, 2017.
- [161] Solar Impulse Foundation. „KEYOU-inside,“ 2021. Available: <https://solarimpulse.com/efficient-solutions/keyou-inside> [visited on 02/18/2021].
- [162] D. Koch, S. C. Zeilinga, H. Rottengruber and A. Sousa, „Simulationsgestützte Entwicklung eines Wasserstoffmotors für einen emissionsfreien Verkehr [Simulation-based development of a hydrogen engine for zero-emission traffic],“ *MTZ - Motortechnische Zeitschrift*, vol. 78, no. 11, pp. 38–43, 2017, DOI: 10.1007/s35146-017-0116-x.

- [163] C. Vogel, „Wasserstoff-Dieselmotor mit Direkteinspritzung, hoher Leistungsdichte und geringer Abgasemission [Hydrogen diesel engine with direct injection, high power density and low exhaust emissions],“ *MTZ - Motortechnische Zeitschrift*, vol. 60, no. 10, pp. 704–708, 1999, DOI: 10.1007/BF03226534.
- [164] M. Borchers, K. Keller, P. Lott and O. Deutschmann, „Selective Catalytic Reduction of NO_x with H₂ for Cleaning Exhausts of Hydrogen Engines: Impact of H₂O, O₂, and NO/H₂ Ratio,“ *Industrial & Engineering Chemistry Research*, 2021, DOI: 10.1021/acs.iecr.0c05630.
- [165] A. Wimmer, T. Wallner, J. Ringler and F. Gerbig, „H₂-Direct Injection – A Highly Promising Combustion Concept,“ in *SAE Technical Paper Series*, 2005, DOI: 10.4271/2005-01-0108.
- [166] P. Kumar, P. Anil Kishan, M. Nikhil Mathew and A. Dhar, „Flame kernel growth study of spark ignited hydrogen air premixed combustion at engine conditions,“ *Thermal Science and Engineering Progress*, vol. 21, p. 100769, 2021, DOI: 10.1016/j.tsep.2020.100769.
- [167] R. van Basshuysen, *Ottomotor mit Direkteinspritzung und Direkteinblasung*, Wiesbaden, Springer Fachmedien Wiesbaden, 2017, ISBN: 978-3-658-12214-0. DOI: 10.1007/978-3-658-12215-7.
- [168] R. Heindl, H. Eichseder, C. Spuller, F. Gerbig and K. Heller, „New and Innovative Combustion Systems for the H₂-ICE: Compression Ignition and Combined Processes,“ *SAE International Journal of Engines*, vol. 2, no. 1, pp. 1231–1250, 2009, DOI: 10.4271/2009-01-1421.
- [169] H. Rottengruber, U. Wiebicke, G. Woschni and K. Zeilinger, „Wasserstoff-Dieselmotor mit Direkteinspritzung, hoher Leistungsdichte und geringer Abgasemission [Hydrogen diesel engine with direct injection, high power density and low exhaust emissions],“ *MTZ - Motortechnische Zeitschrift*, vol. 61, no. 2, pp. 122–128, 2000, DOI: 10.1007/BF03226557.
- [170] S. Verhelst, „Recent progress in the use of hydrogen as a fuel for internal combustion engines,“ *International Journal of Hydrogen Energy*, vol. 39, no. 2, pp. 1071–1085, 2014, DOI: 10.1016/j.ijhydene.2013.10.102.
- [171] P. Pechtl and F. Dorer, „Wasserstoff-Dieselmotor mit Direkteinspritzung, hoher Leistungsdichte und geringer Abgasemission [Hydrogen diesel engine with direct injection, high power density and low exhaust emissions],“ *MTZ - Motortechnische Zeitschrift*, vol. 60, no. 12, pp. 830–837, 1999, DOI: 10.1007/BF03226544.
- [172] K. Klepatz, H. Rottengruber, S. Zeilinga, D. Koch and W. Prümm, „Loss Analysis of a Direct-Injection Hydrogen Combustion Engine,“ in *SAE Technical Paper Series*, 2018, DOI: 10.4271/2018-01-1686.
- [173] A. Boretti, „Stoichiometric H₂ICE with water injection and exhaust and coolant heat recovery through organic Rankine cycles,“ *International Journal of Hydrogen Energy*, vol. 36, no. 19, pp. 12591–12600, 2011, DOI: 10.1016/j.ijhydene.2011.06.124.
- [174] M. Berckmüller et al., „Potentials of a Charged SI-Hydrogen Engine,“ in *SAE Technical Paper Series*, 2003, DOI: 10.4271/2003-01-3210.
- [175] N. Eidkum, „Simulation und Analyse von Wasserstoffverbrennungsmotoren als Zero-Emission Technologie für Nutzfahrzeuge [Simulation and Analysis of Hydrogen Combustion Engines as Zero-Emission Technology for Heavy-Duty Vehicles],“ Bachelor’s thesis, Institute of Automotive Technology, Technical University of Munich, Munich, Germany, 2021.
- [176] W. Arlt, *Machbarkeitsstudie - Wasserstoff und Speicherung im Schwerlastverkehr: Teil 2*, Erlangen, 2018. Available: <https://www.tvt.tf.fau.de/> [visited on 12/14/2021].

- [177] P. Kurzweil and O. K. Dietlmeier, *Elektrochemische Speicher [Electrochemical storage]*, Wiesbaden, Springer Fachmedien Wiesbaden, 2018, ISBN: 978-3-658-21828-7. DOI: 10.1007/978-3-658-21829-4.
- [178] H. S. Roh, T. Q. Hua and R. K. Ahluwalia, „Optimization of carbon fiber usage in Type 4 hydrogen storage tanks for fuel cell automobiles,“ *International Journal of Hydrogen Energy*, vol. 38, no. 29, pp. 12795–12802, 2013, DOI: 10.1016/j.ijhydene.2013.07.016.
- [179] A. Agostini et al., „Role of hydrogen tanks in the life cycle assessment of fuel cell-based auxiliary power units,“ *Applied Energy*, vol. 215, pp. 1–12, 2018, DOI: 10.1016/j.apenergy.2018.01.095.
- [180] M. Baricco et al., „SSH2S: Hydrogen storage in complex hydrides for an auxiliary power unit based on high temperature proton exchange membrane fuel cells,“ *Journal of Power Sources*, vol. 342, pp. 853–860, 2017, DOI: 10.1016/j.jpowsour.2016.12.107.
- [181] M. Niermann, S. Timmerberg, S. Drünert and M. Kaltschmitt, „Liquid Organic Hydrogen Carriers and alternatives for international transport of renewable hydrogen,“ *Renewable and Sustainable Energy Reviews*, vol. 135, p. 110171, 2021, DOI: 10.1016/j.rser.2020.110171.
- [182] Dover Fueling Solutions, „Tokheim Quantum 510M FHR Zapfsäule,“ 2020. Available: https://www.tsg-solutions.com/app/uploads/2020/09/Q510M-FHR-FINAL-DE_P.pdf [visited on 03/18/2021].
- [183] M. Q. Wang, „GREET 1.0 – Transportation fuel cycles model: Methodology and use,“ Argonne National Laboratory, Argonne, USA, 1996, DOI: 10.2172/266652.
- [184] A. Burnham, M. Q. Wang and Y. Wu, „Development and applications of GREET 2.7 – The Transportation Vehicle-CycleModel,“ Energy Systems Division, Argonne National Laboratory, Oak Ridge, 2006, DOI: 10.2172/898530.
- [185] Argonne National Lab. „AFLEET Online,“ 2021. [Online]. Available: <https://afleet-web.es.anl.gov/afleet/> [visited on 12/14/2021].
- [186] M. Wang et al., „Summary of Expansions and Updates in GREET® 2021,“ Argonne, USA, 2021.
- [187] M. A. Delucchi, „A Lifecycle Emissions Model (LEM): Lifecycle Emissions from Transportation Fuels, Motor Vehicles, Transportation Modes, Electricity Use, Heating and Cooking Fuels, and Materials,“ UC Davis: Institute of Transportation Studies, Davis, 2003. Available: <http://citeseerx.ist.psu.edu/viewdoc/download?doi=10.1.1.208.9765&rep=rep1&type=pdf> [visited on 12/14/2021].
- [188] R. Sacchi, C. Bauer and B. L. Cox, „Does Size Matter? The Influence of Size, Load Factor, Range Autonomy, and Application Type on the Life Cycle Assessment of Current and Future Medium- and Heavy-Duty Vehicles,“ *Environmental science & technology*, 2021, DOI: 10.1021/acs.est.0c07773.
- [189] B. Reuter, „Die Bewertung von Nachhaltigkeitsaspekten für die Rohstoff- und Technologieauswahl während des Entwicklungsprozesses von Elektrofahrzeugen [The evaluation of sustainability aspects for raw material and technology selection during the development process of electric vehicles],“ Dissertation, Institute of Automotive Technology, Technical University of Munich, Munich, Germany, 2016. [Visited on 12/19/2018].
- [190] I. Rüdener et al., „Costs and Benefits of Green Public Procurement in Europe,“ 2007. Available: <https://www.oeko.de/oekodoc/590/2007-140-en.pdf>.

- [191] G. Rebitzer and D. Hunkeler, „Life cycle costing in LCM: ambitions, opportunities, and limitations,” *The International Journal of Life Cycle Assessment*, vol. 8, no. 5, pp. 253–256, 2003, DOI: 10.1007/BF02978913. Available: <https://link.springer.com/article/10.1007/BF02978913>.
- [192] International Energy Agency. „Energy Prices 2020,” 2021. [Online]. Available: <https://www.iea.org/reports/energy-prices-2020> [visited on 04/22/2021].
- [193] R. Frischknecht et al., „The ecoinvent Database: Overview and Methodological Framework (7 pp),” *The International Journal of Life Cycle Assessment*, vol. 10, no. 1, pp. 3–9, 2005, DOI: 10.1065/lca2004.10.181.1.
- [194] G. Wernet et al., „The ecoinvent database version 3 (part I): overview and methodology,” *The International Journal of Life Cycle Assessment*, vol. 21, no. 9, pp. 1218–1230, 2016, DOI: 10.1007/s11367-016-1087-8.
- [195] A. Mehmeti, A. Angelis-Dimakis, G. Arampatzis, S. McPhail and S. Ulgiati, „Life Cycle Assessment and Water Footprint of Hydrogen Production Methods: From Conventional to Emerging Technologies,” *Environments*, vol. 5, no. 2, p. 24, 2018, DOI: 10.3390/environments5020024.
- [196] A. König et al., „An Overview of Parameter and Cost for Battery Electric Vehicles,” *World Electric Vehicle Journal*, vol. 12, no. 1, p. 21, 2021, DOI: 10.3390/wevj12010021.
- [197] C. Kost and T. Schlegl, „Stromgestehungskosten erneuerbarer Energien [Electricity production costs of renewable energies],” Freiburg, 2018. Available: https://www.ise.fraunhofer.de/content/dam/ise/de/documents/publications/studies/DE2018_ISE_Studie_Stromgestehungskosten_Erneuerbare_Energien.pdf [visited on 05/07/2020].
- [198] N. A. Burton, R. V. Padilla, A. Rose and H. Habibullah, „Increasing the efficiency of hydrogen production from solar powered water electrolysis,” *Renewable and Sustainable Energy Reviews*, vol. 135, p. 110255, 2021, DOI: 10.1016/j.rser.2020.110255. Available: <https://www.sciencedirect.com/science/article/pii/S136403212030544X>.
- [199] M. Wang et al. „Greenhouse gases, Regulated Emissions, and Energy use in Technologies Model ® (2020 .Net),” 2020. DOI: 10.11578/GREET-NET-2020/DC.20200913.1.
- [200] G. Zang, P. Sun, A. Elgowainy, A. Bafana and M. Wang, „Life Cycle Analysis of Electrofuels: Fischer-Tropsch Fuel Production from Hydrogen and Corn Ethanol Byproduct CO₂,” *Environmental science & technology*, vol. 55, no. 6, pp. 3888–3897, 2021, DOI: 10.1021/acs.est.0c05893.
- [201] CharIN, „Position Paper of Charging Interface Initiative e.V. CharIN DC CCS Power Classes V7.2,” Berlin, Germany, 2021. Available: https://www.charin.global/media/pages/technology/knowledge-base/c6574dae0e-1639130326/charin_dc_ccs_power_classes.pdf [visited on 06/29/2022].
- [202] lastauto omnibus, *Lastauto Omnibus-Katalog 2016*, 1. Aufl., Stuttgart, EuroTransportMedia Verlags- und Veranstaltungs-GmbH, 2015, ISBN: 9783613308008.
- [203] M. Fries, M. Lehmeyer and M. Lienkamp, „Multi-criterion optimization of heavy-duty powertrain design for the evaluation of transport efficiency and costs,” in *IEEE ITSC 2017: 20th International Conference on Intelligent Transportation Systems : Mielparque Yokohama in Yokohama, Kanagawa, Japan, October 16-19, 2017*, Yokohama, 2017, pp. 1–8, ISBN: 978-1-5386-1526-3. DOI: 10.1109/ITSC.2017.8317753.

- [204] S. Rohr, S. Wagner, M. Baumann, S. Müller and M. Lienkamp, „A techno-economic analysis of end of life value chains for lithium-ion batteries from electric vehicles,“ in *2017 Twelfth International Conference on Ecological Vehicles and Renewable Energies (EVER)*, 2017, pp. 1–14, DOI: 10.1109/EVER.2017.7935867.
- [205] J. E. Harlow et al., „A Wide Range of Testing Results on an Excellent Lithium-Ion Cell Chemistry to be used as Benchmarks for New Battery Technologies,“ *Journal of The Electrochemical Society*, vol. 166, no. 13, A3031–A3044, 2019, DOI: 10.1149/2.0981913jes.
- [206] A. Lajunen, „Lifecycle costs and charging requirements of electric buses with different charging methods,“ *Journal of Cleaner Production*, vol. 172, pp. 56–67, 2017, DOI: 10.1016/j.jclepro.2017.10.066.
- [207] H2 Mobility, „Wasserstoffbetankung von Schwerlastfahrzeugen – die Optionen im Überblick [Hydrogen refueling of heavy-duty vehicles - the options at a glance],“ Berlin, Germany, 2021. Available: https://h2-mobility.de/wp-content/uploads/sites/2/2021/09/H2M_Ueberblick_Betankungsoptionen.pdf [visited on 10/27/2021].
- [208] P. Mock and S. Diaz, „European vehicle market statistics 2020/21,“ Berlin, Germany, 2020. Available: https://theicct.org/sites/default/files/publications/ICCT_EU_Pocketbook_2020_Web_Dec2020.pdf [visited on 11/04/2021].
- [209] Vda, „Market commercial vehicles, trailers, bodies and buses,“ 2021. [Online]. Available: <https://en.vda.de/en/topics/automotive-industry-and-markets/sector-commercial-vehicles/overview-of-the-commercial-vehicle-sector.html> [visited on 11/04/2021].
- [210] P. Gerbert et al., „Klimapfade für Deutschland [Climate Pathways for Germany],“ Munich, Germany, 2018. Available: https://image-src.bcg.com/Images/Klimapfade-fuer-Deutschland_tcm108-181356.pdf [visited on 11/03/2021].
- [211] A. Kemmler et al., „Energiewirtschaftliche Projektionen und Folgeabschätzungen 2030/2050 [Energy Industry Projections and Impact Assessments 2030/2050],“ Berlin, Germany, 2020. Available: https://www.bmwi.de/Redaktion/DE/Publikationen/Wirtschaft/klimagutachten.pdf?__blob=publicationFile&v=8 [visited on 11/03/2021].
- [212] M. Rathmann, „Interesse an Gas-Lkw ungebrochen [Interest in gas trucks continues unabated],“ *Eurotransport*, 2021. Available: <https://www.eurotransport.de/artikel/run-auf-foerderprogramm-interesse-an-gas-lkw-ungebrochen-11180994.html> [visited on 11/05/2021].
- [213] Nationale Plattform Zukunft der Mobilität, „Technologisches Factsheet der Fokusgruppe 1, Technologische Elektromobilitätskonzepte [Technological Factsheet of Focus Group 1, Technological Electromobility Concepts],“ Berlin, Germany, 2019.
- [214] R. D. Reid and N. R. Sanders, *Operations management: An integrated approach*, 7th edition, EMEA edition, Hoboken, NJ, Wiley, 2020, ISBN: 1119668174.
- [215] P. Mauk, „Lebenszyklusanalyse eines wasserstoffbetrieben schweren Nutzfahrzeugs im Fernverkehr [Life Cycle Assessment of a Fuel Cell Powered Heavy-Duty Truck],“ Bachelor’s thesis, Institute of Automotive Technology, Technical University of Munich, Munich, Germany, 2020.
- [216] A. Simons and C. Bauer, „A life-cycle perspective on automotive fuel cells,“ *Applied Energy*, vol. 157, pp. 884–896, 2015, DOI: 10.1016/j.apenergy.2015.02.049.
- [217] Q. Dai, J. C. Kelly, L. Gaines and M. Wang, „Life Cycle Analysis of Lithium-Ion Batteries for Automotive Applications,“ *Batteries*, vol. 5, no. 2, p. 48, 2019, DOI: 10.3390/batteries5020048.

- [218] K. Gordon, „Comparative Environmental Life Cycle Assessment of Conventional and Alternative Heavy-Duty Truck Drivetrains,“ Master’s thesis, Institute of Automotive Technology, Technical University of Munich, Munich, Germany, 2019.
- [219] S. Alvarez, „Comparative Environmental Life Cycle Assessment of Heavy-Duty Trucks in Different Geographical Locations,“ Master’s thesis, Institute of Automotive Technology, Technical University of Munich, Munich, Germany, 2019.
- [220] thinkstep AG. „GaBi,“ Stuttgart, 2017.
- [221] PE International, „Handbook for Life Cycle Assessment (LCA): Using the GaBi Education Software Package,“ Leinfelden-Echterdingen, Germany, 2009. Available: https://gabi.sphera.com/fileadmin/gabi/tutorials/tutorial1/GaBi_Education_Handbook.pdf [visited on 11/12/2021].
- [222] thinkstep AG, „Professional Database 2017,“ 2017. Available: https://gabi.sphera.com/fileadmin/GaBi_Databases/Database_Upgrade_2017_Upgrades_and_improvements.pdf.
- [223] A. Nordelöf, E. Grunditz, A.-M. Tillman, T. Thiringer and M. Alatalo, „A scalable life cycle inventory of an electrical automotive traction machine—Part I: design and composition,“ *The International Journal of Life Cycle Assessment*, vol. 23, no. 1, pp. 55–69, 2018, DOI: 10.1007/s11367-017-1308-9.
- [224] M. Seidenfus, „Ökoeffizienz von alternativen Antrieben für den schweren Güterverkehr [Eco-Efficiency of Alternative Drive Trains for Heavy Duty Vehicles in the Transport Sector],“ Semester project thesis, Institute of Automotive Technology, Technical University of Munich, Munich, Germany, 2020.
- [225] Bundesverband Güterkraftverkehr Logistik und Entsorgung. „Modellrechnungen zur Kostentwicklung im Güterkraftverkehr [Model calculations for the development of costs in road freight transport],“ 2021. [Online]. Available: https://www.bgl-ev.de/web/der_bgl/informationen/branchenkostenentwicklung.htm?v=2#form [visited on 12/14/2021].
- [226] L. Guzzella and A. Sciarretta, *Vehicle Propulsion Systems*, 3rd revised ed. 2013, Berlin, Springer-Verlag Berlin and Heidelberg GmbH & Co. KG, 2012, ISBN: 978-3-642-35912-5.
- [227] H. Naunheimer, B. Bertsche and J. Ryborz, *Fahrzeuggetriebe: Grundlagen, Auswahl, Auslegung und Konstruktion [Vehicle transmission: Basics, selection, design and construction]*, 3rd ed. 2019, 2019, ISBN: 9783662588833. DOI: 10.1007/978-3-662-58883-3.
- [228] K.-L. Haken, *Grundlagen der Kraftfahrzeugtechnik: Mit 36 Tabellen [Fundamentals of automotive engineering: With 36 tables]*, (Fahrzeugtechnik), 2., aktualisierte und erw. Aufl., Munich, Germany, Hanser, 2011, ISBN: 978-3-446-42849-2. DOI: 10.3139/9783446428492. Available: <http://www.hanser-elibrary.com/action/showBook?doi=10.3139/9783446428492>.
- [229] European Commission. „Commission Regulation (EU) 2017/1151 of 1 June 2017,“ 2017. Available: <https://eur-lex.europa.eu/legal-content/EN/TXT/?uri=celex%3A32017R1151>.
- [230] M. Rexeis et al., „VECTO tool development: Completion of methodology to simulate Heavy Duty Vehicles’ fuel consumption and CO2 emissions: Upgrades to the existing version of VECTO and completion of certification methodology to be incorporated into a Commission legislative proposal.“ 2017. Available: https://ec.europa.eu/clima/sites/clima/files/transport/vehicles/docs/sr7_lot4_final_report_en.pdf [visited on 02/15/2019].
- [231] M. Fries, M. Kruttschnitt and M. Lienkamp, „Multi-objective optimization of a long-haul truck hybrid operational strategy and a predictive powertrain control system,“ in *Twelfth International Conference on Ecological Vehicles and Renewable Energies (EVER)*, Monte-Carlo, Monaco, 2017, pp. 1–7, DOI: 10.1109/EVER.2017.7935872.

- [232] M. Fries, M. Sinning and M. Lienkamp, „Virtual Combination of Commercial Vehicle Modules (Virtual Truck) for characterization of future Concepts,“ in *Conference on Future Automotive Technology*, 2015. Available: https://www.researchgate.net/publication/275947875_Virtual_Combination_of_Commercial_Vehicle_Modules_Virtual_Truck_for_Characterization_of_Future_Concepts.
- [233] M. Fries, M. Sinning, M. Lienkamp and M. Höpfner, „Virtual Truck - A Method for Customer Oriented Commercial Vehicle Simulation,“ in *Commercial vehicle technology 2016: Proceedings of the 4th Commercial Vehicle Technology Symposium (CVT 2016), March 8-10, 2016, University of Kaiserslautern, Kaiserslautern, Germany*, K. Berns et al., ed. Aachen: Shaker Verlag, 2016, ISBN: 978-3-8440-4229-0. DOI: 10.2370/9783844042290.
- [234] C. Mährle, S. Wolff, S. Held and G. Wachtmeister, „Influence of the Cooling System and Road Topology on Heavy Duty Truck Platooning,“ in *The 2019 IEEE Intelligent Transportation Systems Conference - ITSC: Auckland, New Zealand, 27-30 October 2019*, Auckland, New Zealand, 2019, pp. 1251–1256, ISBN: 978-1-5386-7024-8. DOI: 10.1109/ITSC.2019.8917050.
- [235] A. Süßmann and A. Förg, „Erzeugung und Anwendung von kundenspezifischen Fahrzyklen bei schweren Nutzfahrzeugen [Generation and utilization of customer-specific driving cycles for heavy-duty vehicles],“ in *4. VDI Conference on Transmissions in Commercial Vehicles*, Friedrichshafen, Germany, 2015.
- [236] M. Fries, A. Baum, M. Wittmann and M. Lienkamp, „Derivation of a real-life driving cycle from fleet testing data with the Markov-Chain-Monte-Carlo Method,“ in *2018 21st International Conference on Intelligent Transportation Systems (ITSC)*, Maui, HI, USA, 2018, pp. 2550–2555, ISBN: 978-1-7281-0321-1. DOI: 10.1109/ITSC.2018.8569547.
- [237] F. Verbruggen, V. Rangarajan and T. Hofman, „Powertrain design optimization for a battery electric heavy-duty truck,“ in *2019 American Control Conference (ACC)*, Philadelphia, PA, USA, 2019, pp. 1488–1493, ISBN: 978-1-5386-7926-5. DOI: 10.23919/ACC.2019.8814771.
- [238] European Parliament. „*Regulation (EC) No 595/2009 of the European Parliament and of the Council of 18 June 2009 on type-approval of motor vehicles and engines with respect to emissions from heavy duty vehicles (Euro VI) and on access to vehicle repair and maintenance information and amending Regulation (EC) No 715/2007 and Directive 2007/46/EC and repealing Directives 80/1269/EEC, 2005/55/EC and 2005/78/EC: Regulation (EC) No 595/2009*,“ 18.06.2009. Available: <http://data.europa.eu/eli/reg/2009/595/oj> [visited on 08/30/2019].
- [239] P.-L. Ragon and F. Rodríguez, „Estimated cost of diesel emissions control technology to meet future Euro VII standards,“ Berlin, Germany, 2021. Available: <https://theicct.org/sites/default/files/publications/tech-cost-euro-vii-210428.pdf> [visited on 11/26/2021].
- [240] Environmental Protection Agency, „Heavy-Duty Highway Engine: Clean Fuel Fleet Exhaust Emission Standards (EPA-420-B-16-017, March 2016),“ 2016. Available: <https://nepis.epa.gov/Exe/ZyPDF.cgi?Dockkey=P100O9ZY.pdf> [visited on 12/14/2021].
- [241] California Air Resources Board, „Facts about the Low NOx Heavy-Duty Omnibus Regulation,“ Sacramento, USA, 2020. Available: https://ww2.arb.ca.gov/sites/default/files/classic/msprog/hdlownox/files/HD_NOx_Omnibus_Fact_Sheet.pdf [visited on 12/14/2021].
- [242] Continental, „Worldwide Emission Standards and Related Regulations: Passenger Cars / Light and Medium Duty Vehicles May 2019,“ Regensburg, 2019. Available: https://www.continental-automotive.com/getattachment/8f2dedad-b510-4672-a005-3156f77d1f85/EMISSIONBOOKLET_2019.pdf/ [visited on 12/14/2021].

- [243] European Parliament. „COMMISSION REGULATION (EU) No 582/2011 of 25 May 2011 implementing and amending Regulation (EC) No 595/2009 of the European Parliament and of the Council with respect to emissions from heavy duty vehicles (Euro VI) and amending Annexes I and III to Directive 2007/46/EC of the European Parliament and of the Council: Regulation (EU) No 582/2011,“ 18.06.2009. Available: <http://data.europa.eu/eli/reg/2011/582/oj> [visited on 08/30/2019].
- [244] T. Grigoratos and G. Martini, „Non-exhaust traffic related emissions - Brake and tyre wear PM,“ Luxembourg, Luxembourg rep. JRC89231, 2014, DOI: 10.2790/21481. Available: <https://publications.jrc.ec.europa.eu/repository/handle/JRC89231>.
- [245] C. Pan, „Modeling and Simulation of Real-Driving, Non-CO2 Emissions for Heavy-Duty Trucks,“ Semester project thesis, Institute of Automotive Technology, Technical University of Munich, Munich, Germany, 2020.
- [246] M. Barth, T. Younglove and G. Scora, „Development of a heavy-duty diesel modal emissions and fuel consumption model,“ Berkeley, USA, 2005. Available: <https://escholarship.org/uc/item/67f0v3zf> [visited on 12/14/2021].
- [247] W. Zhang, J. Lu, P. Xu and Y. Zhang, „Moving towards Sustainability: Road Grades and On-Road Emissions of Heavy-Duty Vehicles—A Case Study,“ *Sustainability*, vol. 7, no. 9, pp. 12644–12671, 2015, DOI: 10.3390/su70912644.
- [248] Environmental Protection Agency, *Exhaust Emission Rates for Heavy-Duty On-road Vehicles in MOVES2014*, Washington DC, USA, U.S. Environmental Protection Agency, Office of Transportation and Air Quality, Assessment and Standards Division, 2014. Available: <https://nepis.epa.gov/Exe/ZyPDF.cgi?Dockey=P100NO46.pdf> [visited on 01/28/2021].
- [249] X. Lu, H.-B. Huang, T. Zhang and J.-N. Dong, „Numerical simulation on diffusion characteristics of car tire wear particles [Original language: Chinese],“ *Journal of Ningbo University (Science and Technology)*, 2019.
- [250] A. Iijima et al., „Emission factor for antimony in brake abrasion dusts as one of the major atmospheric antimony sources,“ *Environmental science & technology*, vol. 42, no. 8, pp. 2937–2942, 2008, DOI: 10.1021/es702137g.
- [251] S. Ko et al., „NOx Emissions from Euro 5 and Euro 6 Heavy-Duty Diesel Vehicles under Real Driving Conditions,“ *Energies*, vol. 13, no. 1, p. 218, 2020, DOI: 10.3390/en13010218.
- [252] S. Weiß, „Modellierung einer Brennstoffzelle für Fernverkehrs Lkw [Modeling a PEM Fuel-Cell for Long-Distance Trucks],“ Semester project thesis, Institute of Automotive Technology, Technical University of Munich, Munich, Germany, 2019.
- [253] S. M. Njoya, O. Tremblay and L.-A. Dessaint, „A generic fuel cell model for the simulation of fuel cell vehicles,“ in *IEEE Vehicle Power and Propulsion Conference, 2009: VPPC '09 ; 7 - 10 Sept. 2009, Dearborn, Michigan, USA*, Dearborn, MI, 2009, pp. 1722–1729, ISBN: 978-1-4244-2600-3. DOI: 10.1109/VPPC.2009.5289692.
- [254] S. N. Motapon, O. Tremblay and L. A. Dessaint, „Development of a generic fuel cell model: application to a fuel cell vehicle simulation,“ *International Journal of Power Electronics*, vol. 4, no. 6, p. 505, 2012, DOI: 10.1504/IJPELEC.2012.052427.

- [255] J. Haubrock, „Parametrierung elektrischer Äquivalentschaltbilder von PEM Brennstoffzellen [Parameterization of electrical equivalent circuit diagrams of PEM fuel cells],“ Zugl.: Magdeburg, Univ., Fak. für Elektrotechnik und Informationstechnik, Diss., 2007, Faculty of Electrical Engineering and Information Technology, Otto-von-Guericke-University, Magdeburg, 2008. Available: <http://journals.ub.uni-magdeburg.de/ubjournals/index.php/MAFO/issue/view/69>.
- [256] W. Schmid et al., „A Longitudinal Simulation Model for a Fuel Cell Hybrid Vehicle: Experimental Parameterization and Validation with a Production Car,“ in *2019 Fourteenth International Conference on Ecological Vehicles and Renewable Energies (EVER)*, Monte-Carlo, Monaco, 2019, pp. 1–13, ISBN: 978-1-7281-3703-2. DOI: 10.1109/EVER.2019.8813648.
- [257] R. Isermann, *Elektronisches Management motorischer Fahrzeugantriebe: Elektronik, Modellbildung, Regelung und Diagnose für Verbrennungsmotoren, Getriebe und Elektroantriebe [Electronic management of motor vehicle drives: Electronics, modeling, control and diagnostics for combustion engines, transmissions and electric drives]*, (ATZ / MTZ-Fachbuch), Wiesbaden, Vieweg+Teubner Verlag / GWV Fachverlage GmbH Wiesbaden, 2010, ISBN: 9783834893895. DOI: 10.1007/978-3-8348-9389-5. Available: <http://gbv.ebib.com/patron/FullRecord.aspx?p=749382>.
- [258] M. Tschochner, *Comparative assessment of vehicle powertrain concepts in the early development phase*, (Berichte aus der Fahrzeugtechnik), [1. Auflage], Aachen, Shaker Verlag, 2019, ISBN: 9783844064612.
- [259] S. Munshi, G. Garner, H. Theissl, F. Hofer and B. Raser, „Total Cost of Ownership (TCO) Analysis for Heavy Duty Hydrogen Fueled Powertrains,“ Vancouver, Canada and Graz, Austria, 2021. Available: https://wfsinc.com/file_library/files/wpt-wfsinc/20201225_Westport_AVL_Whitepaper_Hydrogen_HPDI_final.pdf.
- [260] A. Shen, „Auslegung und Simulation von Ladestrategien für batterieelektrische Oberleitungs-Lkws [Design and simulation of charging strategies for battery electric overhead line trucks],“ Semester project thesis, Institute of Automotive Technology, Technical University of Munich, Munich, Germany, 2020.
- [261] W. Baldauf, R. Blaschko, W. Behr, C. Heine and M. Kolbe, „Development of an actively controlled, acoustically optimised single arm pantograph,“ in *Proceedings of the World Congress of Railway Research WCRR 2001*, Cologne, Germany, 2001.
- [262] Z. Luo, X. Wei, M. G. S. Pearce and G. A. Covic, „Multiobjective Optimization of Inductive Power Transfer Double-D Pads for Electric Vehicles,“ *IEEE Transactions on Power Electronics*, vol. 36, no. 5, pp. 5135–5146, 2021, DOI: 10.1109/TPEL.2020.3029789.
- [263] H. Yu et al., „Dimensioning and Power Management of Hybrid Energy Storage Systems for Electric Vehicles With Multiple Optimization Criteria,“ *IEEE Transactions on Power Electronics*, vol. 36, no. 5, pp. 5545–5556, 2021, DOI: 10.1109/TPEL.2020.3030822.
- [264] S. F. Da Silva, J. J. Eckert, F. L. Silva, L. C. Silva and F. G. Dedini, „Multi-objective optimization design and control of plug-in hybrid electric vehicle powertrain for minimization of energy consumption, exhaust emissions and battery degradation,“ *Energy Conversion and Management*, vol. 234, p. 113909, 2021, DOI: 10.1016/j.enconman.2021.113909.
- [265] F. Ju, W. Zhuang, L. Wang and Z. Zhang, „Comparison of four-wheel-drive hybrid powertrain configurations,“ *Energy*, vol. 209, p. 118286, 2020, DOI: 10.1016/j.energy.2020.118286.

- [266] A. Pathak, S. Scheuermann, A. Ongel and M. Lienkamp, „Conceptual Design Optimization of Autonomous Electric Buses in Public Transportation,“ *World Electric Vehicle Journal*, vol. 12, no. 1, p. 30, 2021, DOI: 10.3390/wevj12010030.
- [267] R. J. Kruse et al., *Computational Intelligence: Eine methodische Einführung in Künstliche Neuronale Netze, Evolutionäre Algorithmen, Fuzzy-Systeme und Bayes-Netze*, (Studium), Wiesbaden, Vieweg + Teubner, 2012, ISBN: 978-3-8348-1275-9. DOI: 10.1007/978-3-8348-8299-8. Available: <http://dx.doi.org/10.1007/978-3-8348-8299-8>.
- [268] C. A. C. Coello, G. B. Lamont and D. A. van Veldhuizen, *Evolutionary algorithms for solving multi-objective problems*, (Genetic and evolutionary computation series), 2. ed., New York, NY, Springer, 2007, ISBN: 978-0-387-33254-3. DOI: 10.1007/978-0-387-36797-2.
- [269] K. Deb, S. Agrawal, A. Pratap and T. Meyarivan, „A Fast Elitist Non-dominated Sorting Genetic Algorithm for Multi-objective Optimization: NSGA-II,“ in *Parallel Problem Solving from Nature PPSN VI: 6th International Conference Paris, France, September 18-20, 2000 Proceedings* (Lecture Notes in Computer Science). vol. 1917, M. Schoenauer et al., ed. Berlin and Heidelberg: Springer, 2000, pp. 849–858, ISBN: 978-3-540-41056-0. DOI: 10.1007/3-540-45356-3_83.
- [270] K. Deb, „Multi-objective Optimisation Using Evolutionary Algorithms: An Introduction,“ in *Multi-objective Evolutionary Optimisation for Product Design and Manufacturing*. vol. 18, L. Wang, A. H. C. Ng and K. Deb, ed. London: Springer-Verlag London Limited, 2011, pp. 3–34, ISBN: 978-0-85729-617-7. DOI: 10.1007/978-0-85729-652-8_1.
- [271] B. P. Miller, „Automotive Lithium-Ion Batteries,“ *Johnson Matthey Technology Review*, vol. 59, no. 1, pp. 4–13, 2015, DOI: 10.1595/205651315X685445.
- [272] T. Goel and N. Stander, „A non-dominance-based online stopping criterion for multi-objective evolutionary algorithms,“ *International Journal for Numerical Methods in Engineering*, vol. 84, no. 6, pp. 661–684, 2010, DOI: 10.1002/nme.2909.
- [273] C. Y. Suen, P. D. Grogono, R. Shinghal and F. Coallier, „Verifying, validating, and measuring the performance of expert systems,“ *Expert Systems with Applications*, vol. 1, no. 2, pp. 93–102, 1990, DOI: 10.1016/0957-4174(90)90019-Q.
- [274] R. S. Sojda, „Empirical evaluation of decision support systems: Needs, definitions, potential methods, and an example pertaining to waterfowl management,“ *Environmental Modelling & Software*, vol. 22, no. 2, pp. 269–277, 2007, DOI: 10.1016/j.envsoft.2005.07.023.
- [275] B. Danquah, S. Riedmaier, J. Rühm, S. Kalt and M. Lienkamp, „Statistical Model Verification and Validation Concept in Automotive Vehicle Design,“ *Procedia CIRP*, vol. 91, pp. 261–270, 2020, DOI: 10.1016/j.procir.2020.02.175.
- [276] M. Wentker, M. Greenwood and J. Leker, „A Bottom-Up Approach to Lithium-Ion Battery Cost Modeling with a Focus on Cathode Active Materials,“ *Energies*, vol. 12, no. 3, p. 504, 2019, DOI: 10.3390/en12030504.
- [277] Agora Verkehrswende, „Klimaschutz 2030 im Verkehr: Maßnahmen zur Erreichung des Sektorziels [Climate Protection 2030 in Transport: Measures to Achieve the Sector Target],“ Berlin, Germany, 2018. Available: https://www.agora-verkehrswende.de/fileadmin/Projekte/2017/Klimaschutzszenarien/Agora_Verkehrswende_Klimaschutz_im_Verkehr_Massnahmen_zur_Erreichung_des_Sektorziels_2030.pdf [visited on 12/14/2021].
- [278] A. Ciroth and H. Becker, „Validation – The Missing Link in Life Cycle Assessment. Towards pragmatic LCAs,“ *The International Journal of Life Cycle Assessment*, vol. 11, no. 5, pp. 295–297, 2006, DOI: 10.1065/lca2006.09.271.

- [279] European Commission DG Energy, *EU energy in figures: Statistical pocketbook 2019*, Luxembourg, Publications Office of the European Union, 2019, ISBN: 978-92-76-08818-9.
- [280] M. Ram et al., „Global Energy System based on 100% Renewable Energy – Power, Heat, Transport and Desalination Sectors,“ Lappeenranta, Finland and Berlin, Germany, 2017.
- [281] J. Reinhard, G. Wernet, R. Zah, R. Heijungs and L. M. Hilty, „Contribution-based prioritization of LCI database improvements: the most important unit processes inecoinvent,“ *The International Journal of Life Cycle Assessment*, vol. 24, no. 10, pp. 1778–1792, 2019, DOI: 10.1007/s11367-019-01602-0.
- [282] B. Danquah, S. Riedmaier and M. Lienkamp, „Potential of statistical model verification, validation and uncertainty quantification in automotive vehicle dynamics simulations: a review,“ *Vehicle System Dynamics*, pp. 1–30, 2020, DOI: 10.1080/00423114.2020.1854317.
- [283] T. J. Sullivan, *Introduction to Uncertainty Quantification*, (Texts in Applied Mathematics). vol. 63, Cham et al., Springer, 2015, ISBN: 9783319233956. DOI: 10.1007/978-3-319-23395-6.
- [284] K. Marti, Y. Ermoliev, M. Makowski and G. Pflug, *Coping with Uncertainty: Modeling and Policy Issues*, (Lecture Notes in Economics and Mathematical Systems). vol. 581, Berlin, Heidelberg, Springer-Verlag Berlin Heidelberg, 2006, ISBN: 9783540352624. DOI: 10.1007/3-540-35262-7.
- [285] J. C. Helton, J. D. Johnson, W. L. Oberkampf and C. J. Sallaberry, „Representation of analysis results involving aleatory and epistemic uncertainty,“ *International Journal of General Systems*, vol. 39, no. 6, pp. 605–646, 2010, DOI: 10.1080/03081079.2010.486664.
- [286] M. Seidenfus, „Unsicherheitsquantifizierung der ökonomischen und ökologischen Modellierung alternativer Antriebskonzepte für schwere Nutzfahrzeuge [Uncertainty Quantification of the Economic and Ecological Modeling of Alternative Powertrain-Concepts for Heavy-Duty Vehicles],“ Masterthesis, Institute of Automotive Technology, Technical University of Munich, Munich, Germany, 2021.
- [287] C. J. Roy and W. L. Oberkampf, „A comprehensive framework for verification, validation, and uncertainty quantification in scientific computing,“ *Computer Methods in Applied Mechanics and Engineering*, vol. 200, no. 25-28, pp. 2131–2144, 2011, DOI: 10.1016/j.cma.2011.03.016.
- [288] S. Sankararaman and S. Mahadevan, „Integration of model verification, validation, and calibration for uncertainty quantification in engineering systems,“ *Reliability Engineering & System Safety*, vol. 138, pp. 194–209, 2015, DOI: 10.1016/j.ress.2015.01.023.
- [289] B. Danquah, S. Riedmaier, Y. Meral and M. Lienkamp, „Statistical Validation Framework for Automotive Vehicle Simulations Using Uncertainty Learning,“ *Applied Sciences*, vol. 11, no. 5, p. 1983, 2021, DOI: 10.3390/app11051983.
- [290] S. Riedmaier, B. Danquah, B. Schick and F. Diermeyer, „Unified Framework and Survey for Model Verification, Validation and Uncertainty Quantification,“ *Archives of Computational Methods in Engineering*, 2020, DOI: 10.1007/s11831-020-09473-7.
- [291] B. Danquah et al., „VVUQ Framework,“ Technical University of Munich, Munich, Germany, 2021, DOI: 10.13140/RG.2.2.12259.48168. Available: <https://github.com/TUMFTM/VVUQ-Framework>.
- [292] D. Wolff and A. Duffy, „Development and demonstration of an uncertainty management methodology for life cycle assessment in a tiered-hybrid case study of an Irish apartment development,“ *The International Journal of Life Cycle Assessment*, 2021, DOI: 10.1007/s11367-021-01872-7.

- [293] M. A. Sabará, „Uncertainties in Life Cycle Inventories: Monte Carlo and Fuzzy Sets Treatments,“ in *Proceedings of the 5th International Symposium on Uncertainty Quantification and Stochastic Modelling* (Lecture Notes in Mechanical Engineering), Cursi and Castro, ed. [S.I.]: Springer International Publishing, 2021, pp. 177–197, ISBN: 978-3-030-53668-8. DOI: 10.1007/978-3-030-53669-5_14.
- [294] C.-Y. Baek, K.-H. Park, K. Tahara and Y.-Y. Chun, „Data Quality Assessment of the Uncertainty Analysis Applied to the Greenhouse Gas Emissions of a Dairy Cow System,“ *Sustainability*, vol. 9, no. 10, p. 1676, 2017, DOI: 10.3390/su9101676.
- [295] S. A. Ross and L. Cheah, „Uncertainty Quantification in Life Cycle Assessments: Exploring Distribution Choice and Greater Data Granularity to Characterize Product Use,“ *Journal of Industrial Ecology*, vol. 23, no. 2, pp. 335–346, 2019, DOI: 10.1111/jiec.12742.
- [296] A. Candar, „Life Cycle Sustainability Assessment von Traktionsbatterien für Automobile Anwendungen [Life Cycle Sustainability Assessment of Traction Batteries for Automotive Applications],“ Semester project thesis, Institute of Automotive Technology, Technical University of Munich, Munich, Germany, 2021.
- [297] H. André and M. Ljunggren, „Short and long-term mineral resource scarcity impacts for a car manufacturer: The case of electric traction motors,“ *Journal of Cleaner Production*, vol. 361, p. 132140, 2022, DOI: 10.1016/j.jclepro.2022.132140. Available: <https://www.sciencedirect.com/science/article/pii/S0959652622017462>.
- [298] P. Slowik, N. Lutsey and C.-W. Hsu, „How technology, recycling, and policy can mitigate supply risks to the long-term transition to zero-emission vehicles,“ 2020, DOI: 10.13140/RG.2.2.30613.35041.
- [299] A. Barré, „Heavy-Duty Vehicle Decarbonization–A Stakeholder Analysis,“ Semester project thesis, Institute of Automotive Technology, Technical University of Munich, Munich, Germany, 2021.
- [300] B. Heid, R. Hensley, S. Knupfer and A. Tschiesner, „What’s sparking electric-vehicle adoption in the truck industry?,“ *McKinsey & Company*, 2017. Available: <https://www.mckinsey.com/industries/automotive-and-assembly/our-insights/whats-sparking-electric-vehicle-adoption-in-the-truck-industry> [visited on 05/02/2022].
- [301] R. Mihelic, M. Roeth, K. Otto and J. Lund, „Viable Class 7/8 Electric, Hybrid and Alternative Fuel Tractors,“ 2019, DOI: 10.13140/RG.2.2.33200.92160.
- [302] M. Altenburg, N. R. Anand, S. H. Balm and W. van Ploos Amstel, „Electric freight vehicles in city logistics: insights into decision making process of frontrunner companies,“ in *European Battery, Hybrid and Fuel Cell Electric Vehicle Congress*, Geneva, Switzerland, 2017. Available: https://www.researchgate.net/publication/317101896_Electric_freight_vehicles_in_city_logistics_Insights_into_decision-making_process_of_frontrunner_companies.
- [303] F. Kleiner et al., „Current status of the electrification of transport logistic vehicles - Early niche markets and commercialization opportunities,“ in *European Battery, Hybrid and Fuel Cell Electric Vehicle Congress*, Geneva, Switzerland, 2017. Available: <https://elib.dlr.de/111577/>.
- [304] B. Anderhofstadt, „The transition of road transport toward autonomous and alternative fuel-powered heavy-duty trucks in Germany,“ Dissertation, WHU - Otto Beisheim School of Management, 2020. Available: <https://opus4.kobv.de/opus4-whu/frontdoor/index/index/year/2020/docId/825>.

- [305] I. Lai, Y. Liu, X. Sun, H. Zhang and W. Xu, „Factors Influencing the Behavioural Intention towards Full Electric Vehicles: An Empirical Study in Macau,“ *Sustainability*, vol. 7, no. 9, pp. 12564–12585, 2015, DOI: 10.3390/su70912564.
- [306] K. Zhang et al., „Modeling Acceptance of Electric Vehicle Sharing Based on Theory of Planned Behavior,“ *Sustainability*, vol. 10, no. 12, p. 4686, 2018, DOI: 10.3390/su10124686.
- [307] E. Higuera-Castillo, S. Molinillo, J. A. Coca-Stefaniak and F. Liébana-Cabanillas, „Perceived Value and Customer Adoption of Electric and Hybrid Vehicles,“ *Sustainability*, vol. 11, no. 18, p. 4956, 2019, DOI: 10.3390/su11184956.
- [308] G. Lozzi, „Specification of city & PT stakeholders strategies and needs: Deliverable 2.1 - Fast and Smart Charging Solutions for Full Size Urban Heavy Duty Applications (ASSURED),“ Brussels, 2018. Available: https://assured-project.eu/storage/files/d21-specification-of-city-pt-stakeholders-strategies-and-needs_1.pdf [visited on 05/02/2022].
- [309] L. Mathieu, „Recharge EU: How many charging points will Europa and its Member States need in the 2020s,“ Transport and Environment, Brussels, Belgium, 2020. Available: <https://www.transportenvironment.org/wp-content/uploads/2021/07/01%202020%20Draft%20TE%20Infrastructure%20Report%20Final.pdf> [visited on 05/02/2022].
- [310] Association des Constructeurs Européens d’Automobiles, „Position Paper: Heavy-duty vehicles: Charging and refuelling infrastructure,“ Brussels, Belgium, 2021. Available: https://www.acea.auto/files/ACEA_Position_Paper-Heavy-duty_vehicles-Charging_and_refuelling_infrastructure.pdf [visited on 05/02/2022].
- [311] B. Nykvist and O. Olsson, „The feasibility of heavy battery electric trucks,“ *Joule*, vol. 5, no. 4, pp. 901–913, 2021, DOI: 10.1016/j.joule.2021.03.007.
- [312] J. Schneider, O. Teichert, M. Zähringer and M. Lienkamp, „How low can we go? // Minimizing battery size of battery-electric long-haul trucks,“ in *Advanced Automotive Battery Conference (AABC)*, Mainz, Germany, 2022, DOI: 10.13140/RG.2.2.31302.96327.
- [313] M. Zähringer, S. Wolff, J. Schneider, G. Balke and M. Lienkamp, „Time vs. Capacity—The Potential of Optimal Charging Stop Strategies for Battery Electric Trucks,“ *Energies*, vol. 15, no. 19, p. 7137, 2022, DOI: 10.3390/en15197137.
- [314] O. Teichert, S. Link, J. Schneider, S. Wolff and M. Lienkamp, „Techno-economic cell selection for battery-electric long-haul trucks,“ *eTransportation*, p. 100225, 2022, DOI: <https://doi.org/10.1016/j.etrans.2022.100225>. Available: <https://www.sciencedirect.com/science/article/pii/S2590116822000704>.
- [315] F. Duffner et al., „Post-lithium-ion battery cell production and its compatibility with lithium-ion cell production infrastructure,“ *Nature Energy*, vol. 6, no. 2, pp. 123–134, 2021, DOI: 10.1038/s41560-020-00748-8.

List of Pre-publications

During the writing of this dissertation, publications and student research projects were published, in which partial aspects of this work are presented.

Journals; Scopus/Web of Science listed (peer-reviewed)

- [7] S. Wolff, M. Brönnner, M. Held and M. Lienkamp, „Transforming automotive companies into sustainability leaders: A concept for managing current challenges,“ *Journal of Cleaner Production*, vol. 276, p. 124179, 2020, DOI: 10.1016/j.jclepro.2020.124179.
- [55] S. Wolff, M. Fries and M. Lienkamp, „Technoecological analysis of energy carriers for long-haul transportation,“ *Journal of Industrial Ecology*, vol. 49, no. 11, p. 6402, 2019, DOI: 10.1111/jiec.12937.
- [56] S. Wolff, M. Seidenfus, M. Brönnner and M. Lienkamp, „Multi-disciplinary design optimization of life cycle eco-efficiency for heavy-duty vehicles using a genetic algorithm,“ *Journal of Cleaner Production*, vol. 318, p. 128505, 2021, DOI: 10.1016/j.jclepro.2021.128505.
- [100] S. Wolff, M. Seidenfus, K. Gordon, S. Álvarez, S. Kalt and M. Lienkamp, „Scalable Life-Cycle Inventory for Heavy-Duty Vehicle Production,“ *Sustainability*, vol. 12, no. 13, p. 5396, 2020, DOI: 10.3390/su12135396.
- [138] S. Wolff, S. Kalt, M. Bstieler and M. Lienkamp, „Influence of Powertrain Topology and Electric Machine Design on Efficiency of Battery Electric Trucks—A Simulative Case-Study,“ *Energies*, vol. 14, no. 2, p. 328, 2021, DOI: 10.3390/en14020328.
- [196] A. König, L. Nicoletti, D. Schröder, S. Wolff, A. Waclaw and M. Lienkamp, „An Overview of Parameter and Cost for Battery Electric Vehicles,“ *World Electric Vehicle Journal*, vol. 12, no. 1, p. 21, 2021, DOI: 10.3390/wevj12010021.
- [313] M. Zähringer, S. Wolff, J. Schneider, G. Balke and M. Lienkamp, „Time vs. Capacity—The Potential of Optimal Charging Stop Strategies for Battery Electric Trucks,“ *Energies*, vol. 15, no. 19, p. 7137, 2022, DOI: 10.3390/en15197137.
- [314] O. Teichert, S. Link, J. Schneider, S. Wolff and M. Lienkamp, „Techno-economic cell selection for battery-electric long-haul trucks,“ *eTransportation*, p. 100225, 2022, DOI: <https://doi.org/10.1016/j.etrans.2022.100225>. Available: <https://www.sciencedirect.com/science/article/pii/S2590116822000704>.

Conferences, Periodicals; Scopus/Web of Science listed (peer-reviewed)

- [35] L. Nicoletti, M. Bronner, B. Danquah, A. Koch, A. König, S. Krapf, A. Pathak, F. Schockenhoff, G. Sethuraman, S. Wolff and M. Lienkamp, „Review of Trends and Potentials in the Vehicle Concept Development Process,“ in *2020 Fifteenth International Conference on Ecological Vehicles and Renewable Energies (EVER)*, Monte-Carlo, Monaco, 2020, pp. 1–15, ISBN: 978-1-7281-5641-5. DOI: 10.1109/EVER48776.2020.9243115.
- [54] M. Fries, S. Wolff, L. Horlbeck, M. Kerler, M. Lienkamp, A. Burke and L. Fulton, „Optimization of hybrid electric drive system components in long-haul vehicles for the evaluation of customer requirements,“ in *2017 IEEE 12th International Conference on Power Electronics and Drive Systems (IEEE PEDS 2017): Hawaii Convention Center, Honolulu, Hawaii, USA, 12-15 December 2017*, Honolulu, HI, 2017, pp. 1, 141–1, 146, ISBN: 978-1-5090-2364-6. DOI: 10.1109/PEDS.2017.8289236.
- [234] C. Mährle, S. Wolff, S. Held and G. Wachtmeister, „Influence of the Cooling System and Road Topology on Heavy Duty Truck Platooning,“ in *The 2019 IEEE Intelligent Transportation Systems Conference - ITSC: Auckland, New Zealand, 27-30 October 2019*, Auckland, New Zealand, 2019, pp. 1251–1256, ISBN: 978-1-5386-7024-8. DOI: 10.1109/ITSC.2019.8917050.

Journals, Conferences, Periodicals, Reports, Conference Proceedings and Poster, etc.; not Scopus/Web of Science listed

- [31] M. Lienkamp, W. Schmid, S. Wolff, M. Hessel and F. Homm, *Status Elektromobilität: Das Endspiel nach der Corona Krise*, Munich, Germany, 2020. Available: https://www.researchgate.net/publication/341670568_Status_Elektromobilitat_2020_Das_Endspiel_nach_der_Corona-Krise [visited on 05/28/2020].
- [33] S. Wolff, M. Lienkamp and K.-V. Schaller, *Status Nutzfahrzeuge 2020: Alles auf eine Karte? [Status Commercial Vehicles 2020: All on One Card?]*, Munich, Germany, 2021. Available: https://www.researchgate.net/publication/350580546_STATUS_NUTZFAHRZEUGE_2020_ALLES_AUF_EINE_KARTE [visited on 05/28/2020].

Non-thesis-relevant publications; Scopus/Web of Science listed (peer-reviewed)

S. Wolff, J. Auernhammer, F. Schockenhoff, C. Angerer and M. Wittmann, „MOBILITY BOX: A DESIGN RESEARCH METHODOLOGY TO EXAMINE PEOPLE’S NEEDS IN RELATION TO AUTONOMOUS VEHICLE DESIGNS AND MOBILITY BUSINESS MODEL,“ *Proceedings of the Design Society: DESIGN Conference*, vol. 1, pp. 1185–1194, 2020, DOI: 10.1017/dsd.2020.285.

M. Brönnner, S. Wolff, J. Jovanovic, K. Keuthen and M. Lienkamp, „Production Strategy Development: Simulation of Dependencies Using Recurrent Fuzzy Systems,“ *Systems*, vol. 8, no. 1, p. 1, 2020, DOI: 10.3390/systems8010001.

S. Kalt, S. Wolff and M. Lienkamp, „Impact of Electric Machine Design Parameters and Loss Types on Driving Cycle Efficiency,“ in *2019 8th International Conference on Power Science and Engineering (ICPSE)*, Dublin, Ireland, 2019, pp. 6–12, ISBN: 978-1-7281-6081-8. DOI: 10.1109/ICPSE49633.2019.9041132.

M. Lienkamp, M. Brönner and S. Wolff, „Coronakrise - Was Ingenieure und Virologen gemeinsam haben,“ in *Wissenschaft, Vernunft & Nachhaltigkeit: Denkanstösse für die Zeit nach Corona* (TUM Forum sustainability), M. Molls, J. Eberspächer, H. Auernhammer, G. Färber, B. Herbst-Gaebel, U. Lindemann, K. Mainzer, W. Petry, R. Reichwald, J. Scheurle, J. L. van Hemmen and P. A. Wilderer, ed. Munich, Germany: Technical University of Munich, 2020, pp. 160–161, ISBN: 9783000659669.

M. Lienkamp, M. Brönner and S. Wolff, „Corona Crisis - What Engineers and Virologists Have in Common,“ in *Science, Reason & Responsibility: Forward Thinking for the Post-Corona Era* (TUM Insights), M. Molls, J. Eberspächer and a. et al, ed. Munich, Germany: TUM.University Press, 2021, pp. 158–159, ISBN: 9783958840553.

Thesis-relevant open-source software

- [116] S. Wolff. „LOTUS - Long-Haul Truck Simulation: Longitudinal Dynamic Simulation for Heavy Duty Vehicles,“ [Online]. Available: <https://github.com/TUMFTM/LOTUS>.

Supervised Student's Thesis

The following student research projects were developed within the framework of the dissertation under the author's supervision in terms of content, subject matter, and scientific research, as well as under his author's authoritative guidance. In the following, the bachelor, semester, and master theses related to this dissertation are listed. Many thanks to the authors for their extensive support within the scope of this research project.

References

- [117] B. Mustafić, „Technische und politische Rahmenbedingungen für den wirtschaftlichen Einsatz von elektrischen schweren Nutzfahrzeugen [Technical and political framework conditions for the economic use of electric heavy commercial vehicles],“ Master's thesis, Institute of Automotive Technology, Technical University of Munich, Munich, Germany, 2020.
- [120] M. Bstieler, „Packageanalyse zur Bewertung von Zero-Emission Technologien für schwere Nutzfahrzeugkonzepte [Package-Analysis for the Evaluation of Zero-Emission Technologies for Heavy-Duty Vehicle Concepts],“ Semester project thesis, Institute of Automotive Technology, Technical University of Munich, Munich, Germany, 2021.
- [175] N. Eidkum, „Simulation und Analyse von Wasserstoffverbrennungsmotoren als Zero-Emission Technologie für Nutzfahrzeuge [Simulation and Analysis of Hydrogen Combustion Engines as Zero-Emission Technology for Heavy-Duty Vehicles],“ Bachelor's thesis, Institute of Automotive Technology, Technical University of Munich, Munich, Germany, 2021.
- [215] P. Mauk, „Lebenszyklusanalyse eines wasserstoffbetrieben schweren Nutzfahrzeugs im Fernverkehr [Life Cycle Assessment of a Fuel Cell Powered Heavy-Duty Truck],“ Bachelor's thesis, Institute of Automotive Technology, Technical University of Munich, Munich, Germany, 2020.
- [218] K. Gordon, „Comparative Environmental Life Cycle Assessment of Conventional and Alternative Heavy-Duty Truck Drivetrains,“ Master's thesis, Institute of Automotive Technology, Technical University of Munich, Munich, Germany, 2019.
- [219] S. Alvarez, „Comparative Environmental Life Cycle Assessment of Heavy-Duty Trucks in Different Geographical Locations,“ Master's thesis, Institute of Automotive Technology, Technical University of Munich, Munich, Germany, 2019.
- [224] M. Seidenfus, „Ökoeffizienz von alternativen Antrieben für den schweren Güterverkehr [Eco-Efficiency of Alternative Drive Trains for Heavy Duty Vehicles in the Transport Sector],“ Semester project thesis, Institute of Automotive Technology, Technical University of Munich, Munich, Germany, 2020.

- [245] C. Pan, „Modeling and Simulation of Real-Driving, Non-CO₂ Emissions for Heavy-Duty Trucks,“ Semester project thesis, Institute of Automotive Technology, Technical University of Munich, Munich, Germany, 2020.
- [252] S. Weiß, „Modellierung einer Brennstoffzelle für Fernverkehrs Lkw [Modeling a PEM Fuel-Cell for Long-Distance Trucks],“ Semester project thesis, Institute of Automotive Technology, Technical University of Munich, Munich, Germany, 2019.
- [260] A. Shen, „Auslegung und Simulation von Ladestrategien für batterieelektrische Oberleitungs-Lkws [Design and simulation of charging strategies for battery electric overhead line trucks],“ Semester project thesis, Institute of Automotive Technology, Technical University of Munich, Munich, Germany, 2020.
- [286] M. Seidenfus, „Unsicherheitsquantifizierung der ökonomischen und ökologischen Modellierung alternativer Antriebskonzepte für schwere Nutzfahrzeuge [Uncertainty Quantification of the Economic and Ecological Modeling of Alternative Powertrain-Concepts for Heavy-Duty Vehicles],“ Masterthesis, Institute of Automotive Technology, Technical University of Munich, Munich, Germany, 2021.
- [296] A. Candar, „Life Cycle Sustainability Assessment von Traktionsbatterien für Automobile Anwendungen [Life Cycle Sustainability Assessment of Traction Batteries for Automotive Applications],“ Semester project thesis, Institute of Automotive Technology, Technical University of Munich, Munich, Germany, 2021.
- [299] A. Barré, „Heavy-Duty Vehicle Decarbonization-A Stakeholder Analysis,“ Semester project thesis, Institute of Automotive Technology, Technical University of Munich, Munich, Germany, 2021.

Appendix

A	EU Vehicle Concepts	xxxix
B	BEV Topologies	xl
C	Hydrogen Combustion Properties and Processes	xli
D	Average Vehicle Fleet Derivation	xliv
E	Material Mix Vehicle Design Parameters	xlvi
F	Fuel Cell Parameter Derivation	xlviii
G	Convergence Studies	I
H	Uncertainty Quantification	lii
I	Infrastructure Cost Sensitivity	lvi
J	Stakeholder Analysis	lvii
	J.1 Survey	lvii
	J.2 Confirmatory Factor Analysis	lix

A EU Vehicle Concepts

Table A.1 summarizes the vehicle concepts according to the current EU legislation. The EU categorizes heavy-duty vehicles by the number of axles, the cab type and their engine power.

Table A.1: The regulation 2019/1241 defines the vehicle concepts, respectively subgroups, subject CO₂ targets for heavy-duty vehicles. [Note: urban delivery (UD); regional delivery (RD); long-haul (LH)]

Heavy-Duty Vehicles	Cab Type	Engine Power	Vehicle Sub-Group
4x2 rigid lorries, GCW > 16 t	All	< 170 kW	4-UD
	Day cab	≥170 kW	4-RD
	Sleeper cab	≥170 kW and < 265 kW	4-LH
	Sleeper cab	≥265 kW	4-LH
6x2 rigid lorries	Day cab	All	9-RD
	Sleeper cab		9-LH
4x2 tractors, GCW > 16 t	Day cab	All	5-RD
	Sleeper cab	< 265 kW	5-LH
	Sleeper cab	≥265 kW	5-LH
6x2 tractors	Day cab	All	10-RD
	Sleeper cab		10-LH

B BEV Topologies

Figure B.1 shows the six drivetrain topologies for BET, which were examined in a preliminary publication [138]. The topologies can be categorized by the number and position of the electric machine, as well as the number of (shiftable) gears. The number of gears influences the size of the transmission, which is not shown for reasons of clarity.

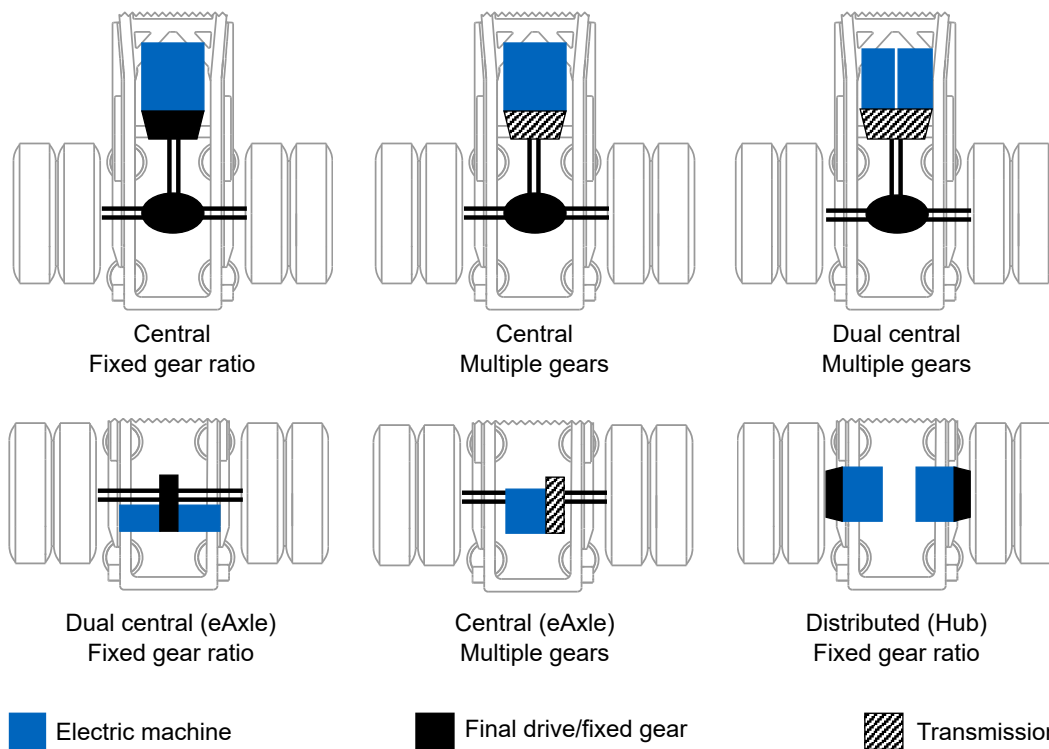


Figure B.1: Depending on the number and position of the electric machine(s), and the number of shiftable gears, there are six BET drivetrain topologies. The topologies are based on a preliminary publication [138].

C Hydrogen Combustion Properties and Processes

Table C.1 summarizes the relevant properties for a hydrogen internal combustion engine. Additionally, Figure C.1 - C.5 show the hydrogen combustion processes, analyzed by Eidkum [175].

Table C.1: General and combustion specific properties of hydrogen and hydrogen-air-mixtures [155, p. 54f]. While the ignition limits describe the general flammability of hydrogen, the narrower detonation limits represent the application for combustion engines with sufficient flame speeds [155, p. 277].

Property	Value	Unit
Fluid at 1.013 25 bar and 20.271 K		
Density	70.828	g/L
Volumetric calorific value	2.333	kW h/L
Gaseous at 1.013 25 bar and 273.15 K		
Density	0.898 82	g/L
Volumetric calorific value	2.9918	W h/L
Gravimetric calorific value	33.286	kW h/kg
Hydrogen-air-mixtures		
Lower ignition limit	4 ($\lambda = 10.1$)	vol %H ₂
Lower detonation limit	18 ($\lambda = 1.9$)	vol %H ₂
Stoichiometric	29.6 ($\lambda = 1$)	vol %H ₂
Upper detonation limit	58.9 ($\lambda = 0.29$)	vol %H ₂
Upper ignition limit	75.6 ($\lambda = 0.13$)	vol %H ₂
Ignition temperature	585	°C
Minimal ignition energy	0.017	mJ
Maximum laminar flame speed	3	m/s

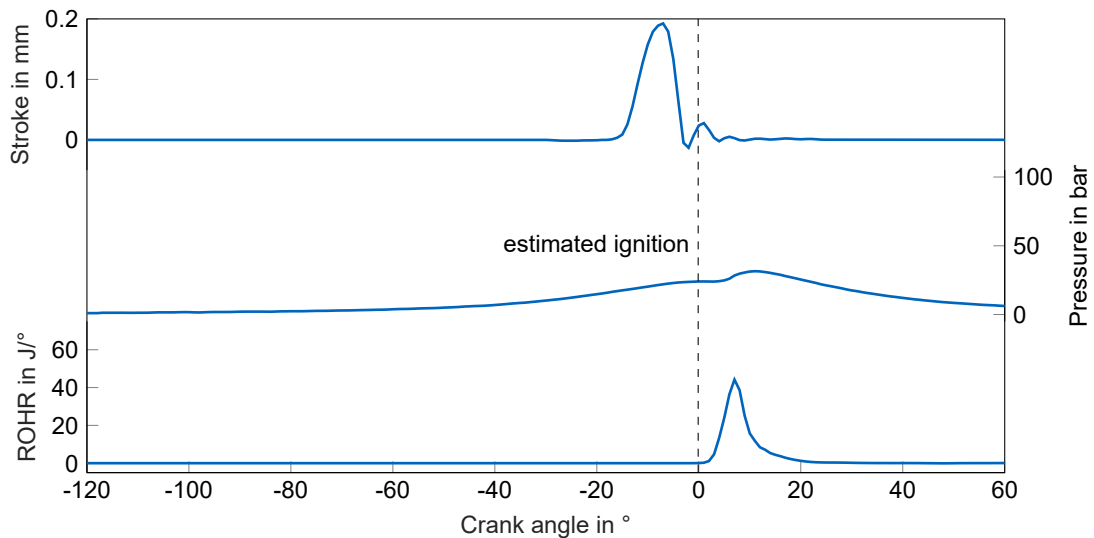


Figure C.1: Operating point of a hydrogen engine with late direct injection and spark plug ignition at 2000 rpm at part load [175].

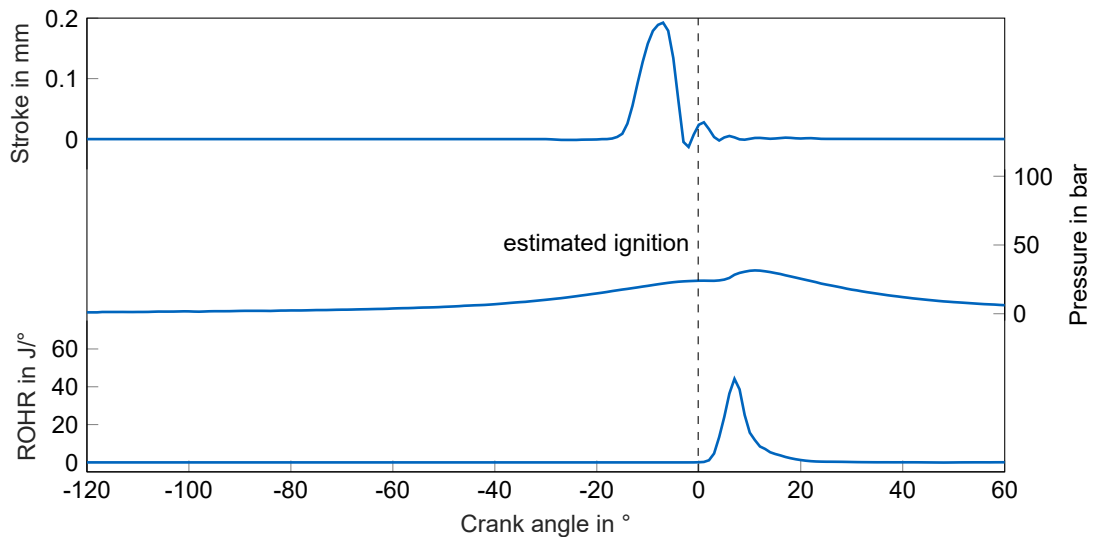


Figure C.2: Operating point of a hydrogen engine with direct injection and compression ignition at 2000 rpm at part load [175].

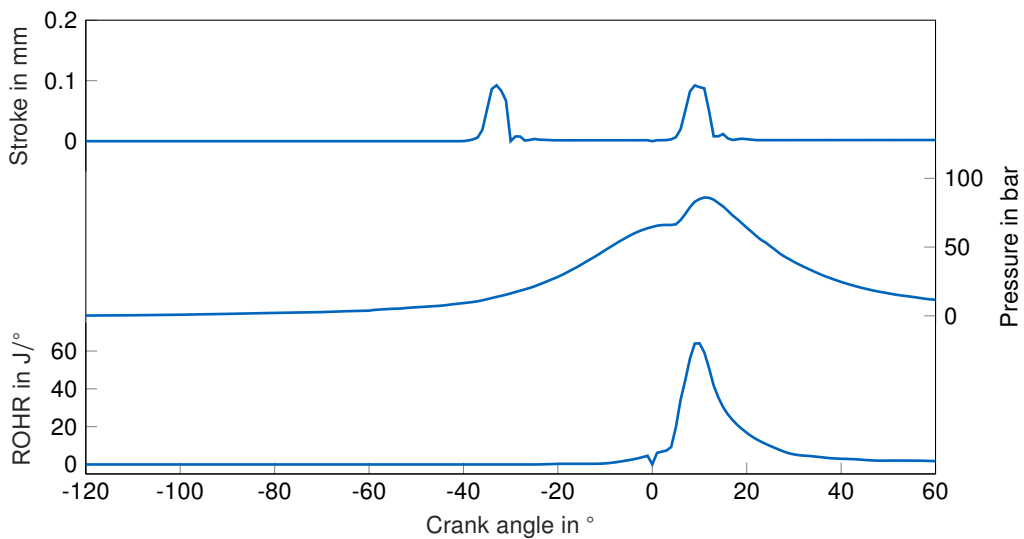


Figure C.3: Operating point of a hydrogen engine with dual direct injection and compression ignition at 2000 rpm in partial load [175].

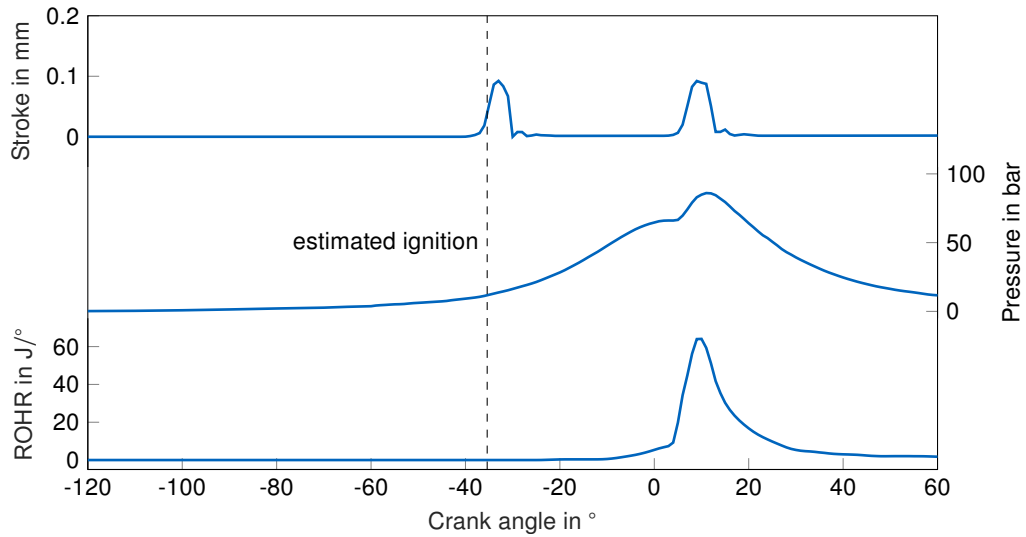


Figure C.4: Operating point of a hydrogen engine with dual direct injection, spark ignition, and compression ignition at 2000 rpm at part load [175].

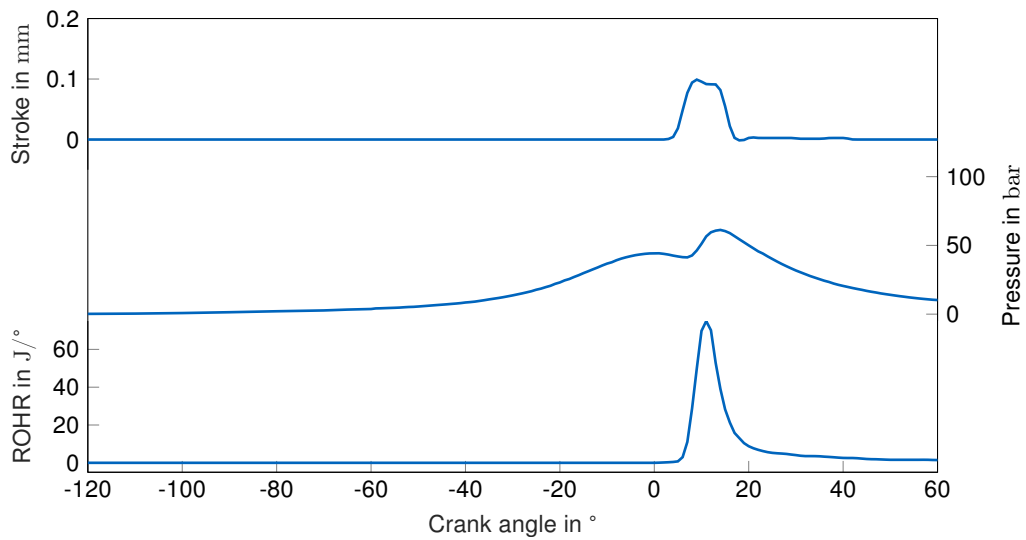


Figure C.5: Operating point of a hydrogen engine with direct injection and glow plug at 2000 rpm at part load [175].

D Average Vehicle Fleet Derivation

Table D.1 shows the 2019 heavy-duty sales data of six major European truck OEMs. Based on this data, Mustafić [117] derived an average vehicle fleet in order to estimate the penalties that arise with the new EU regulation.

Table D.1: Based on the vehicle sales for six major European truck OEMs, Mustafić [117] derived an average vehicle heavy-duty fleet to estimate the penalties due to the EU legislation. Semi tractors and chassis with a 4x2 and 6x2 configuration were considered.

OEM	Number	Tractor			Chassis		
		Total Tractor	4x2	6x2	Total Chassis	4x2	6x2
DAF	34 740	22 029	20 786	1242	10 868	3469	7399
Daimler	63 767	40 435	38 154	2281	19 949	6368	13 581
Iveco	35 041	22 220	20 966	1253	10 962	3499	7463
MAN	46 366	29 401	27 742	1658	14 050	4630	9875
Scania	37 867	24 012	22 657	1354	11 847	3781	8065
Volvo	41 653	25 412	24 922	1490	13 031	4159	8871
Renault	24 169	15 326	14 461	864	7561	2414	5148
Average	40 515	25 548	24 241	1449	12 610	4046	8629

To obtain data for new vehicle registration, several assumptions were made. First, the average, annually registered heavy-duty vehicles are calculated. In 2019, new 66 428 new heavy-duty vehicles were registered. Under an assumed market decline of 2.5 %/a until 2030 (11 years), Equation (D.1) yields the average registration:

$$\text{New Registrations} := n_{\text{new}} = \frac{66428 + 66428 \times (1 - 0.025)^{11}}{2} = 58354. \quad (\text{D.1})$$

Since current non-diesel vehicle registrations are near-zero, the vehicle stock in 2030 must consist entirely of vehicles newly registered in the next decade. Therefore, for each category (diesel, gas, hybrid, and zero-emission), the share of the 2030 vehicle stock must equal the average share of new registrations (Equation (D.2) and (D.3)).

$$\text{Total New Registrations} := n_{\text{new, total}} = n_{\text{years}} n_{\text{new}} = 11 \times 58354 = 641898. \quad (\text{D.2})$$

$$\text{Total Share of New Registrations} := p_{\text{new, cat., total}} = \frac{n_{\text{new, cat., total}}}{n_{\text{new, total}}}. \quad (\text{D.3})$$

Assuming that the vehicle registrations increase linearly per category, Equation (D.4) yields the annual share of new registrations:

$$\text{Annual Share of New Registrations} := p_{\text{new, cat.}} = \frac{p_{\text{new, cat.}}}{n_{\text{years}}}. \quad (\text{D.4})$$

With the annual share of new registrations per category, the data for each year can be calculated recursively according to Equation (D.5). This is based on the assumption that the share of new registrations per category doubles annually.

$$\text{Annual New Registrations} := n_{\text{new, cat., } i+1} = n_{\text{new, cat., } i} \cdot 2 p_{\text{new, cat.}} \quad (\text{D.5})$$

The period under consideration is known and extends from 2019 to 2030. The start value $n_{\text{new, cat., } i+1} = 0$ is assumed. Thus, for any given year n_{year} , the number of new registrations per category can also be calculated using Equation (D.6) together with Equation (D.2) - (D.4):

$$n_{\text{new, cat.}} = n_{\text{new}} \cdot 2 p_{\text{new, cat.}} \cdot (2019 - n_{\text{year}}). \quad (\text{D.6})$$

E Material Mix Vehicle Design Parameters

The design parameters are based on a previous publication [100]. From this publication, the concept PHEV and BEV1 are shown. The FCET design parameters are derived from the pre-published vehicle design optimization [56]. Analogously, the HICET parameters are the optimization results presented in this work. Table E.1 summarizes the parameters. Additionally, Figure E.1 shows the relative material mix. Each bar is relative to the respective total vehicle weight.

Table E.1: Powertrain design parameters for five different long haul vehicle concepts. The capacity indicates the gross capacity. Depths-of-discharge of 31% for HET, and 80% for both BET and FCET were assumed [54, 55, 237].

Configuration	Unit	ICE	HEV	BEV	FCEV	HICE
Internal Combustion Engine						
Maximum Power	kW	352	320	-	-	323
Maximum Torque	N m	2100	1900	-	-	801
Transmission						
No. Of Gears	-	12	10	1	1	8
Electric Machine						
Nominal Power	kW	-	94	774	2x469	-
Nominal Torque	N m	-	679	1720	2x1600	-
Battery						
Capacity	kWh	-	71.5	675	219	-

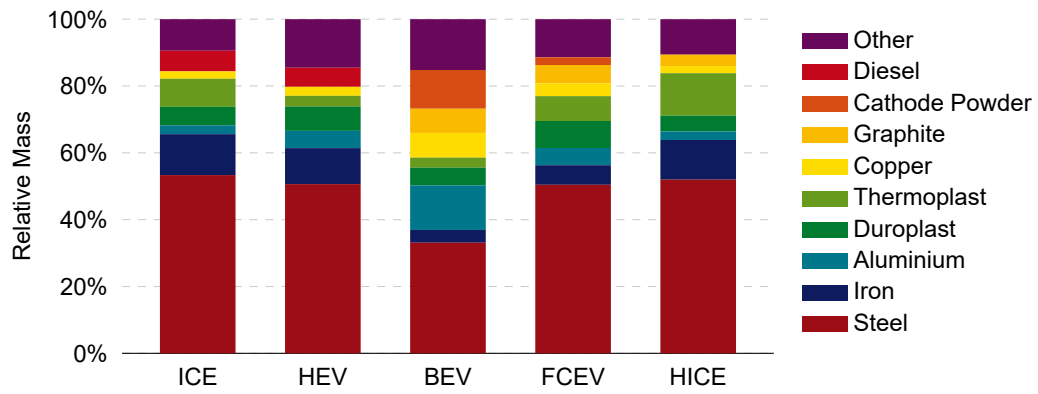


Figure E.1: The LCI analysis of the relative material masses shows decreases of steel and iron materials and an increase of battery related materials (NMC111 powder, graphite and aluminum) for the BEV concept. Only materials >5% are shown. Diesel is only present in ICET and PHET, while NMC111 powder and graphite are only relevant for BET and FCET, although in different quantities. [Note: NMC: nickel manganese cobalt]

F Fuel Cell Parameter Derivation

The nominal current is a key parameter of a fuel cell design. To ensure intuitive compatibility to the existing vehicle simulation model, the required voltage and consequently the fuel cell stack power are the input parameters of the fuel cell design model:

$$I_{\text{nom}} = \frac{P_{\text{nom}}}{U_{\text{nom}}}, \quad (\text{F.1})$$

where:

I_{nom} = Nominal stack current in A

P_{nom} = Nominal stack power in kWh

U_{nom} = Nominal stack voltage in V.

The area depends on the required, nominal current and the cell current density:

$$A = \frac{I_{\text{nom}}}{i_{\text{nom,cell}}}, \quad (\text{F.2})$$

where:

A = Cell surface area in cm^2

$i_{\text{nom,cell}}$ = Current density per cell, estimated at 0.175 A/cm^2 [255]

The number of cells depends on the electro-chemical reaction and thus the resulting voltages:

$$N = \frac{U_{\text{nom}}}{u_{\text{nom,cell}}} = \frac{zFU_{\text{nom}}}{\Delta H_{\text{m,LHV}}\eta_{\text{nom}}}, \quad (\text{F.3})$$

where:

$u_{\text{nom,cell}}$ = Nominal cell voltage in V

z = Number of moving electrons ($z = 2$)

F = Faraday constant (96 485 A s/mol)

$\Delta H_{\text{m,LHV}}$ = Lower heating value 241.83 MJ/mol

η_{nom} = Nominal stack efficiency (55 %) [253]

The Tafel slope as a simplification of the Butler-Volmers-equation

$$b_{\text{Tafel}} = \frac{RT}{z\alpha F}, \quad (\text{F.4})$$

where:

R = Ideal gas constant (8.3145 J/kmol)

T = Operating temperature (338 K) [253]

α = Charge transfer coefficient (0.264 02 at 338 K [253])

With the assumption that all cells are connected in serial, the internal resistance is:

$$R_{i,\text{stack}} = R_{i,\text{cell}}N, \quad (\text{F.5})$$

where

$R_{i,\text{cell}}$ = Internal cell resistance, estimated at 0.7378 m Ω [253].

The stack exchange current is:

$$i_0 = \frac{zFk(p_{\text{H}_2} + p_{\text{O}_2})\Delta v}{Rh} e^{\frac{-\Delta G}{RT}}, \quad (\text{F.6})$$

where:

k = Boltzmann constant ($1.380\,649 \times 10^{-23}$ J/K)

p_{H_2} = Absolute hydrogen supply pressure, estimated at 151 988 Pa [253]

p_{O_2} = Absolute air supply pressure, estimated at 101 325 Pa [253]

Δv = Activation barrier volume factor, estimated at 1 m³ [253]

ΔG = Activation energy barrier, estimated at 129 kJ [253]

h = Planck constant ($6.626\,070\,15 \times 10^{-34}$ J s)

Eventually the stack current at the end of the Ohmic region equals to:

$$I_{\text{end}} = Ai_{\text{end}}, \quad (\text{F.7})$$

where

i_{end} = Cell current density at end of Ohmic region, estimated at 0.25 A/cm² [255].

G Convergence Studies

Figure G.1 - G.4 show the remaining convergence studies.

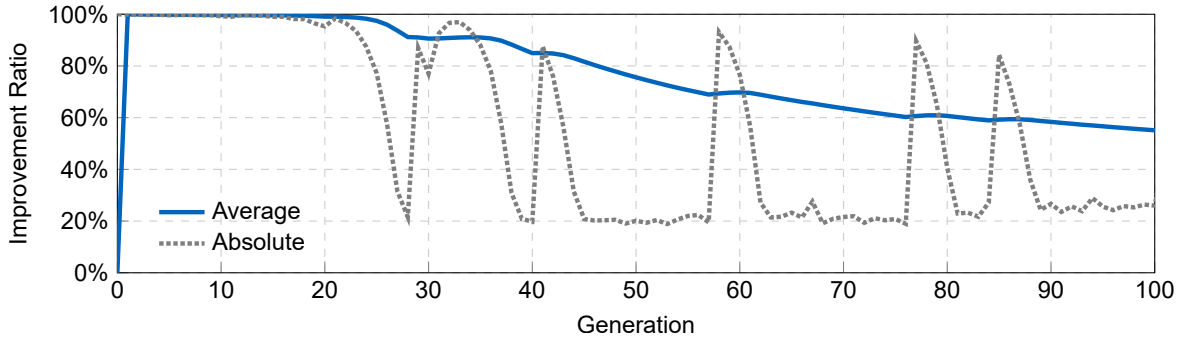


Figure G.1: The absolute improvement ratio shows that the diesel optimization converges after 15 generations. Locally random evolution creates noise, which the average improvement ratio filters out [272].

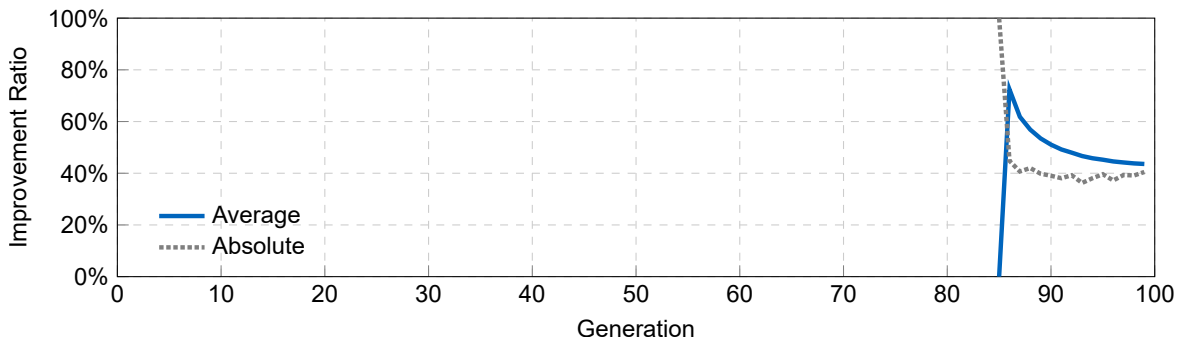


Figure G.2: The absolute improvement ratio shows that the HET optimization converges within the set generations. Locally random evolution creates noise, which the average improvement ratio filters out [272]. The optimization terminated at generation 85 and had to be restarted. Due to server issues, the earlier generation data was lost, which is why the plot starts at generation 85. The proof of convergence as well as the final optimization results are not affected by this.

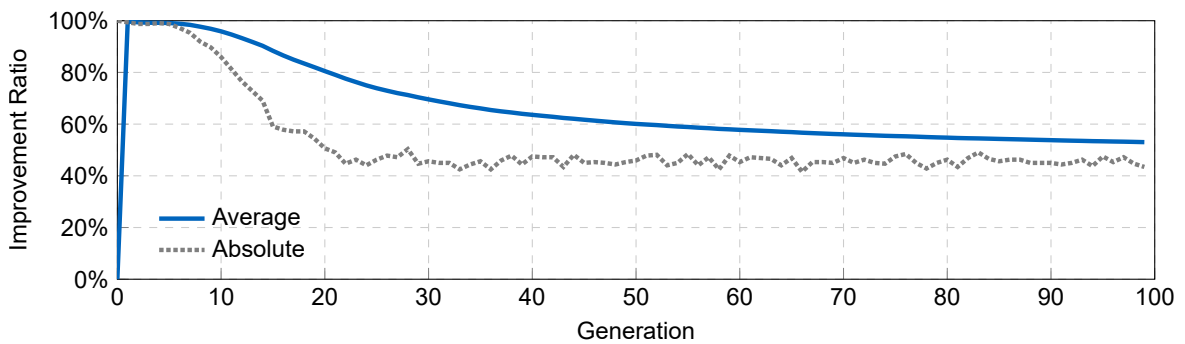


Figure G.3: The absolute improvement ratio shows that the FCET optimization converges after 70 generations. Locally random evolution creates noise, which the average improvement ratio filters out [272].

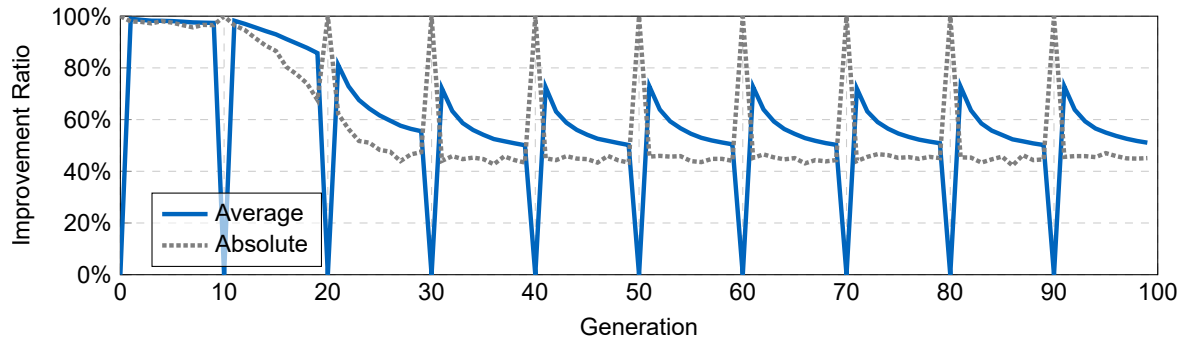


Figure G.4: The absolute improvement ratio shows that the HICET optimization converges after 70 generations. Locally random evolution creates noise, which the average improvement ratio filters out [272].

H Uncertainty Quantification

The results for diesel, hybrid, fuel cell and hydrogen combustion engine are analogous to the BEV results presented in Section 6.2.

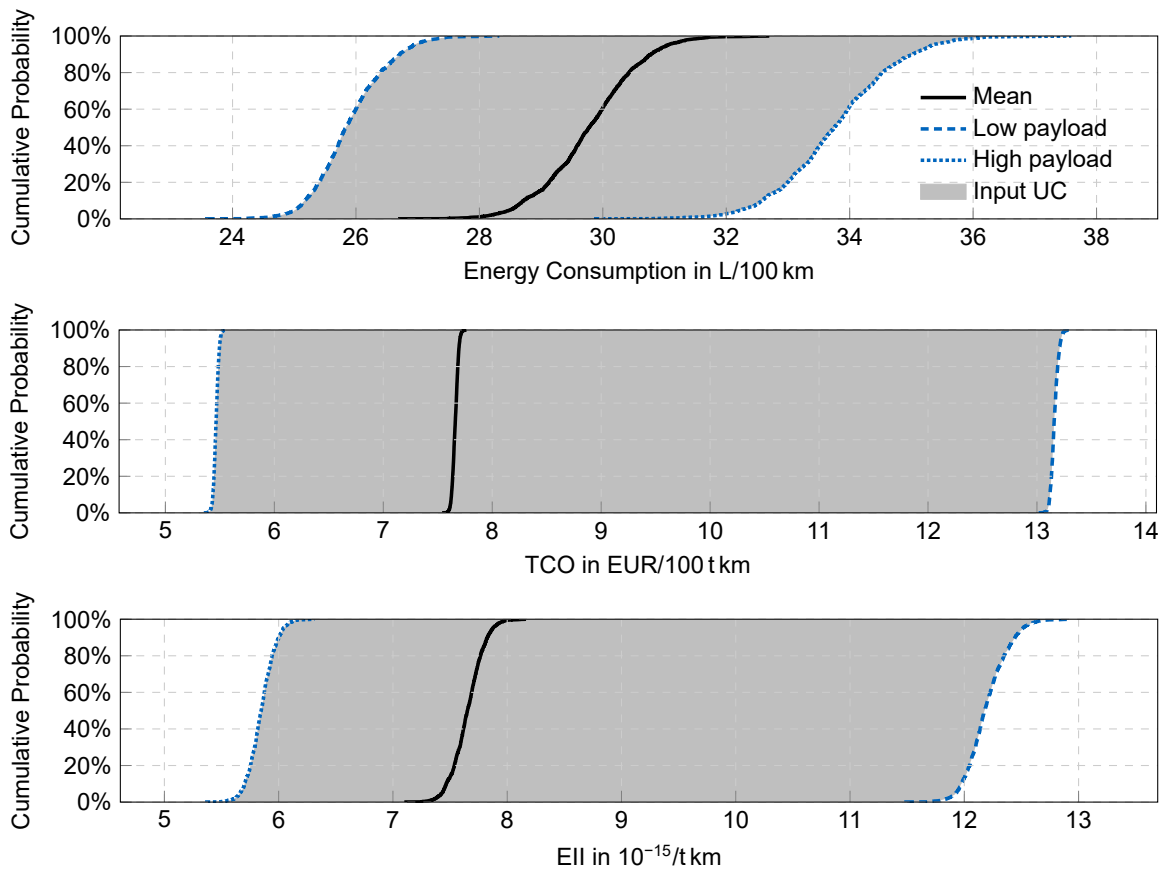


Figure H.1: The cumulative distribution function shows the diesel's uncertainty quantification of the two optimization objectives and its energy consumption. For each of the three aleatoric scenarios (mean, low, and high payload), the vehicle input parameters are altered in their epistemic intervals (Table 6.2). While the epistemic errors are clearly visible in the energy consumption's uncertainty, their effect diminishes for the two objectives. Furthermore, the aleatoric uncertainty associated with differing payloads exceeds the epistemic uncertainties.

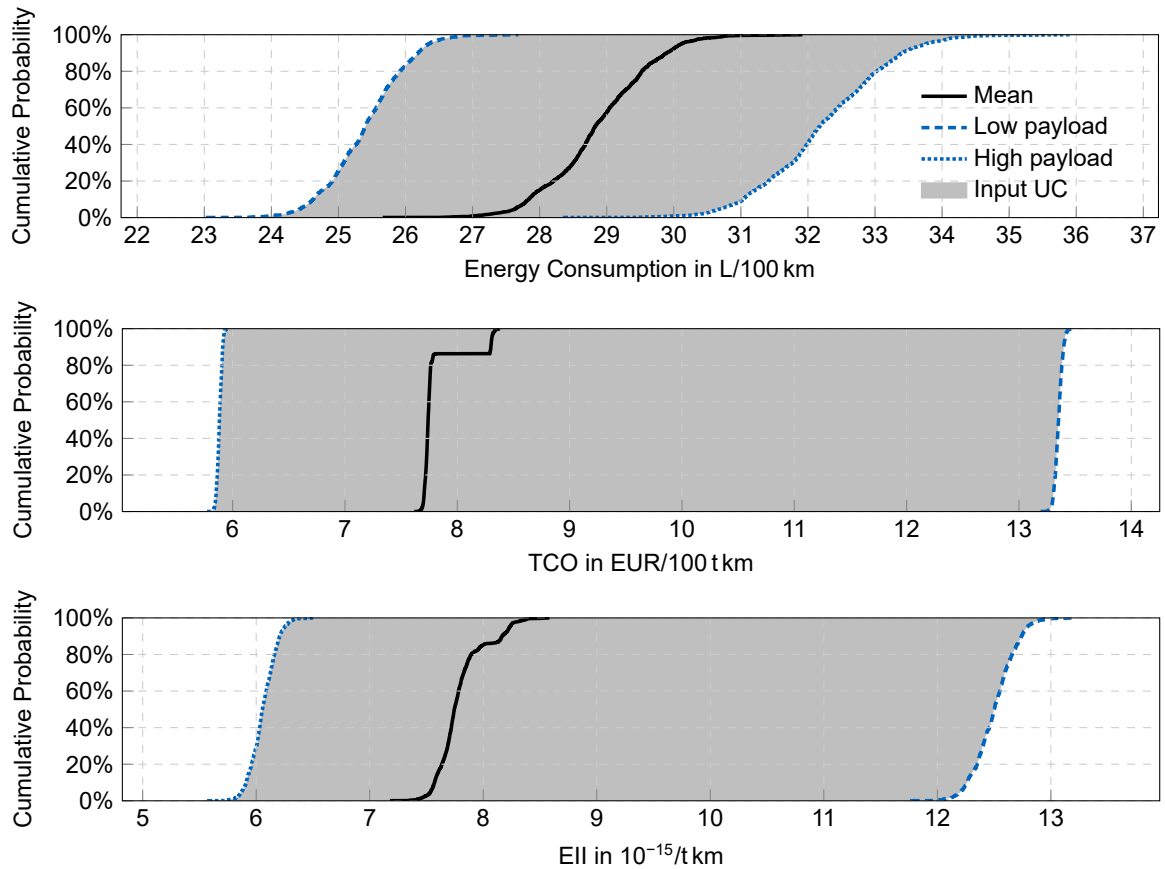


Figure H.2: The cumulative distribution function shows the HET's uncertainty quantification of the two optimization objectives and its energy consumption. For each of the three aleatoric scenarios (mean, low, and high payload), the vehicle input parameters are altered in their epistemic intervals (Table 6.2). While the epistemic errors are clearly visible in the energy consumption's uncertainty, their effect diminishes for the two objectives. Furthermore, the aleatoric uncertainty associated with differing payloads exceeds the epistemic uncertainties.

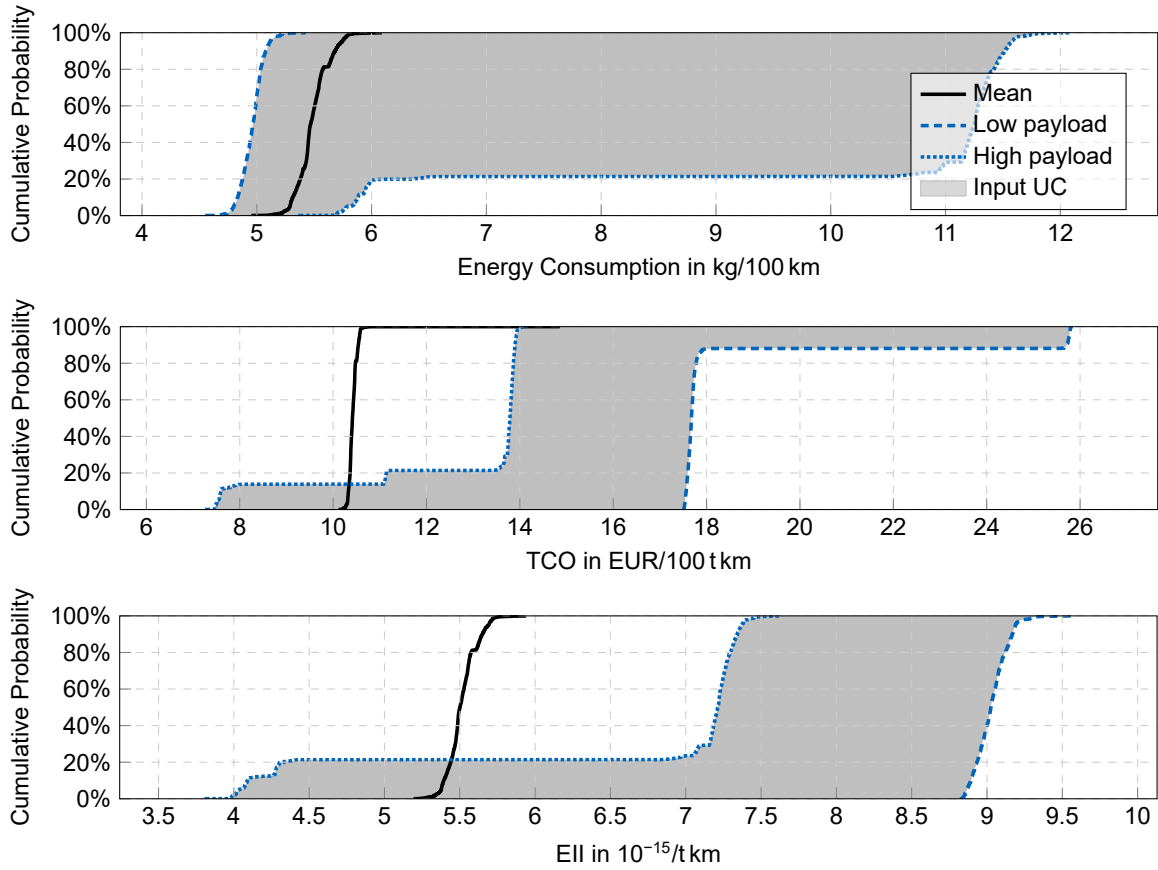


Figure H.3: The cumulative distribution function shows the FCET’s uncertainty quantification of the two optimization objectives and its energy consumption. For each of the three aleatoric scenarios (mean, low, and high payload), the vehicle input parameters are altered in their epistemic intervals (Table 6.2). While the epistemic errors are clearly visible in the energy consumption’s uncertainty, their effect diminishes for the two objectives. Furthermore, the aleatoric uncertainty associated with differing payloads exceeds the epistemic uncertainties.

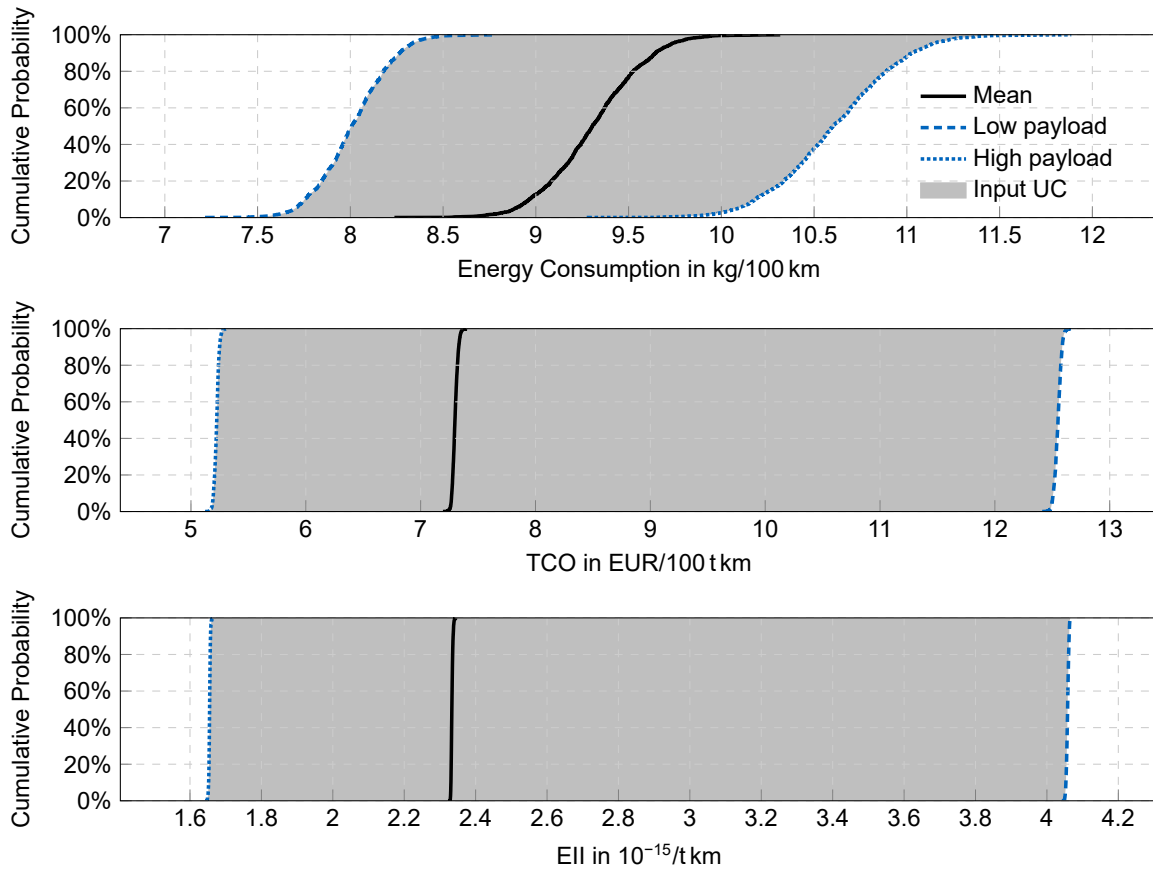


Figure H.4: The cumulative distribution function shows the HICET's uncertainty quantification of the two optimization objectives and it's energy consumption. For each of the three aleatoric scenarios (mean, low, and high payload), the vehicle input parameters are altered in their epistemic intervals (Table 6.2). While the epistemic errors are clearly visible in the energy consumption's uncertainty, their effect diminishes for the two objectives. Furthermore, the aleatoric uncertainty associated with differing payloads exceeds the epistemic uncertainties.

I Infrastructure Cost Sensitivity

To test the infrastructure costs sensitivity to the usage parameter, it is varied in the range of $\pm 20\%$. The system costs model assumes a usage of 10 h/d, consequently, the margins are at 8 h/d and 12 h/d, respectively. The area of overlap between charging and hydrogen infrastructure is small and only present if the low charging and high hydrogen usage exist.

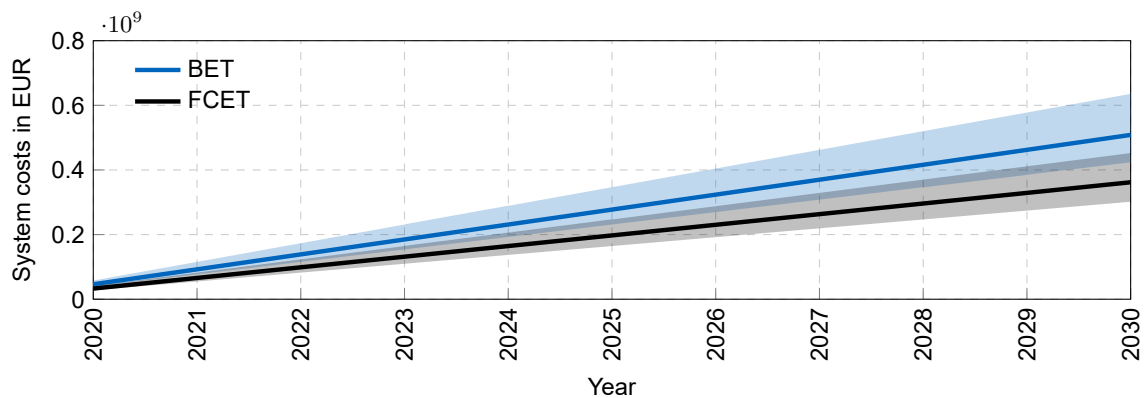


Figure I.1: The infrastructure costs (BCG E scenario) for BET and FCET are sensitive to the usage parameter. However, if the same assumptions for both are used, the relative results are not affected.

J Stakeholder Analysis

The stakeholder analysis consists of a survey Section J.1, which was conducted by Barré [299] in 2021. A confirmatory factor analysis (Section J.2) matches the survey's results to the overall trust and support for the transition towards zero-emission trucks.

J.1 Survey

Barré [299] acquired the survey participants according to the following procedure:

- Find out the usual e-mail layout of the targeted company.
- Target on LinkedIn the respondents among the employees with respect to the targeting strategy.
- E-Mailing.

Table J.1 shows the response rate for each of the four stakeholders. In total, he received 61 valid answers. Table J.2 summarizes the survey form, Barré [299] used.

Table J.1: The total number of valid (i.e., complete answering of all questions) answers for each stakeholder sums up to $n = 61$. Despite direct inquiries, the response rates were low for OEMs and fleet owners. Because drivers were reached via flyers, it is not possible to determine a response rate [299].

Stakeholder	Valid answers	Response rate
Manufacturers	10	11 %
Fleet companies	14	16 %
Drivers	11	n.a.
Public	26	62 %

Table J.2: Stakeholder survey developed by Barré [299]. The survey was conducted online. Participants were acquired via direct e-mailing or, in the case of the drivers, flyers.

Participant Affiliation	
<input type="checkbox"/>	Driver
<input type="checkbox"/>	Fleet company
<input type="checkbox"/>	Public
<input type="checkbox"/>	Charging Operators
<input type="checkbox"/>	OEMs

J Stakeholder Analysis

□ Government

Operational-economic, Likert scale, same for each technology

	Very poor (1)	Poor (3.5)	Good (6.5)	Very good (10)
Travel Range	<input type="checkbox"/>	<input type="checkbox"/>	<input type="checkbox"/>	<input type="checkbox"/>
Charging time	<input type="checkbox"/>	<input type="checkbox"/>	<input type="checkbox"/>	<input type="checkbox"/>
Purchase price	<input type="checkbox"/>	<input type="checkbox"/>	<input type="checkbox"/>	<input type="checkbox"/>
Energy price	<input type="checkbox"/>	<input type="checkbox"/>	<input type="checkbox"/>	<input type="checkbox"/>
Need for maintenance	<input type="checkbox"/>	<input type="checkbox"/>	<input type="checkbox"/>	<input type="checkbox"/>
Infrastructure price	<input type="checkbox"/>	<input type="checkbox"/>	<input type="checkbox"/>	<input type="checkbox"/>
Infrastructure availability	<input type="checkbox"/>	<input type="checkbox"/>	<input type="checkbox"/>	<input type="checkbox"/>
Level of incentive needed	<input type="checkbox"/>	<input type="checkbox"/>	<input type="checkbox"/>	<input type="checkbox"/>

Socio-environmental impact of the transition

	Very negative (0)	Negative (2.5)	No impact (5)	Positive (7.5)	Very positive (10)
Local Air quality	<input type="checkbox"/>	<input type="checkbox"/>	<input type="checkbox"/>	<input type="checkbox"/>	<input type="checkbox"/>
CO2 emissions	<input type="checkbox"/>	<input type="checkbox"/>	<input type="checkbox"/>	<input type="checkbox"/>	<input type="checkbox"/>
Traffic noise	<input type="checkbox"/>	<input type="checkbox"/>	<input type="checkbox"/>	<input type="checkbox"/>	<input type="checkbox"/>
Traffic safety	<input type="checkbox"/>	<input type="checkbox"/>	<input type="checkbox"/>	<input type="checkbox"/>	<input type="checkbox"/>
Job creation	<input type="checkbox"/>	<input type="checkbox"/>	<input type="checkbox"/>	<input type="checkbox"/>	<input type="checkbox"/>
Industry attractiveness	<input type="checkbox"/>	<input type="checkbox"/>	<input type="checkbox"/>	<input type="checkbox"/>	<input type="checkbox"/>
Energetic national independency	<input type="checkbox"/>	<input type="checkbox"/>	<input type="checkbox"/>	<input type="checkbox"/>	<input type="checkbox"/>
Economic development perspectives	<input type="checkbox"/>	<input type="checkbox"/>	<input type="checkbox"/>	<input type="checkbox"/>	<input type="checkbox"/>

Endogenous trust variable assessment					
	<2025	2025-2030	2030-2040	>2040	No believe in the technology
Natural Gas	<input type="checkbox"/>	<input type="checkbox"/>	<input type="checkbox"/>	<input type="checkbox"/>	<input type="checkbox"/>
Electric battery	<input type="checkbox"/>	<input type="checkbox"/>	<input type="checkbox"/>	<input type="checkbox"/>	<input type="checkbox"/>
Fuel cell battery	<input type="checkbox"/>	<input type="checkbox"/>	<input type="checkbox"/>	<input type="checkbox"/>	<input type="checkbox"/>
Overhead Catenary	<input type="checkbox"/>	<input type="checkbox"/>	<input type="checkbox"/>	<input type="checkbox"/>	<input type="checkbox"/>

Stakeholder responsibility distribution					
	Very low (1)	Low (3.5)	High (6.5)	Very High (10)	
Driver	<input type="checkbox"/>	<input type="checkbox"/>	<input type="checkbox"/>	<input type="checkbox"/>	
Fleet company	<input type="checkbox"/>	<input type="checkbox"/>	<input type="checkbox"/>	<input type="checkbox"/>	
Public	<input type="checkbox"/>	<input type="checkbox"/>	<input type="checkbox"/>	<input type="checkbox"/>	
Charging Operators	<input type="checkbox"/>	<input type="checkbox"/>	<input type="checkbox"/>	<input type="checkbox"/>	
OEMs	<input type="checkbox"/>	<input type="checkbox"/>	<input type="checkbox"/>	<input type="checkbox"/>	
Government	<input type="checkbox"/>	<input type="checkbox"/>	<input type="checkbox"/>	<input type="checkbox"/>	

Endogenous Support variable assessment					
	1 (No actions)	2	3	4	5 (Many actions)
Support	<input type="checkbox"/>	<input type="checkbox"/>	<input type="checkbox"/>	<input type="checkbox"/>	<input type="checkbox"/>

J.2 Confirmatory Factor Analysis

Barré [299] performed the confirmatory factor analysis according to the following steps:

1. Review of the literature to support modelling
2. Specification of a model

3. Model identification
4. Collection of the relevant data
5. Statistical analysis
6. Estimation of the model's parameters
7. Evaluation of the fitness of the model
8. Interpretation of the results

The model's fitness is assessed with two indices. To indicate the amount of variance, the R^2 -test was performed. The R^2 -value should be greater than 0.1, for the model to be valid [299]. As part of the CFA, R^2 indicates the percentage of variance present in the endogenous variables. Table J.3 shows the results for the R^2 -test.

Table J.3: R^2 -test for the two exogenous variables of the CFA. A threshold for $R^2 \geq 0.1$ renders a model valid.

	OEM	Fleet Owner	Drivers	Public
Trust	0.474	0.962	0.744	-
Support	0.914	0.979	0.834	0.742

Additionally, two criteria evaluate the correlation between endogenous and exogenous variables. The p-Value describes the statistical significant relationships. The value should be lower than 0.05, for the relationship to be significant. If the value is below 0.1, the relationship is labeled as barely non-significant. The second criteria is the β -coefficient, or coefficient of regression, describes the direction (positive or negative) of a relationship between endogenous and exogenous variables. Table J.4 shows the p-Value and β -coefficient for each exogenous variable and each stakeholder.

Table J.4: The p-value and β -coefficient, describe the correlation between endogenous and exogenous variables. A p-value lower than 0.05 classifies a variable statistically relevant. Additionally, a p-value lower than 0.1 is rated as barely significant.

	Manufacturer		Fleet Owner		Drivers		Public	
	p-value	β -coef.	p-value	β -coef	p-value	β -coef	p-value	β -coef
Technical	0.586	0.122	0.469	0.087	0.48	0.106	0.245	-0.37
Economic	0.002	0.764	0.01	0.792	0.15	0.215	0.801	0.144
Infrastructure	0.064	0.299	0.092	0.389	0	0.493	0.507	0.33
Environmental Impact	0.99	0	0.103	0.177	0.017	0.447	0	0.63
Development Potetial	0	1.16	0.999	0	0.3	0.115	0	1.068
Traffic Impact	0.001	0.395	0.001	0.395	0	0.652	0.848	-0.02